On Coding for Orthogonal Frequency Division Multiplexing Systems

Alan Clark

Department of Electrical and Computer Engineering

A thesis presented for the degree of
Doctor of Philosophy

University of Canterbury
Christchurch, New Zealand
January 2006

The fundamental problem of communication is that of reproducing at one point either exactly or approximately a message selected at another point.

Claude E. Shannon [1], 1948

Abstract

The main contribution of this thesis is the statistical analysis of orthogonal frequency division multiplexing (OFDM) systems operating over wireless channels that are both frequency selective and Rayleigh fading. We first describe the instantaneous capacity of such systems using a central limit theorem, as well as the asymptotic capacity of a power limited OFDM system as the number of subcarriers approaches infinity. We then analyse the performance of uncoded OFDM systems by first developing bounds on the block error rate. Next we show that the distribution of the number of symbol errors within each block may be tightly approximated, and derive the distribution of an upper bound on the total variation distance. Finally, the central result of this thesis proposes the use of lattices for encoding OFDM systems. For this, we detail a particular method of using lattices to encode OFDM systems, and derive the optimal maximum likelihood decoding metric. Generalised Minimum Distance (GMD) decoding is then introduced as a lower complexity method of decoding lattice encoded OFDM. We derive the optimal reliability metric for GMD decoding of OFDM systems operating over frequency selective channels, and develop analytical upper bounds on the error rate of lattice encoded OFDM systems employing GMD decoding.

Acknowledgements

I wish to thank my supervisor, Professor Des Taylor, for the excellent tutelage, support, guidance and conversation that he has provided. I also extend sincerest thanks to Professor Peter Smith for the encouragement, ideas, time and effort he has given me in helping to address some of the interesting statistical problems associated with this thesis. To Des and Pete I apologise for all the errors and ambiguities they had to overcome in reading my papers. Over the years many other people have given their time to offer suggestions regarding the problems I have encountered. I am grateful to these people, in particular Lee Garth, Phillipa Martin, Dave Rankin and Peter Green. Of course, I also extend my thanks and best wishes to Alan Coulson for his continual support and for suggesting OFDM as a research topic. Finally, the writing of this thesis would not have been possible without the continual support of my family and friends, to whom I am indebted.

Contents

Chapter 1

Introduction

Communications have always been fundamental to human existence. The 21st Century will no doubt see wireless communications become ubiquitous, and the expectations of wireless services increase. Today, more than one in three New Zealanders own a cellular phone [2], and services such as high quality video and music, as well as high speed internet are available to wireless mobile users throughout the country. Over time the data rates of wireless systems must grow to support increasing consumer expectations of wireless services, while the system error rate, the proportion of data that is incorrectly received, must remain at an acceptable level.

Achieving high data rates at low error rates is a difficult task, since wireless transmission of data is impeded by the physical properties of the atmosphere, the surrounding environment and electromagnetic interference from other devices [3]. Furthermore, these impairments are typically random in nature, although statistical descriptions are possible. A method for reducing the error rate in a system is *error control coding*, entailing the transmission of some extra data used for verification of the required original data. However, the penalty for coding is usually a reduction in data rate and an increase in system complexity.

One method for transmitting at high data rates is orthogonal frequency division multiplexing (OFDM) [4]. In this thesis we undertake mathematical analysis of the properties of OFDM systems. Such analysis of a transmission method is critical to accurately predict its behaviour, and thus allow for future improvements to the system. We investigate the error performance of uncoded OFDM systems, then propose a coding method based on the rich mathematical subject of lattices.

1.1 Problem Outline

Assume we have some communications system where the transmitter sends symbols over a channel, and occupies a bandwidth of $B\,(\mathrm{Hz})$. At the receiver we obtain the transmitted symbols perturbed by additive white Gaussian noise [1], such that the ratio of received symbol energy to noise power spectral density within the bandwidth B is γ. In 1948 Claude Shannon theorised [1] that the *capacity* of a communications system is

$$C = B \log_2 (1 + \gamma) \text{ bits per second,} \tag{1.1}$$

where the capacity is the maximum rate at which information bits may be transmitted and correctly estimated at the receiver. That is, the channel capacity defines the fundamental maximum limit of the rate at which we may transmit symbols and receive them without error, in the presence of additive white Gaussian noise. For over fifty years, it has been the goal of coding theorists and communications engineers to design and construct systems which operate at, or close to, this capacity. The development of coding theory during the 20^{th} Century is summarised in [5].

Shannon's theorem encapsulates four critical parameters of any communications system: the bandwidth occupied, the ratio of transmitted power to noise (signal to noise ratio), the data rate throughput and the error rate. A fifth parameter is the system complexity. We ideally desire systems that achieve high data rates at low error rates, with low complexity, small signal to noise ratio and small occupied bandwidth. However, communications engineers are required to trade these parameters off against each other during system design. For example, current digital video broadcasting systems [6] have high data rates, low error rates, yet require large bandwidth and signal to noise ratio at moderate complexity. Similarly, deep space satellite communications systems typically provide low signal to noise ratio, yet have low data throughput. In order to design better systems, an accurate mathematical model of system behaviour with respect to these parameters is therefore essential.

This thesis combines analysis of two concepts in communications: OFDM and error control coding. OFDM is a useful transmission method that is resilient to some of the detrimental effects of the wireless radio channel [4]. However, in order to achieve low error rates it is still necessary to employ some form of error control coding in conjunction with OFDM. We thus also consider OFDM systems using error control coding. Specifically, we propose a method of using mathematical lattices [7] as an error control scheme for wireless OFDM systems. We concern ourselves with OFDM systems designed to transmit high data rates. Such systems typically occupy a large bandwidth, and their operation is computationally expensive.

The two key goals of this thesis are to mathematically describe the capacity and error rate

of OFDM systems and to investigate coding using lattices specifically adapted for wireless OFDM systems, in order to achieve low error rates at high data rates, with low complexity. Furthermore, we wish to complement the new coding method with a thorough analysis of its error performance. In undertaking the mathematical analysis within this thesis we hope to construct accurate models to describe the behaviour of OFDM systems, in an effort to afford better system design and analysis of these systems.

1.2 Thesis Contributions

This thesis begins by outlining the key concepts behind a wireless communications system in the following chapter, with emphasis on the effect of the wireless radio channel upon transmitted signals. We then introduce error control coding in Chapter 3, specifically discussing linear block codes, soft decision decoding, generalised minimum distance decoding, coded modulation and the concept of lattices. In Chapter 4 we detail the orthogonal frequency division multiplexing technique and consider the effects of OFDM transmission on the achievable channel capacity. The error performance of uncoded OFDM systems is addressed in Chapter 5. Chapter 6 develops a powerful coding method using lattices, and describes the use of this coding method with OFDM. We then propose generalised minimum distance decoding as a low complexity approach to lattice decoding. Conclusions are presented in Chapter 7.

The contributions considered original are found in Chapter 4, Chapter 5 and Chapter 6, and are outlined as follows. In Chapter 4 we show that the instantaneous capacity of an OFDM system with a large number of subcarriers is approximately Gaussian distributed for certain wireless channels. We also show that in the case of power limited, infinite bandwidth systems no capacity loss is incurred by employing OFDM. In Chapter 5 we derive accurate bounds on the block error rate for OFDM systems, as well as a model for approximating the number of errors within a single OFDM block. We show that the number of symbol errors within a block is Poisson binomial distributed, but accurately approximated with the Poisson distribution. In Chapter 6 we prove requirements for optimal lattice decoding of OFDM, and outline lattice properties that will give the best error performance. We then analyse the error performance of generalised minimum decoding of lattice encoded OFDM systems transmitting over wireless channels, including a derivation of the optimal reliability metric for such systems.

The work described in this thesis was completed during the period from February 2002 to November 2005. The following papers and reports stemming from this work have been published or submitted for publication:

A. Clark and D.P. Taylor, "Lattice Codes and Generalized Minimum Distance Decoding

for OFDM Systems", accepted for publication in IEEE Transactions on Communications, January 2006.

A. Clark and D.P. Taylor, "Lattice Codes and Generalized Minimum Distance Decoding for OFDM Systems", Univ. Canterbury Technical Report, Univ. Canterbury, New Zealand, 2005.

A. Clark, P.J. Smith and D.P. Taylor, "Approximating the Probability Distribution of OFDM Symbol Errors", Univ. Canterbury Technical Report, Univ. Canterbury, New Zealand, 2005.

A. Clark, P.J. Smith and D.P. Taylor, "Approximating the Probability Distribution of OFDM Symbol Errors", in Proc. IEEE WirelessCom 2005, Kaanapali, Hawaii, June 2005.

A. Clark, P.J. Smith and D.P. Taylor, "Instantaneous Capacity of OFDM on Rayleigh Fading Channels", submitted to IEEE Transactions on Information Theory, November 2005.

A. Clark, P.J. Smith and D.P. Taylor, "Simple Expressions for the Correlation between Fading Channel Error Rates", in Proc. IEEE International Symposium on Information Theory, Seattle, WA, July 2006.

Chapter 2

Communications System Overview

This chapter provides a brief introduction to wireless communications systems, a necessary primer before discussion of error control coding and OFDM systems in following chapters. A general overview of the physical layer of a typical wireless communications system is given, and the roles of error control coding, modulation and demodulation are discussed. System performance is severely limited by the wireless radio channel, and we thus give a detailed outline of its underlying mechanisms, statistical descriptions and methods of simulating the channel response. Readers familiar with mobile communications and fading channels may wish to omit this chapter. Further details of communications systems may be found in [8–10], while [9, 11, 12] review the wireless radio channel.

2.1 System Outline

We represent a digital communications system as the following elements: an information source, a transmitter, the communications channel, and a receiver. The transmitter consists of a source encoder, an error control encoder and a digital modulator, while the receiver consists of a digital demodulator, error control decoder and a source decoder. Figure 2.1 displays these basic elements. The information source output is a sequence of binary data, such as a computer file or digitised audio or video. The source encoder compresses the data to remove redundancy for more efficient transmission. We do not consider source encoding and decoding in this thesis; details on these may be found in [13, 14]. The information sequences are often corrupted during transmission, and the error control encoder thus adds redundancy in a controlled fashion, so that error corrupted sequences may be corrected at the receiver without retransmission. The joint operations of error control encoding and error control decoding are referred to as *error control coding*, *channel coding* or simply *coding*. Chapter 3 provides an introduction to error control coding.

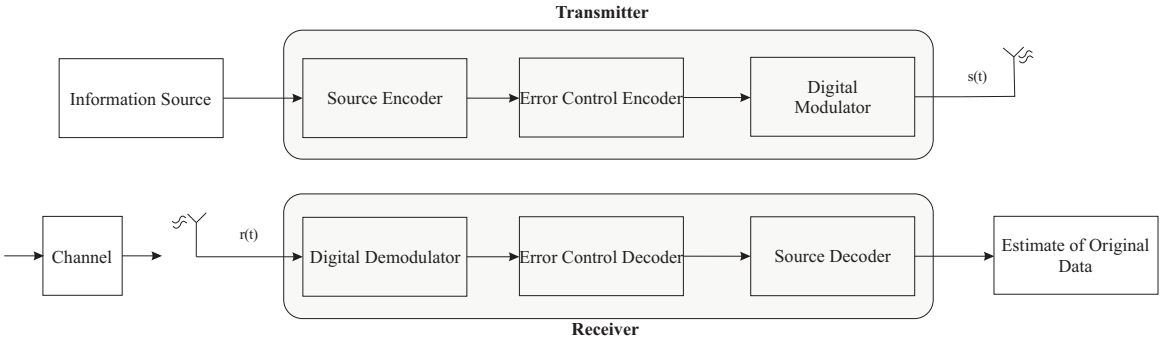

Figure 2.1 Mobile communications system overview

The digital modulator maps the data sequence from the error control encoder to analog waveforms. The digital modulator switches (keys) the amplitude, frequency or phase of a sinusoidal carrier in some manner representing the digital data. The most prevalent modulation method used worldwide is the nonlinear Gaussian Minimum Shift Keying (GMSK) method [8]. However, throughout this thesis we assume that either binary phase shift keying (BPSK), pulse amplitude modulation (PAM) or quadrature amplitude modulation (QAM) is used [8], which are highly prevalent linear modulation schemes. For a BPSK system with carrier frequency f_c and symbol period $T = \frac{1}{f_c}$, signals $s_0(t)$ and $s_1(t)$ with differing phases are used to transmit binary symbols 0 and 1 respectively, where

$$s_1(t) = \sqrt{\frac{2E_0}{T}}\cos(2\pi f_c t) \qquad s_2(t) = \sqrt{\frac{2E_0}{T}}\cos(2\pi f_c t + \pi) \tag{2.1}$$

for $0 \leq t \leq T$, and E_0 is the transmitted energy per bit. For an M-ary modulation scheme we map binary data to M possible signals, $s_1(t)$, $s_2(t)$, $\ldots$, $s_M(t)$, such that each signal represents a unique sequence of $\log_2(M)$ bits. For example, an M-ary PAM system transmits a signal of differing amplitude for each sequence, namely

$$s_i(t) = \sqrt{\frac{2E_0}{T}}a_i \sin(2\pi f_c t) \tag{2.2}$$

for $0 \leq t \leq T$, $i \in \{1, \ldots, M\}$ and $a_i \in \{-M+1, -M+3, \ldots, -1, 1, \ldots, M-3, M-1\}$, assuming M is even. An M-ary square QAM modulator transmits two $\sqrt{M}$-ary PAM carriers in quadrature, so that the signals are defined as

$$s_i(t) = \sqrt{\frac{2E_0}{T}}a_i \cos(2\pi f_c t) + \sqrt{\frac{2E_0}{T}}b_i \sin(2\pi f_c t)\,, \tag{2.3}$$

for $0 \leq t \leq T$, and $a_i, b_i \in \left\{-\sqrt{M}+1, -\sqrt{M}+3, \ldots, -1, 1, \ldots, \sqrt{M}-3, \sqrt{M}-1\right\}$, assuming M and $\sqrt{M}$ are even, positive integers. $2E_0$ is then the energy of the signals with

the lowest amplitude, corresponding to $(a_i, b_i) \in \{(1,1),(1,-1),(-1,1),(-1,-1)\}$. The average energy for an M-ary QAM system is, assuming a square constellation [8],

$$E_{av} = \frac{2(M-1)E_0}{3}. \tag{2.4}$$

The *signal constellation* $\mathcal{M}$ is a representation of the transmitted signals $s_1(t), \ldots, s_M(t)$ as vectors in Euclidean space, referred to as the signal space [9]. Each complex vector has magnitude equal to the signal energy, and phase equal to the signal phase. For example, BPSK and 16-QAM signal constellations are shown in Figure 2.2. For the BPSK constellation, points s_0 and s_1 represent signals $s_0(t)$ and $s_1(t)$, which represent binary symbols 0 and 1, respectively. Each point in the 16-QAM constellation represents a distinct 4-bit sequence. Generally, each point in an M-ary signal constellation is isomorphic to some

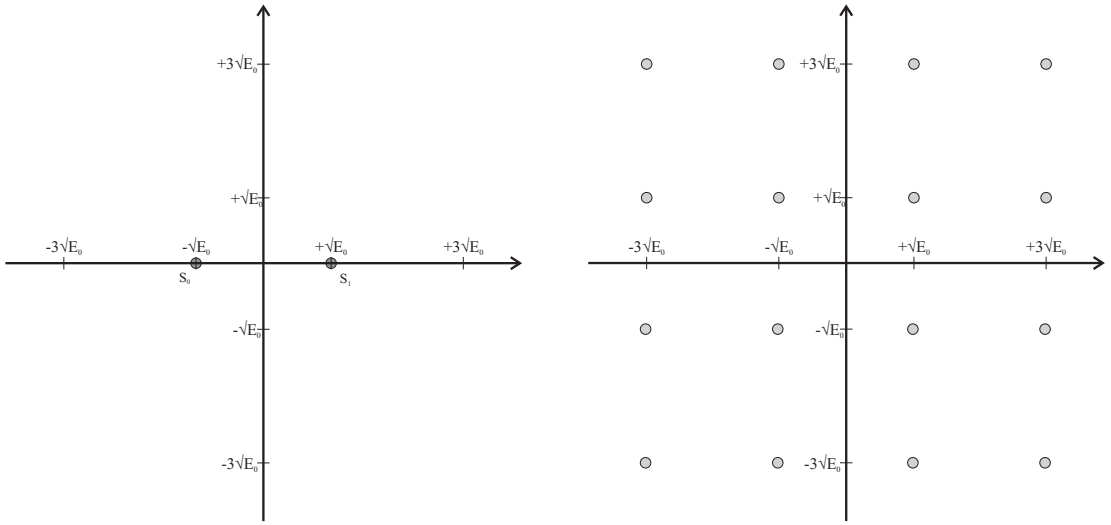

(a) BPSK (b) 16-QAM

Figure 2.2 Signal space constellations

sequence of $\log_2 M$ bits. We denote this mapping as $m : \{0,1\}^{\log_2 M} \to \mathbb{R}^2$. A vector $\mathbf{c}_i = \{c_1, c_2, \ldots, c_{\log_2 M}\}$ of $\log_2 M$ binary bits, is thus isomorphic to a signal point $m(\mathbf{c}_i)$. A length n sequence of $\log_2 M$ bit vectors $\{\mathbf{c}_1, \mathbf{c}_2, \ldots, \mathbf{c}_n\}$ is then isomorphic to the sequence $\{m(\mathbf{c}_1), m(\mathbf{c}_2), \ldots, m(\mathbf{c}_n)\}$ of n signal points. We thus map $n \log_2 M$ bits to n complex signal points. In a slight abuse of notation we again use m to denote this n dimensional mapping as

$$m : \{0,1\}^{n \log_2 M} \to \mathbb{R}^{2n} \tag{2.5}$$

with the inverse mapping denoted $m^{-1} : \mathbb{R}^{2n} \to \{0,1\}^{n \log_2 M}$.

The transmitted signals we consider are *bandpass signals*, that is, they occupy some finite

bandwidth B. The signals are transmitted at some carrier frequency f_c, and therefore occupy frequencies from $f_c - \frac{B}{2}$ to $f_c + \frac{B}{2}$. However, without loss of generality we represent the transmitted signal by its complex baseband equivalent [8], that is, the signal $s(t)$ occupying frequencies from 0 to B. We likewise represent the channel impulse response (detailed in Section 2.2) by its complex baseband equivalent $h(t, \tau)$, so that the channel is modelled as a time varying linear filter. Furthermore, interference encountered in transmission and thermal noise from electronic components is modelled as a zero mean complex Gaussian process, with constant power spectral density $\frac{N_0}{2}$ for both the real and imaginary components (dimensions). Assuming the noise is filtered such that it occupies an identical bandwidth to the transmitted signal, we may then denote the received noise process as $w(t)$, so that a sample $w(t_1)$ of $w(t)$ at time t_1 is a complex Gaussian random variable with variance $\frac{N_0}{2}$ per dimension [8]. Furthermore, we assume samples $w(t_1)$ and $w(t_2)$ are independent, for all t_1 and t_2 such that $t_1 \neq t_2$. The received signal is then

$$r(t) = \int_{-\infty}^{+\infty} h(t, \tau) s(t - \tau) d\tau + w(t) = s(t) \otimes h(t, \tau) + w(t) \tag{2.6}$$

where $\otimes$ denotes convolution between t and τ. In certain cases $h(t, \tau)$ may be represented as a constant, which we assume, without loss of generality, to be unity. The received signal is then perturbed by $w(t)$ only, so that

$$r(t) = s(t) + w(t) \tag{2.7}$$

and we refer to this as an *additive white Gaussian noise* (AWGN) channel. Assuming symbols are transmitted at rate B so that the average symbol power is $B\, E_{av}$, the average signal to noise ratio (SNR) of the bandlimited received signals is $\gamma = \frac{E_{av}}{N_0}$. Although the AWGN channel is one of the simplest channel models, it generally does not fully describe the wireless channel. For wireless channels, we examine the complicated nature of $h(t, \tau)$ in the following section.

The digital demodulator maps the received analog waveform back to some set of data points. The demodulator must first account for the effects of the channel, typically by applying the inverse channel response $h^{-1}(t, \tau)$, and then attempt to apply the inverse mapping from a noise corrupted point in signal space to a sequence of bits, $m^{-1} : \mathbb{R}^2 \rightarrow \{0, 1\}^{\log_2 M}$. We assume the digital demodulator employs a *matched filter* or *correlation receiver* [8] to estimate the data sequence associated with the received waveform. The received data sequence is then passed to the error control decoder, which attempts to correct any erroneous data symbols using the redundancy added by the error control encoder. Finally, the corrected data is passed to the source decoder to reconstruct an estimate of the original binary information.

2.2 Wireless Radio Channels

This section outlines fundamental characterisations of the mobile radio channel, providing a reference for the remainder of this thesis. The properties of the wireless radio channel are determined by the environment surrounding the transmit and receive antennas. The behaviour of the channel is thus typically random, and simple deterministic models are not adequate. We introduce several statistical descriptions of the channel which accurately model its behaviour, largely summarising the work of [12] and [11].

Channel characterisation may be split into two categories [10]. Models which characterise mean received signal strength over large separation distances, hundreds or thousands of metres, between transmitter and receiver are called *large-scale path loss* or *shadowing*. This mean received signal strength varies very slowly, over the order of millions of received symbols, for a given receiver velocity and symbol rate. We neglect the effects of shadowing and assume that the mean received power is constant over a long period of time. That is, we assume the shadowing effects are adequately compensated for using some transmit power control, as in [15] or [16, Chp. 3].

Channel models which consider only the rapid changes in the received signal over small distances or short time are called *small scale fading*, *multipath fading* or simply *fading*. In this thesis we consider *multipath fading* only, since the systems we consider either transmit over short time intervals, or have fixed separation distances. OFDM systems have been proposed for future mobile technologies, and as such we must consider multipath fading. Even fixed point to point OFDM systems may experience multipath fading, particularly if no line of sight path is present. Fixed wireless systems are perturbed by changes in the surrounding environment, such as the movement of people, cars, or flora. These effects may also be modelled as multipath fading.

2.2.1 Multipath Fading Characteristics

Objects, such as buildings, people and trees, in the vicinity of a transmitter or receiver reflect, diffract and scatter radio signals. Multipath fading is caused by the interference from several different versions of the transmitted signal arriving at the receiver at slightly different times. This phenomenon is referred to as *multipath propagation*, and is illustrated in Figure 2.3. Receiver or transmitter movement changes the distribution of the amplitude, phase and arrival times of the incoming signal versions, which may cause rapid fluctuations in the amplitude and phase of the received signal. Note that even for a fixed transmitter and receiver such rapid fluctuations may be caused by motion of surrounding objects [17]. For the context of this thesis, we may assume that the transmitter and surrounding environment are fixed, and thus model multipath fading as due to receiver motion only. The most

important effects of fading are rapid received signal strength changes over a small distance or time interval, random frequency modulation due to Doppler effects and time dispersion due to multipath delays. We outline statistical characterisations of these effects.

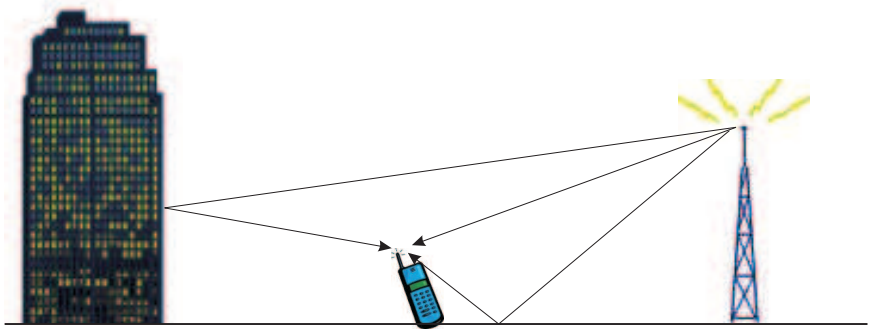

Figure 2.3 Multipath Fading Mechanism

In certain cases it is appropriate to model the received signal as being composed of a dense continuum of delayed transmitted signal versions, referred to as *diffuse multipath*. However, unless noted we assume the received signal is the superposition of a finite number P of versions of the transmitted signal $s(t)$, referred to as *discrete multipath*. Since the path that each version of the transmitted signal travels is distinct, each version has a distinct arrival time, attenuation and phase. We denote the complex gain of the p^{th} version as a_p, and the relative delay in arrival time between the first signal and p^{th} signal as τ_p. We can then write the bandpass representation of the received signal $r(t)$ as

$$r(t) = \text{Re}\left\{ \exp(j2\pi f_c t) \sum_{p=1}^{P} a_p \exp(-j2\pi f_c \tau_p) s(t-\tau_p) \right\} \tag{2.8}$$

where f_c is the carrier frequency of the transmitted signal. The summation in (2.8) is the complex envelope, denoted $\tilde{r}(t)$, of the received signal, which is a function of the delay times, path gains, carrier frequency and the transmitted signal $s(t)$. The phenomenon of several relatively delayed signal versions being received is known as *time dispersion*, and creates *intersymbol interference* (ISI) between successive transmitted signals.

The path gains a_p and delays τ_p may change at different locations, giving rise to rapid spatial fluctuation in the complex envelope $\tilde{r}(t)$. When there is receiver motion this may be viewed as a temporal phenomenon since the receiver changes position over time. We therefore refer to the mobile radio channel as being time varying, although the cause of this is typically spatial variation.

Receiver motion causes a Doppler shift in the received signals. The fading channel there-

fore induces a random frequency modulation and spectral broadening of the transmitted signal. The Doppler shift is dependent on the relative velocity between the transmitter and receiver. Spectral broadening of the transmitted signal due to receiver or environment motion is known as *Doppler spread*.

We now consider the impact of the transmitted signal on the channel classification. Given a transmitted signal $s(t)$ with bandwidth B, carrier frequency f_c, and maximum velocity v, the channel may be classified as either *static* or *fading* and either *narrowband* or *wideband*, as outlined below.

Static Channels

First consider the case when the receiver is stationary and the surrounding environment changes negligibly, or equivalently when the carrier frequency is much less than the inverse of the longest path delay, in other words $f_c \ll \frac{1}{\tau_p}$, for all p. The path delays τ_p and amplitudes a_p are then considered invariant. If the transmitted signal period $T = \frac{1}{B}$ is such that $T \gg \tau_p$, for all p, then the received signal varies slowly and is largely unperturbed by the arriving relatively delayed signals. We can then write $s(t - \tau_p) \approx s(t)$, and thus write (2.8) as

$$r(t) \approx \mathrm{Re}\left\{ s(t) \sum_{p=1}^{P} \exp(-j2\pi f_c \tau_p) \right\} = h_0 s(t). \tag{2.9}$$

The channel is therefore modelled as a time invariant constant h_0. We refer to this channel as a *static narrowband* or *static flat* channel, where *static* refers to the time invariance, and *flat* or *narrowband* implies invariance of the channel gain with respect to frequency.

In the case where $\tau_p \not\ll \frac{1}{B}$, for some $p \in \{1, 2, \ldots, P\}$, the delayed versions of the transmitted signal have a significant effect on the received signal. In this case we write (2.8) as

$$r(t) = \int_{-\infty}^{+\infty} h(\tau) s(t - \tau) d\tau \tag{2.10}$$

where the delay dependent channel gains are $h(\tau) = \sum_{p=1}^{P} h_p \delta(\tau - \tau_p)$ in which $h_p = a_p \exp(j2\pi f_c \tau_p)$. If one or more delays τ_p is greater than the transmitted signal resolution time T, the channel may have a severe distorting effect on the received signal,

$$r(t) \approx \mathrm{Re}\left\{ \sum_{p=1}^{P} \exp(-j2\pi f_c \tau_p) s(t - \tau_p) \right\} = \sum_{p=1}^{P} h_p s(t - \tau_p) \,, \tag{2.11}$$

that is, the channel now behaves like a time invariant linear filter, with impulse response $h(\tau)$. We may find the channel frequency response $H(f)$ by taking the Fourier transform of $h(\tau)$. Conceptually, the transmitted signal is spread over time, and this type of channel is

therefore known as a *static, time dispersive* channel. It is also referred to as a *static dispersive*, *static wideband* or *static frequency selective* channel, since the channel response varies for different frequency components of the transmitted signal.

Many of the systems we consider operate in time varying channels. However, many systems transmit data in short bursts during short time intervals. If the channel time variance is negligible during these periods we refer to the channel as being *quasi-static*. In these cases the assumption of a static channel model is valid.

Time Varying Channels

If the receiver moves at some nonzero velocity v, with respect to the transmitter, then the path delays are time varying, and denoted $\tau_p(t)$. Consider first the case where the time varying path delays are small in comparison to the signal bandwidth, that is $\tau_p(t) \ll \frac{1}{B}$ for all p and t. The transmitted signal then varies slowly enough so that it is unaffected by the received delayed signals, and $s(t - \tau_p(t)) \approx s(t)$. We can then write (2.8) as

$$r(t) \approx s(t) \sum_{p=1}^{P} a_p \exp[-j2\pi\tau_p(t)] = h(t)s(t) \ , \tag{2.12}$$

where $h(t)$ is the time-varying complex channel gain. We refer to this type of channel as a *flat*, *fading* or *time-selective* channel, since there is no variation in the channel gain with transmitted signal frequency. This is also referred to as a *flat fading* channel.

Consider next the case where the delay durations have a significant effect on the received signal. That is, $\tau_p(t) \not\ll \frac{1}{B}$, for some p at time t. Then the transmitted signal is spread over time, and we may write

$$r(t) = \int_{-\infty}^{+\infty} h(t,\tau)s(t-\tau)d\tau \ , \tag{2.13}$$

where $h(t,\tau) = \sum_{p=1}^{P} h_p(t)\delta(\tau - \tau_p)$ and $h_p(t) = a_p(t)\ \exp[-j2\pi\tau_p(t)]$, that is, the channel may be modelled as a linear filter, with time varying impulse response $h(t,\tau)$. This channel is referred to equivalently as a *wideband fading*, *frequency selective fading*, *time and frequency selective* or *dispersive fading* channel.

The wideband fading channel is the most general model, and it is readily seen that the time invariant and flat channel models are special cases of this channel model. We consider only wideband fading channels for the remainder of this chapter.

Since the path delays $\tau_p(t)$ are time variant, the phases of the arriving transmitted signal versions also vary with time. It is typically assumed that the arrival angles ϑ_p of the received signal plane waves at the receiver are constant, a valid assumption when the trans-

mitter is far away from the receiver [11]. Then, the phase of the transmitted signal taking the p^{th} path may be written as $2\pi f_c \tau_p(t)$, relative to a signal with delay $\tau_p(t) = 0$, and the phase change may be written [11] as

$$\theta_p(t_2) - \theta_p(t_1) = \frac{2\pi v(t_2 - t_1)}{\lambda_c} \cos\vartheta_p. \tag{2.14}$$

Differentiating (2.14) with respect to time, we obtain

$$\frac{\partial \theta_p}{\partial t} = \frac{2\pi v}{\lambda_c} \cos\vartheta_p = f_d \cos\vartheta_p \tag{2.15}$$

where $f_d \triangleq \frac{v}{\lambda_c} = \frac{v f_c}{c}$ is the *maximum Doppler shift* due to receiver motion, and c is the ambient speed of light. Thus, the frequency components of the p^{th} version of the transmitted signal are shifted by a maximum of f_d, a phenomenon know as *Doppler spreading* which manifests itself as a spectral broadening of the received signal.

2.2.2 Statistical Channel Description

It is almost impossible to deterministically describe the channel impulse response $h(t, \tau)$, due to stochastic receiver motion and the typically large number of multipath components, whose path gains and delays are themselves stochastic. However, several methods of characterising the stochastic nature of the channel exist [10–12].

We may model the channel response $h(t, \tau)$ as a two dimensional stochastic process. We assume that the number of paths P is large, and that the distribution of propagation delays and amplitudes is random. By the central limit theorem, samples of the channel response $h(t, \tau)$ follow a complex Gaussian distribution, with probability density function

$$f_h(\mathbf{x}) = \frac{1}{(2\pi)^k \det(\mathbf{R_x})} \exp\left(-\frac{1}{2}[\mathbf{x} - \overline{\mathbf{x}}]^\dagger \mathbf{R_x}^{-1} [\mathbf{x} - \overline{\mathbf{x}}]\right) \tag{2.16}$$

where $\mathbf{x} = \{x_1, x_2, \ldots, x_k\}$ is a vector of k samples of the random process $h(t, \tau)$, $\overline{\mathbf{x}} = \mathbb{E}[\mathbf{x}]$ and the correlation matrix is $\mathbf{R_x} = \frac{1}{2}\mathbb{E}\left[(\mathbf{x} - \overline{\mathbf{x}})(\mathbf{x} - \overline{\mathbf{x}})^\dagger\right]$, with † denoting the matrix Hermitian transpose. This distribution is fully described by its mean

$$\overline{h(t, \tau)} = \mathbb{E}[h(t, \tau)] \tag{2.17}$$

and the elements of $\mathbf{R_x}$, defined by the autocorrelation function

$$R_h(t_1, t_2; \tau_1, \tau_2) = \mathbb{E}\left[\left(h(t_1, \tau_1) - \overline{h(t_1, \tau_1)}\right).\left(h(t_2, \tau_2) - \overline{h(t_2, \tau_2)}\right)\right]. \tag{2.18}$$

It is typically assumed that $\overline{h(t, \tau)}$ is time independent and $R_h(t_1, t_2; \tau_1, \tau_2)$ is dependent only on $\Delta t = t_2 - t_1$ rather than t_1 and t_2, so that $h(t, \tau)$ is a second order stationary

process [18]. This is known as the *wide sense stationary* assumption. When a line of sight (LoS) path between the transmitter and receiver is present, this path will usually have far greater magnitude $|a_p|$ than the other paths, and $\overline{h(t,\tau)}$ is nonzero. However, in the non-LoS case we may assume that $\overline{h(t,\tau)} = 0$. We now consider these cases individually.

Rayleigh Fading Channels

We typically model the non-LoS channel as being both wide sense stationary and exhibiting *uncorrelated scattering* (WSSUS) [11, 12], that is, the response at delays τ_1 and τ_2 are uncorrelated so that $R_h(t_1, t_2, \tau_1, \tau_2) = 0$, for all $\tau_1 \neq \tau_2$. In a slight abuse of notation we retain $R_h(\cdot)$ as the WSSUS channel autocorrelation function at fixed delay $\tau_1 = \tau_2$, and time separation $\Delta t = t_2 - t_1$. We then write

$$R_h(t_1, t_2; \tau_1, \tau_2) \equiv R_h(\Delta t; \tau_1, \tau_2)\delta(\tau_1 - \tau_2) \equiv R_h(\Delta t; \tau_1). \tag{2.19}$$

Since the channel is a complex Gaussian process with $\overline{h(t,\tau)} = 0$, the channel envelope $|h(t,\tau)|$ follows a Rayleigh distribution, with probability density function (PDF)

$$f_{|h(t,\tau)|}(x) = \frac{x}{\sigma_h^2} \exp\left(-\frac{x^2}{2\sigma_h^2}\right) \text{ for } x \geq 0 \tag{2.20}$$

where σ_h^2 is the variance of the underlying Gaussian random variables. The channel gain $|h(t,\tau)|^2$ then follows an exponential distribution, with PDF [19]

$$f_{|h(t,\tau)|^2}(y) = \frac{1}{2\sigma_h^2} \exp\left(-\frac{y}{2\sigma_h^2}\right) \text{ for } y \geq 0. \tag{2.21}$$

We thus refer to such non-LoS, time varying channels as *Rayleigh fading channels*.

The average squared magnitude of the channel response as a function of delay τ is described by the *delay power profile* $\sigma_h^2(\tau)$, defined as the channel autocorrelation function at $\Delta t = 0$, that is,

$$\sigma_h^2(\tau) = R_h(0, \tau). \tag{2.22}$$

The *mean delay* and *rms delay spread* are defined, respectively, as

$$\overline{\tau} = \frac{\sum_{p=1}^{P} \tau_p \sigma_h^2(\tau_p)}{\sum_{p=1}^{P} \sigma_h^2(\tau_p)} \quad \text{and} \quad \tau_{rms} = \sqrt{\frac{\sum_{p=1}^{P} \tau_p^2 \sigma_h^2(\tau_p)}{\sum_{p=1}^{P} \sigma_h^2(\tau_p)} - \overline{\tau}^2}. \tag{2.23}$$

The range of τ over which $\sigma_h^2(\tau) \neq 0$ is referred to as the *maximum delay spread* $\tau_{\max}$. If the transmitted symbol period $T \gg \tau_{\max}$, then intersymbol interference is negligible, and the

system is narrowband. At delay τ the channel autocorrelation can be written as

$$R_h(\Delta t, \tau_1) = \sigma_h^2(\tau)\rho_\tau(\Delta t) \tag{2.24}$$

where $\rho_\tau(\Delta t)$ is the time autocorrelation function, normalised so that $\rho_\tau(0) = 1$. The statistical behaviour of the channel is uniquely described by the power delay profile and the time autocorrelation functions, that is, in the τ and Δt domains. By taking the Fourier transform of $h(t, \tau)$ with respect to τ, we may also describe the channel in the time and frequency domains. We then obtain

$$H(t, f) = \int_{-\infty}^{+\infty} h(t, \tau) \exp(-j2\pi f\tau) d\tau \tag{2.25}$$

which is the time varying channel frequency response. Since the Fourier transform is a linear operation the autocorrelation functions of $H(t, f)$ will give an equivalent channel description to the autocorrelation functions of $h(t, \tau)$ [18]. Taking the autocorrelation with respect to time, we obtain the *time-frequency correlation function*

$$\begin{aligned} R_H(\Delta t; f_1, f_2) &= \mathbb{E}\left[H(t, f_1).H^*(t + \Delta t, f_2)\right] \\ &= \mathbb{E}\left[\int_{-\infty}^{+\infty} h(t, \tau) \exp(-j2\pi f_1\tau) d\tau . \int_{-\infty}^{+\infty} h(t + \Delta t, \tau) \exp(-j2\pi f_2\tau) d\tau\right] \\ &= \int_{-\infty}^{+\infty} R_h(\Delta t, \tau) \exp(-j2\pi\Delta f\tau) d\tau \\ &\equiv R_H(\Delta t, \Delta f) \end{aligned} \tag{2.26}$$

where $\Delta f = f_2 - f_1$. Observe that under the WSSUS assumption, the channel autocorrelation is dependent only on the time and frequency separations, Δt and Δf, respectively. Therefore, we may refer to the channel as being stationary in time and frequency. The Fourier transform of the channel autocorrelation $R_h(\Delta t, \tau)$ with respect to Δt yields the *channel scattering function*

$$S_h(v, \tau) = \int_{-\infty}^{+\infty} R_h(\Delta t, \tau) \exp(-j2\pi v\Delta t) d\Delta t \tag{2.27}$$

which gives a measure of the channel gain as a function of the Doppler spread v. Finally, the *Doppler cross-power spectral density* or *spaced-frequency Doppler spread spectrum* is the Fourier transform of the channel autocorrelation, defined as

$$S_H(v, \Delta f) = \int_{-\infty}^{+\infty} R_H(\Delta t, \Delta f) \exp(-j2\pi v\Delta t) d\Delta t \; . \tag{2.28}$$

This gives a measure of the channel frequency response correlation with respect to the

Doppler spread v. A WSSUS Rayleigh fading channel is fully and equivalently described by any of the autocorrelation functions $S_H(v, \Delta f)$, $S_h(v, \tau)$, $R_H(\Delta t, \Delta f)$ or $R_h(\Delta t, \tau)$.

We now consider some important channel parameters which give a partial description of the channel. Firstly, the autocorrelation function of (2.26) at $\Delta t = 0$ yields

$$R_H(\Delta f) = \int_{-\infty}^{+\infty} R_h(\tau) \exp(-j2\pi\Delta f\tau) d\tau. \tag{2.29}$$

The range of Δf for which $R_H(\Delta f)$ is essentially non-zero is known as the channel *coherence bandwidth* B_c. The channel response for transmitted signal components of frequency separation greater than B_c is uncorrelated. It may be seen [12] that the the coherence bandwidth is related to the maximum delay spread by $B_c \approx \frac{1}{\tau_{\max}}$. Averaging the scattering function over all delays yields

$$S_h(v) = \int_{-\infty}^{+\infty} S_h(v, \tau) d\tau \tag{2.30}$$

which is referred to as the channel *Doppler power spectrum*. The range of v over which this is non-zero is referred to as the *Doppler spread* B_d of the channel, which characterises the rate of channel variation, that is, the rate of fading. The channel Doppler spread is related to the receiver velocity by $B_d = 2f_d = 2\frac{v}{\lambda_c}$. Finally, the range of Δt over which the channel response $R_H(\Delta t, \Delta f)$ is essentially non-zero is referred to as the channel coherence time T_h. Intuitively, channel gains within a time interval less than T_h will have some measurable correlation, while channel gains at time separation $\Delta t > T_h$ will appear uncorrelated. From the Fourier transform relationship of the autocorrelation functions, the channel coherence time and Doppler spread are related by $T_h \approx \frac{1}{B_d}$.

Given the channel parameters B_d, T_h, τ_{rms} and $\tau_{\max}$, and signal parameters B, T and f_c, we may more informally classify the channel. We refer to the channel as *fast fading* if $T > T_h$ and $B < B_d$, and in this case the channel response changes significantly during the symbol period of the transmitted signal. Conversely, if $T \ll T_h$ and $B \gg B_d$ then the channel is *slow fading* and the channel response will be approximately constant during the symbol period of the transmitted signal. Note that static and quasi-static channels are special cases of slow fading channels, when the coherence time T_h is very large. The channel coherence bandwidth and delay spread determine whether a channel may be considered narrowband or wideband. If $B > B_c$ and $T < \tau_{rms}$ then a channel is wideband, or frequency selective. Conversely, a channel is narrowband, or flat, if $B \ll B_c$ and $T \gg \tau_{rms}$.

Rician Fading Channels

When there is a LoS or dominant path between the transmitter and receiver, the channel response is modelled as a Gaussian process $h(t,\tau)$ with non-zero mean. We model the LoS path as having constant amplitude a_0 and time varying phase $\tau_0(t)$ and we may then separate the channel response into the LoS and non-LoS components. We express the channel impulse response as

$$h(t,\tau) = a_0 \exp(-j2\pi f_c \tau_0(t)) + h_s(t,\tau) \tag{2.31}$$

where $h_s(t,\tau)$ is the channel response due to the reflected, diffused and scattered paths. We define a_0 so that $h_s(t,\tau)$ is a zero mean, wide sense stationary Gaussian process. Assuming uncorrelated scattering, $h_s(t,\tau)$ then follows the Rayleigh fading channel response, as previously described.

We consider only coherent systems [8], so that the receiver obtains phase lock on the dominant path. The time varying phase $\tau_0(t)$ may then be set to zero and we may model the phase locked channel response as

$$h_{PL}(t,\tau) = a_0 + h_s(t,\tau). \tag{2.32}$$

The channel envelope $|h_{PL}(t,\tau)|$ follows a Rician distribution [20],

$$f_{|h_{PL}(t,\tau)|}(x) = \frac{x}{\sigma_h^2} \exp\left(-\frac{x^2}{2\sigma_h^2} - K_R\right) \mathrm{I}_0\left(\frac{x\sqrt{2K_R}}{\sigma_h}\right) \tag{2.33}$$

where σ_h^2 is the variance of the underlying Gaussian random variables, $\mathrm{I}_0(\cdot)$ is the zeroth order modified Bessel function of the first kind [21] and K_R is the *Rice factor*, defined as

$$K_R = \frac{a_0^2}{2\sigma_h^2}. \tag{2.34}$$

The Rice factor is the ratio of the received power in the LoS component to the received power in the scattering component. The channel gain $|h_{PL}(t,\tau)|^2$ follows a non-central chi squared distribution, with PDF [19]

$$f_{|h_{PL}(t,\tau)|^2}(y) = \frac{1}{2\sigma_h^2} \exp\left(-\frac{y + a_0^2}{2\sigma_h^2}\right) \mathrm{I}_0\left(\sqrt{\frac{a_0^2 y}{\sigma_h^4}}\right). \tag{2.35}$$

We thus refer to this model as a *Rician fading channel*. Note that the Rayleigh fading channel is a special case of the Rician channel, with $K_R = a_0 = 0$.

Channel parameters vary significantly depending on the environment [22], so we give some examples of the typical magnitude of some channel parameters. For tropospheric

super high frequency (SHF) scattering channels the delay spread usually ranges from 0.1μs to 0.2μs [23] with Doppler spread from 0.1Hz to 10Hz. However for ionospheric high frequency (HF) channels the delay spread ranges from 100μs to 5ms with Doppler spread usually 0.01Hz to 2Hz. For terrestrial multipath channels operating at about $f_c = 900$MHz the delay spread can be up to 20μs in an open rural environment, and in the order of 100ns to 10μs in a dense urban environment, with maximum Doppler spread approximately $f_D = 50$Hz for receiver speed of 60km/h. Surveys of the delay spread and other characteristics of such channels include [24–26], [27, pp. 55–66] and [28, Chp. 7].

Jakes' Model

The channel model we most often use is the ubiquitous Jakes' model [11] (actually first proposed by Clarke[1] [29]), which specifies a non-LoS, narrowband Rayleigh fading channel. Furthermore, this model describes the correlation between the channel response of two narrowband fading channels occupying different frequencies, which we will later use to model the correlation between OFDM subchannels. Isotropic scattering is assumed and the channel autocorrelation function is found to be

$$R_h(\Delta t, \tau) = \sigma_h^2(\tau) \mathrm{J}_0\left(2\pi f_d |\Delta t|\right) \tag{2.36}$$

where $\mathrm{J}_0(\cdot)$ is the zeroth order Bessel function of the first kind [21]. The Jakes' model normalised exponential power delay profile is

$$\sigma_h^2(\tau) = \frac{1}{\tau_{rms}} \exp\left(-\frac{\tau}{\tau_{rms}}\right) \tag{2.37}$$

with arbitrary rms delay τ_{rms}. Taking the Fourier transform of (2.36), the normalised Doppler spectrum is then

$$S_H(v) = \begin{cases} \frac{1}{\pi\sqrt{f_d^2 - v^2}} & \text{for } |v| \leq f_d \\ 0 & \text{for } |v| > f_d \end{cases} \tag{2.38}$$

which yields the well-known 'U'-shape shown in Figure 2.4. (Here we have arbitrarily chosen f_c and v so that the maximum Doppler shift is 50Hz.)

The channel gains $H(t_1, f_1)$ and $H(t_2, f_2)$, at times t_1 and t_2 and frequencies f_1 and f_2 respectively, can be written as samples of the complex Gaussian process $H(t, f)$,

$$\begin{aligned} H(t_1, f_1) &= X_1 + jY_1 \,, \\ H(t_2, f_2) &= X_2 + jY_2 \,, \end{aligned} \tag{2.39}$$

[1] In keeping with popular terminology we refer to the model as the Jakes' model. It is unclear why this model is oft credited to Jakes, it may perhaps be due to greater availability of [11] over [29]

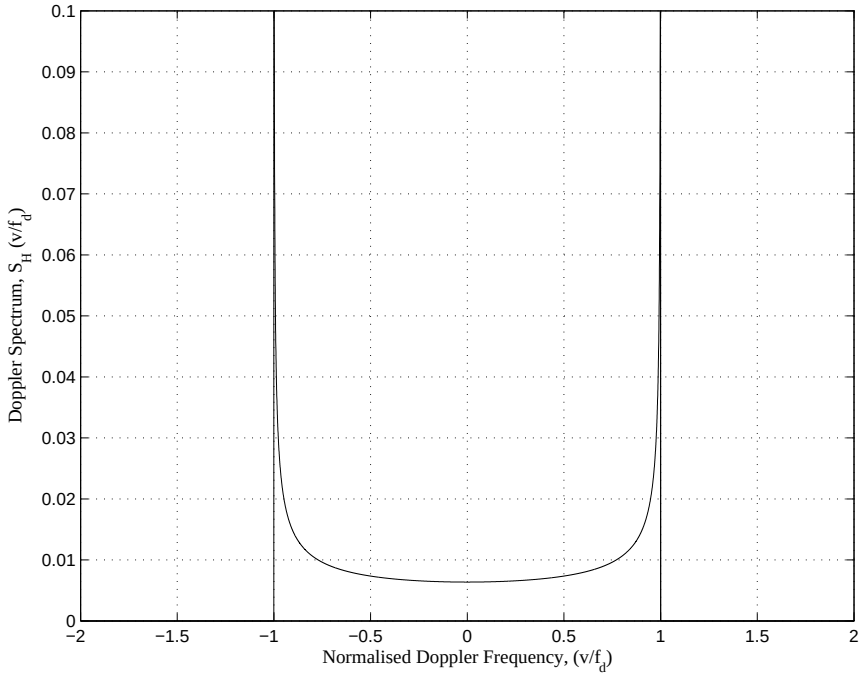

Figure 2.4 Jakes' model Doppler spectrum for a channel with $f_d = 50\text{Hz}$.

where X_1, Y_1, X_2 and Y_2 are identically distributed Gaussian random variables. With no LoS path $\mathbb{E}[X_1] = \mathbb{E}[X_2] = \mathbb{E}[Y_1] = \mathbb{E}[Y_2] = 0$, and without loss of generality we may set $\mathbb{E}\left[X_1^2\right] = \mathbb{E}\left[X_2^2\right] = \mathbb{E}\left[Y_1^2\right] = \mathbb{E}\left[Y_2^2\right] = \frac{1}{2}$. The following correlation properties are then readily shown [11]:

$$\begin{aligned}
\mathbb{E}[X_1 Y_1] &= \mathbb{E}[X_2 Y_2] = 0 \\
\mathbb{E}[X_1 X_2] &= \mathbb{E}[Y_1 Y_2] = \frac{1}{2} \cdot \frac{\mathrm{J}_0(2\pi f_d \Delta t)}{1 + (2\pi \Delta f \tau_{rms})^2} \\
\mathbb{E}[X_1 Y_2] &= -\mathbb{E}[X_2 Y_1] = -\frac{1}{2} \cdot \frac{(2\pi \Delta f \tau_{rms})\,\mathrm{J}_0(2\pi f_d \Delta t)}{1 + (2\pi \Delta f \tau_{rms})^2} \,.
\end{aligned} \tag{2.40}$$

It may be seen that $\{X_1, Y_1\}$ and $\{X_2, Y_2\}$ form a *circular pair* [30] and the channel envelopes $|H(t_1, f_1)|$ and $|H(t_2, f_2)|$ are marginally Rayleigh distributed, with

$$\mathbb{E}[|H(t,f)|] = \frac{1}{\sqrt{2}} \quad \mathbb{E}\left[|H(t,f)|^2\right] = 1, \text{ for all } t, f \tag{2.41}$$

and correlation coefficient

$$\rho = \frac{\mathrm{J}_0^2(2\pi f_d \Delta t)}{1 + (2\pi \tau_{rms} \Delta f)^2} \,. \tag{2.42}$$

The joint distribution of the channel envelope at time $t_1 = t_2$ and frequencies f_1 and f_2 is

then [30]

$$f_{|H_1||H_2|}(x,y) = \frac{xy}{\sigma^4\,(1-\varrho)} \exp\left(-\frac{x^2+y^2}{2\sigma^2[1-\varrho]}\right) \mathrm{I}_0\left(\frac{\sqrt{\varrho}xy}{\sigma^2[1-\varrho]}\right) \tag{2.43}$$

where $\sigma^2 = \frac{1}{2}$ and $\varrho = \frac{1}{1+(2\pi\tau_{rms}\Delta f)^2}$. The channel gains $|H(t_1,f_1)|^2$ and $|H(t_2,f_2)|^2$ have a marginal exponential distribution, with

$$\mathbb{E}\left[|H(t,f)|^2\right] = 1 \quad \mathrm{var}\left[|H(t,f)|^2\right] = 1, \text{for all } t,f \tag{2.44}$$

and the same correlation coefficient

$$\rho = \frac{\mathrm{J}_0^2(2\pi f_d \Delta t)}{1+(2\pi\tau_{rms}\Delta f)^2}. \tag{2.45}$$

The bivariate exponential distribution is then [30]

$$f_{|H_1|^2|H_2|^2}(x,y) = \frac{1}{\sigma^4\,(1-\rho^2)} \exp\left(-\frac{x+y}{2\sigma^2[1-\rho^2]}\right) \mathrm{I}_0\left(\frac{\rho.\sqrt{xy}}{\sigma^2[1-\rho^2]}\right). \tag{2.46}$$

In Figure 2.5 we display the time varying frequency response $H(t,f)$ of a wideband, Rayleigh fading channel defined by the Jakes' model. The transmitted signal has carrier frequency $f_c = 5.1\mathrm{GHz}$ and bandwidth $B = 20\mathrm{MHz}$. We assume rms delay spread of $50\mathrm{ns}$ and a receiver velocity of $100\mathrm{km/h}$.

Other Channel Models

Several other statistical descriptions of the channel model exist. In particular the Nakagami-m [31] and Weibull [32] distributions have been proposed to represent the amplitude of the narrowband fading channel. There is no underlying physical justification for applying these distributions, although empirical data supports their use [33]. Note that the Rayleigh PDF is a special case of both distributions. Furthermore, [34] models the envelope with a generalised gamma distribution. Despite these other models, we persist with the more widely accepted Rayleigh and Rician models.

2.2.3 Simulating the Wireless Channel

Throughout this thesis we verify analytical results with simulated results. A simulation model of the wireless channel is thus essential. Our method of simulating the wireless channel follows that outlined by [23] and [35]. From (2.13) we observe that the channel behaves like a linear time variant filter, so we may simulate the channel using a tapped delay line (TDL) filter [23]. Since the channel maximum delay spread τ_{max} represents the range over which the channel response is essentially non-zero, we may model the channel as a finite impulse response (FIR) filter with maximum delay τ_{max}.

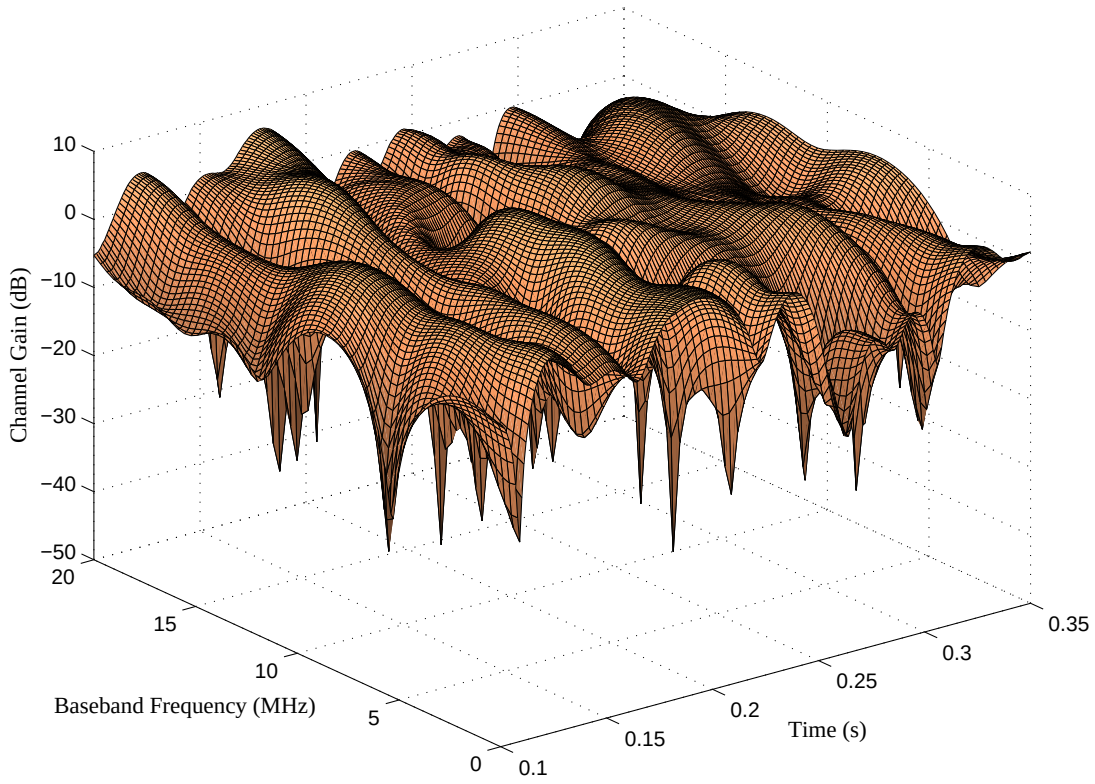

Figure 2.5 Baseband channel gain $20\log_{10}(|H(t,f)|)$ for a Jakes' model, wideband Rayleigh fading channel, with exponential power delay profile and parameters $f_c = 5.1\text{GHz}$, $B = 20\text{MHz}$, $\tau_{rms} = 50\text{ns}$ and $v = 100\text{km/h}$.

The transmitted signal and channel fading processes are generally bandlimited, so we may sample the received signal at rate T_s, with no loss of information provided the Nyquist criterion is satisfied, that is at time intervals $T_s \geq \frac{2}{B_r}$, where B_r is the bandwidth of the received signal. We may write the transmitted symbol as [23]

$$s(t) = \sum_{\ell=-\infty}^{+\infty} s_\ell \,\text{sinc}\left(\frac{t - \ell T_s}{T_s}\right) \tag{2.47}$$

where $s_\ell = s(\ell T_s)$ is the ℓ^{th} sample of $s(t)$. We may also sample the channel response at time intervals T_s, to obtain the ℓ^{th} sample at delay mT_s as

$$c_{\ell,m} = \int_{-\infty}^{+\infty} h(\ell T_s, \tau)\,\text{sinc}\left(\frac{mT_s - \tau}{T_s}\right) d\tau. \tag{2.48}$$

Then following (2.13) we may write the ℓ^{th} sample of the received signal as

$$\begin{aligned} r_\ell &= \int_{-\infty}^{+\infty} h(\ell T_s, \tau) s(\ell T_s - \tau) d\tau \\ &= \sum_{m=-\infty}^{+\infty} s_{\ell-m} \int_{-\infty}^{+\infty} h(\ell T_s, \tau) \operatorname{sinc}\left(\frac{m T_s - \tau}{T_s}\right) d\tau \\ &= \sum_{m=-\infty}^{+\infty} h_{\ell,m} s_{\ell-m}. \end{aligned} \tag{2.49}$$

Since the channel response is negligible for delays greater than $\tau_{\max}$, we can approximate (2.49) as

$$r_\ell \approx \sum_{m=0}^{M} h_{\ell,m} s_{\ell-m} \tag{2.50}$$

where $M = \lceil \frac{\tau_{\max}}{T_s} \rceil$. Thus, for the ℓ^{th} time sample, the channel response may be approximated as a FIR tapped delay line filter, with uncorrelated tap weights $h_{\ell,m}$. The tap gains $h_{\ell,m}$ are samples of a stationary random process with Gaussian probability density functions and power spectral density functions equal to the channel Doppler power spectral density [23]. The mean squared gain of a filter tap at delay ℓT_s is the channel power delay profile at ℓT_s. The simplest method of generating each tap gain is by filtering a white Gaussian noise process, with some FIR filter with transfer function so that the desired Doppler power spectral density is obtained. For example, to obtain the required Jakes' model Doppler power spectral density (2.38) we require a filter with normalised frequency response [23, 36]

$$H_d(f) = \begin{cases} \frac{1}{\sqrt[4]{1-\left(\frac{f}{f_d}\right)^2}} & \text{for } |f| < f_d \\ 0 & \text{otherwise,} \end{cases} \tag{2.51}$$

and corresponding impulse response

$$h_d(t) = \begin{cases} \sqrt[4]{\pi f_d} \,/\, \Gamma\left(\frac{5}{4}\right) & \text{for } t = 0 \\ t^{-\frac{1}{4}} \, \mathrm{J}_{\frac{1}{4}}(2\pi f_d t) & \text{otherwise,} \end{cases} \tag{2.52}$$

where $\Gamma(\cdot)$ is the gamma function and $\mathrm{J}_{\frac{1}{4}}(\cdot)$ is the one-fourth order Bessel function of the first kind [36, 37].

2.3 Summary

We have presented a brief overview of the physical layer of a wireless communications system, with discussion of the concepts of digital modulation and wireless radio channels. Key assumptions have been established, such as the use of QAM or BPSK and a coherent

receiver. A detailed outline of the multipath fading mechanism is provided, as well as statistical descriptions of multipath fading channels. The difficulties of accurately demodulating signals transmitted through multipath channels motivate the discussion of OFDM in Chapter 4.

Chapter 3

Error Control Coding

This chapter introduces error control coding. We limit our discussion to block codes and their derivatives. A general overview of block coding is first given, followed by a discussion of hard and soft decision decoding. We then review signal space codes and lattices, which naturally leads to a discussion of trellis coding. References [5, 38, 39] provide a further introduction to error control coding.

3.1 Introduction

The goal of error control coding is to minimise the number of bit errors in the received data. At the transmitter the channel encoder adds redundant data according to some rule, and the channel decoder exploits this redundancy to decide whether any bits are in error. The addition of redundancy implies either reduced data throughput, or increased system bandwidth, as well as additional system complexity. These constraints are design trade-offs in the choice of error control coding scheme to achieve some acceptable error performance.

Error correcting codes are traditionally separated into *block* codes and *convolutional* codes. Convolutional encoders accept some arbitrary length stream of data symbols, and output a stream of encoded symbols at a higher rate. Block encoders accept a fixed length vector of k data symbols, and a longer length vector of n encoded symbols is output. Many deployed OFDM systems employ convolutional encoders [6, 40, 41]. However, we consider block codes only, since they form the basis for *lattice coding*.

We later introduce lattices, a necessary preliminary to coset coding and lattice coding. Lattice coding is a technique that combines modulation and coding, and allows powerful error correction. Recent results [42–44] have shown that lattice coding techniques may be applied to approach the AWGN channel capacity. Furthermore, lattice coding for fading

channels has also been shown to achieve high coding gains [45].

3.2 Binary Linear Block Codes

An (n, k, d) binary linear block encoder [38] accepts information in k-bit message *blocks*, denoted $\mathbf{m} = \{m_0, m_1, \ldots, m_i, \ldots, m_{k-1}\}$ where $m_i \in \{0, 1\}$. The encoder adds $n - k$ redundant bits to each block, and outputs an encoded block of n bits. We refer to the output block as a *codeword*, denoted $\mathbf{c} = \{c_0, c_1, \ldots, c_i, \ldots, c_{n-1}\}$, where $c_i \in \{0, 1\}$. Each sequence of input bits produces a distinct codeword. The ratio $r = \frac{k}{n}$ is called the *code rate*, which gives a measure of the redundancy added. The set of all distinct codewords is referred to as the *code*, and denoted $\mathcal{C}$. It is readily shown that $|\mathcal{C}| = 2^k$. A code is *linear* if the modulo-two sum of any two codewords $\mathbf{c}_a, \mathbf{c}_b \in \mathcal{C}$, produces another codeword. That is, $\mathbf{c}_a + \mathbf{c}_b \in \mathcal{C}$.

Any binary linear block code may be defined by a generator matrix $\mathbf{G}$, a $k \times n$ binary matrix, which may be used to produce codewords by left multiplication,

$$\mathbf{c} = \mathbf{mG}. \tag{3.1}$$

A generator matrix of a code is necessarily a binary matrix with full row rank. When a binary linear block code is employed, the channel encoder multiplies each block of k message bits by the generator matrix, as in (3.1). A *parity check matrix* $\mathbf{H}$ of a code is defined as the $(n - k) \times n$ matrix such that

$$\mathbf{HG}^T = \mathbf{0}_{(n-k),k} \tag{3.2}$$

where $\mathbf{0}_{(n-k),k}$ is the $(n - k) \times k$ all zero matrix.

The *Hamming distance* $\mathrm{d_H}(\mathbf{c}_a, \mathbf{c}_b)$ between two codewords $\mathbf{c}_a$ and $\mathbf{c}_b$ is defined as the number of elements in which $\mathbf{c}_a$ and $\mathbf{c}_b$ differ. We define the *minimum code distance* $d_{\mathcal{C}}$ of a code $\mathcal{C}$ as the minimum Hamming distance between any two codewords, that is

$$d_{\mathcal{C}} \triangleq \min\left\{\mathrm{d_H}(\mathbf{c}_a, \mathbf{c}_b) : \mathbf{c}_a, \mathbf{c}_b \in \mathcal{C}, \mathbf{c}_a \neq \mathbf{c}_b\right\}. \tag{3.3}$$

We may generally describe a block code as an (n, k, d) code, with length n, k input bits and Hamming distance d.

Generally, linear codes accept k q-ary symbols as input, and output n q-ary, such that the symbols are elements of the order q Galois field [38, 46] $\mathbf{F}_q$, and each codeword is then an element of the Cartesian product $\mathbf{F}_q^n$. Linear codes are thus linear subspaces of $\mathbf{F}_q^n$, and form commutative groups [46]. Linear codes are thus often referred to as *group codes*.

Note that binary codes may be described in this fashion, since $\mathbf{F}_2 = 0, 1$. The code rate is $r = \frac{1}{n} \log_2 q$ bits/symbol. The code distance d is again the minimum Hamming distance between any two codewords, and generally the larger the Hamming distance, the more errors a code can correct.

The *error correcting code problem* is: given n and d, find the (n, k, d) group code with the maximal number of codewords q^k. This will then maximise the rate of a code with length n and fixed error correcting capability d. In general, this problem this problem is unsolved, however a large number of good constructions have been found, and many bounds are known [38]. There are many families of known good binary, and non-binary, linear block codes, each with different error correcting properties, including Hamming codes [47], Reed-Solomon codes [48], Bose-Chaudhuri-Hocquenghem (BCH) [49–51] and Reed-Muller (RM) [52, 53] codes.

Broadly speaking, the attractiveness of block codes is the ability to construct codes with large distance d that can correct many errors, and which have decoding complexity of polynomial order in d. As such, block codes have been, and continue to be, used in many wireless applications.

3.3 Hard and Soft Decision Decoding

Assuming an M-ary transmission scheme with signal constellation $\mathcal{M}$, each signal point represents $\log_2 M$ binary bits. To transmit a length n binary codeword the transmitter then selects a sequence of $\lceil \frac{n}{\log_2 M} \rceil$ waveforms of period T to represent each set of n bits. The receiver obtains $\lceil \frac{n}{\log_2 M} \rceil$ signal points which represent the noise corrupted transmitted points. The demodulator then produces an output corresponding to the received signals. Depending on the demodulator design, the output, for each of the n waveforms, may be a real number or a discrete value. In the case of *hard decision decoding* the demodulator directly estimates the transmitted bit sequence then outputs n binary bits. These bits are then passed to an algebraic decoder whose output is an estimate of the k transmitted information bits. In the case of *soft decision decoding* the demodulator outputs real numbers, or binary words of length greater than n, which are then passed to some decoder to estimate the k information bits. The additional demodulator output information during soft decision decoding typically provides a measure of the reliability of the demodulator estimates, and affords improved decoder performance. We now outline decoding procedures for hard and soft decision decoding.

As an example, consider a BPSK constellation ($M = 2$), where S_0 is equivalent to bit 0, and S_1 is equivalent to bit 1. We may receive point y, as shown in Figure 3.1. A maximum a posteriori (MAP) [8] demodulator hard decision would be to output bit 1, since the received

point is closest to the constellation point S_1.

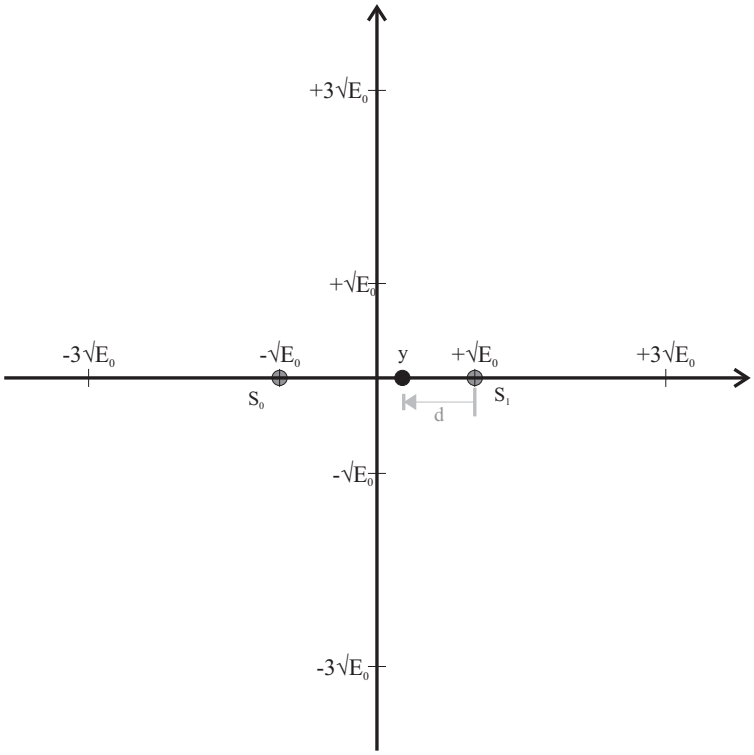

Figure 3.1 Transmitted BPSK constellation and received point $\mathbf{y}$

If we transmit all n bits of a codeword, a hard decision demodulator outputs a length n binary codeword estimate $\mathbf{r} = \{r_0, r_1, \ldots, r_{n-1}\}$. Since $\mathbf{r}$ is possibly error corrupted, we may write

$$\mathbf{r} = \mathbf{c} + \mathbf{e}, \tag{3.4}$$

where $\mathbf{e}$ is a length n binary vector, known as the *error vector*: if $e_i = 1$, then the i^{th} element of r is in error, and conversely if $e_i = 0$ then the i^{th} element of r is correct. The *syndrome* of $\mathbf{r}$ is a vector identifying each correctable error pattern, and is calculated as

$$\mathbf{s} = \mathbf{r}\mathbf{H}^T = (\mathbf{e} + \mathbf{c})\mathbf{H}^T = \mathbf{e}\mathbf{H}^T + \mathbf{c}\mathbf{H}^T = \mathbf{e}\mathbf{H}^T\,, \tag{3.5}$$

since $\mathbf{c}\mathbf{H}^T = \mathbf{0}$ for all codewords. Therefore $\mathbf{r}$ is a codeword if and only if $\mathbf{s} = \mathbf{0}$. We may identify the errors, $\mathbf{e}$ from $\mathbf{s}$. However, it is possible that $\mathbf{r}$ contains errors and $\mathbf{s} = \mathbf{0}$, since, if $\mathbf{e}$ is equal to some nonzero codeword, so that $\mathbf{c} + \mathbf{e} \in \mathcal{C}$, then

$$\mathbf{s} = (\mathbf{c} + \mathbf{e})\mathbf{H}^T = \mathbf{c}\mathbf{H}^T + \mathbf{c}_e\mathbf{H}^T = \mathbf{0}. \tag{3.6}$$

This decoding method is called *syndrome decoding*. We note that many other hard decision

decoding methods exist. For example, the Reed-Muller codes are best decoded using majority logic decoding [38]. It may be shown [39] that hard decision decoding is guaranteed to correct t errors in $\mathbf{r}$, up to half the minimum Hamming distance of the code, that is, provided $2t < d_{\mathcal{C}}$, or equivalently $t \leq \frac{d_{\mathcal{C}}-1}{2}$.

Soft decision decoding offers significant benefits over hard decision decoding. Intuitively, information is discarded by the demodulator when hard decisions are made, while soft decision decoding retains and exploits some or all of this information. The simplest type of soft decision decoder uses *erasures* to indicate certain bits in a codeword which may contain errors. For example, for a system receiving BPSK signal points, as in Figure 3.1, we may decide received points close to S_0 or S_1 are output as 0 or 1 respectively, and received points near the decision boundary are unreliable and thus labelled as erasures. For example, received points where $d > 0.8\sqrt{E_0}$ could be labelled erasures. Given a binary demodulator output $\mathbf{r}$ where t bits are in error and s bits are erased, we may correctly decode $\mathbf{r}$ provided $2t + s < d_{\mathcal{C}}$ [38]. We now outline a simple binary erasure decoding algorithm.

Given a received word $\mathbf{r}$, we place zeros in all the erased positions, and decode normally, labelling the resulting codeword $\mathbf{c}_0$. We then place ones in all erased positions of $\mathbf{r}$, and decode normally, labelling the resulting codeword $\mathbf{c}_1$. The decoder output is then $\mathbf{c}_i$, $i \in \{0, 1\}$, such that $\mathrm{d_H}(\mathbf{c}_i, \mathbf{r})$ is minimised. Analysis of this algorithm is straightforward [38]. Note that this decoding algorithm requires twice the complexity of simple hard decision decoding, as we perform two hard decision decoding operations. The coding gain of this approach is dependent on the choice of erasures. However, soft decision decoding algorithms can generally achieve about 3dB of coding gain over hard decision decoding algorithms, with appropriate demodulator and decoder design [39].

Non-binary erasure decoding algorithms also exist, such as the Berlekamp-Massey [54, 55] algorithm. In particular Bose-Chaudhuri-Hocquenghem and Reed-Solomon codes permit very efficient erasure decoding.

3.3.1 Generalised Minimum Distance Decoding

Generalised minimum distance decoding (GMD) is a soft decision decoding algorithm first introduced in [56]. We transmit codewords from an (n, k, d) linear block code $\mathcal{C}$ by mapping the codeword to a sequence $m(\mathbf{u})$ of signal points in Euclidean space. The demodulator outputs a hard decision word $\mathbf{u} = \{u_1, u_2, \ldots, u_i, \ldots, u_n\}$ and a vector of corresponding reliability values $\boldsymbol{\alpha} = \{\alpha_1, \alpha_2, \ldots, \alpha_i, \ldots, \alpha_n\}$, where $0 \leq \alpha_i \leq 1$ and $\alpha_i \in \mathbb{R}$. Here $\alpha_i = 0$ indicates the hard decision u_i is unreliable while $\alpha_i = 1$ indicates high reliability.

We define the *trial enumerator set* $\mathcal{K}$ as $\mathcal{K} = \{0, 2, \ldots, d-3, d-2\}$ if d is odd, or $\mathcal{K} =$

$\{1, 3, \ldots, d-3, d-1\}$ if d is even. Thus $|\mathcal{K}| = \lfloor \frac{d+1}{2} \rfloor$. The GMD decoder then performs $|\mathcal{K}|$ erasure decoding trials, for all $s \in \mathcal{K}$, where in each trial the s least reliable positions in $\mathbf{u}$ are erased. The trial with s erasures will then produce a candidate codeword, labelled $\hat{\mathbf{c}}_s$, if and only if the number of errors $t = \mathrm{d_H}(\mathbf{u}, \hat{\mathbf{c}}_s)$ satisfies $2t + s < d$. Otherwise, a decoding failure is declared and no candidate codeword is produced. A set of candidate codewords $\mathcal{L}(\mathbf{r}) = \{\hat{\mathbf{c}}_s : s \in \mathcal{K}\}$ is thus obtained, such that $|\mathcal{L}(\mathbf{r})| \leq |\mathcal{K}|$. We refer to this stage as the *algebraic decoding phase*.

Following the algebraic decoding phase, the decoder selects the codeword with the smallest *generalised distance* $\delta(\mathbf{c}, \mathbf{u})$ from $\mathbf{u}$. The generalised distance is defined [56] by

$$\delta^2(\mathbf{c}, \mathbf{u}) = \delta^2(c_1, u_1) + \delta^2(c_2, u_2) + \cdots + \delta^2(c_n, u_n) \tag{3.7}$$

where

$$\delta(c_i, u_i) = \begin{cases} 1 - \alpha_i & \text{for } c_i = u_i \\ 1 + \alpha_i & \text{for } c_i \neq u_i. \end{cases} \tag{3.8}$$

The candidate codeword closest, in generalised minimum distance, to $\mathbf{u}$ is then selected as the decoder output. It is shown in [56] that GMD decoding will decode to the codeword $\mathbf{c} \in \mathcal{C}$, when $\delta(\mathbf{c}, \mathbf{u}) < d$.

We now outline the calculation of a reliability metric α_i, $i = 0, 1, \ldots, N-1$, for Gaussian channels, from [57]. Given a received signal space point r_i the demodulator finds the closest and second closest constellation points labelled s_i and s_i' respectively. The hard decision boundary between s_i and s_i' is their perpendicular bisector. The projection of $r_i - s_i$ in the direction of $s_i' - s_i$ is denoted d_i, and the reliability is the scaled distance of r_i from the decision boundary. Thus,

$$\alpha_i \triangleq \begin{cases} 0 & \text{for } d_i > 1 \\ 1 - d_i & \text{for } 0 \leq d_i \leq 1 \\ 1 & \text{for } d_i < 0 \end{cases} \quad \text{and} \quad d_i \triangleq \frac{\langle r_i - s_i, s_i' - s_i \rangle}{\|s_i' - s_i\|} \tag{3.9}$$

where $\langle \quad , \quad \rangle$ is the standard inner product [1]. Figure 3.2 shows the geometry of α_i, d_i, r_i, s_i and s_i'. The hard decision codeword is the inverse mapping $\mathbf{u} = m^{-1}(\mathbf{s})$ of the vector of closest points $\mathbf{s} = \{s_1, s_2, \ldots, s_n\}$. A received point r_i therefore has unity reliability if it is equal to a signal constellation point s_i. Conversely, r_i is assigned zero reliability if it lies on the decision boundary between two signal constellation points.

It is shown in [57] that GMD decoding using this metric achieves bounded distance decoding. Specifically, if the received point $\mathbf{r}$ produces some hard decision point $\mathbf{s}$ equivalent to

[1] Note that [57, p. 1998] labels this quantity d_j, and there is a typographical error in the definition.

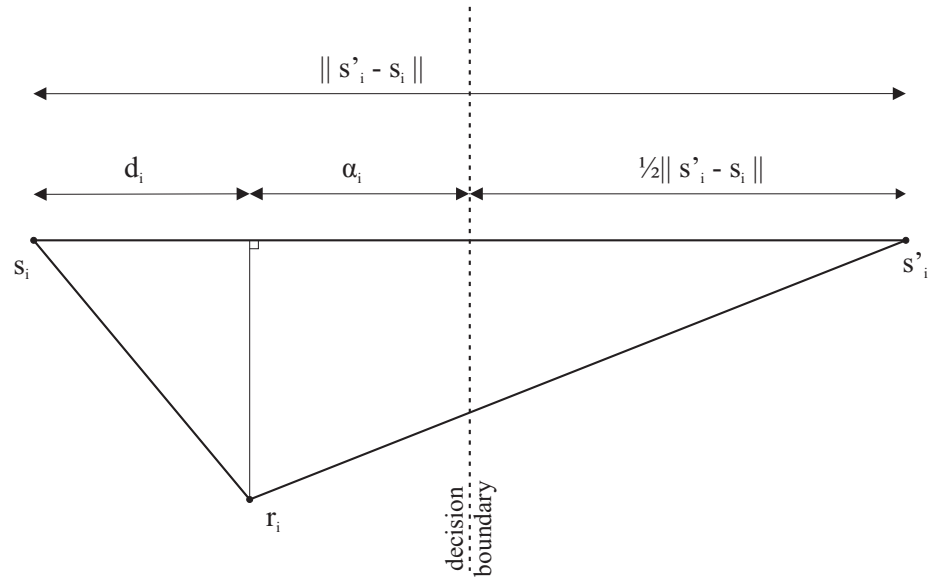

Figure 3.2 GMD AWGN channel reliability calculation

$\mathbf{u}$, then GMD decoding is guaranteed to produce $\mathbf{c}$, provided $\mathbf{z} = m(\mathbf{c})$ satisfies $\|\mathbf{r}-\mathbf{z}\| < d$. Therefore, GMD decoding has performance close to that of maximum likelihood decoding at moderate to high signal to noise ratio.

3.4 Lattices

We now summarise the basic theory of lattices, necessary for later discussion of *lattice codes*. Lattices have been studied by mathematicians for many decades, particularly the *densest sphere packing problem*: 'what is the densest way of packing equal radius N dimensional spheres together? [7]' Reference [7] provides a thorough introduction to lattices and sphere packings, and describes the state of the art.

Informally, a lattice is a regular array of points in Euclidean N-space. More formally, an N dimensional lattice Λ is defined as

$$\Lambda \triangleq \{\mathbf{x} : \mathbf{x} = i_1\mathbf{b}_1 + i_2\mathbf{b}_2 + \cdots + i_N\mathbf{b}_N\} \tag{3.10}$$

where $\mathbf{b_1}, \ldots, \mathbf{b_N}$ are N linearly independent vectors in $\mathbb{R}^N$ and $i_1, \ldots, i_N$ are integers. A lattice may then be thought of as a vector space[2], where the coefficients $\{i_k\}$ must be integers. From (3.10) we observe that a lattice forms a discrete additive subgroup of $\mathbb{R}^N$. A simple example is the two dimensional *integer lattice* $\mathbb{Z}^2$ with basis vectors $\mathbf{b}_1 = \{0, 1\}$ and

[2]Strictly speaking a $\mathbb{Z}$-free module [46]

$\mathbf{b}_2 = \{1, 0\}$. Another simple example is the two dimensional *diagonal lattice* $\mathcal{D}_2$ with basis vectors $\mathbf{b}_1 = \{1, 0\}$ and $\mathbf{b}_2 = \{\frac{1}{2}, \frac{1}{2}\sqrt{3}\}$. These examples are illustrated in Figure 3.3.

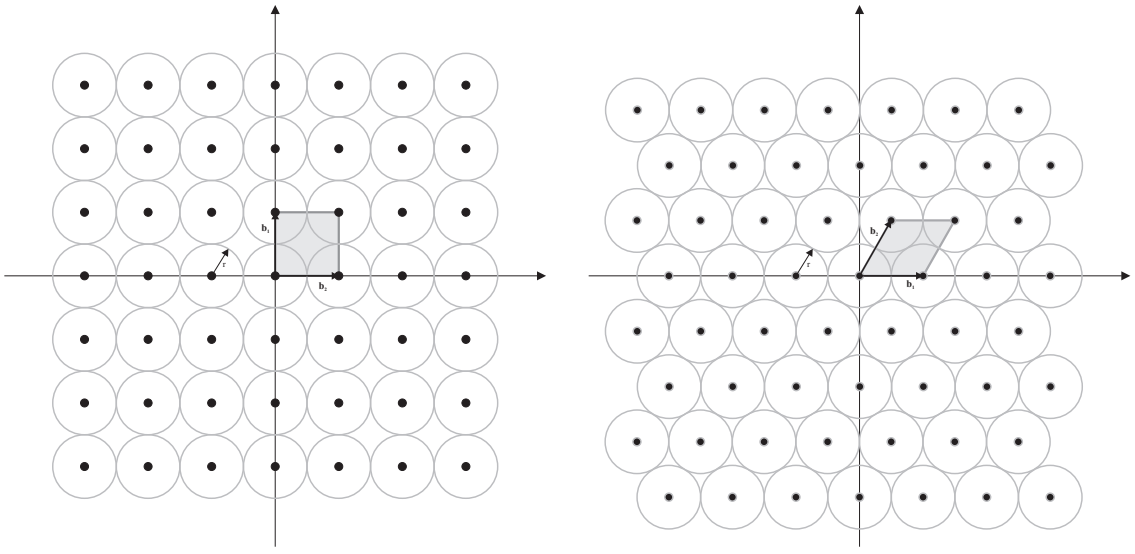

(a) Integer lattice, $\mathbb{Z}^2$. (b) Diagonal lattice, $\mathcal{D}_2$.

Figure 3.3 Two dimensional lattices $\mathbb{Z}^2$ and $\mathcal{D}_2$: illustration of sphere packings, basis vectors $\mathbf{b}_1$,$\mathbf{b}_2$ and fundamental parallelotopes (shaded).

Each lattice point $\mathbf{x}$ may be considered the centre of an N dimensional sphere with radius r as large as possible such that the spheres are non-overlapping. This is illustrated for the lattices $\mathcal{D}_2$ and $\mathbb{Z}^2$ in Figure 3.3. An N dimensional *sphere packing* [7] is then described by the centres of all non-overlapping N-spheres of radius r. While a lattice defines a sphere-packing, the converse is not necessarily true, since a sphere packing need not contain the origin $\mathbf{x} = \mathbf{0}$, and thus may not be a subgroup of $\mathbb{R}^N$.

From (3.10) the vectors $\mathbf{b_1}, \ldots, \mathbf{b_N}$ are called a *basis* for the lattice. The region defined by

$$\{r_1\mathbf{b_1} + r_2\mathbf{b_2} + \cdots + r_N\mathbf{b_N} : 0 \leq r_1, r_2, \ldots, r_N < 1\} \ , \tag{3.11}$$

is the lattice *fundamental region* or *fundamental parallelotope*. Figure 3.3 shows the fundamental region for $\mathbb{Z}^2$ and $\mathcal{D}_2$. A lattice *generator matrix* $\mathbf{G}_\Lambda$ is a matrix whose rows form a set of basis vectors. For example, $\mathbf{G}_\Lambda = \left[\mathbf{b}_1^T, \mathbf{b}_2^T \ldots \mathbf{b}_N^T\right]^T$. The lattice can then be defined as

$$\Lambda = \{\mathbf{x} : \mathbf{x} = [i_1, i_2, \ldots, i_N]\mathbf{G}_\Lambda \, ; \, i_1, \ldots, i_N \in \mathbb{Z}\}. \tag{3.12}$$

It follows that the volume $V(\Lambda)$ of the fundamental region of a lattice is

$$V(\Lambda) = \sqrt{\det\left[\mathbf{G}_\Lambda \mathbf{G}_\Lambda^T\right]} \tag{3.13}$$

which is independent of the choice of generator matrix. The density $\Delta(\Lambda)$ of a lattice is the proportion of space occupied by the spheres, or equivalently the ratio of the volume of one sphere to the volume of the fundamental region, where the volume of an N dimensional sphere of radius r is [7]

$$V_n(r) = \frac{2^N \pi^{\frac{N-1}{2}} \left(\frac{N-1}{2}\right)!}{N!} r^N. \tag{3.14}$$

The aforementioned examples have densities $\Delta\left(\mathbb{Z}^2\right) = \frac{\pi}{4} \approx 0.7854$ and $\Delta\left(\mathcal{D}_2\right) = \frac{\pi}{\sqrt{12}} \approx 0.9069$: in Figure 3.3 observe that the spheres in $\mathcal{D}_2$ appear more closely packed than in $\mathbb{Z}^2$. The lattice *centre density* $\delta(\Lambda)$ is the density normalised by the unit N-sphere volume, namely $\delta(\Lambda) = \frac{\Delta(\Lambda)}{V_n(1)}$.

The *minimum distance* of a lattice (or sphere packing) $d_{\min}(\Lambda)$ is the smallest distance between two lattice points (or sphere centres), and is equal to twice the sphere packing radius $2r$. The *kissing number* $\tau(\Lambda)$ is the number of sphere centres at minimum distance from any other sphere centre. This gives the number of spheres that 'touch' or 'kiss' any one sphere. Observe from Figure 3.3, that $\tau(\mathbb{Z}^2) = 4$ and $\tau(\mathcal{D}_2) = 6$. Finally, the *coding gain* $\gamma(\Lambda)$ of an N dimensional lattice is a measure of minimum distance relative to the fundamental volume per two dimensions, and may be written [58] as

$$\gamma(\Lambda) = \frac{d_{\min}(\Lambda)}{V(\Lambda)^{\frac{2}{N}}}. \tag{3.15}$$

Furthermore, it is readily seen [7] that the centre density is related to the coding gain by

$$\gamma(\Lambda) = 4\left[\delta(\Lambda)\right]^{\frac{2}{N}}. \tag{3.16}$$

A key problem in lattice theory is identifying the densest lattice or sphere packing in N dimensions. For $N = 1$, 2 or 3 this is trivial. For $N \geq 4$ this is a nontrivial problem. However, the densest possible lattices are known for dimensions one through eight, although the densest possible sphere packings are known in dimensions one to three only. However, the coding gain of any N dimensional sphere packing is bounded by the Rogers bound [59, 60], expressed in [61] as

$$\log_2(\gamma(\Lambda)) \leq \frac{N}{2}\log_2\left(\frac{N}{4e\pi}\right) + \frac{3}{2}\log_2(N) - \log_2\left(\frac{e}{\pi}\right) + \frac{5.25}{N+2.5} \tag{3.17}$$

with the last term being approximate, although the exact expression is given in [59]. For $N \geq 42$ a stronger bound was found by Kabatiansky and Levenshtein [62], which may be approximated as

$$\frac{1}{N}\log_2(\Delta(\Lambda)) \leq -0.5990. \tag{3.18}$$

While the densest possible lattices are known in dimensions one through eight, Minkowski's

N	Name	Symbol	Centre Density	Bound ((3.17), (3.18))	Ref.
1	Integer	$\mathbb{Z}$	0.5	0.5	[7]
2	Diagonal	$\mathcal{D}_2$	$\frac{1}{2\sqrt{3}} \approx 0.28868$	0.28868	[7]
3	Diagonal	$\mathcal{D}_3$	$\frac{1}{4\sqrt{2}} \approx 0.17678$	0.1847	[7,64]
4	Schläfli	$\mathcal{D}_4$	$\frac{1}{8} = 0.125$	0.13127	[7]
8	Gosset	$\mathcal{E}_8$	$\frac{1}{16} = 0.0625$	0.06326	[65]
12	Coxeter-Todd	$\mathcal{K}_{12}$	$\frac{1}{27} \approx 0.03704$	0.06559	[66]
24	Leech	Λ_{24}	1	1.2741	[61]
32	Quebbemann	$\mathcal{Q}_{32}$	$\frac{3^{15}}{2^{24}} \approx 1.359$	45.886	[67]
32	Barnes-Wall	$\mathcal{BW}_{32}$	1	45.886	[68]
48	Nebe	$\mathcal{P}_{48n}$	$\frac{3^{24}}{2^{24}} \approx 16834.1$	39512	[69]
64	Barnes-Wall	$\mathcal{BW}_{64}$	$2^{16} \approx 6.5536 \times 10^4$	2.3663×10^9	[68]
64	Nebe	$\mathcal{N}e_{64}$	$3^{16} \approx 4.3047 \times 10^7$	2.3663×10^9	[69]
128	Barnes-Wall	$\mathcal{BW}_{128}$	$2^{64} \approx 1.8447 \times 10^{19}$	5.0368×10^{35}	[68]
128	Elkies	$\mathcal{MW}_{128}$	$2^{97.40} \approx 2.0908 \times 10^{29}$	5.0368×10^{35}	[7]

Table 3.1 Densest known and Barnes-Wall lattices in selected dimensions $N \leq 128$, and Minkowski's existence theorem bound [7]

non-constructive proof [63] states that there exist N dimensional lattices such that

$$\Delta(\Lambda) \geq \frac{\zeta(N)}{2^{N-1}} \tag{3.19}$$

where $\zeta(N) = \sum_{k=1}^{\infty} k^{-N}$ is the Riemann zeta-function [37]. For high dimensions, no lattices have been found that satisfy (3.19). Table 3.4 outlines the densest known sphere packings, and the upper bound on the density given by (3.17) and (3.18) for various dimensions.

Any *sublattice* Λ' of a lattice Λ is defined as a subset of the elements of Λ, such that Λ' is a subgroup of Λ and itself a lattice. Then, by elementary group theory [46], Λ' induces a *factor group* or *partition* Λ/Λ' of Λ into equivalence classes, modulo Λ'. The order of the partition is the number $|\Lambda/\Lambda'|$ of such equivalence classes. Each equivalence class is a *coset* of Λ', that is a translate $\Lambda' + \mathbf{t}$ of Λ', for some $\mathbf{t} \in \Lambda$. We refer to $\mathbf{t}$ as the *coset representative* and the set of all coset representatives for the partition is labelled $[\Lambda/\Lambda']$. It follows that $\Lambda = \Lambda' + [\Lambda/\Lambda']$ is called the *coset decomposition* of Λ. For example, we can partition the lattice $\mathbb{Z}^2$ into the sublattice of even integer only coordinates $2\mathbb{Z}^2$ and its cosets. The coset representatives may be defined as $[\mathbb{Z}^2/2\mathbb{Z}^2] = \{(0,0),(0,1),(1,0),(1,1)\}$. This partition is illustrated in Figure 3.4.

A *partition chain* $\Lambda/\Lambda'/\Lambda''/\ldots$ is a sequence of lattices such that each is a sublattice of the former. For example, $\mathbb{Z}^2/2\mathbb{Z}^2/4\mathbb{Z}^2/\ldots$ is an infinite partition chain. A partition chain de-

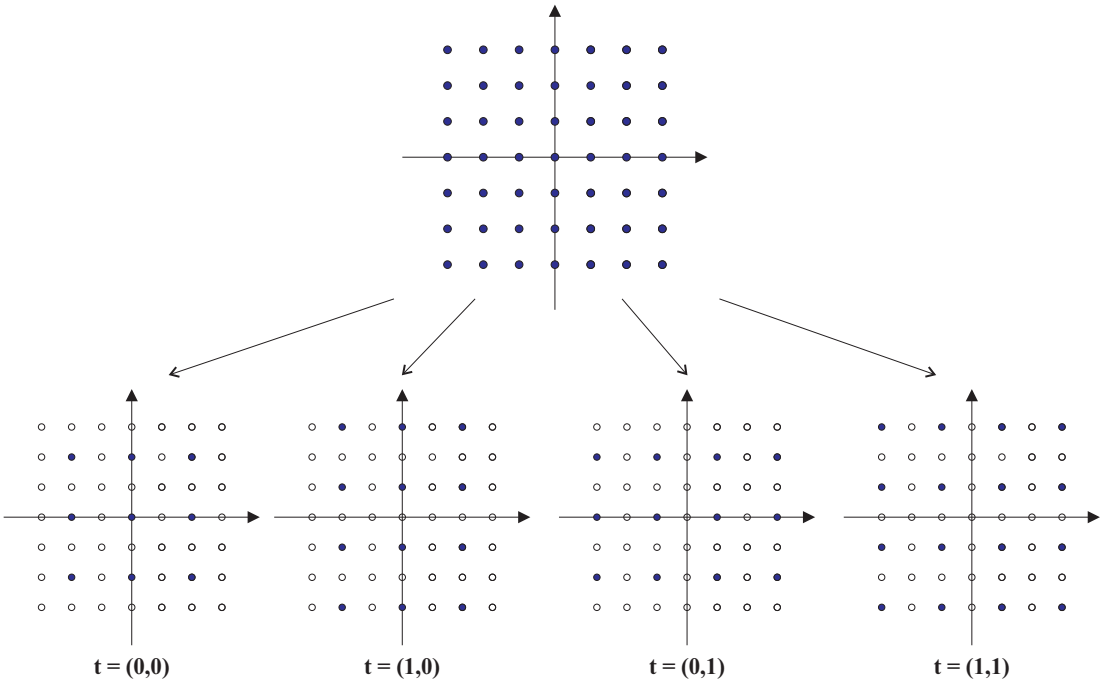

Figure 3.4 Cosets of the lattice partition $\mathbb{Z}^2/2\mathbb{Z}^2$.

fines a coset decomposition chain, that is

$$\begin{aligned}\Lambda =& \Lambda' + \left[\Lambda/\Lambda'\right] \\ =& \Lambda'' + \left[\Lambda'/\Lambda''\right] + \left[\Lambda/\Lambda'\right] \text{ et cetera,}\end{aligned} \tag{3.20}$$

so that each element of Λ may be expressed as an element of the final sublattice in the partition chain, plus a coset representative of each partition chain coset.

3.4.1 Elementary Constructions

We introduce two elementary methods of constructing lattices from binary linear block codes. We then present the special case of the Barnes-Wall lattice construction. There are strong connections between the error control coding problem (Section 3.2) and lattice constructions, since the error control coding problem is the problem of packing as many points as possible into the Galois field $\mathbf{F}_q^n$, with minimum Hamming distance d between any two points. This is equivalent to packing the most number of spheres of radius d into $\mathbf{F}_q^n$. Further discussion of the connections between error control coding and sphere packing are contained in [7, 42].

Construction A [7] is a method of constructing an n dimensional sphere packing from an (n, k, d) binary linear block code $\mathcal{C}$. We may define a lattice $\Lambda_{\mathcal{C}}$ as all n dimensional integer

vectors $\mathbf{x}$ that are equivalent, modulo 2, to a codeword $\mathbf{c} \in \mathcal{C}$. That is,

$$\Lambda_{\mathcal{C}} \triangleq \{\mathbf{x} \equiv \mathbf{c} \,(\mathrm{mod}\ 2) : \mathbf{c} \in \mathcal{C}\}. \tag{3.21}$$

This construction may be generalised [57] as follows. Given an ℓ dimensional lattice Λ and sublattice $\Lambda' \subseteq \Lambda$, we assume there exists some group $\mathcal{G}$ isomorphic to Λ/Λ'. Any $c \in \mathcal{G}$ is therefore equivalent to some coset representative $t \in [\Lambda/\Lambda']$ by some mapping $\xi : c \to t$. Therefore, each $\Lambda' + \xi(c)$ specifies a coset of Λ' and there exists some inverse mapping $\xi^{-1} : t \to c$ from the elements of the coset $\Lambda' + \mathbf{c}$ to the label u. *Generalised Construction A* then defines a lattice from an (n, k, d) group code $\mathcal{C} \subset \mathcal{G}^n$, as

$$\Lambda_{\mathcal{C}} \triangleq \bigcup_{\mathbf{c} \in \mathcal{C}} \xi(\mathbf{c}) \tag{3.22}$$

with

$$\xi(\mathbf{c}) = \left(\Lambda'\right)^n + \{\xi(c_1), \xi(c_2), \ldots, \xi(c_N)\}. \tag{3.23}$$

$\Lambda_{\mathcal{C}}$ is then an $\ell \times n$ dimensional lattice, with [7]

$$\begin{aligned} V(\Lambda_{\mathcal{C}}) =& \frac{V(\Lambda')^n}{|\mathcal{C}|} \\ d_{\min}(\Lambda_{\mathcal{C}}) \geq& \min\left\{d_{\min}\left(\Lambda'\right), d_{\mathcal{C}}.d_{\min}(\Lambda)\right\} \end{aligned} \tag{3.24}$$

where $d_{\mathcal{C}}$ is the minimum Hamming distance of the code $\mathcal{C}$. If $\Lambda = \mathbb{Z}$ and $\Lambda' = 2\mathbb{Z}$, then any binary linear code is isomorphic to Λ/Λ'. Then, letting $\xi(0) = 0$ and $\xi(1) = 1$, generalised construction A reduces to construction A. Note that generalised construction A may be used to define lattices from non-binary codes, as in [57].

Generalised Construction C is a multilevel extension of generalised construction A. [3] Consider a partition chain of ℓ dimensional lattices $\Lambda_m/\Lambda_{m-1}/\ldots/\Lambda_0$, where each partition Λ_k/Λ_{k-1} is isomorphic to a group $\mathcal{G}_k$, for $k = 1, 2, \ldots, m$. We denote each label group to coset mapping as $\xi_k : \mathcal{G}_k \to [\Lambda_k/\Lambda_{k-1}]$, with inverse $\xi_k^{-1} : [\Lambda_k/\Lambda_{k-1}] \to \mathcal{G}_k$. Now consider some sequence of length n codes $\mathcal{C}_1$, $\mathcal{C}_2$,..., $\mathcal{C}_m$, over $\mathcal{G}_1$, $\mathcal{G}_2$,...,$\mathcal{G}_m$ respectively. We can then define a generalised construction C lattice as

$$\Lambda_{\mathcal{C}_{1,\ldots,m}} \triangleq \bigcup_{\mathbf{c}^{(1)} \in \mathcal{C}_1, \ldots, \mathbf{c}^{(m)} \in \mathcal{C}_m} \left\{(\Lambda_0)^n + \xi_1\left(\mathbf{c}^{(1)}\right) + \ldots + \xi_m\left(\mathbf{c}^{(m)}\right)\right\} \tag{3.25}$$

where $\xi_k\left(\mathbf{c}^{(k)}\right) = \left\{\xi_k\left(c_1^{(k)}\right), \xi_k\left(c_2^{(k)}\right), \ldots, \xi_k\left(c_n^{(k)}\right)\right\}$ and $(\Lambda_0)^n$ is the n-fold Cartesian product of Λ_0. It is then readily shown [7] that $\Lambda_{\mathcal{C}_{1,\ldots,m}}$ is an $\ell \times n$ dimensional sphere

[3] [57] generalises this construction further, calling it *Multilevel Construction A*, but in keeping with [7] we use *Generalised Construction C*

packing, with

$$\begin{aligned} V\left(\Lambda_{\mathcal{C}_{1,\ldots,m}}\right) =& \frac{V(\Lambda_m)^n}{\prod_{k=1}^{m}|\mathcal{C}_k|}\,, \\ d_{\min}\left(\Lambda_{\mathcal{C}_{1,\ldots,m}}\right) =& \min\left\{d_{\min}\left(\Lambda_m\right)\,,\, d_{\mathcal{C}_m} d_{\min}\left(\Lambda_{m-1}\right)\,,\ldots,\, d_{\mathcal{C}_1} d_{\min}\left(\Lambda_0\right)\right\}. \end{aligned} \tag{3.26}$$

Although many dense lattices are known for high dimensions ($n \geq 32$) throughout this thesis we use the Barnes-Wall family of lattices [68], or similar sphere packings, as an example, since they are readily constructed from the binary linear Reed-Muller codes. We construct the n dimensional Barnes-Wall lattice, for $n = 2^a, a \in \mathbb{Z}, a \geq 2$, denoted $\mathcal{BW}_n$, using the codes $\mathcal{C}_0, \mathcal{C}_1, \ldots, \mathcal{C}_m$, where $m = \lfloor \frac{a}{2} \rfloor$ and $\mathcal{C}_k$ is the length n, $(2k)^{\text{th}}$ order Reed-Muller code [38]. We use the partition chain $\mathbb{Z}/2\mathbb{Z}/\ldots/2^m\mathbb{Z}$. The mappings from $\mathcal{C}_k$ to $[\Lambda_k/\Lambda_{k-1}]$ are defined as

$$\xi_k\left(\mathbf{c}^{(k)}\right) = \left\{\xi_i\left(c_1^{(k)}\right), \xi_i\left(c_2^{(k)}\right), \ldots, \xi_k\left(c_n^{(k)}\right)\right\} \tag{3.27}$$

where

$$\xi_k\left(c_i^{(k)}\right) = 2^k c_i. \tag{3.28}$$

The n dimensional Barnes-Wall lattice is then given by

$$\mathcal{BW}_n \triangleq \bigcup_{\mathbf{c}^{(0)}\in\mathcal{C}_0,\ldots,\mathbf{c}^{(m-1)}\in\mathcal{C}_{m-1}} \left\{(2^m\mathbb{Z})^n + \xi_0\left(\mathbf{c}^{(0)}\right) + \ldots + \xi_{m-1}\left(\mathbf{c}^{(m-1)}\right)\right\}. \tag{3.29}$$

The Barnes-Wall lattices have kissing number [7]

$$\tau(\mathcal{BW}_n) = (2+2)\times(2+2^2)\times\ldots\times(2+2^m) \approx 4.768\times 2^{\frac{m(m+1)}{2}} \tag{3.30}$$

and centre density

$$\delta\left(\mathcal{BW}_n\right) = 2^{-\frac{5n}{4}} n^{\frac{n}{4}} \tag{3.31}$$

and are among the densest known lattices in dimensions $n \geq 16$.

3.5 Coded Modulation

Coset coding combines coding and modulation so that bandwidth efficient signals are transmitted with reduced error rate. Coded modulation largely stems from the work of Ungerboek [70], while [71,72] provide a thorough examination of the subject. A coset coder has three basic elements: a binary encoder which accepts uncoded data and outputs a larger number of coded bits, a method of using these to select a coset of the signal constellation, and a scheme for choosing an individual signal point from the selected subset with the uncoded bits. We assume a block encoder is used, although many schemes employ convo-

lutional encoding, as described in [58]. The basic elements of coset coding are outlined by Figure 3.5.

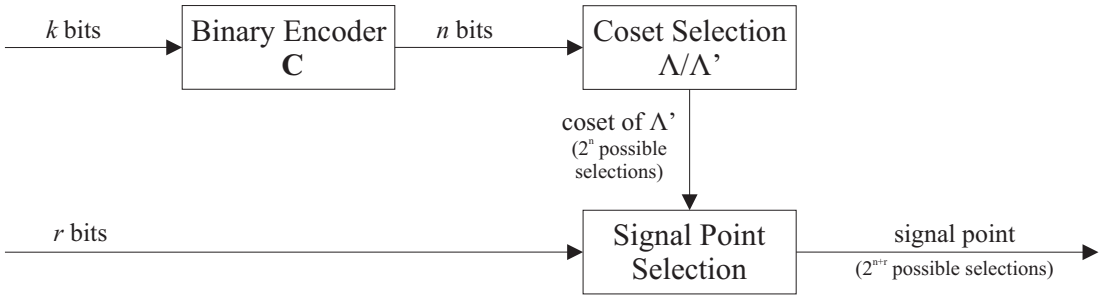

Figure 3.5 Basic elements of coset coding: coset selection and signal point selection.

Note that subsets of a generalised construction A lattice can be formulated as a coset code, since each codeword selects a coset in the signal constellation Λ', and any remaining uncoded bits select a distinct point from this lattice coset. Likewise, subsets of generalised construction C lattices can be formulated as coset codes. We refer to coset coding schemes that are equivalent to selecting a point in a lattice as *lattice coding*.

Strictly speaking, transmitting a point from a lattice dictates that our signal constellation is the lattice Λ. However, we typically transmit some translation $\Lambda + \mathbf{t}$ of Λ, so that $\mathbf{0} \notin \Lambda + \mathbf{t}$, where t is some n dimensional vector, so that our signal constellation has no DC component. Furthermore, any signal constellation must be finite, so we select some finite subset $\mathcal{M}_f \subset \Lambda + \mathbf{t}$ as our transmitted signal constellation. The choice of finite subset determines the *shape gain* of the lattice code [73]. The total coding gain of the lattice code is determined by the product of the shape gain and the lattice coding gain [71]. However, for large constellations, that is $|\mathcal{M}_f| \gg 1$, the total coding gain is largely determined by the lattice properties [71]. Thus, for simplicity we assume the signal constellation is the set of points within an n dimensional cube so that the *shape gain* is unity. A detailed discussion of the effects of signal constellation choice upon shape gain, implementation complexity, and compatibility with existing systems is contained in [74].

As an example of a lattice code, consider transmission of points in the 16 dimensional Barnes-Wall lattice $\mathcal{BW}_{16}$. The construction C representation of $\mathcal{BW}_{16}$ is

$$\mathcal{BW}_{16} = \bigcup_{\mathbf{c}^{(1)} \in RM(0,4), \mathbf{c}^{(2)} \in RM(2,4)} \left\{ (4\mathbb{Z})^{16} + 2\mathbf{c}^{(1)} + \mathbf{c}^{(0)} \right\} \tag{3.32}$$

where $RM(0,4)$ and $RM(2,4)$ are the length 16 Reed-Muller codes of order 0 and 2 respec-

tively. The operation of the $\mathcal{BW}_{16}$ lattice encoder may be described by Figure 3.6. Note that $RM(4,4)$ is the trivial code which adds no redundancy, and simply outputs the uncoded input bits. The output of the $RM(0,4)$ and $RM(2,4)$ encoders select cosets in the lattices partitions $\mathbb{Z}/2\mathbb{Z}$ and $2\mathbb{Z}/4\mathbb{Z}$ respectively, so that a distinct coset of $4\mathbb{Z}$ is chosen. The uncoded bits then select a point from this coset. The selected point is then from the subset of $\mathcal{BW}_{16}$ whose points lie within the 16 dimensional cube with opposite vertices at $\{0,0,\ldots,0\}$ and $\{7,7,\ldots,7\}$. If we set the translation vector $\mathbf{t} = \{-3.5,-3.5,\ldots,-3.5\}$, the signal constellation is symmetric about the origin, and the DC component is removed.

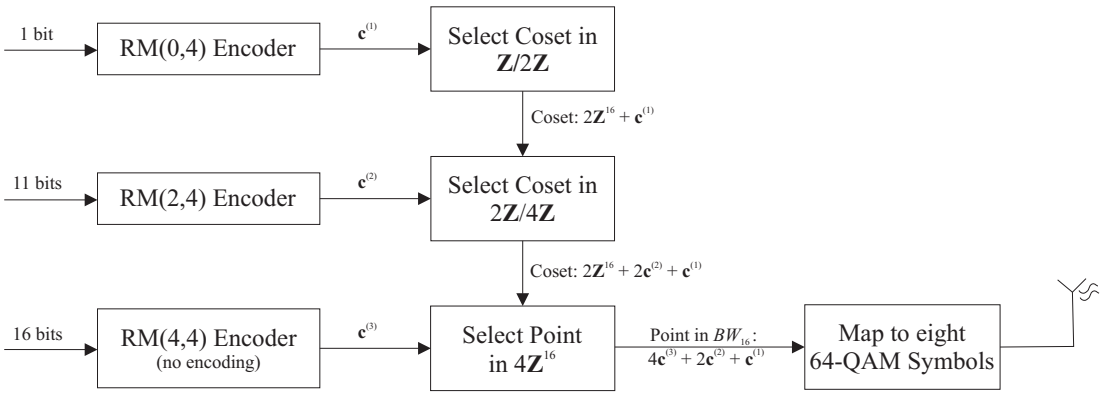

Figure 3.6 Lattice coding using the 16 dimensional Barnes-Wall lattice $\mathcal{BW}_{16}$.

We may then map each point $\mathbf{x} = \{x_1, x_2, \ldots, x_8\} \in \mathcal{BW}_{16}$ to an 8-PAM constellation. For example, we may use the mapping $m(x_i) = 2\sqrt{E_0}(x_i - 3.5)$ so that each coordinate of $\mathbf{x}$ is mapped to the 8-PAM constellation

$$\mathcal{M}_{8-\mathrm{PAM}} = \left\{-7\sqrt{E_0}, -5\sqrt{E_0}, -3\sqrt{E_0}, -\sqrt{E_0}, \sqrt{E_0}, 3\sqrt{E_0}, 5\sqrt{E_0}, 7\sqrt{E_0}\right\}. \tag{3.33}$$

Furthermore, we may transmit two 8-PAM constellations in quadrature as a 64-QAM constellation, so that pairs of coordinates in $\mathbf{x}$ are transmitted. Therefore, we may represent our point in $\mathcal{BW}_{16}$ with eight transmitted 64-QAM symbols.

Note that we may view this as multilevel coding, a powerful method of coding analysed by [75–78]. This is illustrated in Figure 3.6. Generally, any coset coding equivalent to selection from a finite subset of a construction C lattice may be viewed as multilevel coding. We concern ourselves only with this type of coset coding for the remainder of the thesis. A thorough and more general analysis of coset coding is found in [71] and [72].

At the receiver we are presented with the apparently difficult task of estimating the transmitted point $\mathbf{x}$ from a large constellation $\mathcal{M}_f$. However, multilevel codes are elegantly decoded using multistage decoding [75,76]. For our example, given some noise corrupted re-

ceived word $\mathbf{r} \in \mathbb{R}^n$, we first find the closest point in the coset $2\mathbb{Z}^{16} + \xi_0\left(\mathbf{c}^{(0)}\right) = 2\mathbb{Z}^{16} + \mathbf{c}^{(0)}$, and label this $\hat{\mathbf{x}}^{(0)}$. We label the binary vector isomorphic to this point as $\mathbf{u}^{(0)} = \xi_0^{-1}(\hat{\mathbf{x}}^{(0)}) = \hat{\mathbf{x}}^{(0)}$. We can then decode $\mathbf{u}^{(0)}$ to obtain an estimate $\hat{\mathbf{c}}^{(0)}$ of the codeword $\mathbf{c}^{(0)}$. In the next stage, we estimate $\mathbf{c}^{(1)}$ by finding the closest point to $\mathbf{r} - \hat{\mathbf{c}}^{(0)}$ in $4\mathbb{Z}^{16} + \xi_1\left(\mathbf{c}^{(1)}\right) = 4\mathbb{Z}^{16} + 2\mathbf{c}^{(1)}$, which we label $\hat{\mathbf{x}}_1$. From this we obtain $\hat{\mathbf{u}}^{(1)} = \xi_1^{-1}(\hat{\mathbf{x}}^{(1)}) = \frac{1}{2}\hat{\mathbf{x}}^{(1)}$, and we decode this to obtain an estimate $\hat{\mathbf{c}}^{(1)}$ of $\mathbf{c}^{(1)}$. Finally, to estimate the uncoded bits, we find the closest point to $\mathbf{r} - \hat{\mathbf{c}}^{(0)} - 2\hat{\mathbf{c}}^{(1)}$ in $4\mathbb{Z}^{16}$, and estimate the uncoded bits as $\mathbf{c}^{(2)} = \xi_2^{-1}\left(\hat{\mathbf{x}}^{(2)}\right)$. This method is readily generalised to decode any construction C lattice code [57]. We have thus estimated the transmitted bits in stages, with each stage corresponding to estimation of a specific coset of each partition in the lattice partition chain.

In the above example, at the m^{th} level, for $m \in \{0, 1, 2\}$, we estimate the codeword associated with each hard decision. We have implied the use of algebraic hard decision decoding, although, this does not achieve the best error performance. We may also use maximum likelihood sequence estimation of each codeword given $\mathbf{r}$. However, the computational complexity of maximum likelihood decoding increases exponentially with code length n, and thus lattice dimension. We may also employ GMD decoding at each stage to achieve near maximum likelihood performance with only polynomial complexity in n. GMD decoding of Euclidean space codes is summarised in sections 3.3.1 and 6.3.1, and described in detail in [57] and [79].

3.6 Summary

We have introduced error control coding and lattices, including the concept of lattice coding, an attractive method of exploiting the properties of dense lattices. We may transmit points from complicated lattices using simple multilevel constructions, then decode using simple multistage techniques. Near maximum likelihood decoding performance can be obtained by applying soft decision coding at each stage, specifically GMD decoding. We can thus achieve high coding gains with low computational complexity. GMD decoding of wireless OFDM systems employing lattice codes is a major topic of the work in this thesis.

Chapter 4

Orthogonal Frequency Division Multiplexing

In this chapter we summarise the important aspects of orthogonal frequency division multiplexing (OFDM), a method for transmitting high data rates via parallel streams. We begin with a discussion of the motivation for using OFDM, outline the transmitter and receiver structures, and then conclude with the limitations and requirements of OFDM systems. This chapter introduces concepts and notation that will be used throughout the remainder of the thesis. We then show that the distribution of the capacity of an OFDM system with a large number of subcarriers, transmitting over a frequency selective, Rayleigh fading channel, is approximately Gaussian distributed. Furthermore, we prove a theorem, which states that as the number of subcarriers, and system bandwidth, approaches infinity, the asymptotic capacity is the same as that for an infinite bandwidth narrowband system. These capacity results are original work. A comprehensive treatment of OFDM systems is found in [4, 80].

4.1 Motivation

To transmit high data rates we must either increase the size of the transmitted symbol constellation, or decrease the duration of each transmitted symbol. In the unavoidable presence of noise, the error rate will increase if the constellation size is increased, unless the transmitted power is also increased. Battery powered mobile systems or systems operating near people should not transmit high power, and therefore high data rate systems typically employ a short symbol duration, and thus a large transmission bandwidth. The increase in system capacity as bandwidth or power is increased is elegantly shown by Shannon's capacity theorem, stated in Equation 1.1.

As outlined in Chapter 2, systems that employ a large transmission bandwidth are affected by channel frequency selectivity. Traditional single carrier systems transmitting over frequency selective channels are perturbed by intersymbol interference (ISI) which severely limits the transmission rate, unless difficult and complicated equalisation techniques are employed [4].

Parallel data stream systems split the data into N lower rate streams that are simultaneously transmitted, then recombined at the receiver into a single high rate stream. Classical parallel systems divide the total bandwidth into N *subchannels* that do not overlap in frequency, onto which each parallel data stream is modulated. The advantage of the parallel approach is that each data stream occupies a small bandwidth, referred to as a subchannel. Thus, the symbol duration within each subchannel is large compared to the maximal delay spread of the channel, the subchannels are essentially flat, and intersymbol interference is readily mitigated. Nonoverlapping subchannel systems require stringent filtering to prevent subchannel overlap. A simpler method with more efficient use of bandwidth is to allow the subchannels to overlap in frequency, with an orthogonality constraint such that the subchannels do not interfere and may be separated. This may be obtained very efficiently using Fourier transforms, for which fast algorithms exist [81]. This is the OFDM technique, which is described in the following sections.

Overlapping subchannel systems were first proposed in the mid 1960s [82, 83]. However the technique we refer to as OFDM was first completely described, in 1971, by [84]. The attractiveness of OFDM for transmission over both flat fading and frequency selective fading channels was outlined in [85]. The most ubiquitous use of OFDM technology to date is not wireless, but for asymmetric digital subscriber line (ADSL) high speed internet [86]. However, OFDM has grown rapidly in popularity in the 1990s, and has been incorporated in several wireless networking [40, 87] and broadcasting [6, 41] standards. Furthermore, OFDM has been proposed as a transmission method for ultrawideband technology [88] as well as a possible fourth generation cellular technology [89].

4.2 Transmitter Structure

The OFDM signal is the superposition of N subcarriers spaced ΔfHz apart. We can write the k^{th}, $k = 1, 2, \ldots, N$, subcarrier signal as

$$\tilde{g}_k(t) = \begin{cases} \exp\left(j2\pi k \Delta f t\right) & \text{for } 0 \leq t < T_s \\ 0 & \text{otherwise,} \end{cases} \tag{4.1}$$

where $T_s = \frac{1}{\Delta f}$ is the duration of the modulated symbols on each subcarrier. The total system bandwidth B is divided into N narrowband subchannels, each occupied by a sub-

carrier with symbol duration N times longer than that of a single carrier system employing the same bandwidth. We may then write $B = \frac{N}{T_s} = N\Delta f$.

To each subcarrier symbol we add a guard interval T_g. If T_g is larger than the channel maximal delay spread $\tau_{\max}$ no ISI occurs, since all the delayed signal versions arrive at the receiver before the next signal. Each subcarrier signal duration is then $T = T_s + T_g$. Typically we extend each subcarrier signal by T_g, referred to as a *cyclic prefix* [1], such that the k^{th} subcarrier signal during the n^{th} time interval is

$$g_k(t) = \begin{cases} \exp\left(j2\pi k\Delta f t\right) & \text{for } 0 \leq t < T_s + T_g \\ 0 & \text{otherwise.} \end{cases} \tag{4.2}$$

Note that there exist other methods of adding a guard interval. For example, it is shown in [90] that it is possible to estimate the channel impulse response, and then mitigate ISI, even with transmission of no signal during the guard interval. However, in the remainder of this thesis we assume a cyclic prefix is used during the guard interval. Note that no new information is transmitted in the guard interval. Thus we typically select N so that T_s is large compared to T_g, and the proportion of symbol duration used in the guard interval is then small.

We modulate the k^{th} subcarrier during the n^{th} time interval with data symbol $S_{n,k} \in \mathbb{R}^2$, from some signal constellation such as BPSK, QPSK or QAM. We then superimpose all N subcarriers to form the n^{th} OFDM *block*, denoted

$$s_n(t) = \begin{cases} \frac{1}{\sqrt{N}} \sum_{k=1}^{N} S_{n,k}\, g_k(t - nT) & \text{for } (n-1)T \leq t < nT \\ 0 & \text{otherwise.} \end{cases} \tag{4.3}$$

Then, applying a rectangular window to each OFDM block, we obtain the OFDM signal for all time intervals as

$$s(t) = \frac{1}{\sqrt{N}} \sum_{n=0}^{\infty} \sum_{k=1}^{N} S_{n,k}\, g_k(t - nT). \tag{4.4}$$

The Fourier transform of the signal during the n^{th} time interval is then

$$S_n(f) = \frac{1}{\sqrt{N}} \sum_{k=1}^{N} S_{n,k} G_k(f) \tag{4.5}$$

where each subcarrier has spectrum

$$G_k(f) = T\,\text{sinc}\left(\,\pi T[f - k\Delta f]\,\right). \tag{4.6}$$

[1] Strictly (4.2) describes a cyclic postfix, while a cyclic prefix would define $g_k(t)$ to be nonzero between $-T_g \leq t < T_s$. However, these are equivalent.

Thus, the subcarrier spectra are sinc pulses, which overlap but are mutually orthogonal, as illustrated in Figure 4.1. Note that sampling $s_n(t)$ at rate $k\Delta f$ yields the same result as sampling $g_k(t-nT)$ at rate $k\Delta f$. Thus, the subcarriers are mutually orthogonal, since with correct sampling we may reconstruct each subcarrier signal so that it is unaffected by the other $N-1$ overlapping subcarriers.

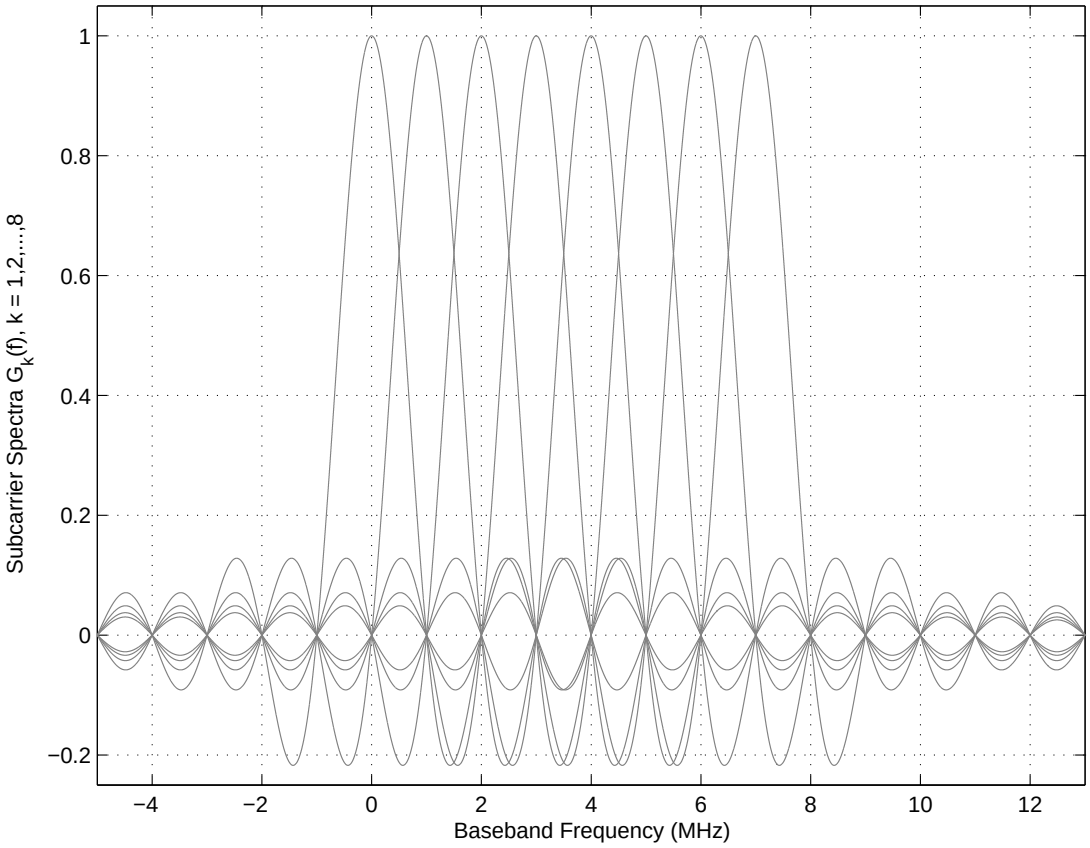

Figure 4.1 Baseband subcarrier frequency spectra for an OFDM system with $N = 8$ and $\Delta f = 1\text{MHz}$.

We sample the signal $s_n(t)$ at rate B and label the samples as $s_{n,i}$ for $i = 1, 2, \ldots, N$. These may be written as

$$s_{n,i} = \frac{1}{\sqrt{N}} \sum_{k=1}^{N} S_{n,k} \exp\left(\frac{j\pi ik}{N}\right) \tag{4.7}$$

which is an inverse discrete Fourier transform (IDFT) operation. We thus efficiently generate $s_n(t)$ by performing an IDFT of the subcarrier symbols $S_{n,k}$, for $k = 1, 2, \ldots, N$, to obtain samples $s_{n,i}$ which are then digital to analog converted to obtain $s_n(t)$. This is illustrated later in Figure 4.2.

4.3 Receiver Structure

Assuming that the transmitted OFDM symbol has guard interval longer than the maximum multipath delay, and that the channel is time invariant during each OFDM block, the received signal $r_n(t)$ for the n^{th} time interval is a channel perturbed version of the transmitted signal. Specifically,

$$r_n(t) = h_n(t) \otimes s_n(t) + w_n(t) \tag{4.8}$$

where $h_n(t)$ is the channel impulse response, and $w_n(t)$ is a complex additive white Gaussian noise process with power spectral density $\frac{N_0}{2}$ per dimension. The orthogonal subcarrier signals are obtained by a correlation technique [4] which may be implemented as a discrete Fourier transform (DFT) of N samples $r_{n,i}$, at rate B, of the received signal $r_n(t)$. That is, we obtain

$$R_{n,k} = \frac{1}{\sqrt{N}} \sum_{i=1}^{N} r_{n,i} \exp\left(-\frac{j2\pi ik}{N}\right) \tag{4.9}$$

where $R_{n,k} \in \mathbb{R}^2$ is a channel and noise perturbed version of $S_{n,k}$. If the channel is approximately constant during each OFDM block, that is the channel coherence time is much greater than T, and the guard interval is sufficient that ISI is negligible, then we may write [84]

$$R_{n,k} = H_{n,k}S_{n,k} + W_{n,k}. \tag{4.10}$$

In this case each subcarrier is multiplied by a complex subchannel gain $H_{n,k}$ and each received symbol is further perturbed by complex additive white Gaussian noise modelled by $W_{n,k}$. It may be shown [80] that $W_{n,k}$ is independent for all n and k, and has variance $\frac{N_0}{2}$ per dimension.

We refer to the set of all N symbols transmitted during the n^{th} time interval as the n^{th} transmitted *OFDM block*, denoted

$$\mathbf{S}_n = \{S_{n,1}, S_{n,2}, \ldots, S_{n,N}\}. \tag{4.11}$$

Similarly the n^{th} received OFDM block is denoted

$$\mathbf{R}_n = \{R_{n,1}, R_{n,2}, \ldots, R_{n,N}\} = \mathbf{S}_n \odot \mathbf{H}_n + \mathbf{W}_n \tag{4.12}$$

where $\mathbf{H}_n = \{H_{n,1}, H_{n,2}, \ldots, H_{n,N}\}$ is the set of n^{th} time interval subchannel gains , $\mathbf{W}_n = \{W_{n,1}, W_{n,2}, \ldots, W_{n,N}\}$ is the set of n^{th} time interval noise process samples, and $\mathbf{S}_n \odot \mathbf{H}_n \triangleq \{S_{n,1}H_{n,1}, S_{n,2}H_{n,2}, \ldots, S_{n,N}H_{n,N}\}$.

The elegance of OFDM is captured in (4.10), since each transmitted subcarrier symbol is not affected by ISI. Each modulation symbol is only multiplied by the subchannel gain, and corrupted by additive white Gaussian noise (AWGN). The components of an OFDM

transmitter and receiver are summarised in Figure 4.2.

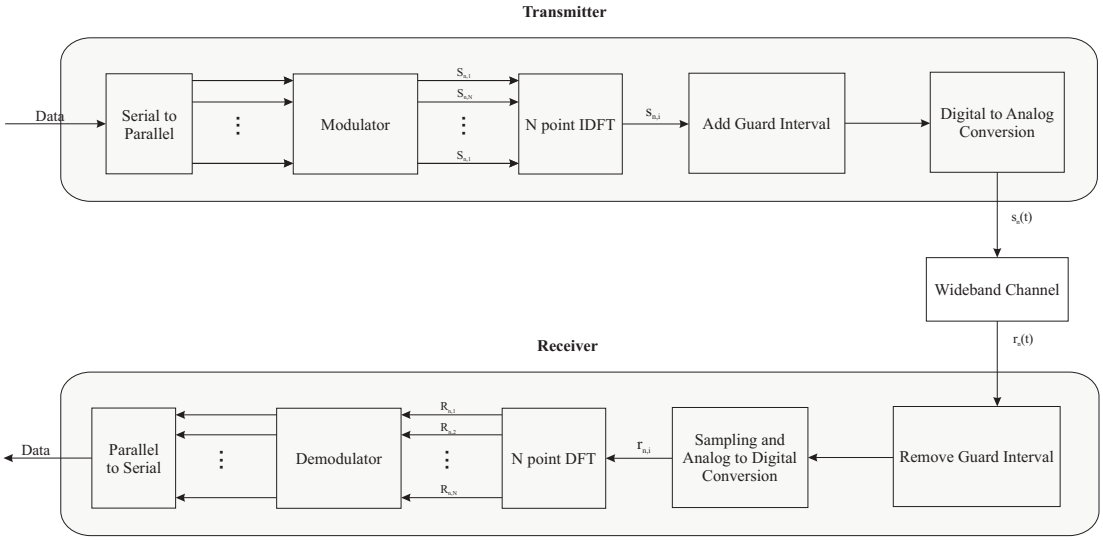

Figure 4.2 OFDM Transmitter and Receiver Structure

4.4 OFDM Channel Model

Following [80, Chp. 2] each subchannel response $H_{n,k}$ may be modelled as the channel response $H(f_k, t)$ at the subchannel centre frequency f_k, assuming a slow fading channel. This is intuitively satisfying, since the spectrum of each subcarrier is a sinc pulse, as in (4.6), centred at f_k with rapidly decaying side lobes, as illustrated in Figure 4.1.

Assuming a Jakes' model Rayleigh fading channel (Section 2.2.2), we may then express the response of subchannels $k_1, k_2 \in \{1, \ldots, N\}$ during time intervals $n_1, n_2 \in \mathbb{Z}$ as complex Gaussian random variables. That is, from (2.39),

$$\begin{aligned} H_{n_1,k_1} &= X_{n_1,k_1} + jY_{n_1,k_1} \\ H_{n_2,k_2} &= X_{n_2,k_2} + jY_{n_2,k_2} \end{aligned} \tag{4.13}$$

where X_{n_1,k_1}, Y_{n_1,k_1}, X_{n_2,k_2} and Y_{n_2,k_2} are real Gaussian random variables with zero mean. Without loss of generality we may assume

$$\mathbb{E}\left[X_{n_1,k_1}^2\right] = \mathbb{E}\left[Y_{n_1,k_1}^2\right] = \mathbb{E}\left[X_{n_2,k_2}^2\right] = \mathbb{E}\left[Y_{n_2,k_2}^2\right] = \frac{1}{2}. \tag{4.14}$$

Furthermore the subchannel gains have cross correlations (Chapter 2):

$$\begin{aligned}
\mathbb{E}\left[X_{n_1,k_1}Y_{n_1,k_1}\right] &= \mathbb{E}\left[X_{n_2,k_2}Y_{n_2,k_2}\right] = 0 \\
\mathbb{E}\left[X_{n_1,k_1}X_{n_2,k_2}\right] &= \mathbb{E}\left[Y_{n_1,k_1}Y_{n_2,k_2}\right] = \frac{1}{2}\frac{\mathrm{J}_0\left(2\pi f_d \Delta n T\right)}{1+\left(2\pi\tau_{rms}\Delta f \Delta k\right)^2} \\
\mathbb{E}\left[X_{n_1,k_1}Y_{n_2,k_2}\right] &= -\mathbb{E}\left[Y_{n_1,k_1}X_{n_2,k_2}\right] = -\frac{1}{2}\frac{\left(2\pi\Delta f\Delta k\tau_{rms}\right)\mathrm{J}_0\left(2\pi f_d\Delta n T\right)}{1+\left(2\pi\tau_{rms}\Delta f\Delta k\right)^2}
\end{aligned} \tag{4.15}$$

where $\Delta k = |k_1 - k_2|$ and $\Delta n = |n_1 - n_2|$. From (4.15) we observe that the cross correlations $\mathbb{E}\left[X_{n_1,k_1}Y_{n_2,k_2}\right]$ and $\mathbb{E}\left[Y_{n_1,k_1}X_{n_2,k_2}\right]$ decrease as $\frac{1}{\Delta k}$, referred to [91] as *strong correlation* or *long range dependence*. This strong correlation prevents the application of classical central limit theorems [92, 93] to functions of the Gaussian distributed subchannel gains.

Note that the channel response magnitudes $|H_{n,k}|$ and channel gains $|H_{n,k}|^2$ have marginal Rayleigh and exponential distributions respectively, as outlined in Section 2.2.2. Furthermore, the joint subchannel gain distribution for subchannels k_1, k_2, $k_1 \neq k_2$, during the same time interval n, is, from (2.46),

$$f_{|H_1|^2|H_2|^2}(x,y) = \frac{1}{\sigma^4\left(1-\rho\right)}\exp\left(-\frac{x+y}{2\sigma^2[1-\rho]}\right)\mathrm{I}_0\left(\frac{\sqrt{\rho}.\sqrt{xy}}{\sigma^2[1-\rho]}\right). \tag{4.16}$$

In this case $\sigma^2 = \frac{1}{2}$ is the variance of the underlying Gaussian random variables, and the correlation coefficient ρ between $|H_{n,k_1}|^2$ and $|H_{n,k_2}|^2$ is

$$\rho = \frac{1}{1+\left(2\pi\tau_{rms}\Delta f\Delta k\right)^2} \tag{4.17}$$

from (2.45) with $\Delta t = 0$ since we consider subchannel gains within the same OFDM block.

4.5 Requirements and Limitations

Although OFDM is an elegant method of combating the effects of channel frequency selectivity, there are several limitations and stringent requirements for the correct operation of OFDM systems. For completeness we discuss the more important requirements and limitations. However, throughout the remainder of this thesis we assume that these requirements are met.

4.5.1 Synchronisation

In Section 4.3 we imply receiver time synchronisation. Time synchronisation requires identification of the beginning of each OFDM block and guard interval. This is typically obtained by first transmitting some known sequence of training blocks, as proposed in [94–97]. Since the OFDM technique employs symbols of duration N times longer than

an equal bandwidth single carrier system, there is less sensitivity to timing offset. However, note that less timing offset is shown to improve carrier frequency offset estimation and also improve channel estimation [96, 98]. A more detailed discussion of the effects of timing jitter is found in [80].

We have also implied perfect receiver frequency synchronisation. The receiver DFT operation correlates the received signal with the subcarrier pulse function $g_k(t)$ for $k = 1, \ldots, N$, (4.2). That is, the received signal is correlated with sinusoids with frequency $f_k = k\Delta f$, $k = 1, \ldots, N$. However, in the presence of frequency offset f_{off} in the receiver, the received signal is correlated with sinusoids of frequency $f_k + f_{\text{off}}$. This violates the orthogonality of subcarriers, and causes intercarrier interference (ICI) over all subcarriers. This is analysed in [80]. The resulting interference power P_{ICI} affecting the ℓ^{th} subcarrier is the sum of the interference from all other subcarriers, and may be written as [99]

$$P_{\text{ICI}} = \sum_{k=1, k\neq\ell}^{N} \text{sinc}^2\left(\pi\left[k - \ell - \frac{f_{\text{off}}}{\Delta f}\right]\right). \tag{4.18}$$

It may be observed, from (4.18), that a frequency offset $f_{\text{off}} = 0.2\Delta f$ causes interference approximately -10dB below the signal power. This significantly reduces the effective signal to noise ratio of each subcarrier and increases the bit error rate. Frequency synchronisation in OFDM systems is therefore critical for correct performance, particularly in systems with small Δf.

Doppler spreading due to receiver motion causes a frequency shift in the received signal. Thus, Doppler effects may be modelled as a frequency offset [100]. This remains a key problem in the use of OFDM in high speed mobile applications and can introduce an unacceptable error floor [100].

Frequency offset must be corrected before performing the receiver DFT. Typically, pilot symbols are used to estimate the frequency offset, as in [99, 101–103]. Reference [104] gives an overview of existing frequency offset correction algorithms.

An alternative approach to synchronisation exploits the cyclic prefix. Estimation of the timing and frequency offset can be derived from the intrinsic redundancy of the samples that constitute the cyclic prefix [105–108]. Conceptually, samples of the subcarrier signal $\tilde{g}_k(t)$ are correlated with samples from the guard interval to provide an accurate estimate of the start of each signal. These methods remove the necessity, or reduce the required number, of pilot symbols. However, cyclic prefix based frequency offset estimation typically has worse performance then pilot based schemes, since the cyclic prefix is typically shorter in duration than a pilot symbol, and the estimate is then based on a sample with lower SNR.

4.5.2 Channel Estimation

At the receiver we obtain symbols $R_{n,k}$, as in (4.10). Thus, we multiply by the normalised conjugate subchannel response $\frac{\overline{H}_{n,k}}{|H_{n,k}|^2}$ to obtain

$$R'_{n,k} = \frac{\overline{H}_{n,k}}{|H_{n,k}|^2} R_{n,k} = S_{n,k} + \frac{\overline{H}_{n,k}}{|H_{n,k}|^2} W_{n,k} = S_{n,k} + W'_{n,k} \tag{4.19}$$

where $W'_{n,k}$ is a complex zero mean Gaussian random variable with variance $\frac{1}{|H_{n,k}|^2}\frac{N_0}{2}$ per dimension. We therefore require knowledge of each subchannel gain. Channel estimation may be performed in static or quasi-static channels by transmitting a pilot sequence prior to data transmission, as in [86]. In faster fading channels, estimation techniques typically require devoting a number of subcarriers within each block to transmitting a pilot symbol. Note, from (4.17), that the gains of neighbouring subchannels are highly correlated, and thus readily estimated using dedicated pilot subcarriers, as in [40, 85, 109].

In the absence of channel state information differential modulation techniques may be used. Conventional differential modulation techniques [110] may be applied to successive subcarrier signals, or the subcarrier symbols may be encoded differentially between adjacent subcarriers within a single OFDM block [111]. Such schemes attract a throughput sacrifice, although pilot symbols are not required and the receiver structure may then be simplified.

4.5.3 Peak to Average Power Ratio

Each OFDM block $s_n(t)$ is the sum of N subcarrier signals modulated by independent and identically distributed symbols $S_{n,k}$. The amplitude of $s_n(t)$ is therefore a random variable. For large N the central limit theorem dictates that $|s_n(t)|$ follows a Gaussian distribution. Thus OFDM signals usually have large peak to average power ratio (PAPR). Specifically, the PAPR is

$$\mathcal{P}_{\text{pk/av}} \triangleq \frac{\max_{0\le t<T} |s_n(t)|^2}{P_{\text{av}}} \tag{4.20}$$

where the average power $P_{\text{av}} = \mathbb{E}\left[|s_n(t)|^2\right]$. The cumulative probability density function (CDF) of $P_{\text{pk/av}}$ is approximately [112]

$$F_{\mathcal{P}_{\text{pk/av}}}(x) = \left(1 - e^{-x}\right)^N. \tag{4.21}$$

Although a more accurate approximation of $F_{\mathcal{P}_{\text{pk/av}}}(x)$ is derived in [112], (4.21) captures one of the major drawbacks with OFDM systems: the PAPR is typically very large. Thus, power amplifiers that remain linear over a large dynamic range are necessary. In the absence of such amplifiers, the signal is clipped and distorted, causing both out of band

emissions and symbol errors at the receiver [80]. The reduction of OFDM PAPR is the subject of a large body of work. Generally, PAPR reduction techniques fall into two categories: restriction of the subcarrier symbols $S_{n,k}$ to eliminate the combinations which produce large amplitudes, as in [113–115]; and filtering or pre-distorting the OFDM signal before amplification to reduce the amplitude peaks, as in [116–118]. A general summary of these techniques is contained in [4].

4.5.4 Further Considerations

There exist many other requirements for reliable operation of OFDM systems. These include suppression of narrowband interference from other systems, methods for which are outlined in [119]; the effects and mitigation of phase noise in the receiver [80, 120]; and methods [121–123] of windowing the signal $s_n(t)$ so that out of band emissions, due to the sinc pulse side lobes (4.6), are suppressed. A summary of the important considerations is given in [124]. Most key considerations are also addressed by the standards [40, 87, 88].

4.6 OFDM Capacity

In this section we consider the capacity of OFDM systems operating over frequency selective Rayleigh fading channels. Recent work concerning the capacity of systems operating over frequency selective channels includes [125–127], while [128] gives an encyclopedic overview of the subject. However, we restrict our capacity analysis to OFDM systems, and concern ourselves with the distribution of instantaneous capacity, that is, the capacity during transmission of each OFDM block.

Similar analysis of OFDM capacity is found in [129], where transmission over twisted pair cables perturbed by crosstalk and thermal noise is analysed. [129] considers OFDM systems with fixed bandwidth, and derives the asymptotic capacity as the subcarrier separation decreases. In contrast, we consider the capacity of power limited OFDM systems with very large finite bandwidth, and derive the asymptotic capacity of systems with infinite bandwidth. This is motivated by recent proposals [88] for the of OFDM in ultrawideband systems. An overview of recent capacity results for power limited systems transmitting over a large bandwidth is given in [130].

From Section 1.1, Shannon's theorem [1] states that a narrowband system occupying a bandwidth Δf and perturbed by additive white Gaussian noise such that the signal to noise ratio within the bandwidth is γ, can transmit at a maximum rate of

$$C = \frac{\Delta f}{\ln 2} \ln (1 + \gamma) \text{ bits/s} \tag{4.22}$$

so that each bit may be estimated without error. Consider an OFDM system transmitting N subcarriers spaced ΔfHz apart, over a frequency selective slow fading Rayleigh channel, where the receiver has perfect synchronisation in time and frequency and perfect channel state information. Furthermore, assume that the total average transmitted energy over all subcarriers is E_N, so that each subcarrier transmits symbols at rate Δf, with average energy $E_0 = \frac{E_N}{N}$. Then, given bandlimited noise with power spectral density of N_0 per dimension across the transmission bandwidth, the received signal to noise ratio on the k^{th} subchannel during the n^{th} block is $\gamma_{n,k} = |H_{n,k}|^2 \frac{\gamma_0}{N}$, where $\gamma_0 = \frac{E_0}{N_0}$. Without loss of generality we may ignore any loss in capacity due to the guard interval, and write the instantaneous k^{th} subchannel capacity as

$$C_{n,k} = \frac{\Delta f}{\ln 2} \ln\left(1 + \gamma_{n,k}\right) = \frac{\Delta f}{\ln 2} \ln\left(1 + \gamma_0 |H_{n,k}|^2\right). \tag{4.23}$$

Note that, for any subcarrier k, $C_{n,k}$ is a random variable in time since the subchannel gain $|H_{n,k}|^2$ is time varying. The pdf of $C_{n,k}$, since $|H_{n,k}|^2$ follows an exponential distribution with unity mean, is then

$$f_{C_{n,k}}(x) = \frac{\ln 2}{\gamma_0 \Delta f} \exp\left(\frac{x \ln 2}{\Delta f}\right) \exp\left(\frac{1}{\gamma_0} - \frac{1}{\gamma_0} \exp\left[\frac{x \ln 2}{\Delta f}\right]\right) \tag{4.24}$$

so that, using Appendix A.1, we may write the mean capacity as

$$\mathbb{E}\left[C_{n,k}\right] = \int_0^\infty \frac{\Delta f}{\ln 2} \ln\left(1 + \gamma_0 y\right) \exp(-y) dy = -\frac{\Delta f}{\ln 2} \exp\left(\frac{1}{\gamma_0}\right) \text{Ei}\left(-\frac{1}{\gamma_0}\right) \tag{4.25}$$

where $\text{Ei}(.)$ is the exponential integral function [37]. This expression is also obtained in [127, 131]. We define the instantaneous total capacity of the OFDM system as

$$C_n = \sum_{k=1}^{N} C_{n,k} \tag{4.26}$$

which is also a random variable in time.

In the remainder of this section we show that, for large N, in a frequency selective Rayleigh fading channel the distribution of C_n is approximated by a Gaussian random variable. Furthermore, we derive the mean and variance of this distribution. This key result allows OFDM system designers to construct confidence intervals on the achievable system capacity, and clearly identifies the statistical behaviour of system capacity. We also prove a theorem which states that, in the limit as $N \to \infty$, the normalised capacity of an OFDM system converges, in probability, to a constant equal to the wideband channel capacity [130]. Therefore no loss in capacity is incurred by using OFDM to transmit over wideband channels.

The derivation of these two results relies on a central limit theorem, introduced in Section 4.6.2. However, use of this theorem first necessitates the definition of the subchannel capacity as a function of each subchannel gain, and the introduction of the Hermite rank of this function, in Section 4.6.1. We then apply the central limit theorem in Section 4.6.3 to show that, for large N, the distribution of C_n is approximated by a Gaussian distribution, whose mean and variance may be found using the subchannel capacity correlation expressions also in this section. We prove the asymptotic total capacity in Section 4.6.4. Finally, we verify our analysis with system simulations shown in Section 4.6.5.

4.6.1 Hermite Rank of Capacity Function

Each subchannel gain may be expressed as a complex Gaussian random variable, $H_{n,k} = X_{n,k} + jY_{n,k}$, as in (4.13). In the Rayleigh fading channel $X_{n,k}$ and $Y_{n,k}$ are zero mean, and without loss of generality we may set $\mathbb{E}\left[X_{n,k}^2\right] = \mathbb{E}\left[Y_{n,k}^2\right] = \frac{1}{2}$. We may then express the subchannel capacity as a function $\mathrm{c}(\cdot)$ of Gaussian random variables. Specifically,

$$C_{n,k} \triangleq \mathrm{c}\left(X_{n,k}, Y_{n,k}\right) = \frac{\Delta f}{\ln 2} \ln\left(1 + \left[X_{n,k}^2 + Y_{n,k}^2\right] \gamma_0\right). \tag{4.27}$$

The Hermite rank [132] of a function is the index of the first nonzero coefficient in its Hermite polynomial [133] expansion. We require the Hermite rank of $\mathrm{c}(\cdot)$ in order to apply a central limit theorem introduced later. The Hermite rank $\varphi(f) \geq 0$ of a measurable function $f : \mathbf{X} \to \mathbb{R}$ for the zero mean Gaussian vector $\mathbf{X} = \{X_1, \ldots, X_d\} \in \mathbb{R}^d$, where f has finite second moment, is defined [132] as

$$\varphi(f) = \inf\left\{\tau : \exists l_j \text{ with } \sum_{j=1}^{d} l_j = \tau \text{ and } \mathbb{E}\left[\left(f(\mathbf{X}) - \mathbb{E}\left[f(\mathbf{X})\right]\right) \prod_{j=1}^{d} H_{l_j}(X_1)\right] \neq 0\right\} \tag{4.28}$$

where H_{l_j} is the $(l_j)^{\text{th}}$ order Hermite polynomial [133]. Equivalently [134], given a polynomial P we may write

$$\varphi(f) \triangleq \inf\left\{\varphi(f) : \exists\, P \text{ of degree } \varphi(f), \text{ with } \mathbb{E}\left[\left(\, f(\mathbf{X}) - \mathbb{E}\left[f(\mathbf{X})\right] \,\right) \cdot P\big(X_1, \ldots, X_d\big)\right] \neq 0\right\}. \tag{4.29}$$

We show that the Hermite rank $\varphi(\mathrm{c})$ of $\mathrm{c}(X_1, X_2)$ is at least two by showing that it is neither zero nor unity. Consider first a zero order polynomial $P_0(X_1, X_2) = \alpha_0$. Then

$$\mathbb{E}\left[\left(\mathrm{c}(X_1, X_2) - \mathbb{E}\left[\mathrm{c}(X_1, X_2)\right]\right) P_0(X_1, X_2)\right] = \alpha_0 \mathbb{E}\left[\mathrm{c}(X_1, X_2)\right] - \alpha_0 \mathbb{E}\left[\mathrm{c}(X_1, X_2)\right] = 0 \tag{4.30}$$

for all α_0, and thus $\varphi(\mathrm{c}) \neq 0$. Now consider a first order polynomial, $P_1(X_1, X_2) = \alpha_2 X_1 +$

$\alpha_1 X_2 + \alpha_0$. With a little manipulation we may then write

$$\begin{aligned}&\mathbb{E}\left[(\mathrm{c}(X_1, X_2) - \mathbb{E}\left[\mathrm{c}(X_1, X_2)\right]) P_1(X_1, X_2)\right] \\ &= \alpha_2 \frac{\Delta f}{\ln 2} \mathbb{E}\left[X_1 \ln\left(1 + \gamma_0\left[X_1^2 + X_2^2\right]\right)\right] + \alpha_1 \frac{\Delta f}{\ln 2} \mathbb{E}\left[X_2 \ln\left(1 + \gamma_0\left[X_1^2 + X_2^2\right]\right)\right].\end{aligned} \tag{4.31}$$

Assuming X_1 and X_2 each have variance σ^2, we may write

$$\begin{aligned}&\mathbb{E}\left[X_1 \ln\left(1 + \gamma_0\left[X_1^2 + X_2^2\right]\right)\right] \\ &= \mathbb{E}\left[X_2 \ln\left(1 + \gamma_0\left[X_1^2 + X_2^2\right]\right)\right] \\ &= \frac{1}{\sqrt{2\pi\sigma^2}} \int_{-\infty}^{\infty} X_2 \ln\left(1 + \gamma_0\left[X_1^2 + X_2^2\right]\right) \exp\left(-\frac{X_2^2}{2\sigma^2}\right) \partial X_2 \\ &= 0\end{aligned} \tag{4.32}$$

since the integrand is the product of an odd function and two even functions in X_2. Thus $\varphi(\mathrm{c}) \neq 1$, and it follows that $\varphi(\mathrm{c}) \geq 2$.

4.6.2 The Arcones-de Naranjo Central Limit Theorem

We now present a central limit theorem, proved by Arcones [134] and de Naranjo [135], for nonlinear functions of strongly correlated vectors of Gaussian random variables. We shall apply this theorem to the capacity function (4.23). The theorem may be stated as

Theorem 4.1. *Let $\{\mathbf{X}_j\}_{j=1}^{\infty}$ be a stationary mean-zero sequence of Gaussian vectors in $\mathbb{R}^d$. Set $\mathbf{X}_j = (X_j^{(1)}, \ldots, X_j^{(d)})$. Let f be a function on $\mathbb{R}^d$ with Hermite rank $\varphi(f)$ such that $1 \leq \varphi(f) < \infty$. Define*

$$r^{(p,q)}(k) = \mathbb{E}\left[X_m^{(p)} X_{m+k}^{(q)}\right] \tag{4.33}$$

for $k \in \mathbb{Z}$, where m is any number large enough that $m \geq 1$ and $m + k \geq 1$. Suppose that

$$\sum_{k=-\infty}^{\infty} \left|r^{(p,q)}(k)\right|^{\varphi(f)} < \infty \tag{4.34}$$

for all $1 \leq p \leq d$ and $1 \leq q \leq d$. Then as $n \to \infty$,

$$\frac{1}{\sqrt{n}} \sum_{j=1}^{n} \left(f(\mathbf{X}_j) - \mathbb{E}\left[f(\mathbf{X}_j)\right]\right) \xrightarrow{D} \mathcal{N}(0, \sigma^2) \tag{4.35}$$

where '$\xrightarrow{D}$' denotes 'convergence in distribution' [91], and

$$\sigma^2 = \mathbb{E}\left[\left(f(X_1) - \mathbb{E}\left[f(X_1)\right]\right)^2\right] + 2 \sum_{k=1}^{\infty} \mathbb{E}\left[\left(f(X_1) - \mathbb{E}\left[f(X_1)\right]\right)\left(f(X_{1+k}) - \mathbb{E}\left[f(X_{1+k})\right]\right)\right]. \tag{4.36}$$

4.6.3 Total Capacity Distribution

The total capacity C_n (4.26) is the sum of nonlinear functions (4.23) of correlated Gaussian random variables. In order to apply the theorem to the capacity function $\mathrm{c}(\cdot)$ requirement (4.34) must be satisfied. This will occur if the sums of the cross-correlations and correlations, of the underlying subchannel gain Gaussian random variables raised to the power of the function Hermite rank, are convergent. Substituting the correlation expressions in (4.15), with $\Delta n = 0$, we may write

$$\sum_{\Delta k=-\infty}^{\infty} \left|\mathbb{E}\left[X_{n,k}Y_{n,k+\Delta k}\right]\right|^{\varphi(\mathrm{c})} = \sum_{\Delta k=-\infty}^{\infty} \left|\mathbb{E}\left[Y_{n,k}X_{n,k+\Delta k}\right]\right|^{\varphi(\mathrm{c})} = \sum_{\Delta k=-\infty}^{\infty} \left|\frac{1}{2}\frac{(2\pi\Delta f \Delta k \tau_{rms})}{1+(2\pi\Delta f \Delta k)^2}\right|^{\varphi(\mathrm{c})} \tag{4.37}$$

which is convergent [136] since $\varphi(\mathrm{c}) \geq 2$. Similarly,

$$\sum_{\Delta k=-\infty}^{\infty} \left|\mathbb{E}\left[X_{n,k}X_{n,k+\Delta k}\right]\right|^{\varphi(\mathrm{c})} = \sum_{\Delta k=-\infty}^{\infty} \left|\mathbb{E}\left[Y_{n,k}Y_{n,k+\Delta k}\right]\right|^{\varphi(\mathrm{c})} = \sum_{\Delta k=-\infty}^{\infty} \left|\frac{1}{2}\frac{1}{1+(2\pi\Delta f \Delta k)^2}\right|^{\varphi(\mathrm{c})} \tag{4.38}$$

is also convergent.

Thus, requirement (4.34) of the theorem is satisfied, and we may write

$$\frac{1}{\sqrt{N}}\sum_{k=1}^{N}\left\{\mathrm{c}\left(X_{n,k},Y_{n,k}\right) - \mathbb{E}\left[\mathrm{c}\left(X_{n,k},Y_{n,k}\right)\right]\right\} \xrightarrow{D} \mathcal{N}\left(0,\Omega_c^2\right) \tag{4.39}$$

where

$$\begin{aligned}\Omega_c^2 &= \mathbb{E}\left[\left(\mathrm{c}\left(X_{n,1},Y_{n,1}\right) - \mathbb{E}\left[\mathrm{c}\left(X_{n,1},Y_{n,1}\right)\right]\right)^2\right] + 2\sum_{\Delta k=1}^{\infty}\mathbb{E}\Big[\left(\mathrm{c}\left(X_{n,1},Y_{n,1}\right) - \mathbb{E}\left[\mathrm{c}\left(X_{n,1},Y_{n,1}\right)\right]\right) \\ &\qquad \times \left(\mathrm{c}\left(X_{n,1+\Delta k},Y_{n,1+\Delta k}\right) - \mathbb{E}\left[\mathrm{c}\left(X_{n,1+\Delta k},Y_{n,1+\Delta k}\right)\right]\right)\Big] \\ &= \mathrm{var}\left[\mathrm{c}\left(X_{n,1},Y_{n,1}\right)\right] + 2\sum_{\Delta k=1}^{\infty}\mathrm{cov}\left[\mathrm{c}\left(X_{n,1},Y_{n,1}\right)\mathrm{c}\left(X_{n,1+\Delta k},Y_{n,1+\Delta k}\right)\right].\end{aligned} \tag{4.40}$$

with the above variance and covariance terms readily calculable using the expression for $\mathbb{E}\left[C_{n,k}\right]$ in (4.25), and the expression for $\mathbb{E}\left[C_{n,k_1}C_{n,k_2}\right]$ later derived in (4.48). The convergence in distribution described in (4.39) clearly motivates the following approximation. For large finite N, the distribution of the instantaneous capacity C_n, may be approximated by that of a Gaussian random variable with mean $N\mathbb{E}\left[C_{n,k}\right]$ and variance $N\Omega_c^2$. Note that since capacity is nonnegative, the Gaussian approximation to the distribution of C_n is invalid at $C_n < 0$. However, for sufficiently large SNR and N, the probability $\Pr\left(C<0\right)$ vanishes, and the deviation from the Gaussian approximation is small, as demonstrated in

Section 4.6.5.

We can then use this result to approximate the distribution of the instantaneous capacity for systems with very large bandwidth, such as ultrawideband systems [88], and fixed total average transmitted energy E_N. The average SNR per subcarrier is $\gamma_0 = \frac{E_N}{NN_0}$, and we may substitute this into (4.25) and (4.48) to obtain $N\mathbb{E}[C_{n,k}]$ and $N\Omega_c^2$ respectively. Simulation results, in Section 4.6.5, show this to be a good approximation to the distribution of the instantaneous capacity for a very large bandwidth, power limited OFDM system. We would expect this approximation to be tighter for larger N, and this is demonstrated by the simulations.

We now derive a series representation of the correlation between the capacity of any two subchannels. This result allows simple calculation of the covariance between subchannel capacities, and thus Ω_c^2.

Subchannel Capacity Correlation

The mean squared capacity $\mathbb{E}\left[C_{n,k}^2\right]$ may be expressed as

$$\mathbb{E}\left[C_{n,k}^2\right] = \left(\frac{\Delta f}{\ln 2}\right)^2 \int_0^\infty \left[\ln\left(1+\gamma_0 y\right)\right]^2 \exp(-y)dy \tag{4.41}$$

which is readily numerically evaluated. We may write the correlation between the capacity of subchannels k_1 and k_2 in time interval n as

$$\mathbb{E}\left[C_{n,k_1}C_{n,k_2}\right] = \left(\frac{\Delta f}{\ln 2}\right)^2 \int_0^\infty \int_0^\infty \ln\left(1+\gamma_0 x\right)\ln\left(1+\gamma_0 y\right) f_{|H_1|^2,|H_2|^2}(x,y)\,dxdy \tag{4.42}$$

where $f_{|H_1|^2,|H_2|^2}(x,y)$ is the joint pdf of two correlated exponential random variables, $|H_{n,k_1}|^2$ and $|H_{n,k_2}|^2$. We assume, without loss of generality, that $\mathbb{E}\left[|H_{n,k}|^2\right] = 1$, for all n,k. Then, we may rewrite (4.16) as

$$f_{|H_1|^2,|H_2|^2}(x,y) = \kappa \exp\left(-\alpha x - \alpha y\right) \mathrm{I}_0\left(\theta\sqrt{xy}\right) \tag{4.43}$$

where

$$\alpha = \kappa = \frac{1}{1-\rho^2} \quad \theta = \frac{\rho}{1-\rho^2} \tag{4.44}$$

and ρ is the correlation coefficient defined in (4.17). Substituting (4.43) into (4.42) we obtain

$$\begin{aligned}
&\mathbb{E}\left[C_{n,k_1}C_{n,k_2}\right] \\
&= \kappa \int_0^\infty \int_0^\infty \left(\frac{\Delta f}{\ln 2}\right)^2 \ln\left(1+\gamma_0 x\right) \ln\left(1+\gamma_0 y\right) \exp\left(-\alpha(x+y)\right) \mathrm{I}_0\left(\theta\sqrt{xy}\right)\, dx\, dy \\
&= \kappa \left(\frac{\Delta f}{\ln 2}\right)^2 \sum_{i=0}^{\infty} \frac{\theta^{2i}}{4^i (i!)^2} \left[\int_0^\infty x^i \ln\left(1+\gamma_0 x\right) \exp\left(-\alpha x\right)\, dx\right]^2
\end{aligned} \tag{4.45}$$

using the series expansion for $\mathrm{I}_0(\cdot)$ in Appendix A.12. Consider the integral in the above expression. We substitute $u = 1+\gamma_0 x$ and use the binomial expansion of $(u-1)^i$, in Appendix A.15, so that after some manipulation we may write

$$\int_0^\infty x^i \ln\left(1+\gamma_0 x\right) e^{-\alpha x}\, dx = \frac{1}{\gamma_0^{i+1}} \exp\left(\frac{\alpha}{\gamma_0}\right) \sum_{r=0}^{i} \binom{i}{r} (-1)^{i-r} \int_1^\infty \ln(u)\, u^r \exp\left(-\frac{\alpha\, u}{\gamma_0}\right)\, du. \tag{4.46}$$

We then integrate by parts and use Appendix A.8 to write

$$\begin{aligned}
&\int_1^\infty \ln(u)\, u^r \exp\left(-\frac{\alpha\, u}{\gamma_0}\right)\, du \\
&= \int_1^\infty \exp\left(-\frac{\alpha\, u}{\gamma_0}\right) \left[\frac{\gamma_0\, u^{r-1}}{\alpha} + \sum_{k=1}^{r} r(r-1)(r-2)\ldots(r-k+1) \left(\frac{\gamma_0}{\alpha}\right)^{k+1} u^{r-k-1}\right] du \\
&= \left(\frac{\gamma_0}{\alpha}\right)^{r+1} \left[\Gamma\left(r, \alpha\gamma_0^{-1}\right) + \sum_{k=1}^{r} \frac{r!}{(r-k)!} \Gamma\left(r-k, \alpha\gamma_0^{-1}\right)\right]
\end{aligned} \tag{4.47}$$

where $\Gamma(\cdot,\cdot)$ is the incomplete Gamma function [21]. We may substitute (4.47) and (4.46) into (4.45) to then write

$$\begin{aligned}
\mathbb{E}\left[C_{n,k_1}C_{n,k_2}\right] = \kappa \left(\frac{\Delta f}{\ln 2}\right)^2 \exp\left(\frac{\alpha}{\gamma_0}\right) \sum_{i=0}^{\infty} \frac{\theta^{2i}}{4^i\, i!} \Bigg\{ &\sum_{r=0}^{i} \frac{1}{(i-r)!} \frac{(-\gamma_0)^{r-i}}{\alpha^{r+1}} \\
&\times \left[\frac{1}{r!} \Gamma\left(r, \alpha\gamma_0^{-1}\right) + \sum_{k=1}^{r} \frac{\Gamma\left(r-k, \alpha\gamma_0^{-1}\right)}{(r-k)!}\right]\Bigg\}^2
\end{aligned} \tag{4.48}$$

for $k_1 \neq k_2$. This series representation is rapidly convergent, and may be used to numerically calculate the variance of the instantaneous capacity distribution.

4.6.4 Asymptotic Total Capacity

We now consider the case of a power limited OFDM system with fixed Δf, and we let the number of subcarriers N approach infinity, so that the bandwidth also approaches infinity.

For such power limited systems E_N is fixed, so that $E_0 = \frac{E_N}{N} \to 0$, as $N \to \infty$. We then prove a new theorem, which states that the limiting capacity $C_\infty = \lim_{N\to\infty} C_n$ of such systems approaches a constant.

Theorem 4.1 is not applicable in this scenario, since the function $\mathrm{c}(\cdot)$ now becomes a function of N, in addition to $X_{n,k}$ and $Y_{n,k}$. Hence we proceed in an alternative manner, and find C_∞ by first proving that the arithmetic average subchannel gain converges, in probability, to the mean gain of a single subchannel. This is outlined in the following lemma.

Lemma 4.2. *Assuming $\mathbb{E}\left[|H_{n,k}|^2\right] = 1$, the distribution of the arithmetic average subchannel gain converges to a degenerate distribution, as $N \to \infty$, such that*

$$\frac{1}{N}\sum_{k=1}^{N} |H_{n,k}|^2 \xrightarrow{P} 1 \tag{4.49}$$

where '$\xrightarrow{P}$' denotes 'convergence in probability'.

Proof. Let $\Omega_H^2(N) = \mathrm{var}\left[\frac{1}{N}\sum_{k=1}^{N} |H_{n,k}|^2\right]$. Then, $\Omega_H^2(N)$ can be expanded as

$$\begin{aligned}\Omega_H^2(N) &= \frac{1}{N^2}\left\{\sum_{k=1}^{N} \mathrm{var}\left[|H_{n,k}|^2\right] + \sum_{r=1}^{N-1} 2(N-r)\mathrm{cov}\left[|H_{n,1}|^2, |H_{n,1+r}|^2\right]\right\} \\ &\leq \frac{1}{N}\mathrm{var}\left[|H_{n,k}|^2\right] + \frac{2}{N}\sum_{r=1}^{N-1} \mathrm{cov}\left[|H_{n,1}|^2, |H_{n,1+r}|^2\right].\end{aligned} \tag{4.50}$$

From (4.17), the covariance between $|H_{n,1}|^2$ and $|H_{n,1+r}|^2$ vanishes as $r \to \infty$ with order r^{-2}. Hence, the right hand side of (4.50) converges to zero as $N \to \infty$, and we have $\Omega_H^2(N) \to 0$ as $N \to \infty$. Since $\mathbb{E}\left[\frac{1}{N}\sum_{k=1}^{N} |H_{n,k}|^2\right] = 1$ for all N, and $\mathrm{var}\left[\frac{1}{N}\sum_{k=1}^{N} |H_{n,k}|^2\right] \to 0$, it follows that

$$\frac{1}{N}\sum_{k=1}^{N} |H_{n,k}|^2 \xrightarrow{ms} 1 \tag{4.51}$$

where '$\xrightarrow{ms}$' denotes mean square convergence. This mean square convergence then implies $\frac{1}{N}\sum_{k=1}^{N} |H_{n,k}|^2 \xrightarrow{P} 1$, as required.

□

We may use this lemma to write the following theorem on the asymptotic capacity C_∞ of a power limited OFDM system, with $E_0 = \frac{E_N}{N}$.

Theorem 4.3. *As N approaches infinity the capacity of an infinite bandwidth, power limited*

OFDM system converges, in probability, to the constant

$$C_\infty = \frac{\Delta f E_N}{N_0 \ln 2} \mathbb{E}\left[|H_{n,k}|^2\right]. \tag{4.52}$$

That is, the limiting capacity is dependent only on the SNR, subchannel separation and mean channel gain. Since we have set $\mathbb{E}\left[|H_{n,k}|^2\right] = 1$*, we may then write*

$$C_\infty = \frac{\Delta f E_N}{N_0 \ln 2}. \tag{4.53}$$

Proof. When $E_0 = \frac{E_N}{N}$, we may write the instantaneous capacity as

$$C_n = \sum_{k=1}^{N} \frac{\Delta f}{\ln 2} \ln\left(1 + \frac{E_N}{NN_0}|H_{n,k}|^2\right). \tag{4.54}$$

From [37] we may write

$$z - \frac{z^2}{1+z} \leq \ln(1+z) \leq z \tag{4.55}$$

for $z > -1$. Then, using (4.54) and (4.55) we may write

$$\frac{\Delta f}{\ln 2} \sum_{k=1}^{N} \left\{ \frac{E_N}{NN_0}|H_{n,k}|^2 - \frac{\left(\frac{E_N}{NN_0}|H_{n,k}|^2\right)^2}{1 + \frac{E_N}{NN_0}|H_{n,k}|^2} \right\} \leq C_n \leq \frac{\Delta f}{\ln 2} \sum_{k=1}^{N} \frac{E_N}{NN_0}|H_{n,k}|^2. \tag{4.56}$$

We now show that the above lower and upper bound converge in probability to the same limit. Consider the lower bound, which we may write as

$$\frac{\Delta f}{\ln 2} \sum_{k=1}^{N} \frac{E_N}{NN_0}|H_{n,k}|^2 - \frac{\Delta f}{\ln 2} \sum_{k=1}^{N} \frac{\left(\frac{E_N}{NN_0}|H_{n,k}|^2\right)^2}{1 + \frac{E_N}{NN_0}|H_{n,k}|^2}. \tag{4.57}$$

The second term in (4.57) satisfies

$$\frac{\Delta f}{\ln 2} \sum_{k=1}^{N} \frac{\left(\frac{E_N}{NN_0}|H_{n,k}|^2\right)^2}{1 + \frac{E_N}{NN_0}|H_{n,k}|^2} \leq \frac{\Delta f}{\ln 2} \frac{E_N^2}{N_0^2} \sum_{k=1}^{N} \frac{|H_{n,k}|^4}{N^2}. \tag{4.58}$$

The random variables $|H_{n,k}|^2$, $k = 1, \ldots, N$, are marginally exponentially distributed, and thus nonnegative with finite second moments. Hence, as $N \to \infty$, we may write

$$\mathbb{E}\left[\frac{1}{N^2} \sum_{k=1}^{N} |H_{n,k}|^4\right] \to 0 \tag{4.59}$$

and

$$\begin{aligned}\text{var}\left[\frac{1}{N^2}\sum_{k=1}^{N}|H_{n,k}|^4\right] &= \frac{1}{N^4}\text{var}\left[\sum_{k=1}^{N}|H_{n,k}|^4\right] \\ &\leq \frac{1}{N^4}N^2\text{var}\left[|H_{n,k}|^4\right] \\ &\to 0.\end{aligned} \tag{4.60}$$

The properties in (4.59) and (4.60) imply that $\frac{1}{N^2}\sum_{k=1}^{N}|H_{n,k}|^4 \xrightarrow{ms} 0$, so that we may then write

$$\frac{1}{N^2}\sum_{k=1}^{N}|H_{n,k}|^4 \xrightarrow{P} 0. \tag{4.61}$$

Thus, the right hand side of (4.58) converges in mean square to zero as $N \to \infty$, so that the expression in (4.57) converges in mean square to the first term only, as $N \to \infty$. Therefore, both the upper and lower bounds in (4.56) converge to the same limit. From Lemma 1, we also have $\frac{1}{N}\sum_{k=1}^{N}|H_{n,k}|^2 \xrightarrow{P} 1$, and we substitute this into (4.56) to write

$$C_n \xrightarrow{P} C_\infty = \frac{\Delta f}{\ln 2}\frac{E_N}{N_0}\mathbb{E}\left[|H_{n,k}|^2\right]. \tag{4.62}$$

□

Note that we may normalise the limit C_∞ by Δf to obtain the limiting *spectral efficiency* [8, 126], defined as the capacity per unit bandwidth. We have thus verified that OFDM systems can achieve the fading wideband channel capacity derived by [126]. Moreover, C_∞ is equal to the capacity of an unlimited bandwidth system transmitting over a flat Rayleigh fading channel [131], or the infinite bandwidth AWGN system [137].

4.6.5 Simulations

We simulate the normalised capacity $\frac{C_n}{\Delta f}$ of two example systems, and compare the observed instantaneous capacity distributions with the analytical approximating distributions. System A is a 1024 subcarrier system and system B is a 32768 subcarrier system. Both systems have subcarrier separation $\Delta f = 0.3125\text{MHz}$, SNR $\frac{E_N}{N_0} = 30\,\text{dB}$, and thus occupy bandwidths of $320\,\text{MHz}$ and $10.24\,\text{GHz}$ respectively. We assume an exponential power delay profile with root mean squared (rms) delay spread of $50\,\text{ns}$, and a receiver velocity of $100\,\text{km/h}$ for all systems.

In Figure 4.3 we plot the analytical approximating distributions and simulated instantaneous capacity distributions for the fading channel response during transmission of 500,000 blocks. Observe that we obtain a reasonable analytical approximation for system A, and a

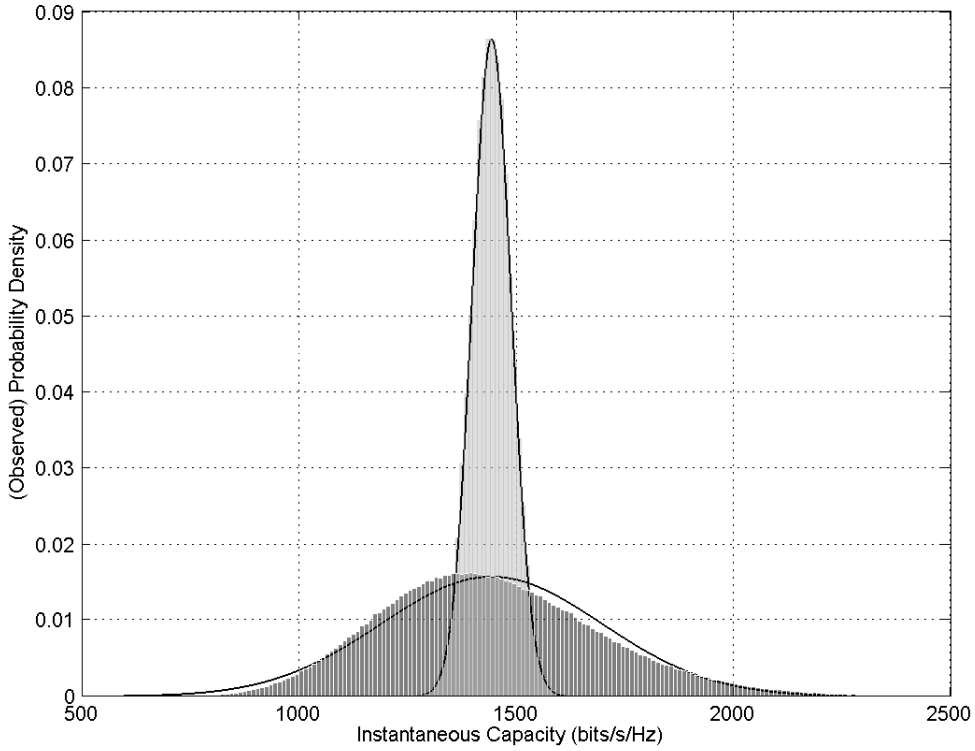

Figure 4.3 Simulated (bars) and theoretical (solid line) distributions of instantaneous capacity, normalised by Δf, for 1024 subcarrier system (larger variance) and 32768 subcarrier systems (smaller variance). Both systems have $\Delta f = 0.3125\text{MHz}$ and SNR $\frac{E_N}{N_0} = 30\text{dB}$.

tight approximation for system B, which has more subcarriers. Furthermore, observe that the variance of the capacity of system B is much smaller than that of system A, consistent with the limiting result of Theorem **??**.

4.7 Summary

In this chapter we have introduced the OFDM technique. OFDM is an elegant technique for combatting channel frequency selectivity. We have outlined the basics of OFDM transmission and reception, including the use of the Fourier transform to efficiently generate the OFDM signal and extract the subcarrier symbols in the receiver. Mathematical models of the OFDM subchannels and their correlation structure have been given. We have briefly surveyed some of the limitations of OFDM.

We have shown that the distribution of the capacity of an OFDM system transmitting a large number of subcarriers over a Rayleigh fading channel is approximately Gaussian. Furthermore, we have derived readily calculable expressions for the mean and variance of this distribution for arbitrary SNR and channel parameters. We have also proved that,

as $N \to \infty$, the capacity of an OFDM system approaches the capacity of an infinite bandwidth single carrier narrowband system, which is also equal to the capacity of an infinite bandwidth AWGN channel system. This proves that as $N \to \infty$, there is no capacity loss incurred by using OFDM to combat the frequency selective nature of the wireless channel.

Throughout the remainder of this thesis we consider OFDM systems with perfect channel knowledge, time synchronisation and frequency synchronisation at the receiver. The effects of amplifier nonlinearities and narrowband interference are not considered. Furthermore, we assume sufficient guard interval such that ISI is negligible, and, unless noted, transmission over a frequency selective, slow fading, Rayleigh channel described by the Jake's model. These are broad assumptions, and as such our analysis pertains to 'ideal' OFDM systems only. That is, the analysis represents a best case scenario.

Chapter 5

OFDM Performance Analysis

This chapter describes analysis of the error performance of uncoded OFDM systems. We first derive bounds on OFDM block error rates. These bounds demonstrate the error performance of uncoded OFDM over a wide range of signal to noise ratios, and thus afford better selection of error control coding methods to reduce block errors. We then extend our analysis to consider multiple symbol errors within each block. We analyse the distribution of the number of OFDM symbol errors within each block. Once again this analysis affords better selection of error control coding, since the probability of decoding failure of any code applied across subcarrier symbols within a single block is determined by the probability distribution of the number of received symbol errors within each block.

These two results are somewhat independent. Therefore, this chapter is organised so that each section is generally independent, necessitating some slight repetition.

5.1 OFDM Block Error Rate

For the n^{th} OFDM block the receiver obtains noise corrupted symbols $R_{n,k}$, for $k = 1, \ldots, N$. From each of these symbols the receiver generates estimates $\hat{S}_{n,1}, \ldots, \hat{S}_{n,N}$ of the transmitted symbols $S_{n,1}, \ldots, S_{n,N}$, respectively. If we employ a non-binary error correction code whose codeword symbols are entire OFDM blocks, $\mathbf{S}_n = \{S_{n,1}, S_{n,2}, \ldots, S_{n,N}\}$, analysis of code performance requires the probability of an OFDM block being in error, that is, the probability that the vector of receiver symbol estimates $\hat{\mathbf{S}}_n = \{\hat{S}_{n,1}, \hat{S}_{n,2}, \ldots, \hat{S}_{n,N}\}$ is not equal to the vector of transmitted symbols $\mathbf{S}_n = \{S_{n,1}, S_{n,2}, \ldots, S_{n,N}\}$. Utility of the block error rate also lies in the analysis of space-time OFDM systems, such as [138, 139], where the space-time code symbols are entire OFDM blocks. Furthermore, the block error rate may be used to obtain readily calculable bounds on the bit error rate of an uncoded OFDM system with any number of subcarriers.

Assuming transmission of BPSK symbols of energy E_0 and coherent reception, we denote the event that symbol $S_{n,k}$ is incorrectly received as $\mathcal{E}_{n,k}$. The probability of this event, assuming maximum likelihood (ML) estimation and perfect channel knowledge at the receiver, is [9]

$$P_{n,k} = \Pr\left(\mathcal{E}_{n,k}\right) = \frac{1}{2}\mathrm{erfc}\left(\sqrt{\gamma_{n,k}}\right) \tag{5.1}$$

where $\mathrm{erfc}(\cdot)$ is the complimentary Gaussian error function, and $\gamma_{n,k} = |H_{n,k}|^2 \frac{E_0}{N_0}$. The event of the n^{th} block being in error is the probability of one or more of the estimates $\hat{S}_{n,1}, \ldots, \hat{S}_{n,N}$ being incorrect, which we denote B_n. Applying the principle of inclusion and exclusion [140] we may write

$$\begin{aligned}\Pr\left(B_n\right) &= \Pr\left(\bigcup_{k=1}^{N} \mathcal{E}_{n,k}\right) \\ &= \sum_{k=1}^{N} \Pr\left(\mathcal{E}_{n,k}\right) - \sum_{\substack{k_2>k_1 \\ k_1,k_2=1}}^{N} \Pr\left(\mathcal{E}_{n,k_1} \cap \mathcal{E}_{n,k_2}\right) + \sum_{\substack{k_3>k_2>k_1 \\ k_1,k_2,k_3=1}}^{N} \Pr\left(\mathcal{E}_{n,k_1} \cap \mathcal{E}_{n,k_2} \cap \mathcal{E}_{n,k_3}\right) \\ &\quad - \cdots + \cdots.\end{aligned} \tag{5.2}$$

Then, averaging over successive OFDM blocks, the mean block error rate may be written as

$$\begin{aligned}\mathbb{E}\left[\Pr\left(B_n\right)\right] &= \sum_{k=1}^{N} \mathbb{E}\left[\Pr\left(\mathcal{E}_{n,k}\right)\right] - \sum_{\substack{k_2>k_1 \\ k_1,k_2=1}}^{N} \mathbb{E}\left[\Pr\left(\mathcal{E}_{n,k_1} \cap \mathcal{E}_{n,k_2}\right)\right] \\ &\quad + \sum_{\substack{k_3>k_2>k_1 \\ k_1,k_2,k_3=1}}^{N} \mathbb{E}\left[\Pr\left(\mathcal{E}_{n,k_1} \cap \mathcal{E}_{n,k_2} \cap \mathcal{E}_{n,k_3}\right)\right] - \cdots + \cdots.\end{aligned} \tag{5.3}$$

Accurate calculation of the block error rate consequently requires a large number of terms. However, by including only the first or second terms in (5.3) we may write the following bounds on the mean block error rate:

$$\begin{aligned}\mathbb{E}\left[\Pr\left(B_n\right)\right] &\leq \min\left\{\sum_{k=1}^{N} \mathbb{E}\left[\Pr\left(\mathcal{E}_{n,k}\right)\right], 1\right\} \\ \mathbb{E}\left[\Pr\left(B_n\right)\right] &\geq \max\left\{\sum_{k=1}^{N} \mathbb{E}\left[\Pr\left(\mathcal{E}_{n,k}\right)\right] - \sum_{\substack{k_2>k_1 \\ k_1,k_2=1}}^{N} \mathbb{E}\left[\Pr\left(\mathcal{E}_{n,k_1} \cap \mathcal{E}_{n,k_2}\right)\right], 0\right\}.\end{aligned} \tag{5.4}$$

The upper bound in (5.4) is often used to approximate the mean block error rate, and is

referred to as a *union bound* approximation. Thus,

$$\mathbb{E}\left[\Pr\left(B_n\right)\right] = \sum_{k=1}^{N} \mathbb{E}\left[\Pr\left(\mathcal{E}_{n,k}\right)\right] + \epsilon \approx \sum_{k=1}^{N} \mathbb{E}\left[\Pr\left(\mathcal{E}_{n,k}\right)\right] \tag{5.5}$$

where, from (5.4),

$$\epsilon \leq \sum_{\substack{k_2 > k_1 \\ k_1, k_2 = 1}}^{N} \mathbb{E}\left[\Pr\left(\mathcal{E}_{n,k_1} \cap \mathcal{E}_{n,k_2}\right)\right]. \tag{5.6}$$

We can thus find an upper bound on the mean error rate by calculating the mean subcarrier error rate $\mathbb{E}\left[\Pr\left(\mathcal{E}_{n,k}\right)\right]$. The union bound approximation is often used at moderate to high SNR, without quantification of the SNR range or the approximation. We now calculate a lower bound and bound the error ϵ in the union bound approximation by calculating the correlation between error probabilities for any two subcarriers $k_1, k_2 \in \{1, \ldots, N\}$, as in (5.6). We outline these calculations for the Rician channel and Rayleigh channels in the following subsections.

For the Rician fading channel we obtain a tight upper bound on the correlation between the mean probability of error on any two subchannels transmitting BPSK symbols. For the Rayleigh fading channel we obtain an exact series representation for this correlation. These simple expressions for the error probability correlation are derived for arbitrary correlation coefficient between the channel gains. The expressions are therefore useful in analysis of other multichannel schemes, such as multiple antenna systems, or Markov modelling of the channel error process as in [141–143].

5.1.1 Rician Channels

Assuming transmission over a Rician fading channel, each OFDM subchannel gain $|H_{n,k}|^2$ is identically marginally distributed, with average squared magnitude

$$\mathbb{E}\left[|H_{n,k}|^2\right] = \overline{|H_0|^2}, \text{ for all } n, k. \tag{5.7}$$

Thus, the mean probability of symbol error for each subchannel is

$$\mathbb{E}\left[\Pr\left(\mathcal{E}_{n,k}\right)\right] = \mathbb{E}\left[P_{n,k}\right] = \overline{P_0} = \int_0^\infty \operatorname{erfc}\left(\sqrt{x\frac{E_0}{N_0}}\right) f_{|H_{n,k}|^2}(x)dx, \text{ for all } n, k \tag{5.8}$$

where $f_{|H_{n,k}|^2}(x)$ is the probability density function (PDF) of the channel gain for Rician distributed $|H_{n,k}|$. Recall from (2.35) that we may write this as

$$f_{|H_{n,k}|^2}(x) = \frac{(K_R+1)}{\overline{\gamma_0}} \exp\left(-\frac{(K_R+1)x}{\overline{\gamma_0}} - K_R\right) \mathrm{I}_0\left(2\sqrt{K_R}\sqrt{\frac{(K_R+1)x}{\overline{\gamma_0}}}\right) \tag{5.9}$$

where K_R is the Rice factor, $\overline{\gamma_0} = \overline{|H_0|^2}\gamma_0$ and $\gamma_0 = \frac{E_0}{N_0}$ is the mean SNR for all subchannels. Substituting (5.9) into (5.8) and using the alternative representation [144] of the $\mathrm{erfc}(\cdot)$ function (Appendix A.10) we may write

$$\begin{aligned}\overline{P_0} =& \frac{2}{\pi}\exp\left(-K_R\right)\int_0^{\infty}\int_0^{\frac{\pi}{2}}\exp\left(-\frac{2x}{2\sin^2\theta}\right)\frac{(K_R+1)}{\overline{\gamma_0}}\exp\left(-\frac{(K_R+1)x}{\overline{\gamma_0}}\right)\\ &\times \mathrm{I}_0\left(2\sqrt{K_R}\sqrt{\frac{(K_R+1)x}{\overline{\gamma_0}}}\right)d\theta dx.\end{aligned} \tag{5.10}$$

Then, recognising that $\mathrm{I}_0(x) = \mathrm{J}_0(jx)$, for $x \in \mathbb{R}$, and applying the result from Appendix A.5 to simplify the integral over x, we may write

$$\overline{P_0} = \frac{2}{\pi}\frac{[K_R+1]\sin^2\theta}{\overline{\gamma_0}+[K_R+1]\sin^2\theta}\int_0^{\frac{\pi}{2}}\exp\left(\frac{-K_R\overline{\gamma_0}}{\overline{\gamma_0}+[K_R+1]\sin^2\theta}\right)d\theta \tag{5.11}$$

a readily calculable expression. Note that this result is also found in [145].

Consider any two subchannels with indices $k_1, k_2 \in \{1,\ldots,N\}$. Since there is independent AWGN on each subcarrier, and the receiver has knowledge of the subchannel gains, the events of incorrectly estimating the symbol transmitted on each subchannel are independent, but not necessarily identically distributed. We may then write

$$\Pr\left(\mathcal{E}_{n,k_1}\cap\mathcal{E}_{n,k_2}\right) = \frac{1}{4}\mathrm{erfc}\left(\sqrt{\gamma_{n,k_2}}\right)\mathrm{erfc}\left(\sqrt{\gamma_{n,k_2}}\right) = P_{n,k_1}P_{n,k_2}. \tag{5.12}$$

Then, averaging in time across the channel response, we obtain

$$\begin{aligned}\mathbb{E}\left[\Pr\left(\mathcal{E}_{n,k_1}\cap\mathcal{E}_{n,k_2}\right)\right] &= \mathbb{E}\left[P_{n,k_1}P_{n,k_2}\right]\\ &= \frac{1}{4}\int_0^{\infty}\int_0^{\infty}\mathrm{erfc}\left(x\sqrt{\frac{E_0}{N_0}}\right)\mathrm{erfc}\left(y\sqrt{\frac{E_0}{N_0}}\right)f_{|H_1|,|H_2|}(x,y)\,dxdy\end{aligned} \tag{5.13}$$

where $f_{|H_1|,|H_2|}(x,y)$ is the joint PDF of two correlated Rician random variables. In our case each Rician random variable is identically marginally distributed, and recall from (2.39) that we may write

$$H_{n,k_1} = a_0 + X_{n,k_1} + jY_{n,k_1} \text{ and } \quad H_{n,k_2} = a_0 + X_{n,k_1} + jY_{n,k_2} \tag{5.14}$$

where X_{n,k_1}, Y_{n,k_1}, X_{n,k_2} and Y_{n,k_2} are zero mean Gaussian random variables with variance σ^2, and a_0 represents the line of sight path amplitude, as in (2.32). The correlation between the random variables is given in (2.40). From [146] we may write the required joint PDF as

[1]

$$f_{|H_1|,|H_2|}(x,y) = \frac{xy}{\sigma^4\left(1-\rho^2\right)} \exp\left(-\frac{1}{2(1-\rho^2)}\left[\frac{x+y}{\sigma^4} + \left(\frac{2\sigma^2-2\rho}{\sigma^4}\right)a_0^2\right]\right) \times \sum_{i=0}^{\infty} \varepsilon_i \, \mathrm{I}_i\left(\frac{xy\rho}{\sigma^2(1-\rho^2)}\right) \mathrm{I}_i\left(\frac{a_0 x(1-\rho)}{\sigma^2(1-\rho^2)}\right) \mathrm{I}_i\left(\frac{a_0 y(1-\rho)}{\sigma^2(1-\rho^2)}\right) \tag{5.15}$$

where ρ is the coefficient of correlation between $|H_{n,k_1}|$ and $|H_{n,k_2}|$, and ε_i is the Neumann factor [37], defined by

$$\varepsilon_i = \begin{cases} 1, \text{ for } i = 0 \\ 2, \text{ for } i > 0. \end{cases} \tag{5.16}$$

A closed form expression for (5.13) thus appears impossible to attain.

We may obtain a tight upper bound to $\mathbb{E}\left[P_{n,k_1}P_{n,k_2}\right]$ by first recognising [9] that

$$P_{n,k} \leq \exp\left(-\gamma_{n,k}\right) \tag{5.17}$$

which is an asymptotically tight bound as $\gamma_{n,k} \to \infty$. We then write the subchannel gains as

$$\begin{aligned} H_{n,k_1} &= a_0 + U_1 + jV_1 \\ H_{n,k_2} &= a_0 + \tilde{U}_2 + j\tilde{V}_2 \end{aligned} \tag{5.18}$$

with

$$\tilde{U}_2 = \rho U_1 + \sqrt{1-\rho^2}U_2, \text{ and } \tilde{V}_2 = \rho V_1 + \sqrt{1-\rho^2}V_2 \tag{5.19}$$

where U_1, U_2, V_1 and V_2 are iid Gaussian random variables with mean zero and (without loss of generality) variance $\frac{1}{2}$. We denote the PDFs of these random variables as $f_{U_1}(x)$, $f_{U_2}(x)$, $f_{V_1}(x)$ and $f_{V_2}(x)$ respectively. We may then write the sum of the squared magnitude of the channel responses as

$$\begin{aligned} &|H_{n,k_1}|^2 + |H_{n,k_2}|^2 \\ &= \left(U_1 + a_0\right)^2 + V_1^2 + \left(\tilde{U}_2 + a_0\right)^2 + \tilde{V}_2^2 \\ &= \left\{U_1^2 + \rho^2 U_1^2 + \left(1-\rho^2\right)U_2^2 + 2\rho\sqrt{1-\rho^2}U_1U_2 + 2a_0U_1 + 2\rho a_0 U_1 + 2a_0\sqrt{1-\rho^2}U_2 + a_0^2\right\} \\ &\quad + \left\{V_1^2 + \rho^2 V_1^2 + \left(1-\rho^2\right)V_2^2\right\} \\ &= \mathrm{q}\left(U_1, U_2, a_0\right) + \mathrm{q}\left(V_1, V_2, 0\right) \end{aligned} \tag{5.20}$$

[1] The commonly used expression for $f_{|H_1|,|H_2|}(x,y)$, found in [19] and [147], is incorrect, as recently noted in [146]. We have previously used the incorrect expressions, in [148], however, this has no effect on the main result. Thanks go to Prof. Norman C. Beaulieu, Queens University, Canada, for pointing out this error.

where the quadratic $\mathrm{q} : \mathbb{R}^3 \to \mathbb{R}$ is defined as

$$\mathrm{q}(x, y, z) = (x + z)^2 + \left(\rho x + \sqrt{1 - \rho^2} y + z\right)^2. \tag{5.21}$$

Using this definition, we may then write an upper bound on the error probability correlation as

$$\begin{aligned} \mathbb{E}\left[P_{n,k_1} P_{n,k_2}\right] &\leq \frac{1}{4}\mathbb{E}\left[\exp\left(-\gamma_{n,k_1}\right)\exp\left(-\gamma_{n,k_2}\right)\right] \\ &= \frac{1}{4}\mathbb{E}\left[\exp\left(-\gamma_0\left|H_{n,k_1}\right|^2\right)\exp\left(-\gamma_0\left|H_{n,k_2}\right|^2\right)\right] \\ &= \frac{1}{4}\mathbb{E}\left[\exp\left(-\gamma_0 \mathrm{q}\left(U_1, U_2, a_0\right)\right)\exp\left(-\gamma_0 \mathrm{q}\left(V_1, V_2, 0\right)\right)\right]. \end{aligned} \tag{5.22}$$

Since U_1, U_2, V_1 and V_2 are iid random variables, we may write the upper bound in (5.22) as

$$\mathbb{E}\left[P_{n,k_1} P_{n,k_2}\right] \leq \frac{1}{4}\mathbb{E}\left[\exp\left(-\gamma_0 \mathrm{q}\left(U_1, U_2, a_0\right)\right)\right]\mathbb{E}\left[\exp\left(-\gamma_0 \mathrm{q}\left(V_1, V_2, 0\right)\right)\right] = \frac{1}{4}\mathrm{g}_1(a_0)\mathrm{g}_1(0) \tag{5.23}$$

where the function $g_1 : \mathbb{R} \to \mathbb{R}$ is defined as

$$\begin{aligned} \mathrm{g}_1(z) &\triangleq \mathbb{E}\left[\exp\left(\gamma_0 \mathrm{q}\left(U_1, U_2, \alpha\right)\right)\right] \\ &= \int_{-\infty}^{+\infty}\int_{-\infty}^{+\infty} \exp\left(\gamma_0 \mathrm{q}\left(x, y, z\right)\right) f_{U_1}(x) f_{U_2}(y)\, dxdy \\ &= \frac{1}{\pi}\int_{-\infty}^{+\infty} \exp\left(\gamma_0\left[(1-\rho^2)y^2 + 2\sqrt{1-\rho^2}zy + 2z^2\right] - y^2\right)\mathrm{g}_2(y, z)\, dy. \end{aligned} \tag{5.24}$$

We have thus implicity defined

$$\begin{aligned} \mathrm{g}_2(y, z) &= \int_{-\infty}^{+\infty} \exp\left(\gamma_0\left[(1+\rho^2)x^2 + 2(1+\rho)zx + 2\rho\sqrt{1-\rho^2}yx\right] - x^2\right)\, dx \\ &= \int_{-\infty}^{+\infty} \exp\left(-C_1 x^2 - x g_3(z)\right)\, dx \end{aligned} \tag{5.25}$$

where $C_1 = 1 - \gamma_0(1+\rho^2)$ and $\mathrm{g}_3(z) = -2\gamma_0\left([1+\rho]z + \rho\sqrt{1-\rho^2}y\right)$. Completing the square and rearranging the integrand as a Gaussian PDF we may then write

$$\begin{aligned} \mathrm{g}_2(y, z) &= \exp\left(\frac{\mathrm{g}_3^2(z)}{4A}\right)\int_{-\infty}^{+\infty} \exp\left(-C_1\left[x + \frac{\mathrm{g}_3(z)}{2C_1}\right]^2\right)\, dx \\ &= \sqrt{\frac{\pi}{C_1}}\exp\left(\frac{\mathrm{g}_3^2(z)}{4C_1}\right)\int_{-\infty}^{+\infty} \frac{1}{\sqrt{2\pi(2C_1)^{-1}}}\exp\left(-\frac{1}{2(2C_1)^{-1}}\left[x - \frac{-\mathrm{g}_3(z)}{2C_1}\right]^2\right)\, dx \\ &= \sqrt{\frac{\pi}{C_1}}\exp\left(\left[\mathrm{g}_4(z) + C_2 y\right]^2\right) \end{aligned} \tag{5.26}$$

where

$$(\mathrm{g}_4(z) + C_2 y)^2 = \frac{{\mathrm{g}_3}^2(z)}{4C_1} = \frac{\left[\gamma_0\left([1+\rho]z + \rho\sqrt{1-\rho^2}y\right)\right]^2}{1-\gamma_0(1+\rho^2)} \tag{5.27}$$

such that $\mathrm{g}_4(z) = \frac{1}{\sqrt{C_1}}\gamma_0(1+\rho)z$, and $C_2 = \frac{1}{\sqrt{C_1}}\gamma_0\rho\sqrt{1-\rho^2}$. Substituting this into (5.26) we may simplify (5.24) to

$$\begin{aligned}\mathrm{g}_1(z) &= \frac{1}{\pi}\sqrt{\frac{\pi}{C_1}}\int_{-\infty}^{+\infty}\exp\left(\gamma_0\left[(1-\rho^2)y^2 + 2\sqrt{1-\rho^2}zy + 2z^2\right] - y^2\right) \\ &\qquad\qquad \times \exp\left([\mathrm{g}_4(z) + C_2 y]^2\right)\, dy \\ &= \frac{1}{\pi}\sqrt{\frac{\pi}{C_1}}\int_{-\infty}^{+\infty}\exp\left(-C_3 y^2 - \mathrm{g}_5(z)y - \mathrm{g}_6(z)\right)\, dy\end{aligned} \tag{5.28}$$

requiring that $C_3 = \gamma_0(1-\rho^2) + C_2^2$, $\mathrm{g}_5(z) = 2\gamma_0\sqrt{1-\rho^2}z + 2C_2\mathrm{g}_4(z)$, and $g_6(z) = 2\gamma_0 z + g_4^2(z)$. Once again manipulating the integrand so that it is in the form of a Gaussian PDF, we may write

$$\begin{aligned}\mathrm{g}_1(z) &= \frac{1}{\pi}\sqrt{\frac{\pi}{C_1}}\exp(-\mathrm{g}_6(z))\int_{-\infty}^{+\infty}\exp\left(-C_3\left[y - \frac{\mathrm{g}_5(z)}{2C_3}\right]^2 + \frac{\mathrm{g}_5^2(z)}{4C_3}\right)\, dy \\ &= \frac{1}{\pi}\sqrt{\frac{\pi}{C_1}}\sqrt{\frac{\pi}{C_3}}\exp\left(\frac{\mathrm{g}_5^2(z)}{4C_3} - \mathrm{g}_6(z)\right)\int_{-\infty}^{+\infty}\exp\left(-\frac{1}{\sqrt{2\pi(2C_3)^{-1}}}\left[y - \frac{\mathrm{g}_5(z)}{2C_3}\right]^2\right)\, dy \\ &= \frac{1}{\sqrt{C_1 C_3}}\exp\left(\frac{\mathrm{g}_5^2(z)}{4C_3} - \mathrm{g}_6(z)\right).\end{aligned} \tag{5.29}$$

Finally, substituting (5.29) into (5.23) we may write the desired upper bound on the correlation between subcarrier error probabilities as

$$\begin{aligned}\mathbb{E}\left[P_{n,k_1}P_{n,k_2}\right] &\leq \frac{1}{4}\mathrm{g}_1(a)\mathrm{g}_1(0) \\ &= \frac{1}{4\sigma^4}\frac{1}{C_1 C_3}\exp\left(\frac{\mathrm{g}_5^2(a)}{4C_3} - \mathrm{g}_6(a)\right)\exp\left(\frac{\mathrm{g}_5^2(0)}{4C_3} - \mathrm{g}_6(0)\right) \\ &= \frac{1}{4\sigma^4}\frac{1}{C_1 C_3}\exp\left(\frac{\mathrm{g}_5^2(a)}{4C_3} - \mathrm{g}_6(a)\right)\end{aligned} \tag{5.30}$$

since it may be observed that $\mathrm{g}_5(0) = \mathrm{g}_6(0) = 0$. This readily calculable expression may be substituted into (5.4) to calculate a lower bound on the block error rate of an OFDM system transmitting over a Rician channel; or into (5.6) to upper bound the error in using the union bound approximation to the block error rate.

5.1.2 Rayleigh Fading Channels

For the special case of the Rayleigh fading channel a more exact calculation of the correlation $\mathbb{E}\left[P_{n,k_1}P_{n,k_2}\right]$ is possible. Each subchannel gain $|H_{n,k}|^2$ is marginally exponentially distributed and we let $\mathbb{E}\left[|H_{n,k}|^2\right] = 1$. The mean probability of error for each subchannel is then

$$\begin{aligned}\mathbb{E}\left[P_{n,k}\right] &\triangleq \overline{P_0} \\ &= \int_0^\infty \operatorname{erfc}\left(\sqrt{x\frac{E_0}{N_0}}\right)\exp\left(-x\right)dx \\ &= \frac{1}{2}\left(1-\sqrt{\frac{\gamma_0}{1+\gamma_0}}\right), \text{for all } n,k\end{aligned} \tag{5.31}$$

from [9]. Equation (5.31) may be used to calculate the union bound approximation to the OFDM block error rate. To calculate the lower bound and approximation error we require the correlation between subcarrier error probabilities, which may be written as

$$\begin{aligned}\mathbb{E}\left[P_{n,k_1}P_{n,k_2}\right] &= \frac{1}{4}\int_0^\infty\int_0^\infty \operatorname{erfc}\left(\sqrt{\gamma_0 x}\right)\operatorname{erfc}\left(\sqrt{\gamma_0 y}\right) f_{|H_1|^2,|H_2|^2}(x,y)\,dx\,dy \\ &= \frac{1}{4}\int_0^\infty\int_0^\infty \frac{1}{(1-\rho^2)}\operatorname{erfc}\left(\sqrt{\gamma_0 x}\right)\operatorname{erfc}\left(\sqrt{\gamma_0 y}\right) \\ &\qquad \exp\left(-\frac{x+y}{1-\rho^2}\right)\mathrm{I}_0\left(\frac{2\rho\sqrt{xy}}{1-\rho^2}\right)dx\,dy, \text{ for } k_1 \neq k_2\end{aligned} \tag{5.32}$$

where we have substituted the bivariate exponential PDF in equation (2.46). Consider the integral

$$\begin{aligned}\mathrm{g}_7(y) &\triangleq \int_0^\infty \operatorname{erfc}\left(\sqrt{\gamma_0 x}\right)\exp\left(-\frac{x}{1-\rho^2}\right)\mathrm{I}_0\left(\frac{2\rho\sqrt{xy}}{1-\rho^2}\right)dx \\ &= \sum_{i=0}^\infty \int_0^\infty \operatorname{erfc}\left(\sqrt{\gamma_0 x}\right)\exp\left(-\frac{x}{1-\rho^2}\right)\frac{1}{(i!)^2}\left[\frac{\rho^2 xy}{(1-\rho^2)^2}\right]^i dx\end{aligned} \tag{5.33}$$

using a series expansion for Bessel functions (Appendix A.12). A general term of this summation contains the integral

$$\begin{aligned}\mathrm{g}_8(i) &\triangleq \int_0^\infty \operatorname{erfc}\left(\sqrt{\gamma_0 x}\right)\exp\left(-\frac{x}{1-\rho^2}\right)x^i\,dx \\ &= 2(i!)(1-\rho^2)^{i+1}\int_0^\infty \frac{1}{2}\operatorname{erfc}\left(\sqrt{\gamma_0 x}\right)\frac{x^i}{(i!)(1-\rho^2)^{i+1}}\exp\left(-\frac{x}{1-\rho^2}\right)dx \\ &= 2(i!)(1-\rho^2)^{i+1}\left[\frac{1}{2}\left(1-\sqrt{\frac{\gamma_0(1-\rho^2)}{2+\gamma_0(1-\rho^2)}}\right)\right]^{i+1} \\ &\quad \times\sum_{n=0}^{i}\binom{i+n}{n}\left[\frac{1}{2}\left(1+\sqrt{\frac{\gamma_0(1-\rho^2)}{2+\gamma_0(1-\rho^2)}}\right)\right]^n\end{aligned} \tag{5.34}$$

using the closed form expression in [9, (14.4-17)]. We substitute $\mathrm{g}_8(i)$ into (5.33) to obtain

$$\begin{aligned}\mathrm{g}_7(y) = \sum_{i=0}^{\infty} \frac{2(\rho^2 y)^i}{i!(1-\rho^2)^{i-1}} \left[\frac{1}{2}\left(1 - \sqrt{\frac{\gamma_0(1-\rho^2)}{2+\gamma_0(1-\rho^2)}}\right)\right]^{i+1} \\ \times \sum_{n=0}^{i} \binom{i+n}{n} \left[\frac{1}{2}\left(1 + \sqrt{\frac{\gamma_0(1-\rho^2)}{2+\gamma_0(1-\rho^2)}}\right)\right]^{n}\end{aligned} \tag{5.35}$$

After substituting this into (5.32), and further use of (5.34), we may write the required correlation expression as

$$\mathbb{E}\left[P_{n,k_1} P_{n,k_2}\right] = \frac{1}{4} \sum_{i=0}^{\infty} \frac{1}{(i!)^2} \frac{\rho^{2i}}{(1-\rho^2)^{2i+1}} \left[\mathrm{g}_8(i)\right]^2 . \tag{5.36}$$

This expression allows simple numerical calculation of $\mathbb{E}\left[P_{n,k_1} P_{n,k_2}\right]$, since it may be shown to be rapidly convergent for $\rho \neq 1$.

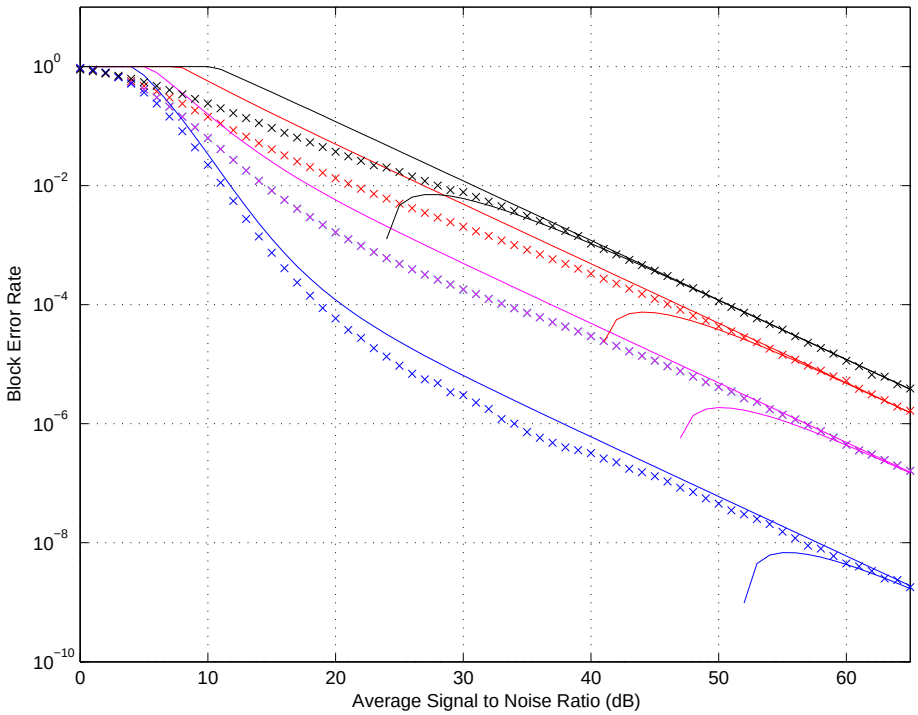

Figure 5.1 Analytical bounds (solid lines) and simulated (crosses) OFDM block error rate for $K_R = 0$ (black), 2 (red), 5 (magenta) and 10 (blue).

5.1.3 Simulations

We use the expressions (5.8), (5.31), (5.36) and (5.30) to calculate upper and lower bounds on the block error rate for a 48 subcarrier OFDM system. We assume the system occupies a total bandwidth of $8\mathrm{MHz}$ and transmits over a channel with exponential power delay profile, and rms delay spread of $15\mathrm{ns}$. This delay spread is consistent with an indoor wireless

environment [23,149], in which an IEEE802.11a [40] system would operate. Although these systems occupy a bandwidth of 16MHz for 48 subcarriers, we present a system with 8MHz bandwidth as this increases correlation between subchannels, and thus the error in the union bound approximation. We consider a Rayleigh fading channel, as well as channels with Rice factors of 2, 5, and 10. The block error rates of this OFDM system are simulated and plotted with the analytical bounds in Figure 5.1.

Observe from Figure 5.1 that the analytical bounds are consistent with the simulation results. The upper bounds are tight at moderate to high SNR, while the lower bound are accurate only at high SNR. However, the utility of the lower bounds is also in identifying the SNR ranges over which the upper bound may be used as an accurate approximation to the block error rate. That is, when the approximation error ϵ is small. Calculation of the higher order terms in (5.3) would afford tighter bounds than (5.4). However, analytical expressions for the higher order terms appear intractable.

5.2 Distribution of OFDM Symbol Errors

For OFDM systems employing a large number of subcarriers and transmitting over frequency selective channels, we may employ a length N block code, so that each block $\mathbf{S}_n$ of transmitted symbols is a codeword. The code redundancy is then contained within the subcarrier symbols of a single OFDM block. For example, consider an OFDM system with a large number of subcarriers, transmitting over a slowly fading channel and occupying a large bandwidth. In this case there will be large frequency diversity, and low time diversity, so that coding within an OFDM block may be more effective than over several blocks. Decoding delay is then less than that caused by error control systems that spread redundancy across consecutive OFDM blocks. It is also conceivable that we may wish to concatenate coding within a block, and across several blocks to exploit both time and frequency diversity.

Analysis of the performance of these codes requires the distribution of the number of symbol errors b within each OFDM block. That is, the probability that $b \in \{0, 1, 2, \ldots, N\}$ of the estimated symbols $\hat{S}_{n,1}, \hat{S}_{n,2}, \ldots, \hat{S}_{n,N}$ are in error. Since the channel response is time varying, b is then a random variable. Throughout this section we assume that the receiver has perfect knowledge of all the subchannel gains, and thus the probability of error on each subchannel. Furthermore, we assume the channel is described using the Jakes' model (Section 2.2.2).

In this section we show a method of estimating the PDF $f_b(x)$ of b. We then outline a measure of the error in our approximation. For the time varying channel this error is a random variable, and we wish to derive its stationary distribution [18]. That is, the long

term distribution of the error, ignoring any short term transient effects, such that we may disregard the effects of correlation in time. In the following sections we derive distributions for lower and upper bounds on the approximation error.

5.2.1 Poisson Approximation

Since we have knowledge of all subchannel gains, and the AWGN on each subcarrier is independent [80], the events $\mathcal{E}_{n,k}$ of estimating symbols $S_{n,k}$ incorrectly are independent for all n and k, with known respective probabilities $P_{n,k}$. The probability of exactly b subcarrier symbols in the n^{th} block being incorrectly estimated is then the probability of exactly b of the events $\mathcal{E}_{n,1}, \ldots, \mathcal{E}_{n,N}$ occurring. This is equivalent to the sum of N independent Bernoulli random variables [150], with probabilities $P_{n,k}$, for $k = 1, ..., N$. The probability mass function of b for the n^{th} block is then

$$\mathcal{L}_n(b) = \sum_{\forall \mathcal{I}_e} \left\{ P_{n,e_1} P_{n,e_2} \ldots P_{n,e_b} \times (1 - P_{n,c_1})(1 - P_{n,c_2}) \ldots \left(1 - P_{n,c_{N-b}}\right) \right\} \tag{5.37}$$

where $\mathcal{I}_e = \{e_1, e_2, \ldots, e_b\}$ is a set of b subcarrier indices, such that $\mathcal{I}_e \subseteq \{1, \ldots, N\}$ and $|\mathcal{I}_e| = b$; and $\mathcal{I}_c = \{c_1, c_2, \ldots, c_{N-b}\}$ is the set of remaining indices not in $\mathcal{I}_e$. Thus, $\mathcal{I}_e \cap \mathcal{I}_c = \{\}$, $\mathcal{I}_e \cup \mathcal{I}_c = \{1, \ldots, N\}$ and $|\mathcal{I}_c| = N - b$. The distribution $\mathcal{L}_n(b)$ is referred to as the *Poisson binomial distribution* or *generalised binomial distribution*. Note that the binomial distribution is a special case of this distribution, when $P_{n,1} = P_{n,2} = \ldots = P_{n,N}$, which arises in the case of a flat fading channel.

There are $\binom{N}{b}$ unique sets $\mathcal{I}_e$, so that calculation of the probability mass function $\mathcal{L}_n(b)$ requires the sum of $\binom{N}{b}$ products for $b = 0, 1, \ldots, N$. For $N \geq 30$ the calculation of so many terms is not practical with current technology. However, the Poisson binomial distribution is well approximated by the Poisson distribution [151–155] with PDF

$$\mathcal{P}_n(b) = \frac{\lambda_n^b e^{-\lambda_n}}{b!}, \text{ where } \lambda_n = \sum_{k=1}^{N} P_{n,k}. \tag{5.38}$$

An example of this approximation for transmission of a single block from a 1024 subcarrier OFDM system is shown in Figure 5.2. We obtain the simulation results in Figure 5.2 by fixing the channel response and simulating transmission of 5000 OFDM blocks, with average SNR of 10dB per subcarrier, to give an approximation to the Poisson binomial PDF of the number of errors for this channel response. The channel response was generated using the Jakes' channel model (Section 2.2.2), with exponential power delay profile and rms delay of 15ns. We assume BPSK transmission on each subcarrier, with perfect knowledge of subchannel gains at the receiver.

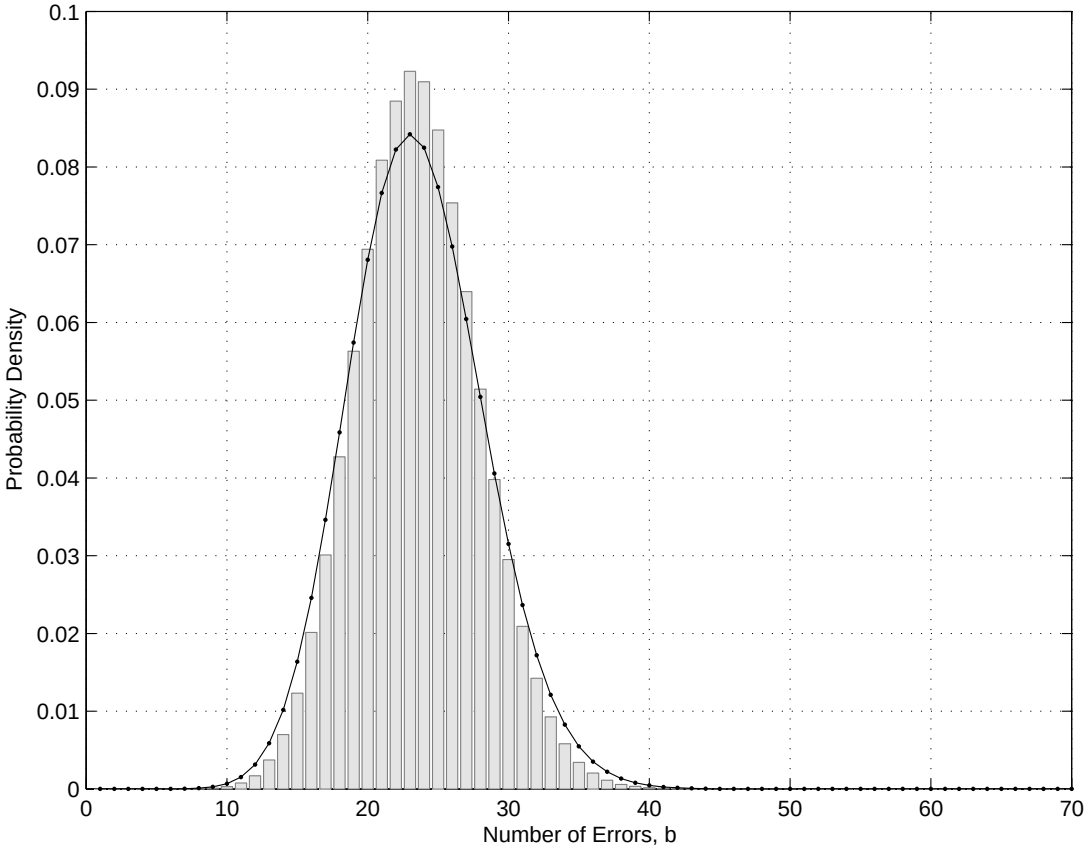

Figure 5.2 Simulated Error Rate Distribution (bars) and Poisson Approximation (solid line) for one Channel Realisation, 10dB SNR

A measure of the error in the approximation is the total variation distance, defined as

$$d\left\{\mathcal{L}_n(b), \mathcal{P}_n(b)\right\} = \frac{1}{2}\sum_{x=0}^{N} \left|\mathcal{L}_n(x) - \mathcal{P}_n(x)\right|. \tag{5.39}$$

Note that the Poisson binomial distribution probability mass function is readily calculated for small or large b, for example b $\in \{0, 1, 2, N-2, N-1, N\}$, so that $\binom{N}{b}$ is small. A residual variation distance measure may then be calculated by excluding these terms from the calculation in (5.39). For example, we could readily calculate

$$\begin{aligned} \tilde{d}\left\{\mathcal{L}_n(b), \mathcal{P}_n(b)\right\} &\triangleq \frac{1}{2}\sum_{x=1}^{N-1} \left|\mathcal{L}_n(x) - \mathcal{P}_n(x)\right| \\ &= d\left\{\mathcal{L}_n(b), \mathcal{P}_n(b)\right\} - \frac{1}{2}\left(\mathcal{L}_n(0) - \mathcal{P}_n(0)\right) - \frac{1}{2}\left(\mathcal{L}_n(N) - \mathcal{P}_n(N)\right) \end{aligned} \tag{5.40}$$

since $\mathcal{L}_n(0)$ and $\mathcal{L}_n(N)$ are readily calculable.

It is proven in [151] that the total variation distance between the Poisson binomial and

Poisson distributions is bounded by

$$\begin{aligned} d\left\{\mathcal{L}_n(b), \mathcal{P}_n(b)\right\} &\leq U_n = \frac{1-\exp\left(-\lambda_n\right)}{\lambda_n} \sum_{k=1}^{N} P_{n,k}^2 \\ d\left\{\mathcal{L}_n(.), \mathcal{P}_n(.)\right\} &\geq L_n = \frac{1}{32} \min\left\{\frac{1}{\lambda_n}, 1\right\} \sum_{k=1}^{N} P_{n,k}^2. \end{aligned} \tag{5.41}$$

Note that these bounds are random variables, since the channel error probabilities, and consequently the distributions $\mathcal{L}_n(b)$ and $\mathcal{P}_n(b)$, are time varying.

In the following subsections we derive approximations to the distributions of the bounds L_n and U_n for large finite N. We first show that the arithmetic average probability of error, and probability of error squared are both Gaussian distributed in the limit as $N \to \infty$. This is achieved by applying the Arcones-de Naranjo central limit theorem [134, 135], stated in Section 4.6.2, which necessitates first describing the Hermite rank of the arithmetic average probability of error and probability of error squared. We then show that U_n and L_n are approximated by the ratio of two correlated Gaussian random variables, for which we derive an explicit PDF. We finally simulate an OFDM system and compare our simulation results with the derived distributions.

5.2.2 Hermite Rank of Error Functions

Recall, from Section 4.4 that we may decompose each complex subchannel response $H_{n,k}$ into real zero mean Gaussian random variables $X_{n,k}$ and $Y_{n,k}$. Assuming BPSK transmission on each subchannel with average energy E_0, the probability of subcarrier symbol error is given in (5.1), and may be expressed as a nonlinear function $\mathrm{e} : \mathbb{R}^2 \to \mathbb{R}$ of the subchannel gain underlying Gaussian random variables. Namely,

$$P_{n,k} = \frac{1}{2}\mathrm{erfc}\left(\left|H_{n,k}\right| \sqrt{\gamma_0}\right) = \frac{1}{2}\mathrm{erfc}\left(\sqrt{\gamma_0}\sqrt{X_{n,k}^2 + Y_{n,k}^2}\right) \triangleq \mathrm{e}\left(X_{n,k}, Y_{n,k}\right). \tag{5.42}$$

In order to apply the Arcones-de Naranjo central limit theorem, we now prove that the Hermite rank $\varphi(\mathrm{e})$ of the function $\mathrm{e}\left(\cdot\right)$ is at least two, using the methodology of Section 4.6.1. Consider first a zero order polynomial $P_0(X_1, X_2) = \alpha_0$ of two zero mean iid Gaussian random variables X_1 and X_2. We may then write

$$\mathbb{E}\left[\left(\mathrm{e}\left(X_1, X_2\right) - \mathbb{E}\left[\mathrm{e}\left(X_1, X_2\right)\right]\right) P_0(X_1, X_2)\right] = \mathbb{E}\left[\mathrm{e}\left(X_1, X_2\right)\right] \alpha_0 - \mathbb{E}\left[\mathrm{e}\left(X_1, X_2\right)\right] \alpha_0 = 0 \tag{5.43}$$

for all $\alpha_0 \in \mathbb{R}$. Thus $\varphi(\mathrm{e}) \neq 0$. Now consider a first order polynomial $P_1(X_1, X_2) = \alpha_2 X_2 + \alpha_1 X_1 + \alpha_0$. We may then write

$$\mathbb{E}\left[\left(\mathrm{e}\left(X_1, X_2\right) - \mathbb{E}\left[\mathrm{e}\left(X_1, X_2\right)\right]\right) P_1(X_1, X_2)\right] = (\alpha_2 + \alpha_1)\mathbb{E}\left[X_1 \mathrm{e}\left(X_1, X_2\right)\right] \tag{5.44}$$

since X_1 and X_2 are zero mean and iid. Furthermore, substituting the Gaussian PDF and an alternative representation of the error function [144] we may write

$$\begin{aligned}\mathbb{E}\left[X_1 \mathrm{e}\left(X_1, X_2\right)\right] &= \frac{1}{2}\int_{-\infty}^{+\infty}\int_{-\infty}^{+\infty} \operatorname{erfc}\left(\sqrt{\gamma_0}\sqrt{x_1^2+x_2^2}\right)\exp\left(-\frac{x_1^2}{2}\right)\exp\left(-\frac{x_2^2}{2}\right)\,dx_1dx_2 \\ &= \frac{1}{\pi}\int_0^{\frac{\pi}{2}}\int_{-\infty}^{+\infty}\left\{\int_{-\infty}^{+\infty} x_1\exp\left(-\frac{2\gamma_0 x_1^2}{\sin^2\theta}\right)\exp\left(-\frac{x_1^2}{2}\right)\,dx_1\right\} \\ &\qquad\qquad \times\exp\left(-\frac{2\gamma_0 x_2^2}{\sin^2\theta}\right)\exp\left(-\frac{x_2^2}{2}\right)\,dx_2d\theta \\ &= 0\end{aligned} \tag{5.45}$$

since the integrand in x_1 is the product of two even functions and an odd function. Substituting (5.45) into (5.44) we may write

$$\mathbb{E}\left[\left(\mathrm{e}\left(X_1, X_2\right) - \mathbb{E}\left[\mathrm{e}\left(X_1, X_2\right)\right]\right)P_1(X_1, X_2)\right] = 0 \tag{5.46}$$

and therefore the Hermite rank $\varphi(\mathrm{e}) \neq 1$, so that $\varphi(\mathrm{e}) \geq 2$.

We similarly define the squared probability of error as a function, $\mathrm{esq} : \mathbb{R}^2 \to \mathbb{R}$, of the underlying Gaussian random variables of the subchannel response,

$$P_{n,k}^2 = \frac{1}{4}\left[\operatorname{erfc}\left(|H_{n,k}|\sqrt{\gamma_0}\right)\right]^2 = \frac{1}{4}\left[\operatorname{erfc}\left(\sqrt{\gamma_0}\sqrt{X_{n,k}^2+Y_{n,k}^2}\right)\right]^2 \triangleq \mathrm{esq}\left(X_{n,k}, Y_{n,k}\right). \tag{5.47}$$

Using the same methodology as above, it is readily shown that the Hermite rank $\varphi(\mathrm{esq})$ is greater than or equal to two. The condition requiring multiplication by the zero order polynomial follows from (5.43). For the case of a first order polynomial we find, as in (5.44), that

$$\mathbb{E}\left[\left(\mathrm{esq}\left(X_1, X_2\right) - \mathbb{E}\left[\mathrm{esq}\left(X_1, X_2\right)\right]\right)P_1(X_1, X_2)\right] = (\alpha_2+\alpha_1)\mathbb{E}\left[X_1\mathrm{esq}\left(X_1, X_2\right)\right]. \tag{5.48}$$

Using the Gaussian PDF and the $\operatorname{erfc}(\cdot)$ function representation of [144] we write

$$\begin{aligned}&\mathbb{E}\left[X_1\mathrm{esq}\left(X_1, X_2\right)\right] \\ &= \frac{1}{4}\int_{-\infty}^{+\infty}\int_{-\infty}^{+\infty}\left[\operatorname{erfc}\left(\sqrt{\gamma_0}\sqrt{x_1^2+x_2^2}\right)\right]^2\exp\left(-\frac{x_1^2}{2}\right)\exp\left(-\frac{x_2^2}{2}\right)\,dx_1dx_2 \\ &= \frac{1}{\pi^2}\int_0^{\frac{\pi}{2}}\int_0^{\frac{\pi}{2}}\int_{-\infty}^{+\infty}\exp\left(-\frac{2\gamma_0 x_2^2}{\sin^2\theta_1}\right)\exp\left(-\frac{2\gamma_0 x_2^2}{\sin^2\theta_2}\right)\exp\left(-\frac{x_2^2}{2}\right) \\ &\times\left\{\int_{-\infty}^{+\infty} x_1\exp\left(-\frac{2\gamma_0 x_1^2}{\sin^2\theta_1}\right)\exp\left(-\frac{2\gamma_0 x_1^2}{\sin^2\theta_2}\right)\exp\left(-\frac{x_1^2}{2}\right)dx_1\right\}dx_2d\theta_1d\theta_2 \\ &= 0\end{aligned} \tag{5.49}$$

since the integrand in $\{\cdot\}$ is the product of three even functions in x_1 and an odd function. It follows that $\varphi(\mathrm{esq}) \neq 1$, and therefore $\varphi(\mathrm{esq}) \geq 2$.

5.2.3 Distribution of the Average Error and Average Squared Error

Given that the Hermite rank of the probability of error function satisfies $\varphi(\mathrm{e}) \geq 2$ we may write

$$\begin{aligned} \sum_{\Delta k=-\infty}^{\infty} |\mathbb{E}\left[X_{n,1}X_{n,1+\Delta k}\right]|^{\varphi(\mathrm{e})} < \infty, \qquad \sum_{\Delta k=-\infty}^{\infty} |\mathbb{E}\left[Y_{n,1}Y_{n,1+\Delta k}\right]|^{\varphi(\mathrm{e})} < \infty \\ \sum_{\Delta k=-\infty}^{\infty} |\mathbb{E}\left[X_{n,1}Y_{n,1+\Delta k}\right]|^{\varphi(\mathrm{e})} < \infty, \qquad \sum_{\Delta k=-\infty}^{\infty} |\mathbb{E}\left[Y_{n,1}X_{n,1+\Delta k}\right]|^{\varphi(\mathrm{e})} < \infty \end{aligned} \tag{5.50}$$

since the above correlation terms approach zero with order $\frac{1}{\Delta k}$ or $\frac{1}{\Delta k^2}$, as shown in (4.15). We may then apply Theorem 4.1 to write

$$\frac{1}{\sqrt{N}} \sum_{k=1}^{N} \left\{\mathrm{e}\left(X_{n,k}, Y_{n,k}\right) - \mathbb{E}\left[\mathrm{e}\left(X_{n,k}, Y_{n,k}\right)\right]\right\} = \frac{1}{\sqrt{N}} \sum_{k=1}^{N} \left\{P_{n,k} - \mathbb{E}\left[P_{n,k}\right]\right\} \xrightarrow{D} \mathcal{N}\left(0, \Omega_P\right) \tag{5.51}$$

in the limit as $N \to \infty$, where

$$\Omega_P = \mathrm{var}\left[P_{n,k}\right] + 2\sum_{k=2}^{N} \mathrm{cov}\left[P_{n,1}P_{n,k}\right]. \tag{5.52}$$

This limiting distribution motivates the following statement. For large finite N the distribution of the arithmetic average probability of error $P_{n,av} = \frac{1}{N}\sum_{k=1}^{N} P_{n,k} = \frac{\lambda_n}{N}$ is approximated by the Gaussian distribution

$$\mathcal{N}\left(\overline{P_0}, \frac{1}{N}\Omega_P\right) \tag{5.53}$$

where $\overline{P_0}$ is the mean error probability, defined in (5.31). Note that $P_{n,av}$ is the sample mean of N correlated random variables $P_{n,1}, P_{n,2}, \ldots, P_{n,N}$. The variance $P_{n,av}$ of is

$$\mathrm{var}\left[P_{n,av}\right] = \mathrm{var}\left[P_{n,k}\right] + 2\sum_{k=2}^{N} \mathrm{cov}\left[P_{n,1}P_{n,k}\right]. \tag{5.54}$$

Readily calculable expressions for the variance and covariance terms in (5.52) may be found from Section 5.1.2. Therefore, the sample mean $P_{n,av}$ is approximately Gaussian distributed for large N, with known mean and variance.

We similarly apply Theorem 4.1 to the squared probability of error function. Since $\varphi(\mathrm{esq}) \geq$

2, the requisite series are convergent. That is,

$$\begin{aligned} \sum_{\Delta k=-\infty}^{\infty} |\mathbb{E}\left[X_{n,1}X_{n,1+\Delta k}\right]|^{\varphi(\text{esq})} < \infty, \qquad \sum_{\Delta k=-\infty}^{\infty} |\mathbb{E}\left[Y_{n,1}Y_{n,1+\Delta k}\right]|^{\varphi(\text{esq})} < \infty \\ \sum_{\Delta k=-\infty}^{\infty} |\mathbb{E}\left[X_{n,1}Y_{n,1+\Delta k}\right]|^{\varphi(\text{esq})} < \infty, \qquad \sum_{\Delta k=-\infty}^{\infty} |\mathbb{E}\left[Y_{n,1}X_{n,1+\Delta k}\right]|^{\varphi(\text{esq})} < \infty. \end{aligned} \tag{5.55}$$

We may then apply the Arcones-de Naranjo central limit theorem to the subchannel gain Gaussian random variables and the squared error probability function, to write

$$\frac{1}{\sqrt{N}} \sum_{k=1}^{N} \left\{ \text{esq}\left(X_{n,k}, Y_{n,k}\right) - \mathbb{E}\left[\text{esq}\left(X_{n,k}, Y_{n,k}\right)\right] \right\} = \frac{1}{\sqrt{N}} \sum_{k=1}^{N} \left\{ P_{n,k}^2 - \mathbb{E}\left[P_{n,k}^2\right] \right\} \xrightarrow{D} \mathcal{N}\left(0, \Omega_{P^2}\right) \tag{5.56}$$

in the limit as $N \to \infty$, where

$$\Omega_{P^2} = \text{var}\left[P_{n,k}^2\right] + 2\sum_{k=2}^{N} \text{cov}\left[P_{n,1}^2 P_{n,k}^2\right]. \tag{5.57}$$

This limiting distribution then motivates the following approximation. For large, finite N the distribution of the arithmetic average squared probability of error $P_{n,av}^2 = \frac{1}{N}\sum_{k=1}^{N} P_{n,k}^2$ is approximated by the Gaussian distribution

$$\mathcal{N}\left(\overline{P_0^2}, \frac{1}{N}\Omega_{P^2}\right) \tag{5.58}$$

where the mean of the squared probability of error $\overline{P_0^2} = \mathbb{E}\left[P_{n,k}^2\right]$ is given by (5.59). The variance and covariance terms in (5.57) are readily calculated using the following expressions.

Mean and Variance of the Squared Error Probability

Given BPSK transmission and unity mean Rayleigh fading subchannels, the mean of the probability of error squared is

$$\begin{aligned} \overline{P_0^2} &= \frac{1}{4}\int_0^{\infty} \left[\text{erfc}\left(\sqrt{\gamma_0 x}\right)\right]^2 f_{|H_{n,k}|^2}(x)\, dx \\ &= \frac{1}{4}\int_0^{\infty} \left[\text{erfc}\left(\sqrt{\gamma_0 x}\right)\right]^2 \exp(-x)\, dx \\ &= \frac{1}{4} - \frac{\arctan\left(\sqrt{\gamma_0^{-1}+1}\right)}{\pi\sqrt{\gamma_0^{-1}+1}} \end{aligned} \tag{5.59}$$

as shown in [145, App. 5A].

Using the Jakes' channel model, the correlation between the squared probability of error on any two distinct subchannels is

$$\begin{aligned}
&\mathbb{E}\left[P_{n,k_1}^2 P_{n,k_2}^2\right] \\
&= \frac{1}{4}\int_0^\infty \int_0^\infty \left[\operatorname{erfc}\left(\sqrt{\gamma_0 x}\right)\right]^2 \left[\operatorname{erfc}\left(\sqrt{\gamma_0 y}\right)\right]^2 f_{|H_{n,k_1}|^2,|H_{n,k_2}|^2}(x,y)\,dxdy \\
&= \frac{1}{1-\rho^2}\int_0^\infty \int_0^\infty \left[\operatorname{erfc}\left(\sqrt{\gamma_0 x}\right)\right]^2 \left[\operatorname{erfc}\left(\sqrt{\gamma_0 y}\right)\right]^2 \exp\left(-\frac{x+y}{1-\rho^2}\right) \mathrm{I}_0\left(\frac{2\rho\sqrt{xy}}{1-\rho^2}\right) dxdy \\
&= \frac{1}{1-\rho^2}\int_0^\infty \mathrm{g}_9(y) \left[\operatorname{erfc}\left(\sqrt{\gamma_0 y}\right)\right]^2 \exp\left(-\frac{y}{1-\rho^2}\right) dy, \text{ for } k_1 \neq k_2
\end{aligned} \tag{5.60}$$

where we have substituted the PDF from (2.46), with $\sigma^2 = \frac{1}{2}$. Furthermore, we have

$$\begin{aligned}
\mathrm{g}_9(y) &\triangleq \int_0^\infty \left[\operatorname{erfc}\left(\sqrt{\gamma_0 x}\right)\right]^2 \mathrm{I}_0\left(\frac{2\rho\sqrt{xy}}{1-\rho^2}\right) \exp\left(-\frac{x}{1-\rho^2}\right) dx \\
&= \sum_{i=0}^{\infty} \int_0^\infty \left[\operatorname{erfc}\left(\sqrt{\gamma_0 x}\right)\right]^2 \exp\left(-\frac{x}{1-\rho^2}\right) \frac{1}{(i!)^2} \left(\frac{\rho^2 xy}{[1-\rho^2]^2}\right)^i dx.
\end{aligned} \tag{5.61}$$

using a series expansions for Bessel functions (Appendix A.12). The i^{th} term in the summation of (5.61) may be rearranged to express the integral as

$$\begin{aligned}
D_i &= \frac{1}{i!}\int_0^\infty \left[\operatorname{erfc}\left(\sqrt{\gamma_0 x}\right)\right]^2 \exp\left(-\frac{x}{1-\rho^2}\right) x^i\,dx \\
&= \frac{1}{i!}\int_0^\infty \frac{4}{\pi^2}\int_0^{\frac{\pi}{2}}\int_0^{\frac{\pi}{2}} \exp\left(-\frac{x[\sin^2\theta_1+\sin^2\theta_2]}{\sin^2\theta_1\sin^2\theta_2}\right) \exp\left(-\frac{x}{1-\rho^2}\right) x^i\,d\theta_1 d\theta_2 dx \\
&= \frac{4}{\pi^2}\int_0^{\frac{\pi}{2}}\int_0^{\frac{\pi}{2}} \left(\frac{\sin^2\theta_1+\sin^2\theta_2}{\sin^2\theta_1\sin^2\theta_2} + \frac{1}{1-\rho^2}\right)^{-i-1} d\theta_1 d\theta_2
\end{aligned} \tag{5.62}$$

after applying an integral representation in Appendix A.6. This is readily evaluated numerically. We may then write (5.61) as

$$\mathrm{g}_9(y) = \sum_{i=0}^{\infty} \frac{1}{i!}\left(\frac{\rho^2 y}{[1-\rho^2]^2}\right)^i D_i \tag{5.63}$$

and substituting this into (5.60) we obtain

$$\begin{aligned}
&\mathbb{E}\left[P_{n,k_1}^2 P_{n,k_2}^2\right] \\
&= \frac{1}{1-\rho^2}\sum_{i=0}^{\infty}\frac{1}{i!}\left(\frac{\rho^2}{[1-\rho^2]^2}\right)^i D_i \int_0^\infty y^i \left[\operatorname{erfc}\left(\sqrt{\gamma_0 y}\right)\right]^2 \exp\left(-\frac{y}{1-\rho^2}\right) dy \\
&= \frac{1}{1-\rho^2}\sum_{i=0}^{\infty}\left(\frac{\rho^2}{[1-\rho^2]^2}\right)^i D_i^2, \text{ for } k_1 \neq k_2
\end{aligned} \tag{5.64}$$

which is a numerically calculable, since it may be show that the series converges rapidly.

For the special case of $k_1 = k_2$ we require

$$\mathbb{E}\left[P_{n,k}^4\right] = \frac{1}{16}\int_0^\infty \left[\operatorname{erfc}\left(\sqrt{\gamma_0 x}\right)\right]^4 \exp(-x^2)dx. \tag{5.65}$$

Substituting $u = \sqrt{\gamma_0 x}$ and integrating by parts we may write

$$\begin{aligned}
\mathbb{E}\left[P_{n,k}^4\right] &= \frac{1}{16}\left[\operatorname{erfc}(0)\right]^4 - \frac{1}{2\sqrt{\pi}}\int_0^\infty \left[\operatorname{erfc}(u)\right]^3 \exp\left(-\frac{u^2[1+\gamma_0]}{\gamma_0}\right) du \\
&= \frac{1}{16} - \frac{2}{\pi^2\sqrt{\pi}}\int_0^{\frac{\pi}{2}}\int_0^{\frac{\pi}{2}}\int_0^\infty \operatorname{erfc}(u) \\
&\qquad \times \exp\left(-\frac{-u^2\left[\sin^2\theta_1 + \left(\sin^2\theta_1 + \gamma_0 + \gamma_0\sin^2\theta_1\right)\sin^2\theta_2\right]}{\gamma_0\sin^2\theta_1\sin^2\theta_2}\right) d\theta_1 d\theta_2 du \\
&= \frac{1}{16} - \frac{2}{\pi^3}\int_0^{\frac{\pi}{2}}\int_0^{\frac{\pi}{2}} \frac{\arctan\left(\sqrt{\frac{\sin^2\theta_1+\left(\sin^2\theta_1+\gamma_0+\gamma_0\sin^2\theta_1\right)\sin^2\theta_2}{\gamma_0\sin^2\theta_1\sin^2\theta_2}}\right)}{\sqrt{\frac{\sin^2\theta_1+\left(\sin^2\theta_1+\gamma_0+\gamma_0\sin^2\theta_1\right)\sin^2\theta_2}{\gamma_0\sin^2\theta_1\sin^2\theta_2}}} d\theta_1 d\theta_2
\end{aligned} \tag{5.66}$$

where we have applied an integral representation from Appendix A.7. We have therefore obtained a finite range integral expression for the fourth moment of the subcarrier probability of error. This expression may then be numerically evaluated.

5.2.4 Accuracy of Poisson Approximation

In the limit as $N \to \infty$ we may write the bounds (5.41) on the total variation distance as

$$\begin{aligned}
\lim_{N\to\infty}\{L_n\} &= \lim_{N\to\infty}\left\{\frac{1}{32}\min\left\{\frac{1}{\lambda_n}, 1\right\}\sum_{k=1}^N P_{n,k}^2\right\} = \frac{\sum_{k=1}^N P_{n,k}^2}{32\lambda_n} = \frac{P_{n,av}^2}{32\,P_{n,av}} \\
\lim_{N\to\infty}\{U_n\} &= \lim_{N\to\infty}\left\{\frac{1-\exp(-\lambda_n)}{\lambda_n}\sum_{k=1}^N P_{n,k}^2\right\} = \frac{\sum_{k=1}^N P_{n,k}^2}{\lambda_n} = \frac{P_{n,av}^2}{P_{n,av}}.
\end{aligned} \tag{5.67}$$

For large, finite N we may then approximate L_n and U_n as the respective limits in (5.67). The upper and lower bounds then have the limiting distribution of the ratio of the Gaussian random variables, $P_{n,av}^2$ and $P_{n,av}$. However, these random variables are correlated. This distribution of the ratio of two correlated Gaussian random variables may be found from the distribution of the ratio of two independent Gaussian random variables, as shown in Appendix B. Using this result we may then approximate the distribution of U_n, for large N, as

$$f_U(x) = \frac{a_1\exp\left(-\frac{1}{2}\left[a_2^2+a_3^2\right]\right)}{\pi\left[a_1^2+(x-a_4^2\right]}\left[1+\sqrt{\frac{\pi}{2}}\,h(x)\operatorname{erf}\left(\frac{h(x)}{\sqrt{2}}\right)\exp\left(\frac{[h(x)]^2}{2}\right)\right] \tag{5.68}$$

where

$$\begin{aligned} a_1 &= \sqrt{1-\rho(P_{av},P_{av}^2)}\sqrt{\frac{\Omega_{P^2}}{\Omega_P}} \\ a_2 &= \frac{1}{\sqrt{1-\rho(P_{av},P_{av}^2)}}\left[\frac{\mathbb{E}\left[P_{n,av}^2\right]}{\sqrt{\frac{1}{N}\Omega_{P^2}}} - \frac{\rho(P_{av},P_{av}^2)\mathbb{E}\left[P_{n,av}\right]}{\sqrt{\frac{1}{N}\Omega_P}}\right] \\ a_3 &= \frac{\mathbb{E}\left[P_{n,av}\right]}{\sqrt{\frac{1}{N}\Omega_P}} \qquad a_4 = \rho(P_{av},P_{av}^2)\sqrt{\frac{\Omega_{P^2}}{\Omega_P}} \\ h(x) &= \frac{a_1a_3 + a_2(x-a_4)}{\sqrt{a_1^2+(x-a_4)^2}} \end{aligned} \tag{5.69}$$

and $\rho(P_{av},P_{av}^2)$ is the coefficient of correlation between $P_{n,av}$ and $P_{n,av}^2$. The limiting distribution of L_n has a similar form to (5.68). The correlation coefficient $\rho(P_{av},P_{av}^2)$ is readily calculated using the following result.

Correlation between $P_{n,av}$ and $P_{n,av}^2$

We may calculate the correlation coefficient $\rho(P_{av},P_{av}^2)$ given the correlation

$$\mathbb{E}\left[P_{n,k_1}^2 P_{n,k_2}\right] = \frac{1}{8}\int_0^\infty\int_0^\infty \left[\operatorname{erfc}\left(\sqrt{\gamma_0 x}\right)\right]^2 \operatorname{erfc}\left(\sqrt{\gamma_0 y}\right) f_{|H_1|^2|H_2|^2}(x,y)\,dxdy. \tag{5.70}$$

Note that this may be expressed as

$$\mathbb{E}\left[P_{n,k_1}^2 P_{n,k_2}\right] = \frac{1}{2[1-\rho^2]}\int_0^\infty \left[\operatorname{erfc}\left(\sqrt{\gamma_0 y}\right)\right]^2 \exp\left(-\frac{y}{1-\rho^2}\right)\mathrm{g}_7(y)dy \tag{5.71}$$

where $\mathrm{g}_7(y)$ is defined in (5.33). Furthermore, substituting (5.34), (5.35) and (5.62) we obtain the readily calculable expression

$$\mathbb{E}\left[P_{n,k_1}^2 P_{n,k_2}\right] = \sum_{i=0}^{\infty}\frac{1}{2i!}\frac{\rho^{2i}}{(1-\rho^2)^{2i+1}}\left[\frac{1-\rho^2}{2-\rho^2}\right]^{-\frac{i+1}{2}} D_i\,\mathrm{g}_8(i). \tag{5.72}$$

For the special case where $k_1 = k_2$ we may write

$$\begin{aligned} &\mathbb{E}\left[P_{n,k}^3\right] = \\ &\frac{1}{8}\int_0^\infty \left[\operatorname{erfc}\left(\sqrt{\gamma_0 x}\right)\right]^3 f_{|H_{n,k}|^2}(x)\,dx \\ &= \frac{1}{8} - \frac{3}{2\pi\sqrt{\pi}}\int_0^{\frac{\pi}{2}}\int_0^\infty \exp\left(\frac{-u^2[\gamma_0+\gamma_0\sin^2\theta+\sin^2\theta]}{\gamma_0\sin^2\theta}\right)\operatorname{erfc}(u)\,dud\theta \\ &= \frac{1}{8} - \frac{3}{2\pi^2}\int_0^{\frac{\pi}{2}} \arctan\left(\sqrt{\frac{\gamma_0+\gamma_0\sin^2\theta+\sin^2\theta}{\gamma_0\sin^2\theta}}\right)\left[\frac{\gamma_0+\gamma_0\sin^2\theta+\sin^2\theta}{\gamma_0\sin^2\theta}\right]^{-\frac{1}{2}} d\theta \end{aligned} \tag{5.73}$$

where we have substituted $u = \sqrt{\gamma_0 x}$, integrated by parts and applied the result in Appendix A.7.

5.2.5 Simulations and Discussion

We consider a 1024 subcarrier OFDM system transmitting over a Rayleigh fading channel with an exponential power delay profile and maximum excess delay of 50ns. We assume the system occupies a 320MHz bandwidth with carrier frequency 5.1GHz and receiver velocity of 15m/s. Due to the large number of subcarriers, calculation of the exact probability of b errors for $3 \leq b \leq 1022$ is infeasible.

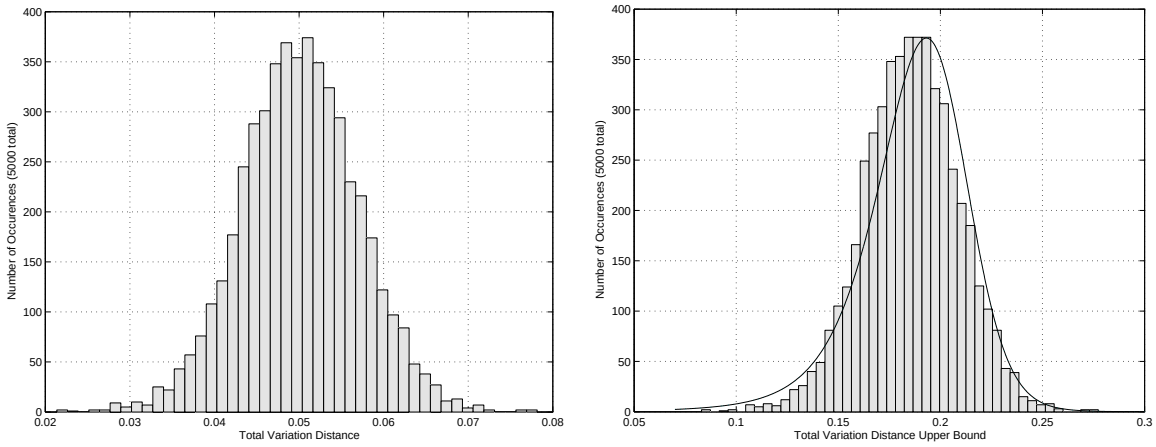

(a) Total variation distance distribution

(b) Upper bound distribution

Figure 5.3 Simulated (bars) and analytical (line) distributions of total variation distance and upper Bound.

We consider transmission over 5000 consecutive simulated fading channel realisations. For each channel realisation we simulate transmission of 10^7 blocks, and thus estimate the Poisson binomial distribution of errors for that channel realisation. We then calculate the total variation distance between the estimated distribution and the Poisson approximation, as well as the upper bound on total variation distance (5.41) for each realisation.

We display the distribution of the total variation distance between the simulated distribution of errors and the Poisson approximation, for all 5000 realisations, in Figure 5.3(a). In Figure 5.3(b) we plot the derived approximating distribution (5.68) of the upper bound on the total variation distance and the simulated distribution of this upper bound. It is observed that the PDF of (5.68) is a good approximation to the density of the simulated upper bound on total variation distance. Similar results are readily obtained for the lower bound. The analytical distribution of the upper bound on total variation distance is skewed to the left of the simulated distribution, as shown in Figure 5.3(b). This skew suggests that the analytical model gives a slightly weaker upper bound to the total variation distance. Thus, the analysis gives a slightly more conservative upper bound on the distribution of the time

varying error incurred when we estimate the distribution of the number of symbol errors in an OFDM block with the Poisson distribution. For systems with larger N it is observed that the approximation appears tighter.

Note that this analysis may be readily extended to the case of QAM transmission, since the error probability for QAM transmission may be written as a linear combination of $\mathrm{erfc}(\cdot)$ functions. For brevity, this is not described here, however the methodology is the same as detailed for the BPSK case. Using the same methods we may show that the Hermite rank of the probability of error for QAM transmission is greater than or equal to two. For QAM, readily calculable expressions for the probability of error correlation are not as forthcoming, however numerical integration may be used.

5.3 Summary

We have presented two analytical results concerning wireless OFDM systems. We have first examined the block error rate of uncoded OFDM systems, an important measure for analysing coding over successive OFDM blocks. We have derived a lower bound on the probability of OFDM block error for both Rician channels and Rayleigh channels with arbitrary parameters. Our analysis includes a readily calculable expression for the correlation between the probability of error on two correlated channels. These correlations are useful in several other applications, including the evaluation of MIMO performance with correlated subchannels, or Markov modelling of receiver error processes [141, 142].

We have then examined the distribution of symbol errors within an OFDM block. We have observed that this follows the Poisson binomial distribution, which is well approximated by the Poisson distribution. For OFDM systems transmitting over Rayleigh fading channels we have derived the distribution of upper and lower bounds on the total variation distance between the true distribution and Poisson approximation. This analysis includes the derivation of useful correlation expressions for the error and squared error probabilities on correlated Rayleigh fading channels.

These two results are useful in the analysis of code design for OFDM systems transmitting over frequency selective, fading channels. OFDM systems with a smaller number of subcarriers may employ codes such that each codeword symbol is an OFDM block. The error performance of these codes is then dependent on the block error rate. The tight bounds on the block error rate will allow judicious choice of code, so that a given rate of decoding error may be satisfied. Larger OFDM systems may employ coding within each block, such that each subcarrier symbol is a codeword symbol. The error performance of the code is then determined by the distribution of the number of erroneously demodulated OFDM symbols within each block. We have shown that this distribution is well approximated

by the Poisson distribution, and we may simplify analysis by using this approximation. Should one wish to bound the error in the approximation we have derived the distribution of an upper bound on the total variation distance between the true Poisson binomial distribution and the Poisson distribution approximation. We use this approximation in the following chapter, where we analyse the performance of a coded OFDM system with a large number of subcarriers.

Chapter 6

Lattice Coding for OFDM Systems

Lattice coding of OFDM systems is considered in this chapter. The analysis herein is original. OFDM data is encoded so that each block represents a lattice point, thereby exploiting the high coding gain of lattices. We first outline the encoding procedure and give some examples, then discuss the problem of decoding the lattice points. Specifically, we detail the optimal decoding metric, as well as the optimal lattice properties for transmission over frequency selective channels. We then propose the use of multistage GMD decoding, and provide a comprehensive analysis of lattice encoded, GMD decoded OFDM systems. As a case study we consider transmission of points from the 128 dimensional Barnes-Wall lattice, over a 64 subcarrier OFDM system, and show that high coding gains are possible with relatively low decoding complexity.

6.1 Lattice Encoding

OFDM systems are well suited to lattice codes. Given an $\frac{N}{2}$ subcarrier OFDM system transmitting two dimensional subcarrier points, the OFDM block may be elegantly represented as a single point $\mathbf{x}$ in N dimensional Euclidean space. Lattice coding of the OFDM block simply requires restriction of $\mathbf{x}$ such that it is an element of some N dimensional lattice Λ, or an equivalent sphere packing. Since OFDM systems typically employ a large number (48 or more) of subcarriers we consider high dimensional lattices ($N \geq 48$), with large coding gain. We outline a simple method for restricting the OFDM block to be points from a lattice, or more strictly speaking, a sphere packing.

Since lattices have infinite cardinality we must choose some finite cardinality subset $\Lambda_f \subset \Lambda$ from which we map a signal constellation. Furthermore, as outlined in Section 3.5 we require some mapping $\mathbf{m} : \Lambda_f \rightarrow \mathcal{M}_N$ from the lattice subset to some subset $\mathcal{M}_N = \mathcal{M}_2^{\frac{N}{2}}$

of the $\frac{N}{2}$-fold Cartesian product of the two dimensional subcarrier constellations $\mathcal{M}_2$. We denote the mapping of the entire lattice by $\mathcal{M} = \mathbf{m}(\Lambda)$, which typically does not form a lattice since we remove the zero point $\mathbf{0} = \{0, 0, \ldots, 0\}$. However, provided the mapping may be expressed as

$$\mathbf{m}(\mathbf{x}) = a\mathbf{T}\mathbf{x} + \mathbf{t} \forall \mathbf{x} \in \Lambda \tag{6.1}$$

where a is a scalar, $\mathbf{T}$ is an orthogonal $N \times N$ matrix and $\mathbf{t} = \{b, b, \ldots, b\}$ is a length N vector containing a single scalar b; the sphere packing $\mathcal{M} = \mathbf{m}(\Lambda)$ then retains the packing density and coding gain of Λ [7].

As in previous chapters, we denote the k^{th} subcarrier symbol transmitted during the n^{th} block as $S_{n,k}$. $S_{n,k}$ is from the constellation $\mathcal{M}_2$, which we restrict to be a square M^2-ary QAM constellation with minimum energy $2E_0$. Assuming (without loss of generality) that Λ has unit minimum distance $d_{\min}(\Lambda) = 1$, this is equivalent to defining the lattice subset to be

$$\Lambda_f \triangleq \{\mathbf{x} = \{x_1, x_2, \ldots, x_N\} \in \Lambda : 0 \leq x_i \leq M\} \tag{6.2}$$

and using the mapping

$$\mathbf{m}(x) = 2\sqrt{E_0}\mathbf{x} + \left\{(M-1)\sqrt{E_0}, \ldots, (M-1)\sqrt{E_0}\right\}, \text{for all } \mathbf{x} \in \Lambda_f. \tag{6.3}$$

We are thus employing a cubic constellation [74], since all points $\mathbf{x}$ are contained within an N dimensional cube of side length M. Although this mapping affords no shaping gain [74] and does not reduce the peak to average power ratio, it ensures compatibility with existing high data rate OFDM systems [40, 87] which use QAM constellations. Each pair of lattice dimensions are mapped to a QAM constellation, or equivalently each lattice dimension is mapped to an M-ary PAM constellation, denoted

$$\mathcal{M}_1 = \left\{-(M-1)\sqrt{E_0}, -(M-3)\sqrt{E_0}, \ldots, -\sqrt{E_0}, \sqrt{E_0}, \ldots, (M-3)\sqrt{E_0}, (M-1)\sqrt{E_0}\right\}. \tag{6.4}$$

Each OFDM block $\mathbf{S}_n = \{S_{n,1}, \ldots, S_{n,\frac{N}{2}}\}$ is then a point from an N dimensional sphere packing $\mathcal{M}_N = \mathcal{M}_2^{N/2} = \mathcal{M}_1^N \subset \mathbb{R}^N$. Note that a single OFDM block comprises $\frac{N}{2}$ orthogonal M^2-ary QAM points, equivalent to N M-ary PAM points.

As an example, consider a 64 subcarrier OFDM system transmitting 256-QAM points from a lattice code based on a 128 dimensional construction C lattice, P_{128}. Specifically,

$$P_{128} \triangleq \bigcup_{\mathbf{c}^{(1)} \in RM(1,7), \mathbf{c}^{(2)} \in RM(3,7), \mathbf{c}^{(3)} \in RM(5,7)} \left\{8\mathbb{Z}^{128} + 4\mathbf{c}^{(3)} + 2\mathbf{c}^{(2)} + \mathbf{c}^{(1)}\right\} \tag{6.5}$$

where $RM(1,7)$, $RM(3,7)$ and $RM(5,7)$ are the first, third and fifth order, length 128 Reed-Muller codes respectively. These are $(128, 8, 64)$, $(128, 64, 16)$ and $(128, 120, 4)$ linear

block codes respectively. P_{128} has 9.03dB coding gain [7, Chap. 5.6]. We refer to P_{128} as the 128 dimensional Barnes-Wall lattice, since P_{128} has the same coding gain and kissing number as this lattice, although it is not strictly equivalent [7]. Since we are employing 256-QAM constellations, we require $M = 16$ and restrict the signal constellation to points mapped from the subset of P_{128} within the 128 dimensional cube with opposite vertices at $\{0, \ldots, 0\}$ and $\{15, \ldots, 15\}$. Thus, the finite lattice subset may be expressed as

$$\Lambda_f = \bigcup_{\mathbf{c}^{(4)} \in RM(7,7), \mathbf{c}^{(3)} \in RM(5,7), \mathbf{c}^{(2)} \in RM(3,7), \mathbf{c}^{(1)} \in RM(1,7)} \left\{ 8\mathbf{c}^{(4)} + 4\mathbf{c}^{(3)} + 2\mathbf{c}^{(2)} + \mathbf{c}^{(1)} \right\} \quad (6.6)$$

where $RM(7,7)$ is the trivial $(128, 128, 1)$ Reed-Muller code, so that $8\mathbf{c}^{(4)} \in 8\mathbb{Z}^{128}$.

In order to choose a point $\mathbf{x} \in \Lambda_f$ we may input blocks of 128, 120, 64 and 8 uncoded data bits to encoders for the codes $RM(7,7)$, $RM(5,7)$, $RM(3,7)$ and $RM(1,7)$, respectively, thus obtaining the four length 128 codewords $\mathbf{c}^{(4)}$, $\mathbf{c}^{(3)}$, $\mathbf{c}^{(2)}$ and $\mathbf{c}^{(1)}$ respectively. Note, however, that $RM(7,7)$ simply outputs the uncoded bits. This lattice code then has rate $\frac{128+120+64+8}{4\times128} = 0.625$. Each coordinate is then mapped to a 16-PAM constellation via

$$\mathbf{m}(\mathbf{x}) = 2\sqrt{E_0}\mathbf{x} - \left\{ 15\sqrt{E_0}, \ldots, 15\sqrt{E_0} \right\} \quad (6.7)$$

so that $\mathbf{m}(x)$ is an element of the 64-fold Cartesian product of a squared 256-QAM constellation within minimum energy $2E_0$ and average energy $E_{av} = 170E_0$.

6.2 Decoding

At the receiver we obtain some channel perturbed and noise corrupted version of the transmitted lattice point. We must then estimate the transmitted lattice point. In the following subsection we extend the work of [156] and [157] to derive the optimal metric for maximum likelihood decoding of lattice encoded OFDM transmission over Rayleigh fading frequency selective channels. We show that this is the Euclidean distance between the received point and the mapped lattice points. In Section 6.2.2 we discuss the criteria for choosing good lattices for lattice encoded OFDM, and show that maximising the lattice product distance is critical for reducing the error rate.

6.2.1 Optimal Decoding Metric for OFDM

We employ an $\frac{N}{2}$ subcarrier OFDM system and transmit a block $\mathbf{S}_n = \{S_{n,1}, S_{n,2}, \ldots, S_{n,N}\}$ $= \mathbf{m}(\mathbf{x})$, mapped from a lattice point $\mathbf{x} \in \Lambda$, so that $\mathbf{S}_n$ is a point in an N dimensional sphere packing. Assuming sufficient guard interval and synchronisation so that intersymbol interference is negligible and subcarrier orthogonality is preserved, at the receiver we obtain a channel perturbed and AWGN corrupted signal point. We may write the transmitted

block as the diagonal $\frac{N}{2}$ by $\frac{N}{2}$ complex matrix

$$\mathbf{S}_n = \begin{bmatrix} S_{n,1} & 0 & 0 & \dots & 0 \\ 0 & S_{n,2} & 0 & \dots & 0 \\ 0 & 0 & S_{n,3} & \dots & 0 \\ \vdots & \vdots & \vdots & \ddots & \vdots \\ 0 & 0 & 0 & \dots & S_{n,N/2} \end{bmatrix}. \tag{6.8}$$

Note that, for the remainder of Section 6.2.1 we retain the symbol $\mathbf{S}_n$ to denote the above matrix of transmitted symbols, although this was previously used to denote the vector of transmitted symbols. Permitting a similar discrepancy, we may also define diagonal complex matrices comprising each subchannel gain and additive white Gaussian noise component as

$$\mathbf{H}_n = \begin{bmatrix} H_{n,1} & 0 & 0 & \dots & 0 \\ 0 & H_{n,2} & 0 & \dots & 0 \\ 0 & 0 & H_{n,3} & \dots & 0 \\ \vdots & \vdots & \vdots & \ddots & \vdots \\ 0 & 0 & 0 & \dots & H_{n,\frac{N}{2}} \end{bmatrix}, \qquad \mathbf{W}_n = \begin{bmatrix} W_{n,1} & 0 & 0 & \dots & 0 \\ 0 & W_{n,2} & 0 & \dots & 0 \\ 0 & 0 & W_{n,3} & \dots & 0 \\ \vdots & \vdots & \vdots & \ddots & \vdots \\ 0 & 0 & 0 & \dots & W_{n,\frac{N}{2}} \end{bmatrix} \tag{6.9}$$

respectively. Each $W_{n,k}$, for $k = 1, \dots, \frac{N}{2}$, is an independent mean zero complex Gaussian random variable with one dimensional variance $\frac{N_0}{2}$. Each $H_{n,k}$, for $k = 1, \dots, \frac{N}{2}$, is a complex Gaussian random variable, which we assume has one dimensional variance $\frac{1}{2}$. Furthermore, letting $\dagger$ denote the matrix Hermitian transpose, we may write the correlation matrices

$$\mathbf{\Theta}_{WW} = \frac{1}{2}\mathbb{E}\left[\mathbf{W}_n \mathbf{W}_n^{\dagger}\right] = \begin{bmatrix} N_0 & 0 & 0 & \dots & 0 \\ 0 & N_0 & 0 & \dots & 0 \\ 0 & 0 & N_0 & \dots & 0 \\ \vdots & \vdots & \vdots & \ddots & \vdots \\ 0 & 0 & 0 & \dots & N_0 \end{bmatrix} = N_0 \mathbf{I}_{\frac{N}{2}} \tag{6.10}$$

$$\mathbf{\Theta}_{HH} = \frac{1}{2}\mathbb{E}\left[(H_{n,1}, \dots, H_{n,N})^{\dagger}(H_{n,1}, \dots, H_{n,N})\right] = \begin{bmatrix} \rho(0) & \rho(1) & \rho(2) & \dots & \rho\left(\frac{N}{2}\right) \\ \rho(1) & \rho(0) & \rho(1) & \dots & \rho\left(\frac{N}{2}\right) \\ \rho(2) & \rho(1) & \rho(0) & \dots & \rho\left(\frac{N}{2}\right) \\ \vdots & \vdots & \vdots & \ddots & \vdots \\ \rho\left(\frac{N}{2}\right) & \rho\left(\frac{N}{2}-1\right) & \rho\left(\frac{N}{2}-2\right) & \dots & \rho(0) \end{bmatrix} \tag{6.11}$$

where $\mathbf{I}_{\frac{N}{2}}$ is the $\frac{N}{2}$ by $\frac{N}{2}$ identity matrix, and the correlation $\rho(\Delta k)$ between subchannel gains is given by (4.17). We may then write the received symbols, in matrix form, as

$$\mathbf{R}_n = \begin{bmatrix} R_{n,1} & 0 & 0 & \dots & 0 \\ 0 & R_{n,2} & 0 & \dots & 0 \\ 0 & 0 & R_{n,3} & \dots & 0 \\ \vdots & \vdots & \vdots & \ddots & \vdots \\ 0 & 0 & 0 & \dots & R_{n,\frac{N}{2}} \end{bmatrix} = \mathbf{S}_n\mathbf{H}_n + \mathbf{W}_n. \tag{6.12}$$

Assuming perfect knowledge of the subchannel gains at the receiver, a maximum likelihood (ML) detector [9] generates an estimate $\hat{\mathbf{S}}_n$ of the transmitted block by choosing

$$\hat{\mathbf{S}}_n = \underset{\mathbf{S}_n}{\operatorname{argmax}} \left\{ \Pr\left(\mathbf{S}_n|\mathbf{R}_n, \mathbf{H}_n\right) \right\} = \underset{\mathbf{S}_n}{\operatorname{argmax}} \left\{ \Pr\left(\mathbf{R}_n, \mathbf{H}_n|\mathbf{S}_n\right) \right\}. \tag{6.13}$$

To determine the maximum likelihood decoding criterion we then require the joint conditional probability density function $\Pr\left(\mathbf{R}_n, \mathbf{H}_n|\mathbf{S}_n\right)$. This is equivalent to calculating the probability density function (PDF) of the vector

$$\mathbf{\Psi}_n = \left[R_{n,1}, R_{n,2}, \dots, R_{n,\frac{N}{2}}, H_{n,1}, H_{n,2}, \dots, H_{n,\frac{N}{2}}\right]^T \tag{6.14}$$

conditioned on $\mathbf{S}_n$. Note that $H_{n,k}$, and $R_{n,k}$ given $S_{n,k}$, are zero mean complex Gaussian random variables, for $k = 1, \dots, \frac{N}{2}$, so that $\mathbf{\Psi}_n$ has a multivariate Gaussian probability distribution function. We may write this as

$$f_{\mathbf{\Psi}_n}\left(\mathbf{\Psi}_n|\mathbf{S}_n\right) = \frac{\exp\left(-\frac{1}{2}\mathbf{\Psi}_n^\dagger \mathbf{\Theta}_{\Psi\Psi|\mathbf{S}_n}^{-1} \mathbf{\Psi}_n\right)}{(2\pi)^N \det\left[\mathbf{\Theta}_{\Psi\Psi|\mathbf{S}_n}\right]} \tag{6.15}$$

where $\mathbf{\Theta}_{\mathbf{\Psi}\mathbf{\Psi}|\mathbf{S}_n}$ is the correlation matrix of $\mathbf{\Psi}_n$. This correlation matrix is defined as

$$\mathbf{\Theta}_{\Psi\Psi|\mathbf{S}_n} = \frac{1}{2}\mathbb{E}\left[\mathbf{\Psi}_n\mathbf{\Psi}_n^\dagger\right] = \begin{bmatrix} \mathbf{\Theta}_{RR} & \mathbf{\Theta}_{RH} \\ \mathbf{\Theta}_{HR} & \mathbf{\Theta}_{HH} \end{bmatrix} \tag{6.16}$$

where

$$\begin{aligned} \mathbf{\Theta}_{RR} &= \frac{1}{2}\mathbb{E}\left[\mathbf{R}_n\mathbf{R}_n^\dagger\right] = \frac{1}{2}\mathbb{E}\left[\left(\mathbf{S}_n\mathbf{H}_n + \mathbf{W}_n\right)\left(\mathbf{S}_n\mathbf{H}_n + \mathbf{W}_n\right)^\dagger\right] = \mathbf{S}_n\mathbf{\Theta}_{HH}\mathbf{S}_n^\dagger + N_0\mathbf{I}_{\frac{N}{2}} \\ \mathbf{\Theta}_{RH} &= \frac{1}{2}\mathbb{E}\left[\mathbf{\Psi}_n\mathbf{H}_n^\dagger\right] = \frac{1}{2}\mathbb{E}\left[\left(\mathbf{S}_n\mathbf{H}_n + \mathbf{W}_n\right)\mathbf{H}_n^\dagger\right] = \mathbf{S}_n\mathbf{\Theta}_{HH} \\ \mathbf{\Theta}_{HR} &= \frac{1}{2}\mathbb{E}\left[\mathbf{H}_n\mathbf{\Psi}_n^\dagger\right] = \frac{1}{2}\mathbb{E}\left[\mathbf{H}_n\left(\mathbf{S}_n\mathbf{H}_n + \mathbf{W}_n\right)^\dagger\right] = \mathbf{\Theta}_{HH}\mathbf{S}_n^\dagger \end{aligned} \tag{6.17}$$

since $\mathbb{E}\left[\mathbf{W}_n\mathbf{H}_n^\dagger\right] = \mathbb{E}\left[\mathbf{H}_n\mathbf{W}_n^\dagger\right] = 0$.

Substituting (6.15) into (6.13) and recognising that the $\ln(\cdot)$ function is monotonic increasing, with some manipulation we may then write the ML decoder output as

$$\begin{aligned}\hat{\mathbf{S}}_n &= \underset{\mathbf{S}_n}{\operatorname{argmax}} \left\{ \frac{\exp\left(-\frac{1}{2}\boldsymbol{\Psi}_n^\dagger \boldsymbol{\Theta}_{\Psi\Psi|\mathbf{S}_n}^{-1} \boldsymbol{\Psi}_n\right)}{(2\pi)^N \det\left[\boldsymbol{\Theta}_{\Psi\Psi|\mathbf{S}_n}\right]} \right\} \\ &= \underset{\mathbf{S}_n}{\operatorname{argmax}} \left\{ \ln\left(\frac{\exp\left(-\frac{1}{2}\boldsymbol{\Psi}_n^\dagger \boldsymbol{\Theta}_{\Psi\Psi|\mathbf{S}_n}^{-1} \boldsymbol{\Psi}_n\right)}{(2\pi)^N \det\left[\boldsymbol{\Theta}_{\Psi\Psi|\mathbf{S}_n}\right]} \right) \right\} \\ &= \underset{\mathbf{S}_n}{\operatorname{argmin}} \left\{ \frac{1}{2}\boldsymbol{\Psi}_n^\dagger \boldsymbol{\Theta}_{\Psi\Psi|\mathbf{S}_n}^{-1} \boldsymbol{\Psi}_n + \ln\left(\det[\boldsymbol{\Theta}_{\Psi\Psi|\mathbf{S}_n}]\right) + N\ln 2\pi \right\} \\ &= \underset{\mathbf{S}_n}{\operatorname{argmin}} \left\{ M_d\left(\mathbf{S}_n\right) \right\}\end{aligned} \tag{6.18}$$

where the ML decoding metric is

$$M_d\left(\mathbf{S}_n\right) = \boldsymbol{\Psi}_n^\dagger \boldsymbol{\Theta}_{\Psi\Psi|\mathbf{S}_n}^{-1} \boldsymbol{\Psi}_n + 2\ln\left(\det\left[\boldsymbol{\Theta}_{\Psi\Psi|\mathbf{S}_n}\right]\right). \tag{6.19}$$

We may further simplify this decoding metric by substituting (6.17) into (6.16) and applying an identity for the inverse of a partitioned matrix from [158, p. 41][1], yielding

$$\boldsymbol{\Theta}_{\Psi\Psi|\mathbf{S}_n}^{-1} = \begin{bmatrix} \frac{1}{N_0}\mathbf{I}_{\frac{N}{2}} & -\frac{1}{N_0}\mathbf{S}_n \\ -\frac{1}{N_0}\mathbf{S}_n^\dagger & \boldsymbol{\Theta}_{HH}^{-1} + \frac{1}{N_0}\mathbf{S}_n^\dagger \mathbf{S}_n \end{bmatrix}. \tag{6.20}$$

With some manipulation we may then write the first term of $M_d\left(\mathbf{S}_n\right)$ as

$$\begin{aligned}\boldsymbol{\Psi}_n^\dagger \boldsymbol{\Theta}_{\Psi\Psi|\mathbf{S}_n}^{-1} \boldsymbol{\Psi}_n &= \begin{bmatrix} \mathbf{S}_n^\dagger & \mathbf{H}_n^\dagger \end{bmatrix} \begin{bmatrix} \frac{1}{N_0}\mathbf{I}_{\frac{N}{2}} & -\frac{1}{N_0}\mathbf{S}_n \\ -\frac{1}{N_0}\mathbf{S}_n^\dagger & \boldsymbol{\Theta}_{HH}^{-1} + \frac{1}{N_0}\mathbf{S}_n^\dagger \mathbf{S}_n \end{bmatrix} \begin{bmatrix} \mathbf{S}_n \\ \mathbf{H}_n \end{bmatrix} \\ &= \frac{1}{N_0}\left(\mathbf{R}_n - \mathbf{S}_n\mathbf{H}_n\right)\left(\mathbf{R}_n - \mathbf{S}_n\mathbf{H}_n\right)^\dagger + \mathbf{H}_n \boldsymbol{\Theta}_{HH}^{-1} \mathbf{H}_n^\dagger \\ &= \mathbf{H}_n \boldsymbol{\Theta}_{HH}^{-1} \mathbf{H}_n^\dagger + \frac{1}{N_0}\sum_{k=1}^{\frac{N}{2}} \left|R_{n,k} - S_{n,k}H_{n,k}\right|^2.\end{aligned} \tag{6.21}$$

[1] Note that there is a typographical error in [158, p.41]. The equation $A^{-1} = \begin{bmatrix} X & XQS^{-1} \\ -S^{-1}RX & W \end{bmatrix}$ should instead read $A^{-1} = \begin{bmatrix} X & -XQS^{-1} \\ -S^{-1}RX & W \end{bmatrix}$.

Furthermore, the second term in $M_d(\mathbf{S}_n)$ may be written as

$$\begin{aligned} 2\ln\left(\det\left[\mathbf{\Theta}_{\Psi\Psi|\mathbf{S}_n}\right]\right) &= 2\ln\left(\det\begin{bmatrix}\mathbf{S}_n\mathbf{\Theta}_{HH}\mathbf{S}_n^\dagger + N_0\mathbf{I}_{\frac{N}{2}} & \mathbf{S}_n\mathbf{\Theta}_{HH}\\ \mathbf{\Theta}_{HH}\mathbf{S}_n^\dagger & \mathbf{\Theta}_{HH}\end{bmatrix}\right) \\ &= 2\ln\left(\det\begin{bmatrix}\mathbf{S}_n & \mathbf{I}_{\frac{N}{2}}\\ \mathbf{I}_{\frac{N}{2}} & \mathbf{0}\end{bmatrix}\det\begin{bmatrix}\mathbf{\Theta}_{HH} & \mathbf{0}\\ \mathbf{0} & N_0\mathbf{I}_{\frac{N}{2}}\end{bmatrix}\det\begin{bmatrix}\mathbf{S}_n^\dagger & \mathbf{I}_{\frac{N}{2}}\\ \mathbf{I}_{\frac{N}{2}} & \mathbf{0}\end{bmatrix}\right) \\ &= 2\ln\left(N_0^{\frac{N}{2}}\det\left[\mathbf{\Theta}_{HH}\right]\right). \end{aligned} \tag{6.22}$$

Finally, substituting (6.21) and (6.22) into (6.19), and removing the terms independent of $\mathbf{S}_n$ we may write an equivalent ML decoding metric as

$$\tilde{M}_d(\mathbf{S}_n) = \sum_{k=0}^{\frac{N}{2}} |R_{n,k} - S_{n,k}H_{n,k}|^2. \tag{6.23}$$

Therefore, a maximum likelihood decoder should select the point $\mathbf{S}_n$ such that the Euclidean distance between the received point $\mathbf{R}_n$ and the channel perturbed point $\mathbf{H}_n\mathbf{S}_n$ is minimised. Note that this is an intuitive result, and is analogous to the derivation of the maximum likelihood sequence detector [9]. Using this result we may then show the important lattice properties for minimising the receiver lattice point error rate, as follows.

6.2.2 Optimal Lattices for Wideband OFDM

In an additive white Gaussian noise or flat fading environment it is well known that lattices with the highest possible density, or coding gain, provide the lowest error rates for moderate to high SNR [7,58]. However, for lattice encoded OFDM systems operating over frequency selective channels, we show that at high SNR the lowest error performance is provided by maximising the product distance of the lattice, which we define. This is analogous to similar results [45] for lattices transmitted with single carrier systems over fading channels.

Consider the maximum likelihood decoder described in Section 6.2.1. Assuming that during the n^{th} time interval we transmit some point $\mathbf{S}_{(1)}$ from the N dimensional sphere packing $\mathcal{M}_N$, then the decoder will incorrectly select the point $\mathbf{S}_{(2)} \neq \mathbf{S}_{(1)}$ if

$$\tilde{M}_d\left(\mathbf{S}_{(2)}\right) < \tilde{M}_d\left(\mathbf{S}_{(1)}\right); \tag{6.24}$$

or equivalently, from (6.19),

$$\mathbf{\Psi}_n^\dagger\mathbf{\Theta}^{-1}_{\Psi\Psi|\mathbf{S}_{(1)}}\mathbf{\Psi}_n + 2\ln\left(\det\left[\mathbf{\Theta}_{\Psi\Psi|\mathbf{S}_{(1)}}\right]\right) < \mathbf{\Psi}_n^\dagger\mathbf{\Theta}^{-1}_{\Psi\Psi|\mathbf{S}_{(2)}}\mathbf{\Psi}_n + 2\ln\left(\det\left[\mathbf{\Theta}_{\Psi\Psi|\mathbf{S}_{(2)}}\right]\right). \tag{6.25}$$

We may then write the probability of the event that the decoder outputs $\mathbf{S}_{(2)}$ when $\mathbf{S}_{(1)}$ is transmitted as

$$\begin{aligned}
&\Pr\left(\mathbf{S}_{(1)} \to \mathbf{S}_{(2)}\right) \\
&= \Pr\left(\boldsymbol{\Psi}_n^\dagger \boldsymbol{\Theta}_{\Psi\Psi|\mathbf{S}_{(1)}}^{-1} \boldsymbol{\Psi}_n + 2\ln\left(\det\left[\boldsymbol{\Theta}_{\Psi\Psi|\mathbf{S}_{(1)}}\right]\right) < \boldsymbol{\Psi}_n^\dagger \boldsymbol{\Theta}_{\Psi\Psi|\mathbf{S}_{(2)}}^{-1} \boldsymbol{\Psi}_n + 2\ln\left(\det\left[\boldsymbol{\Theta}_{\Psi\Psi|\mathbf{S}_{(2)}}\right]\right)\right) \\
&= \Pr\left(\boldsymbol{\Psi}_n^\dagger \left[\boldsymbol{\Theta}_{\Psi\Psi|\mathbf{S}_{(2)}}^{-1} - \boldsymbol{\Theta}_{\Psi\Psi|\mathbf{S}_{(1)}}^{-1}\right] \boldsymbol{\Psi}_n < 2\ln\left(\frac{\det\left[\boldsymbol{\Theta}_{\Psi\Psi|\mathbf{S}_{(1)}}\right]}{\det\left[\boldsymbol{\Theta}_{\Psi\Psi|\mathbf{S}_{(2)}}\right]}\right)\right) \\
&= \Pr\left(\Omega < \omega\right)
\end{aligned} \tag{6.26}$$

where

$$\begin{aligned}
\Omega &= \boldsymbol{\Psi}_n^\dagger \left[\boldsymbol{\Theta}_{\Psi\Psi|\mathbf{S}_{(2)}}^{-1} - \boldsymbol{\Theta}_{\Psi\Psi|\mathbf{S}_{(1)}}^{-1}\right] \boldsymbol{\Psi}_n \\
&= \boldsymbol{\Psi}_n^\dagger \left\{ \begin{bmatrix} \frac{1}{N_0}\mathbf{I}_{\frac{N}{2}} & -\frac{1}{N_0}\mathbf{S}_{(1)} \\ -\frac{1}{N_0}\mathbf{S}_{(1)}^\dagger & \boldsymbol{\Theta}_{HH}^{-1} + \frac{1}{N_0}\mathbf{S}_{(1)}^\dagger \mathbf{S}_{(1)} \end{bmatrix} - \begin{bmatrix} \frac{1}{N_0}\mathbf{I}_{\frac{N}{2}} & -\frac{1}{N_0}\mathbf{S}_{(2)} \\ -\frac{1}{N_0}\mathbf{S}_{(2)}^\dagger & \boldsymbol{\Theta}_{HH}^{-1} + \frac{1}{N_0}\mathbf{S}_{(2)}^\dagger \mathbf{S}_{(2)} \end{bmatrix} \right\} \boldsymbol{\Psi}_n \\
&= \boldsymbol{\Psi}_n^\dagger \begin{bmatrix} 0 & \frac{1}{N_0}\left(\mathbf{S}_{(2)} - \mathbf{S}_{(1)}\right) \\ -\frac{1}{N_0}\left(\mathbf{S}_{(1)}^\dagger - \mathbf{S}_{(2)}^\dagger\right) & \frac{1}{N_0}\left(\mathbf{S}_{(1)}^\dagger \mathbf{S}_{(1)} - \mathbf{S}_{(2)}^\dagger \mathbf{S}_{(2)}\right) \end{bmatrix} \boldsymbol{\Psi}_n \\
\omega &= 2\ln\left(\frac{\det\left[\boldsymbol{\Theta}_{\Psi\Psi|\mathbf{S}_{(1)}}\right]}{\det\left[\boldsymbol{\Theta}_{\Psi\Psi|\mathbf{S}_{(2)}}\right]}\right) = 2\ln\left(\frac{N_0^{\frac{N}{2}} \det\left[\boldsymbol{\Theta}_{HH}\right]}{N_0^{\frac{N}{2}} \det\left[\boldsymbol{\Theta}_{HH}\right]}\right) = 0
\end{aligned} \tag{6.27}$$

from (6.20) and (6.22).

We denote the PDF of Ω, implicitly conditioned on $\mathbf{S}_{(1)}$ and $\mathbf{S}_{(2)}$, as $f_\Omega(x)$. Since $\boldsymbol{\Theta}_{HH}$ is a real symmetric matrix, then $\left(\mathbf{S}_{(1)}\boldsymbol{\Theta}_{HH}\mathbf{S}_{(1)}^\dagger + N_0\mathbf{I}_{\frac{N}{2}}\right)$ and $\left(\mathbf{S}_{(2)}\boldsymbol{\Theta}_{HH}\mathbf{S}_{(2)}^\dagger + N_0\mathbf{I}_{\frac{N}{2}}\right)$ are similarly real and symmetric. Moreover, from (6.16) and (6.17) observe that $\boldsymbol{\Theta}_{\Psi\Psi|\mathbf{S}_{(1)}}$ and $\boldsymbol{\Theta}_{\Psi\Psi|\mathbf{S}_{(2)}}$ are Hermitian matrices, and consequently $\left[\boldsymbol{\Theta}_{\Psi\Psi|\mathbf{S}_{(2)}}^{-1} - \boldsymbol{\Theta}_{\Psi\Psi|\mathbf{S}_{(1)}}^{-1}\right]$ is Hermitian. Since $\boldsymbol{\Psi}_n$ is a zero mean vector of complex Gaussian random variables, we may then use a result from [159] to write the two sided Laplace transform [160] characteristic function of Ω as

$$\begin{aligned}
\phi_\Omega(s) &\triangleq \int_{-\infty}^{\infty} f_\Omega(x)\exp(-sx)\,dx \\
&= \frac{1}{\det\left[\mathbf{I}_{\frac{N}{2}} - 2s\boldsymbol{\Theta}_{\Psi\Psi|\mathbf{S}_{(1)}}\left(\boldsymbol{\Theta}_{\Psi\Psi|\mathbf{S}_{(2)}}^{-1} - \boldsymbol{\Theta}_{\Psi\Psi|\mathbf{S}_{(1)}}^{-1}\right)\right]} \\
&= \frac{1}{\det\left[\mathbf{I}_{\frac{N}{2}} - 2s\boldsymbol{\Theta}_{\Psi\Psi|\mathbf{S}_{(1)}}\boldsymbol{\Theta}_{\Psi\Psi|\mathbf{S}_{(2)}}^{-1} + 2s\mathbf{I}_{\frac{N}{2}}\right]}.
\end{aligned} \tag{6.28}$$

The poles of the characteristic function are then given by the nonsingular eigenvalues of

$\boldsymbol{\Theta}_{\Psi\Psi|\mathbf{S}_{(1)}}\left(\boldsymbol{\Theta}^{-1}_{\Psi\Psi|\mathbf{S}_{(2)}} - \boldsymbol{\Theta}^{-1}_{\Psi\Psi|\mathbf{S}_{(1)}}\right)$.

We may then find the required pairwise error probability by taking the inverse two sided Laplace transform of (6.28) and integrating. Thus,

$$\Pr\left(\mathbf{S}_{(1)} \to \mathbf{S}_{(2)}\right) = \Pr\left(\Omega < 0\right) = \int_{-\infty}^{0}\left[\frac{1}{2\pi j}\oint_{\mathrm{Br}}\phi_{\Omega}(s)\exp(sx)ds\right]dx \tag{6.29}$$

where the integral in $[\cdot]$ above is the Bromwich contour integral [161], extending over $s = \sigma - jR$ to $s = \sigma + jR$, as R approaches infinity.

Since each element of $\boldsymbol{\Psi}_n$ is an independent Gaussian random variable, we may express Ω as a sum of random variables. That is,

$$\begin{aligned}\Omega &= \Omega^{(1)} + \Omega^{(2)} + \ldots + \Omega^{(N)}, \text{ where}\\ \Omega^{(k)} &= \Psi_k \sum_{i=1}^{N}\left\{\boldsymbol{\Theta}^{-1}_{\Psi\Psi|\mathbf{S}_{(1)}}(k,i) - \boldsymbol{\Theta}^{-1}_{\Psi\Psi|\mathbf{S}_{(2)}}(k,i)\right\}\Psi_k^{\dagger} \quad \text{for } k = 1,\ldots,N\end{aligned} \tag{6.30}$$

where $\boldsymbol{\Theta}^{-1}_{\Psi\Psi|\mathbf{S}_{(1)}}(k,i)$ is the element on the k^{th} row, i^{th} column of $\boldsymbol{\Theta}^{-1}_{\Psi\Psi|\mathbf{S}_{(1)}}$. Each $\Omega^{(k)}$ is then the sum of exponential random variables, and manipulating the result in [9, Appendix 4B] we may write the two sided Laplace transform characteristic functions as

$$\phi_{\Omega^{(k)}}(s) = \frac{p_{k,1}\,p_{k,2}}{(s-p_{k,1})\,(s-p_{k,2})} \tag{6.31}$$

with poles

$$p_{k,1}, p_{k,2} = \frac{1}{\frac{1}{N_0}d_k^2 \pm \sqrt{\left(\frac{1}{N_0}d_k^2\right)^2 - \frac{1}{N_0}d_k^2}} \quad \text{for } d_k \neq 0 \tag{6.32}$$

where d_k^2 is the squared Euclidean distance between $S_{(1),k}$ and $S_{(2),k}$; that is

$$d_k^2 = \left|S_{(1),k} - S_{(2),k}\right|^2. \tag{6.33}$$

In the case where the k^{th} elements, $S_{(1),k}$ and $S_{(2),k}$, of the codewords are equal, the corresponding k^{th} columns of $\boldsymbol{\Theta}^{-1}_{\Psi\Psi|\mathbf{S}_{(1)}} - \boldsymbol{\Theta}^{-1}_{\Psi\Psi|\mathbf{S}_{(2)}}$ will be zero. In this case $\Omega^{(k)} = 0$, and the characteristic function is $\phi_{\Omega^{(k)}}(s) = 1$. We define the set of indices where $\mathbf{S}_{(1)}$ and $\mathbf{S}_{(2)}$ differ as

$$L = \left\{k : S_{(1),k} \neq S_{(2),k} : 1 \leq k \leq \frac{N}{2}\right\}. \tag{6.34}$$

so that we may write (6.28) as the product of characteristic functions

$$\phi_{\Omega}(s) = \prod_{k\in L}\phi_{\Omega^{(k)}}(s) = \prod_{k\in L}\frac{p_{k,1}\,p_{k,2}}{(s-p_{k,1})\,(s-p_{k,2})}. \tag{6.35}$$

From (6.28), observe that the non-zero eigenvalues of $\boldsymbol{\Theta}_{\Psi\Psi|\mathbf{S}_{(1)}}\left(\boldsymbol{\Theta}^{-1}_{\Psi\Psi|\mathbf{S}_{(2)}}-\boldsymbol{\Theta}^{-1}_{\Psi\Psi|\mathbf{S}_{(1)}}\right)$ correspond to the $k, k+\frac{N}{2}$ rows of $\boldsymbol{\Theta}_{\Psi\Psi|\mathbf{S}_{(1)}}\left(\boldsymbol{\Theta}^{-1}_{\Psi\Psi|\mathbf{S}_{(2)}}-\boldsymbol{\Theta}^{-1}_{\Psi\Psi|\mathbf{S}_{(1)}}\right)$ where $k \in L$. The non-zero eigenvalues are then equivalent to the eigenvalues of $\tilde{\boldsymbol{\Theta}}_{\Psi\Psi|\mathbf{S}_{(1)}}\tilde{\boldsymbol{\Theta}}^{-1}$, where $\tilde{\boldsymbol{\Theta}}_{\Psi\Psi|\mathbf{S}_{(1)}}$ consists of the $k, k+\frac{N}{2}$ rows and columns of $\boldsymbol{\Theta}_{\Psi\Psi|\mathbf{S}_{(1)}}$, where $k \in L$, and similarly, $\tilde{\boldsymbol{\Theta}}^{-1}$ consists of all $k, k+\frac{N}{2}$ rows and columns of $\left(\boldsymbol{\Theta}^{-1}_{\Psi\Psi|\mathbf{S}_{(2)}}-\boldsymbol{\Theta}^{-1}_{\Psi\Psi|\mathbf{S}_{(1)}}\right)$, such that $k \in L$. Both $\tilde{\boldsymbol{\Theta}}_{\Psi\Psi|\mathbf{S}_{(1)}}$ and $\tilde{\boldsymbol{\Theta}}^{-1}$ are then $2|L| \times 2|L|$ matrices. We may thus write

$$\phi_{\Omega}(s) = \frac{1}{\det\left[\mathbf{I}_N - 2s\tilde{\boldsymbol{\Theta}}_{\Psi\Psi|\mathbf{S}_{(1)}}\tilde{\boldsymbol{\Theta}}^{-1}\right]}. \tag{6.36}$$

The poles of $\phi_{\Omega}(s)$ are then given by the $2|L|$ eigenvalues, denoted $\lambda_{k,1}, \lambda_{k,2}$ for $k \in |L|$, of $\tilde{\boldsymbol{\Theta}}_{\boldsymbol{\Psi\Psi}|\mathbf{S}_{(1)}}\tilde{\boldsymbol{\Theta}}^{-1}$. Specifically,

$$p_{k,1} = -\frac{1}{2\lambda_{k,1}}, \quad p_{k,2} = -\frac{1}{2\lambda_{k,2}}. \tag{6.37}$$

We could find the eigenvalues of $\tilde{\boldsymbol{\Theta}}_{\Psi\Psi|\mathbf{S}_{(1)}}\tilde{\boldsymbol{\Theta}}^{-1}$ and perform the integration of (6.29) to calculate the pairwise error probability. However, following [156] we recognise that the integral of the inverse Laplace transform, in (6.29), may be written as

$$\Pr\left(\mathbf{S}_{(1)} \to \mathbf{S}_{(2)}\right) = \int_{-\infty}^{0}\left[\frac{1}{2\pi j}\oint_{\mathrm{Br}}\phi_{\Omega}(s)ds\right]dx = -\sum_{\forall p_r}\mathrm{Residue}\left\{\frac{1}{s}\phi_{\Omega}(s)\right\} \tag{6.38}$$

where p_r denotes the right half plane poles of $\frac{1}{s}\phi_{\Omega}(s)$. Note, from (6.32) that the poles $\{p_{k,1} : k \in L\}$ of $\phi_{\Omega}(s)$ lie in the right half plane, and the poles $\{p_{k_2} : k \in L\}$ lie in the left half plane. Furthermore, $\frac{1}{s}\phi_{\Omega}(s)$ has an additional pole at $s = 0$, whose residue is $\prod_{k\in L} p_{k,1}p_{k,2}$. Then, using the formula for the residue of a pole [162] we may write (6.38) as

$$\Pr\left(\mathbf{S}_{(1)} \to \mathbf{S}_{(2)}\right) = -\left(\prod_{k\in L} p_{k,1}p_{k,2}\right)\sum_{k\in L}\lim_{s\to p_{k,1}}\left\{\frac{1}{s}\prod_{\substack{i\in L\\ i\neq k}}\frac{1}{(s-p_{i,1})(s-p_{i,2})}\right\}. \tag{6.39}$$

Consider the product of poles term $\prod_{k\in L} p_{k,1}p_{k,2}$ in this expression; we may relate this to the eigenvalues $\lambda_{k,1}, \lambda_{k,2}$ as

$$\prod_{k\in L} p_{k,1}p_{k,2} = \prod_{k\in L}\frac{1}{4\lambda_{k,1}\lambda_{k,2}} = \frac{1}{4^{|L|}\det\left[\tilde{\boldsymbol{\Theta}}_{\boldsymbol{\Psi\Psi}|\mathbf{S}_{(1)}}\tilde{\boldsymbol{\Theta}}^{-1}\right]}. \tag{6.40}$$

It follows from (6.22) that we may write $\det\left[\tilde{\boldsymbol{\Theta}}_{\boldsymbol{\Psi\Psi}|\mathbf{S}_{(1)}}\right] = N_0^{|L|}\det\left[\boldsymbol{\Theta}_{HH}\right]$, and in Appendix

C we show that $\det\left[\tilde{\mathbf{\Theta}}^{-\mathbf{1}}\right] = \frac{(-1)^{|L|}}{N_0^{2|L|}} \prod_{k\in L} d_k^2$. We may then write

$$\prod_{k\in L} p_{k,1}p_{k,2} = \frac{1}{(-4)^{|L|} N_0^{-|L|} \det\left[\mathbf{\Theta}_{HH}\right] \prod_{k\in L} d_k^2}. \tag{6.41}$$

We then consider the behaviour of the poles at high SNR, that is as $\frac{d_k^2}{N_0} \to \infty$, for $k \in L$. Observe from (6.32) that $p_{k,1} \to 0$ and $p_{k,2} \to \frac{1}{2}$, so that we may write

$$\begin{aligned}
\lim_{\frac{d_k^2}{N_0}\to\infty} \sum_{k\in L} \lim_{s\to p_{k,1}} \left\{ \frac{1}{s} \prod_{\substack{i\in L \\ i\neq k}} \frac{1}{(s-p_{k,1})(s-p_{k,2})} \right\} &= \sum_{k\in L} \lim_{s\to p_{k,1}} \frac{1}{s^{|L|+1}\left(s-\frac{1}{2}\right)^{|L|}} \\
&= \lim_{s\to\frac{1}{2}} \frac{1}{(|L|-1)!} \frac{d^{|L|-1}}{ds^{|L|-1}} \left\{ \frac{\left(s-\frac{1}{2}\right)^{|L|}}{s^{|L|+1}\left(s-\frac{1}{2}\right)^{|L|}} \right\} \\
&= \lim_{s\to-\frac{1}{2}} \frac{1}{(|L|-1)!} \frac{(-1)^{|L|}(2|L|-1)!}{|L|!} \frac{1}{s^{2|L|}} \\
&= \frac{(2|L|-1)!(-4)^{|L|}}{(|L|-1)!|L|!}
\end{aligned} \tag{6.42}$$

using the formula [162] for the residue of an n^{th} order pole. Using [163] we recognise that

$$\frac{(2|L|-1)!}{(|L|-1)!|L|!} < \frac{4^{|L|}}{2\sqrt{\pi\left(|L|+\frac{1}{4}\right)}} < 4^{|L|} \tag{6.43}$$

so that substituting (6.42) into (6.39) we may bound the pairwise error probability as

$$\Pr\left(\mathbf{S}_{(1)} \to \mathbf{S}_{(2)}\right) \leq \frac{1}{\det\left[\mathbf{\Theta}_{HH}\right]} \frac{(2|L|-1)!}{|L|!\,(|L|-1)!} \prod_{i\in L} \frac{N_0}{d_i^2} \leq \frac{1}{\det\left[\mathbf{\Theta}_{HH}\right]} \prod_{i\in L} \frac{4N_0}{d_i^2} \tag{6.44}$$

for $\det\left[\mathbf{\Theta}_{HH}\right] > 0$.

The pairwise error probability in (6.44) is worst for the two points $\mathbf{S}_(1), \mathbf{S}_(2) \in \Lambda$ where $\prod_{i\in L} \frac{4N_0}{d_i^2}$ is greatest. We therefore recognise that for lattice coded OFDM transmission over fading and frequency selective channels, the pairwise error probability decreases proportionally to the minimum squared product distance of the lattice Λ, which we define as

$$d_p^2(\Lambda) \triangleq \min_{\forall \mathbf{x},\mathbf{y}\in\Lambda} \prod_{k\in L} |x_k - y_k|^2, \text{ where } L \triangleq \{k : x_k \neq y_k\}. \tag{6.45}$$

Furthermore, we also define the product kissing number $\tau_p(\mathbf{x})$ as the number of lattice points at minimum product distance $d_p(\Lambda)$ from $\mathbf{x} \in \Lambda$, and the lattice Hamming dis-

tance $d_H(\mathbf{x}, \mathbf{y})$ as the number of elements of $\mathbf{x}$ and $\mathbf{y}$ that differ. If the product kissing number is equal for all $\mathbf{x} \in \Lambda$, as in the lattice constructions of interest [7], we denote this $\tau_p(\Lambda)$. We similarly denote the minimum Hamming distance of the lattice as $d_H(\Lambda) = \min_{\mathbf{x},\mathbf{y}\in\Lambda} d_H(\mathbf{x}, \mathbf{y})$. Consider then an OFDM system transmitting points from some lattice Λ mapped to the sphere packing $\mathcal{M}_N$, over a frequency selective Rayleigh fading channel. We may then union bound the probability that a maximum likelihood detector, with perfect channel state information, erroneously estimates the transmitted point as

$$P_e \leq \tau_p\left(\mathcal{M}_n\right) \frac{1}{\det\left[\mathbf{\Theta}_{HH}\right]} (4N_0)^{d_H(\mathcal{M}_N)} \frac{1}{d_p^2\left(\mathcal{M}_N\right)}. \tag{6.46}$$

Moreover, since the sphere packing product distance is lower bounded by the sphere packing minimum distance raised to the power of its Hamming distance, that is, $d_p\left(\mathcal{M}_N\right) \leq \left[d_{\min}\left(\mathcal{M}_N\right)\right]^{d_H(\mathcal{M}_N)}$, we may write

$$P_e \leq \tau_p\left(\mathcal{M}_N\right) \frac{1}{\det\left[\mathbf{\Theta}_{HH}\right]} \left[\frac{4N_0}{d_{min}^2(\mathcal{M}_N)}\right]^{d_H(\mathcal{M}_N)}. \tag{6.47}$$

Note that, since $d_{min}^2\left(\mathcal{M}_N\right)$ is proportional to the transmitted energy per symbol, or equivalently per data bit, $\frac{d_{min}^2(\mathcal{M}_N)}{N_0}$ gives a measures of the SNR.

Equations (6.46) and (6.47) thus describe the key parameters affecting the error rate of lattice coded OFDM. The error rate is inversely proportional to the product kissing number multiplied by the signal to noise ratio raised to the power of the minimum Hamming distance. Therefore, for lattice coded OFDM transmission over fading, frequency selective channels we should select constellations that maximise these quantities; in contrast to maximising the lattice centre density for transmission over AWGN channels. Although we do not describe methods of constructing such lattices, this is the subject of a large body of work including [45, 164, 165].

From (6.46) note that for a fixed lattice constellation, the error probability is inversely proportional to the determinant of the correlation matrix. For a Jakes' model Rayleigh fading channel with exponential power delay profile we may write

$$\begin{aligned}
&\det\left[\mathbf{\Theta}_{HH}\right] \\
&= \det\begin{bmatrix}
1 & \frac{1}{1+[4\pi\tau_{rms}\Delta f]^2} & \frac{1}{1+[6\pi\tau_{rms}\Delta f]^2} & \cdots & \frac{1}{1+[N\pi\tau_{rms}\Delta f]^2} \\
\frac{1}{1+[4\pi\tau_{rms}\Delta f]^2} & 1 & \frac{1}{1+[6\pi\tau_{rms}\Delta f]^2} & \cdots & \frac{1}{1+[(N-2)\pi\tau_{rms}\Delta f]^2} \\
\frac{1}{1+[4\pi\tau_{rms}\Delta f]^2} & \frac{1}{1+[6\pi\tau_{rms}\Delta f]^2} & 1 & \cdots & \frac{1}{1+[(N-4)\pi\tau_{rms}\Delta f]^2} \\
\vdots & \vdots & \vdots & \ddots & \vdots \\
\frac{1}{1+[(N-2)\pi\tau_{rms}\Delta f]^2} & \frac{1}{1+[(N-4)\pi\tau_{rms}\Delta f]^2} & \frac{1}{1+[(N-6)\pi\tau_{rms}\Delta f]^2} & \cdots & 1
\end{bmatrix}.
\end{aligned} \tag{6.48}$$

Therefore, the error rate is a function of $\tau_{rms}\Delta f$, the product of the channel rms delay spread and the subcarrier separation. It is readily observed that as $\tau_{rms}\Delta f$ increases, $\frac{1}{\det[\mathbf{\Theta}_{HH}]}$ decreases, so that for fixed τ_{rms} lower error rates are achievable using greater system bandwidth. This result is expected, since increasing either τ_{rms} or Δf increases the frequency diversity of the system [9].

6.3 High Dimensional Lattice Decoding

Maximum likelihood decoding of points from lattice constellations requires calculation of the Euclidean distance from the received point to all constellation points. For high dimensional lattices the large constellation size renders this approach infeasible. For example, the 64 OFDM subcarrier system transmitting 256-QAM points mapped from a subset of P_{128}, as described in Section 6.1, has a constellation size of $|\mathcal{M}_n| = 2^{128+120+64+8} \approx 10^{96}$. Generally, maximum likelihood decoding of lattices requires exponentially increasing complexity as the lattice dimension increases [38]. A low complexity alternative to maximum likelihood decoding of multilevel lattice constructions is to multistage decode the lattice, employing algebraic decoding of the codes associated with each level. However, algebraic hard decision decoding of codes is suboptimal, and induces a 3dB reduction in the coding gain at low error rates [38], with respect to the maximum likelihood approach.

To avoid much of this loss we employ generalised minimum distance (GMD) decoding of the codes associated with each lattice partition, as proposed and thoroughly discussed in [57] and further analysed in [79]. Although GMD decoding is suboptimal, it is shown to give effectively the same error rate as maximum likelihood decoding at high SNR. However, GMD decoding requires complexity that increases only polynomially with the lattice dimension, as discussed in Section 6.3.3.

We consider GMD decoding of OFDM systems encoded using high dimensional lattices, and transmitting over frequency selective channels. We first outline the technique and derive, using the methods in [56], the optimal reliability metric for transmission of QAM subcarrier constellations. In the remainder of this chapter we then extend the analysis of [79] to the fading and frequency selective channel. We obtain an approximation, that in most cases of interest is an upper bound, to the decoding error rate. We illustrate our analysis by comparing simulated decoding of the 256-QAM, 64 subcarrier OFDM system encoded with P_{128}, to analytical results.

6.3.1 GMD Decoding

Given the lattice encoded $\frac{N}{2}$ subcarrier OFDM system outlined in Section 6.1, we consider transmission of subcarrier symbols $\mathbf{S}_n$ over a frequency selective channel, with complex

Gaussian distributed subchannel responses denoted by $\mathbf{H}_n = \left\{H_{n,1}, H_{n,2}, \ldots, H_{n,N/2}\right\}$. We may equivalently write the $\frac{N}{2}$ M^2-ary QAM points as N M-ary PAM points, denoted

$$\mathbf{s}_n = \{s_{n,1}, s_{n,2}, \ldots, s_{n,N}\} \in \mathcal{M}_1 \tag{6.49}$$

so that the QAM symbol $S_{n,k}$ comprises PAM symbols $s_{n,2k-1}$ and $s_{n,2k}$ transmitted in quadrature, for $k = 1, \ldots, \frac{N}{2}$. Each of the N elements of the mapped lattice point $\mathbf{s}_n \equiv \mathbf{S}_n = \mathbf{m}(\mathbf{x})$, $\mathbf{x} \in \Lambda_f$, are from an M-ary PAM constellation, which without loss of generality we assume has separation $2\sqrt{E_0}$ between points, as in Figure 6.1.

At the receiver, following multiplication by the inverse subchannel gains we obtain $\frac{N}{2}$ noise corrupted QAM points, denoted

$$\mathbf{R}'_n = \left\{R'_{n,1}, R'_{n,2}, \ldots, R'_{n,\frac{N}{2}}\right\} = \mathbf{S}_n + \mathbf{W}'_n \tag{6.50}$$

where $\mathbf{W}'_n = \left\{W'_{n,1}, W'_{n,2}, \ldots, W'_{n,\frac{N}{2}}\right\}$ is a vector of independent zero mean Gaussian random variables, with $\mathbb{E}\left[W'_{n,k}\right] = \frac{1}{|H_{n,k}|^2}\frac{N_0}{2}(1+j)$, for $k = 1, \ldots, \frac{N}{2}$. This is equivalent to reception of N noise corrupted PAM points, denoted

$$\mathbf{r}'_n = \{r'_{n,1}, r'_{n,2}, \ldots, r'_{n,N}\} = \mathbf{s}_n + \mathbf{w}'_n \tag{6.51}$$

where $\mathbf{w}'_n = \{w'_{n,1}, \ldots, w'_{n,N}\}$ is a vector of independent zero mean Gaussian random variables with $\mathbb{E}\left[w'^2_{n,k}\right] = \frac{1}{|h_{n,k}|^2}\frac{N_0}{2}$, and $h_{n,k} = H_{n,\lceil\frac{k}{2}\rceil}$ is the subchannel gain associated with the k^{th} PAM point, for $k = 1, \ldots, N$. Note that we hereafter consider transmission of a single OFDM block, and thus omit the time index n. Readers should note that channel estimation errors will inevitably add further noise terms to (6.51). Depending on channel conditions and estimation method, these may be modelled as Gaussian random variables, and thus incorporated in $\mathbf{w}'_n$. Since channel estimation methods are beyond the scope of this thesis, note that the following analysis is then restricted to cases where the perturbation of the received signal may be modelled as additive white Gaussian noise with arbitrary variance, as in (6.51).

A code $\mathcal{C}_\ell$ is associated with the ℓ^{th} level of an m level lattice construction, as outlined in Section 3.4 and Section 3.5. Any point $\mathbf{x} \in \Lambda$ may then be expressed as a set of coset representatives, $\mathbf{c}_1, \mathbf{c}_2, \ldots, \mathbf{c}_m$, associated with a partition chain of the lattice, where $\mathbf{c}_\ell$ is a codeword from the code $\mathcal{C}_\ell$. Then, after the inverse mapping $\mathbf{m}^{-1} : \mathcal{M}_N \rightarrow \Lambda_f$, defined from (6.7), we may write the received point as

$$\tilde{\mathbf{r}} = \mathbf{x} + \tilde{\mathbf{w}} = 2^m\mathbf{c}_{m+1} + 2^{m-1}\mathbf{c}_m + \cdots + 2\mathbf{c}_2 + \mathbf{c}_1 + \tilde{\mathbf{w}} \tag{6.52}$$

where $\mathbf{x} \in \Lambda_f$, $\mathbf{c}_{m+1}$ is a codeword from the trivial $(N, N, 1)$ repetition code, and $\tilde{\mathbf{w}} = \{\tilde{w}_{n,1}, \ldots, \tilde{w}_{n,N}\}$ is a vector of independent zero mean Gaussian random variables, with $\mathbb{E}\left[\tilde{w}_k^2\right] = \frac{1}{4E_0}\frac{N_0}{2|h_k|^2}$. We may then estimate the transmitted lattice point $\mathbf{x}$, by successively finding estimates $\hat{\mathbf{c}}_1, \hat{\mathbf{c}}_2, \ldots, \hat{\mathbf{c}}_m$ for the codewords $\mathbf{c}_1, \mathbf{c}_2, \ldots, \mathbf{c}_m$, respectively, as discussed in Section 3.5. We apply GMD decoding to estimate the codeword at each stage. We outline this method below, although a more thorough description may be found in [57].

Assuming stages $1, \ldots, \ell - 1$ have been estimated, yielding $\hat{\mathbf{c}}_1, \ldots, \hat{\mathbf{c}}_{\ell-1}$, the component of the received vector $\mathbf{r}$ corresponding to remaining stages is $\tilde{\mathbf{r}}_\ell = \mathbf{r} - \hat{\mathbf{c}}_1 - 2\hat{\mathbf{c}}_2 - \cdots - 2^{\ell-2}\hat{\mathbf{c}}_{\ell-1}$. For each element $\tilde{r}_{\ell,k}$, for $k = 1, \ldots, N$, of $\tilde{\mathbf{r}}_\ell = \{\tilde{r}_{\ell,1}, \ldots, \tilde{r}_{\ell,N}\}$ the GMD decoder first produces a hard decision $u_{\ell,k}$ as to the most likely transmitted codeword symbol $c_{\ell,k}$, given $\tilde{r}_{\ell,k}$, and a metric $0 \leq \alpha_{\ell,k} \leq 1$ that gives a measure of the reliability of this hard decision. Larger values of $\alpha_{\ell,k}$ represent a greater probability of the hard decision being correct, with smaller values representing lesser probability of correct hard decision. The decoder then performs a series of erasures decoding trials, as outlined in Section 3.3.1.

We now consider decoding of the first stage only, since the decoding procedure for the latter stages is identical, and thus omit the subscript ℓ that denotes stage. Finding the hard decision estimate $\mathbf{u} = \{u_1, \ldots, u_N\}$ of the transmitted codeword $\mathbf{c} = \{c_1, \ldots, c_N\} \in \mathcal{C}$, is equivalent to finding the closest points $\mathbf{y} = \{y_1, \ldots, y_N\} \in \Lambda_f$ to each of the received points $\tilde{\mathbf{r}} = \{\tilde{r}_1, \ldots, \tilde{r_N}\}$. This is equivalent to finding each of the closest points $\hat{s}_k \in \mathcal{M}_1$ to each of the noise corrupted M-ary PAM points r'_k, for $k = 1, \ldots, N$. Given a closest point $\hat{s}_k \in \mathcal{M}_1$, we may readily find the point $y_k = m^{-1}(\mathbf{s}_k)$, and then $u_k = rem(y_k, 2)$, namely, the remainder following division of y_k by 2. Each point $\hat{s}_k \in \mathcal{M}_1$ is readily found using a correlation receiver [8] for each PAM constellation.

Note that, following multiplication by the inverse subchannel gains, each PAM constellation is perturbed by independently, but non-identically, distributed noise, since the noise variances $\mathbb{E}\left[{w'_k}^2\right]$ may be distinct for all k. Following [56] we now show that the optimum (such that the probability of decoding error is minimised) reliability metric for each hard decision is the log likelihood ratio for each hard decision.

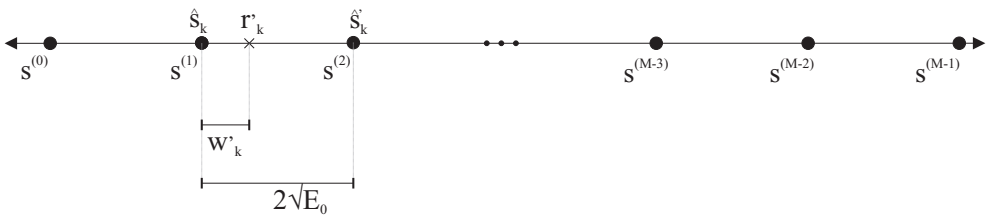

Figure 6.1 Received noise corrupted M-ary PAM point r'_k and associated hard decision $\hat{s}_k$.

6.3.2 Optimal Reliability Metric

We denote the event that the hard decision u_k is correct as G_k, and the event that u_k is incorrect as F_k. We require a metric for the reliability of the hard decision. In Section 3.3.1 we defined a reliability metric α_k for AWGN systems. We now derive the optimal reliability metric for GMD decoding of OFDM systems transmitting over frequency selective channels. We retain the symbol α_k to denote this metric, although the definition will differ from that of Section 3.3.1.

Given the reliability metric $0 \leq \alpha_k \leq 1$ associated with u_k we may write the conditional probability of G_k occurring as $\Pr(G_k|\alpha_k = x)$. Similarly the conditional probability of F_k occurring is denoted $\Pr(F_k|\alpha_k)$. Then, consider the random variable χ_k, which we define as

$$\chi_k \triangleq \begin{cases} 1-\alpha_k & \text{given } \alpha_k \text{ and } G_k \\ 1+\alpha_k & \text{given } \alpha_k \text{ and } F_k. \end{cases} \tag{6.53}$$

The expected value of χ_k is then

$$\mathbb{E}[\chi_k] = \sum_{\forall \alpha_k} \Big\{ (1-\alpha_k)\Pr(G_k|\alpha_k) + (1+\alpha_k)\Pr(F_k|\alpha_k) \Big\} \Pr(\alpha_k) \tag{6.54}$$

where we have taken the expectation over all possible values of α_k, and we imply that α_k takes a discrete value. In the case where the reliability is continuous valued the summation is readily replaced with integration over the appropriate PDF. The moment generating function (MGF) of χ_k is then

$$\begin{aligned} g_k(t) &= \mathbb{E}[\exp(t\chi_k)] \\ &= \sum_{\forall \alpha_k} \Big\{ \exp[t(1-\alpha_k)] \Pr(G_k|\alpha_k) + \exp[t(1+\alpha_k)] \Pr(F_k|\alpha_k) \Big\} \Pr(\alpha_k) \\ &= \sum_{\forall \alpha_k} \Big\{ \exp[t(1-\alpha_k)] \Pr(G_k, \alpha_k) + \exp[t(1+\alpha_k)] \Pr(F_k, \alpha_k) \Big\} \end{aligned} \tag{6.55}$$

where $\Pr(\alpha_k)$ is the probability of observing the reliability metric value α_k. The semi-invariant MGF is defined as

$$\mu_k(t) \triangleq \ln[g_k(t)]. \tag{6.56}$$

Following [56] it is readily shown that GMD decoding is guaranteed to decode to the codeword $\mathbf{c} \in \mathcal{C}$, if the generalised distance $\delta(\mathbf{u}, \mathbf{c})$ between $\mathbf{u}$ and $\mathbf{c}$ satisfies

$$\delta(\mathbf{u}, \mathbf{c}) < d_{\mathcal{C}} \tag{6.57}$$

where $d_{\mathcal{C}}$ is the minimum Hamming distance of the code, and we recall, from (3.7), that

$$\delta^2(\mathbf{c}, \mathbf{u}) = \delta^2(c_1, u_1) + \delta^2(c_2, u_2) + \cdots + \delta^2(c_n, u_n) \tag{6.58}$$

with

$$\delta(c_k, u_k) = \begin{cases} 1 - \alpha_k & \text{for } c_k = u_k \\ 1 + \alpha_k & \text{for } c_k \neq u_k. \end{cases} \tag{6.59}$$

It is readily seen that given reliability values α_k, for $k = 1, \ldots, N$, we may write

$$\sum_{k=1}^{N} \chi_k = \delta(\mathbf{c}, \mathbf{u}) \tag{6.60}$$

so that the probability $P_{e,GMD}$ of GMD decoding error may be bounded by

$$P_{e,GMD} \leq \Pr\left(\sum_{k=1}^{N} \chi_k < d_{\mathcal{C}}\right). \tag{6.61}$$

We may then apply the Chernoff bound [9, Ch.1.1.5] to write

$$\begin{aligned} &\Pr\left(\sum_{k=1}^{N} \chi_k < d_{\mathcal{C}}\right) \\ &\leq \exp(-td_{\mathcal{C}})\mathbb{E}\left[\exp\left(t\sum_{k=1}^{N}\chi_k\right)\right] \\ &= \exp(-td_{\mathcal{C}})\sum_{\forall \alpha_k}\exp\left(t\sum_{k=1}^{N}\chi_k\right)\Pr(\alpha_k) \\ &= \exp(-td_{\mathcal{C}})\sum_{\forall \alpha_k}\prod_{k=1}^{N}\Big\{\Pr(G_k, \alpha_k)\exp(t[1-\alpha_k]) + \Pr(F_k, \alpha_k)\exp(t[1+\alpha_k])\Big\} \\ &= \exp\left(-td_{\mathcal{C}} + \sum_{k=1}^{N}\mu_k(t)\right) \end{aligned} \tag{6.62}$$

for any value of $t \in \mathbb{R}$. We may find the optimum reliability values α_k by minimising the probability of GMD decoding error, with respect to α_k and then with respect to t. That is, we wish to find

$$\underset{\alpha_1,\ldots,\alpha_N,\, t}{\operatorname{argmin}}\left\{\Pr\left(\sum_{k=1}^{N}\chi_k < d_{\mathcal{C}}\right)\right\} = \underset{\alpha_1,\ldots,\alpha_N,\, t}{\operatorname{argmax}}\left\{td_{\mathcal{C}} - \sum_{k=1}^{N}\mu_k(t)\right\}. \tag{6.63}$$

We first minimise $\sum_{k=1}^{N} \mu_k(s)$ with respect to $\{\alpha_1, \alpha_2, \ldots, \alpha_N\}$, so that

$$\frac{\partial}{\partial \alpha_1}\frac{\partial}{\partial \alpha_2}\cdots\frac{\partial}{\partial \alpha_N}\left\{\sum_{k=1}^{N}\mu_k(t)\right\} = 0. \tag{6.64}$$

Recognising that each $\mu_k(t)$ is independent of α_j, for all $j \neq k$, we may write (6.64) as

$$\sum_{k=1}^{N}\frac{\partial}{\partial \alpha_k}\mu_k(t) = \sum_{k=1}^{N}\frac{1}{g_k(t)}\frac{\partial}{\partial \alpha_k}g_k(t) = 0. \tag{6.65}$$

A solution of this equation occurs at $\frac{\partial}{\partial \alpha_k}g_k(t) = 0$, for $k = 1, \ldots, N$. Thus, from (6.55), we may write

$$\Pr\left(G_k|\alpha_k\right)\exp(t[1-\alpha_k]) = \Pr\left(F_k|\alpha_k\right)\exp(t[1+\alpha_k]). \tag{6.66}$$

Taking the logarithm and rearranging we may then write

$$\alpha_k = \begin{cases} 0 & \text{for } \mathcal{L}_k \leq 0 \\ \frac{\mathcal{L}_k}{2t} & \text{for } 0 < \mathcal{L}_k < 1 \\ 1 & \text{for } \mathcal{L}_k \geq 1 \end{cases} \tag{6.67}$$

where we define

$$\mathcal{L}_k \triangleq \log\left\{\frac{\Pr\left(G_k|\alpha_k\right)}{\Pr\left(F_k|\alpha_k\right)}\right\} \tag{6.68}$$

for all $k = 1, \ldots, N$. Note that α_k is limited so that $0 \leq \alpha_k \leq 1$, as required by definition [56]. The optimum reliability metric is thus the logarithm of the likelihood ratio of the probability of correct hard decision to the probability of incorrect hard decision, given the reliability value, the well known *log likelihood ratio*, $\mathcal{L}_k$.

In the case of interest a point $s_k \in \mathcal{M}_1$ is transmitted from an M-ary PAM constellation. From (6.51) we obtain a noise corrupted M-ary PAM point $r'_k = s_k + w'_k$, for $k = 1, \ldots, N$, as illustrated in Figure 6.1. We denote the closest point to s_k as $\hat{s}_k$, and the second closest point as $\hat{s}'_k$. Assuming we receive point r_k, that is assigned reliability value α_k, we may then neglect the effect of constellation end points to approximate the probability of a correct hard decision as

$$\Pr\left(G_k|\alpha_k\right) = \Pr\left(G_k|r_k\right) \approx \frac{1}{\sqrt{\pi\frac{1}{|h_k|^2}N_0}}\exp\left(-\frac{|h_k|^2\,|\hat{s}_k - r_k|^2}{N_0}\right) \tag{6.69}$$

since w'_k is a zero mean Gaussian random variable with variance $\frac{N_0}{2|h_k|^2}$. Similarly we may

write the probability of an incorrect decision, given r_k, being made as

$$\begin{aligned}\Pr\left(F_k|\alpha_k\right) &= \Pr\left(F_k|r_k\right) \\ &\approx \sum_{\substack{k=1 \\ s_k \neq \hat{s}_k}}^{L} \Pr\left(s_k \text{ transmitted, } \hat{s}_k \text{ hard decision}\right) \\ &= \sum_{\substack{k=1 \\ s_k \neq \hat{s}_k}}^{L} \frac{1}{\sqrt{\pi \frac{1}{|h_k|^2} N_0}} \exp\left(-\frac{|h_k|^2 \left|s_k - r_k\right|^2}{N_0}\right).\end{aligned} \tag{6.70}$$

We may then write the likelihood ratio as

$$\frac{\Pr\left(G_k|\alpha_k\right)}{\Pr\left(F_k|\alpha_k\right)} = \frac{\exp\left(-\frac{|h_k|^2 |\hat{s}_k - r_k|^2}{N_0}\right)}{\sum_{\substack{k=1 \\ s_k \neq \hat{s}_k}}^{L} \exp\left(-\frac{|h_k|^2 |s_k - r_k|^2}{N_0}\right)}. \tag{6.71}$$

In the case where the SNR $\frac{E_0}{N_0}$ is large, we may approximate the probability of incorrect hard decision as the probability that point $s_k = \hat{s}'_k$ is transmitted and hard decision $\hat{s}_k$ is made. This results in the well known max-log-MAP approximation to the log-MAP metric [166]. We may then write

$$\begin{aligned}\Pr\left(F_k|r_k\right) &\approx \Pr\left(s_k = \hat{s}'_k \text{ transmitted, } \hat{s}_k \text{ hard decision}\right) \\ &= \frac{|h_k|}{\sqrt{\pi N_0}} \exp\left(-\frac{|h_k|^2 \left|\hat{s}'_k - r_k\right|^2}{N_0}\right)\end{aligned} \tag{6.72}$$

so that the log likelihood ratio may be approximated as

$$\begin{aligned}\ln\left(\frac{\Pr\left(G_k|\alpha_k\right)}{\Pr\left(F_k|\alpha_k\right)}\right) &= \frac{|h_k|^2}{N_0}\left[\left|\hat{s}'_k - r_k\right|^2 - \left|\hat{s}_k - r_k\right|^2\right] \\ &= \frac{|h_k|^2}{N_0}\left[\left(2\sqrt{E_0} - \left|\hat{s}_k - r_k\right|\right)^2 - \left|\hat{s}_k - r_k\right|^2\right] \\ &= \frac{4|h_k|^2 E_0}{N_0}\left[1 - \frac{\left|\hat{s}_k - r_k\right|}{\sqrt{E_0}}\right]\end{aligned} \tag{6.73}$$

The value of $\mathcal{L}_k$ is thus approximated by the normalised distance of the received point r_k to the decision boundary between $\hat{s}_k$ and $\hat{s}'_k$, weighted by $\frac{|h_k|^2 E_0}{N_0}$, the received SNR for each

subchannel. From (6.67) and (6.55) the MGF of χ_k at the optimal t value is

$$\begin{aligned} g_{\text{opt},k}(t) = &\exp(0)\Pr\left(G_k, \mathcal{L}_k \geq 2t\right) + \exp(2t)\Pr\left(F_k, \mathcal{L} \geq 2t\right) \\ &+ \exp\left(t\left[1 - \frac{\mathcal{L}_k}{2t}\right]\right)\Pr\left(G_k, 0 \leq \mathcal{L}_k \leq 2t\right) \\ &+ \exp\left(t\left[1 + \frac{\mathcal{L}_k}{2t}\right]\right)\Pr\left(F_k, 0 \leq \mathcal{L}_k \leq 2t\right) \\ &+ \exp(t)\Pr\left(G_k, \mathcal{L}_k < 0\right) + \exp(t)\Pr\left(F_k, \mathcal{L}_k < 0\right) \\ = &\operatorname{erf}\left(\sqrt{\frac{|h_k|^2E_0}{N_0}}\left[\frac{4|h_k|^2E_0}{N_0} - 2t\right]\right) + \exp(2t)\operatorname{erfc}\left(\sqrt{\frac{|h_k|^2E_0}{N_0}}\left[\frac{N_0}{2|h_k|^2E_0}t + 1\right]\right) \\ &+ \exp\left(t\left[1 - \frac{\mathcal{L}_k}{2t}\right]\right)\left[\operatorname{erf}\left(\sqrt{\frac{|h_k|^2E_0}{N_0}}\right) - \operatorname{erf}\left(\sqrt{\frac{|h_k|^2E_0}{N_0}}\left[1 - \frac{N_0}{2|h_k|^2E_0}t\right]\right)\right] \\ &+ \exp\left(t\left[1 + \frac{\mathcal{L}_k}{2t}\right]\right)\left[\operatorname{erfc}\left(\sqrt{\frac{|h_k|^2E_0}{N_0}}\right) - \operatorname{erf}\left(\sqrt{\frac{|h_k|^2E_0}{N_0}}\left[1 + \frac{N_0}{2|h_k|^2E_0}t\right]\right)\right] \end{aligned} \tag{6.74}$$

where we have recognised that $\Pr\left(F_k, \mathcal{L}_k < 0\right) = \Pr\left(G_k, \mathcal{L}_k < 0\right) = 0$, and manipulated the probability expressions in Appendix D. We then require the value of t such that the right hand side of (6.63) is maximised. From (6.63) we take the derivative with respect to t, and find that the requisite value, denoted t_{opt}, occurs at

$$\frac{\partial}{\partial t}\sum_{k=1}^{N}\mu_{\text{opt,k}}(t) = \sum_{k=1}^{N}\frac{\frac{\partial}{\partial t}g_{\text{opt},k}(t)}{g_{\text{opt},k}(t)} = d_{\mathcal{C}} \tag{6.75}$$

where $\mu_{\text{opt},k}(t) = \ln\left[g_{\text{opt},k}(t)\right]$. Given the subchannel gains $\tilde{h}_k^2$, for $k = 1, \ldots, N$, and the signal to noise measure $\frac{E_0}{N_0}$, the optimal value t_{opt} may be numerically calculated using (6.74) and (6.75). Given the value t_{opt}, substituting (6.73) into (6.67) we may write the optimal GMD decoding metric as

$$\alpha_k \triangleq \begin{cases} 0 & \text{for } |\hat{s}_k - r_k| \geq \sqrt{E_0} \\ \frac{1}{2t_{\text{opt}}}\frac{4|h_k|^2E_0}{N_0}\left[1 - \frac{|\hat{s}_k - r_k|}{\sqrt{E_0}}\right] & \text{for } \left[1 - \frac{N_0}{2|h_k|^2E_0}t_{\text{opt}}\right]\sqrt{E_0} < |\hat{s}_k - r_k| < \sqrt{E_0} \\ 1 & \text{for } |\hat{s}_k - r_k| \leq \left[1 - \frac{N_0}{2|h_k|^2E_0}t_{\text{opt}}\right]\sqrt{E_0}. \end{cases} \tag{6.76}$$

6.3.3 GMD Decoding Complexity

GMD decoding incurs only polynomially increasing complexity as N increases, and is indeed not significantly greater than normal algebraic decoding of a linear block code. In order to bound the number of real operations we consider the maximum number of real

operations required at each decoding step of a single stage of GMD decoding a (N, K, D) linear block code. We assume that this is one stage of decoding a construction C lattice.

To generate the hard decision vector $\mathbf{u}$, we require N decodings of the coset $\mathbb{Z}/2\mathbb{Z}$, which requires N real rounding operations [57]. The reliability values $\boldsymbol{\alpha}$ require a further N operations to generate, since they are the subtraction of the rounded vector $\mathbf{u}$ from the received vector. We then find the $D-1$ least reliable positions in $\mathbf{u}$, requiring no more than

$$N - (D-1) + \sum_{k=N-(D-1)+2}^{N} \log_2 k \tag{6.77}$$

real operations [167]. As outlined in Section 3.3.1, a series of $|\mathcal{K}|$ algebraic decoding trials are then conducted. Both [168] and [169] show that, for use of codes that may be decoded with the Berlekamp-Massey algorithm [54], only a single pass of this algorithm is required to generate all candidate codewords. For the Barnes-Wall lattices of interest, the constituent codes are (r, m) Reed-Muller codes, which may be hard decision decoded [170] [171] with no more than $N \min\{r, m-r\}$ real operations. Errors and erasures decoding requires twice the complexity [38], so that no more than $|\mathcal{K}|N \min\{r, m-r\}$ real operations are required. Finally, we require selection of the candidate codeword with the smallest generalised distance from the received vector. In [57, lemma 5.1] it is shown that this requires at most

$$\frac{t(t+1)}{2} + E(D-E) - 1 \tag{6.78}$$

real operations, where $t = \lfloor \frac{D-1}{2} \rfloor$ and $E = \lfloor \frac{D+1}{4} \rfloor$. The total complexity of decoding a point thus increases polynomially in N, as opposed to exponentially for maximum likelihood decoding.

We consider decoding of the P_{128} sphere packing, constructed from the codes $RM(1,7)$, $RM(3,7)$ and $RM(5,7)$, which are $(128, 8, 64)$, $(128, 64, 16)$ and $(128, 120, 4)$ linear block codes, respectively. Thus, decoding of the first stage requires no more than 256 real operations for generation of $\mathbf{u}$ and $\boldsymbol{\alpha}$, 474 operations for sorting, $2 \times 4 \times 128$ operations for algebraic decoding and 1263 operations for codeword selection, yielding a total of 3017 real operations. Similarly the second stage requires no more than $256 + 210 + 2 \times \times 384 + 75 = 6685$ operations, and the third stage $256 + 139 + 2 \times 2 \times 256 + 3 = 1422$ operations. The final (uncoded) stage requires generation of a hard decision only, and thus requires 128 operations. Therefore, no more than $3017 + 6685 + 1422 + 128 \approx 11500$ real operations are needed to GMD decode a single point transmitted from the P_{128} sphere packing. In comparison, decoding of four uncoded stages would require $4 \times 128 = 512$ real rounding operations. However, as demonstrated in Section 6.4.2 this additional complexity yields excellent coding gains.

6.4 GMD Decoding Performance Analysis

We now extend the analysis of [79] to lattice points transmitted using OFDM, over a frequency selective channel. We obtain an approximation to the error rate of multistage GMD decoding of multilevel construction lattice points, which is an upper bound for the cases of interest. We refer to this as an approximate upper bound. Given an m level construction C lattice we calculate the probability of lattice symbol decoding error. A symbol error occurs if the estimated lattice point $\hat{\mathbf{x}} \in \Lambda$ is not equal to the transmitted lattice point $\mathbf{x} \in \Lambda$, or equivalently if the estimated OFDM block $\hat{\mathbf{S}}_n$ is not equal to the transmitted block $\mathbf{S}_n$ mapped from the lattice Λ. We denote this error event as $\mathcal{E}_\Lambda$, and denote the events of correct and incorrect decoding at the ℓ^{th} stage as $\mathcal{E}_\ell^c$ and $\mathcal{E}_\ell$ respectively. We may then write

$$\mathcal{E}_\Lambda = \bigcup_{\ell=1}^{m} \mathcal{E}_\ell. \tag{6.79}$$

We denote the probability that the ℓ^{th} stage is incorrectly decoded, given that the stages $1, 2, \ldots, \ell-1$ are correctly decoded, as $\Pr\left(\mathcal{E}_\ell | \mathcal{E}_{\ell-1}^c, \mathcal{E}_{\ell-2}^c, \ldots, \mathcal{E}_1^c\right)$. We may then use the principle of inclusion and exclusion [140] to write

$$\Pr\left(\mathcal{E}_\Lambda\right) = \bigcup_{\ell=1}^{m} \Pr\left(\mathcal{E}_\ell\right) \leq \sum_{\ell=1}^{m} \Pr\left(\mathcal{E}_\ell | \mathcal{E}_{\ell-1}^c, \mathcal{E}_{\ell-2}^c, \ldots, \mathcal{E}_1\right) \tag{6.80}$$

with this upper bound being an approximation when the conditional probability of error for each stage is small. In the next subsection we outline a method for approximating the probability of decoding error for a single stage, conditional on all previous stages being correctly decoded. We may then use this result to obtain the probability of lattice decoding error.

6.4.1 Single Stage Performance

We extend the methodology of [79] to the case where each lattice coordinate is perturbed by independent non-identically distributed noise. Since we are concerned with a single stage only, for clarity we omit the subscript ℓ denoting decoding stage. We consider decoding of a single stage only, assuming all previous stages are previously decoded. Furthermore, we assume this stage is constructed with codeword $\mathbf{c}$ from code $\mathcal{C}$, which is mapped to an M-ary PAM constellation, as described, for example, in (6.1) and (6.2). The minimum Hamming distance of $\mathcal{C}$ is denoted $d_{\mathcal{C}}$.

As before, the receiver front end produces a vector of hard decisions $\mathbf{u} = \{u_1, u_2, \ldots, u_N\}$ and corresponding reliability values $\boldsymbol{\alpha} = \{\alpha_1, \alpha_2, \ldots, \alpha_N\}$. We denote the event that there are b hard decision errors as E_b, for $0 \leq b \leq N$ and $b \in \mathbb{Z}$. Furthermore, we let

$\mathcal{I}_F = \{f_1, f_2, \ldots, f_b\} \subseteq \{1, 2, \ldots, N\}$ denote the set of indices of $\mathbf{u}$ corresponding to incorrect hard decisions. That is, u_k is incorrect if $k \in \mathcal{I}_F$. We let $\mathcal{I}_G = \{g_1, g_2, \ldots, g_{N-b}\} \subseteq \{1, 2, \ldots, N\}$ be the complimentary set corresponding to the correct hard decisions u_k, $k \in \mathcal{I}_G$. As before, the event that hard decision u_k is either correct or incorrect is denoted F_k or G_k respectively.

The probability of correct hard decision is

$$\Pr(G_k) = \frac{1}{M} + \frac{M-1}{M}\text{erf}\left(\sqrt{\frac{E_0}{N_0}}\right) \tag{6.81}$$

the well known [8] probability of maximum likelihood decoding for an M-ary PAM signal. Similarly,

$$\Pr(F_k) = \frac{M-1}{M}\text{erfc}\left(\sqrt{\frac{E_0}{N_0}}\right). \tag{6.82}$$

Since the probability of error differs for each hard decision, the probability of exactly b hard decision errors is

$$\Pr(E_b) = \sum_{\forall \mathcal{I}_F, \mathcal{I}_G} \Pr(G_{F_1}) \Pr(G_{F_2}) \ldots \Pr(G_{F_b}) \Pr(F_{G_1}) \Pr(F_{G_2}) \ldots \Pr\left(F_{G_{N-b}}\right) \tag{6.83}$$

where the summation is over all $\binom{N}{b}$ distinct pairs of $\mathcal{I}_F$ and $\mathcal{I}_G$. The probability mass function of (6.83) is recognised to be a Poisson binomial distribution. We may readily approximate this distribution with the Poisson distribution, as outlined in Section 5.2, so that

$$\Pr(E_b) \approx \frac{\lambda^b e^{-b}}{b!}, \text{ with } \lambda = \sum_{k=1}^{N} \Pr(F_k). \tag{6.84}$$

For the special case of a flat fading or AWGN channel the error probability is equal for all subcarrier symbols, so that we may write

$$\Pr(E_b) = \binom{N}{b} [\Pr(G_1)]^b [\Pr(F_1)]^{N-b}. \tag{6.85}$$

We may write the reliability measures corresponding to erroneous hard decisions as the set $\{\alpha_{f_1}, \alpha_{f_2}, \ldots, \alpha_{f_b}\}$. We rank these in nondecreasing order to obtain $\beta_1 \leq \beta_2 \leq \cdots \leq \beta_b$, the ordered set of reliability values associated with incorrect hard decisions. We similarly denote the ordered set of reliability values associated with correct hard decisions as $\gamma_1, \ldots, \gamma_{N-b}$, so that $\gamma_1 \leq \gamma_2 \leq \cdots \leq \gamma_{N-b}$.

Recall, from Section 3.3.1, that the GMD decoding procedure is to first generate a set of $\mathcal{K}$ candidate codewords, which we refer to as the *algebraic decoding phase*. The candidate

codeword $\hat{\mathbf{c}}$ with the smallest generalised minimum distance $\delta(\hat{\mathbf{c}}, \mathbf{u})$ (Section 3.3.1) is then chosen as the decoder output, which we refer to as the *Euclidean space selection phase*. The algebraic decoding phase is successful if the transmitted codeword is a member of the set of candidate codewords, and we denote this event $\mathcal{S}$. As shown in [79], if the transmitted codeword is in the list of candidate codewords, the probability of not choosing this codeword is very small so that the probability of decoding stage ℓ incorrectly may be approximated by $\Pr(\mathcal{S})$, for each stage.

The event of a successful algebraic decoding phase given that b hard decision errors exist is denoted $\mathcal{S}_b$, so that we may write $\mathcal{S} = \mathcal{S}_0 \cup \mathcal{S}_1 \cup \ldots \cup \mathcal{S}_N$. We let $\mathcal{S}$ denote the algebraic decoding phase failure complimentary event, namely, when the transmitted codeword does not appear in the list of candidates. If the number of errors is less than half the minimum Hamming distance of the block code, that is $b \leq t \triangleq \lfloor \frac{d_{\mathcal{C}}-1}{2} \rfloor$, then algebraic decoding is guaranteed to be successful. Furthermore, if the number of errors exceeds the code's minimum Hamming distance then algebraic decoding will fail; that is, $b \geq d_{\mathcal{C}} - 1$. We may then write $\Pr(\mathcal{S}_b) = 1$, for $b = 1, 2, \ldots, \lfloor \frac{d_{\mathcal{C}}-1}{2} \rfloor$ and $\Pr(\mathcal{S}_b) = 0$, for $b = d_{\mathcal{C}} - 1, d_{\mathcal{C}}, \ldots, N$. The probability of algebraic decoding phase error is then

$$\begin{aligned}\Pr(\mathcal{F}) &= 1 - \Pr(\mathcal{S}) \\ &= 1 - [\Pr(\mathcal{S}_1) + \Pr(\mathcal{S}_2) + \cdots + \Pr(\mathcal{S}_N)] \\ &= 1 - [\Pr(E_1) + \Pr(E_2) + \cdots + \Pr(E_t) + \Pr(\mathcal{S}_{t+1}) + \Pr(\mathcal{S}_{t+2}) + \cdots + \Pr(\mathcal{S}_{d_{\mathcal{C}}-1})]\end{aligned} \tag{6.86}$$

The probability of b errors occurring is readily approximated, using (6.84). We now calculate lower bounds on $\Pr(\mathcal{S}_n)$, for $b = t+1, t+2, \ldots, d_{\mathcal{C}} - 1$, and thus upper bound the probability of GMD decoding failure.

The algebraic decoding phase requires $|\mathcal{K}|$ errors and erasures decoding trials, with each trial requiring ν erasures be made, for all $\nu \in \mathcal{K}$. Letting the event $\mathcal{S}_{b,\nu} \subset \mathcal{S}_b$ denote production of the correct codeword when k erasures are made, we may write $\mathcal{S}_b = \cup_{\nu \in \mathcal{K}} \{\mathcal{S}_{b,\nu}\}$. It may then be shown [79] that a tight lower bound is given by

$$\Pr(\mathcal{S}_b) \geq \max_{\nu \in \mathcal{K}} \{\Pr(\mathcal{S}_{b,\nu})\} \tag{6.87}$$

since the events $\mathcal{S}_{b,1}, \mathcal{S}_{b,2}, \ldots, \mathcal{S}_{b,|\mathcal{K}|}$ are highly correlated.

We let $\mathcal{U}_{\tau,\nu}$ be the event that τ or more hard decision errors are erased when ν erasures are made, requiring that $\tau \geq k$ and $b \geq \tau$. Note that, if τ or more errors are erased, this requires $\beta_\tau < \gamma_{\nu-\tau+1}$; that is, the τ^{th} smallest reliability associated with a hard decision error must be less than the $(\nu - \tau + 1)^{\text{th}}$ smallest reliability associated with a correct hard decision, so that at most only $(\nu - \tau)$ correct hard decisions are erased. The probability

of $\mathcal{U}_{\tau,\nu}$ occurring, given that there are b hard decision errors, is then the probability that $\beta_\tau > \gamma_{\nu-\tau+1}$. This is readily calculated given the PDF of β_τ, denoted $f_{\beta_\tau}(x)$, and the PDF and cumulative probability density function (CDF) of $\gamma_{\nu-\tau+1}$, denoted $f_{\gamma_{\nu-\tau+1}}(x)$ and $F_{\gamma_{\nu-\tau+1}}(x)$ respectively. Given these probability functions, described below, we may write

$$\Pr\left(\mathcal{U}_{\tau,\nu}|\mathcal{E}_b\right) = \int_0^\infty f_{\beta_\tau}(x) \int_x^\infty f_{\gamma_{\nu-\tau+1}}(y)\, dydx = \int_0^\infty f_{\beta_\tau}(x) \left[1 - F_{\gamma_{\nu-\tau+1}}(x)\right]\, dx. \quad (6.88)$$

Presuming τ hard decision errors are erased, leaving $b-\tau$ unerased errors, then a necessary and sufficient condition for production of a correct codeword is $\nu+2(b-\tau) < d_{\mathcal{C}}$, since any block code can correct up to p errors and q erasures, provided $2p+q < d_{\mathcal{C}}$. This condition may be equivalently written as $\tau > b - \frac{\nu-d_{\mathcal{C}}}{2} \geq b - \lfloor\frac{d_{\mathcal{C}}-\nu-1}{2}\rfloor$, which corresponds to the event $\mathcal{U}_{\tau,\nu}$. We may thus write

$$\Pr\left(\mathcal{S}_{b,\nu}\right) = \Pr\left(\mathcal{U}_{\tau,k}, E_b\right) = \Pr\left(E_b\right) \Pr\left(\mathcal{U}_{\tau,k}|E_b\right) = \Pr\left(E_b\right) \int_0^\infty f_{\beta_\tau}(x) \left[1 - F_{\gamma_{\nu-\tau+1}}(x)\right]\, dx \quad (6.89)$$

where $\tau = b - \lfloor\frac{d_{\mathcal{C}}-\nu-1}{2}\rfloor$. We can therefore upper bound the probability of GMD algebraic decoding phase failure by first calculating $\Pr\left(\mathcal{S}_{b,\nu}\right)$, for all $\nu \in \mathcal{K}$, and thus obtain a lower bound to $\Pr\left(\mathcal{S}_b\right)$, as in (6.87). With the lower bounds on $\Pr\left(\mathcal{S}_b\right)$, for $b = t+1, t+2, \ldots, d_{\mathcal{C}}-1$, we then calculate an upper bound on the probability of GMD decoding error, $\Pr\left(\mathcal{F}\right)$, as in (6.86). The order statistics distribution functions required for the calculation of (6.89) are given below, as well as tight bounds and approximations to these functions. We may then obtain an approximation to the probability of GMD decoding error for each stage $\ell = 1, \ldots, m$, assuming all previous stages are correctly decoded. In most cases this approximation is an upper bound. With this conditional probability of decoding failure for each stage we may use (6.80) to obtain an approximate upper bound to the probability of error when decoding a multilevel lattice transmitted over a frequency selective channel, using multistage GMD decoding.

Reliability Order Statistics

For a frequency selective channel the PDFs of the reliability order statistics are significantly more difficult to describe and evaluate than for the AWGN case described in [79]. Recall that the reliability statistics associated with incorrect hard decisions are denoted $\alpha_{f_1}, \alpha_{f_2}, \ldots, \alpha_{f_b}$, while those associated with correct hard decisions are $\alpha_{g_1}, \alpha_{g_2}, \ldots, \alpha_{g_{N-b}}$. The order statistics associated with incorrect hard decisions are $\beta_1 \leq \beta_2 \leq \ldots \leq \beta_b$, while those associated with correct hard decisions are $\gamma_1 \leq \gamma_2 \leq \cdots \leq \gamma_{N-b}$.

The variance $\frac{N_0}{2|h_k|^2}$ of the Gaussian noise component w'_k perturbing each received symbol may be different for all $k \in \{1, \ldots, N\}$. Each α_{f_k}, for $f_k \in \mathcal{I}_f$, is then independent but non-identically distributed, with PDF $f_{\alpha_{f_k}}(x)$ and CDF $F_{\alpha_{f_k}}(x)$. These functions are calculated

in the following subsection. Given the indices of incorrect hard decisions $\mathcal{I}_f$, we then use a result from [172] to write the PDF of the i^{th} smallest α_{f_k} given that b hard decisions errors are made, that is the PDF of β_i, as

$$f_{\beta_i}(x|\mathcal{I}_f) = \frac{1}{(i-1)!(N-i)!}\,\text{Per}\begin{bmatrix} F_{\alpha_{f_1}}(x) & F_{\alpha_{f_2}}(x) & \cdots & F_{\alpha_{f_N}}(x) \\ \vdots & \vdots & \ddots & \vdots \\ F_{\alpha_{f_1}}(x) & F_{\alpha_{f_2}}(x) & \cdots & F_{\alpha_{f_N}}(x) \\ f_{\alpha_{f_1}}(x) & f_{\alpha_{f_2}}(x) & \cdots & f_{\alpha_{f_N}}(x) \\ 1-F_{\alpha_{f_1}}(x) & 1-F_{\alpha_{f_2}}(x) & \cdots & 1-F_{\alpha_{f_N}}(x) \\ \vdots & \vdots & \ddots & \vdots \\ 1-F_{\alpha_{f_1}}(x) & 1-F_{\alpha_{f_2}}(x) & \cdots & 1-F_{\alpha_{f_{(N)}}}(x) \end{bmatrix} \begin{matrix} \left.\vphantom{\begin{matrix}a\\a\\a\end{matrix}}\right\} (i-1) \text{ rows} \\ \\ \left.\vphantom{\begin{matrix}a\\a\\a\end{matrix}}\right\} (b-i) \text{ rows,} \end{matrix} \tag{6.90}$$

where $\text{Per}[A]$ denotes the permanent [173] of the matrix A. Similarly, the PDF $f_{\gamma_i}(x|\mathcal{I}_g)$ of the i^{th} smallest reliability associated with a correct hard decision, given $\mathcal{I}_g$, is equal to

$$\frac{1}{(i-1)!(N-b-i)!}\,\text{Per}\begin{bmatrix} F_{\alpha_{g_1}}(x) & F_{\alpha_{g_2}}(x) & \cdots & F_{\alpha_{g_{(N-b)}}}(x) \\ \vdots & \vdots & \ddots & \vdots \\ F_{\alpha_{g_1}}(x) & F_{\alpha_{g_2}}(x) & \cdots & F_{\alpha_{g_{(N-b)}}}(x) \\ f_{\alpha_{g_1}}(x) & f_{\alpha_{g_2}}(x) & \cdots & f_{\alpha_{g_{(N-b)}}}(x) \\ 1-F_{\alpha_{g_1}}(x) & 1-F_{\alpha_{g_2}}(x) & \cdots & 1-F_{\alpha_{g_N}}(x) \\ \vdots & \vdots & \ddots & \vdots \\ 1-F_{\alpha_{g_1}}(x) & 1-F_{\alpha_{g_2}}(x) & \cdots & 1-F_{\alpha_{g_{(N-b)}}}(x) \end{bmatrix} \begin{matrix} \left.\vphantom{\begin{matrix}a\\a\\a\end{matrix}}\right\} (i-1) \text{ rows} \\ \\ \left.\vphantom{\begin{matrix}a\\a\\a\end{matrix}}\right\} (N-b-i) \text{ rows,} \end{matrix} \tag{6.91}$$

where $f_{\alpha_{g_k}}(x)$ and $F_{\alpha_{g_k}}(x)$ are the PDF and CDF of a reliability value associated with a correct hard decision, where $g_k \in \mathcal{I}_g$. These functions are calculated in the following subsection.

Note that typically $\mathcal{I}_F$ and $\mathcal{I}_G$ are unknown, so that the PDFs of β_i and γ_i, given that b hard decision errors occur, are

$$f_{\beta_i}(x) = \sum_{\forall \mathcal{I}_F} \Pr\left(\mathcal{I}_G|\mathcal{E}_b\right) f_{\beta_i}\left(x|\mathcal{I}_F\right) \qquad f_{\gamma_i}(x) = \sum_{\forall \mathcal{I}_G} \Pr\left(\mathcal{I}_G|\,\mathcal{E}_b\right) f_{\gamma_i}\left(x|\,\mathcal{I}_G\right) \tag{6.92}$$

where the above summations are over all $\binom{N}{b}$ distinct $\mathcal{I}_F$ and $\mathcal{I}_G$. We may lower bound the PDFs by considering the first few terms only of these summations. However, it is found that in most cases of interest a sufficiently accurate approximation results from considering the most likely sets $\mathcal{I}_F$ and $\mathcal{I}_G$, namely taking $\mathcal{I}_F$ as the set corresponding to the b hard decisions with the largest probability of error, and $\mathcal{I}_G$ to be the set corresponding to the $N-b$ hard decisions with the smallest probability of error. Thus,

$$f_{\beta_i}(x) \approx \underset{\Pr(\mathcal{I}_F)}{\text{argmax}}\left\{f_{\beta_i}\left(x|\,\mathcal{I}_F\right)\right\}, \text{ and } f_{\gamma_i}(x) \approx \underset{\Pr(\mathcal{I}_G)}{\text{argmax}}\left\{f_{\gamma_i}\left(x|\,\mathcal{I}_G\right)\right\}. \tag{6.93}$$

Note that these approximations may be tightened, at obvious computational expense, by also considering the next most likely sets $\mathcal{I}_F$ and $\mathcal{I}_G$.

While the order statistic PDFs in (6.90) and (6.91) are elegant expressions, they are difficult to compute, since calculation of the permanent of an $N \times N$ matrix requires on the order of $N2^N$ calculations. For large matrices, say $N > 30$, obtaining the exact value of the permanent is not feasible using current technology. Note that there exist various methods of approximating the permanent of a matrix, with tighter approximations obtained at greater computational expense. Recent approaches include that of [174] and [175], while [176] provides a review of some classical approaches.

Since we use the permanent expressions in the calculation of a lower bound, (6.87), we now bound the permanent of the matrices in (6.90) and (6.91). We exploit the fact that the matrices have nonnegative entries to apply the matrix permanent bounds of [177][2]. Specifically, given an $N \times N$ nonnegative matrix A we denote the i^{th} row, j^{th} column element as a_{ij}, and the N-tuple of i^{th} row elements as $A_{(i)} = \{a_{i1}, a_{i2,}, \ldots, a_{iN}\}$. Furthermore, we let $A'_{(i)} = \{a'_{i1}, a'_{i2}, \ldots, a'_{iN}\}$ denote the elements of $A_{(i)}$ rearranged in non-decreasing order, so that $a'_{i1} \leq a'_{i2} \leq \cdots \leq a'_{iN}$. Similarly, $A_{(i)}* = \{a_{i1}*, a_{i2}*, \ldots, a_{iN}*\}$ is the N-tuple representing the elements of $A_{(i)}$ arranged in non-increasing order, so that $a_{i1}* \geq a_{i2}* \geq \cdots \geq a_{iN}*$. From [177] we may then write

$$\begin{aligned} \text{Per}[A] &\geq \prod_{i=1}^{n} \sum_{t=1}^{i} a'_{it} + (A_{1,\Sigma} - n\, a'_{11}) \prod_{j=2}^{n} \sum_{s=1}^{j-1} a'_{js}\,, \\ \text{Per}[A] &\leq \prod_{i=1}^{n} \sum_{t=1}^{i} a^*_{it} + (A_{1,\Sigma} - n\, a^*_{11}) \prod_{j=2}^{n} \sum_{s=1}^{j-1} a'_{js}\,, \end{aligned} \tag{6.94}$$

where $A_{1,\Sigma}$ is the sum of elements of $A_{(1)}$.

We may readily apply the bounds of (6.94) to the permanent expressions in (6.90) and (6.91) to obtain lower and upper bounds on the PDFs of $f_{\beta_i}(x)$ and $f_{\gamma_i}(x)$ respectively. Consequently, we obtain a lower bound on $\Pr(\mathcal{S}_{b,\nu})$ from (6.89), a lower bound on $\Pr(\mathcal{S}_b)$ from (6.87) and then the desired upper bound on $\Pr(\mathcal{F})$, from (6.86).

For the special case of the AWGN channel, obtaining $f_{\beta_i}(x)$ and $f_{\gamma_i}(x)$ is straightforward. All sets $\mathcal{I}_F$ are equally likely to occur, as are all sets $\mathcal{I}_G$. All β_k, for $k \in \mathcal{I}_F$, statistics are iid, with CDF denoted $F_\beta(x)$ and PDF $f_\beta(x)$. Similarly, all γ_k, for $k \in \mathcal{I}_G$, statistics are iid with CDF denoted $F_\gamma(x)$ and PDF $f_\gamma(x)$. Then, using a basic result of order statistics [178], we

[2] Also in the more accessible text [173]

may write

$$f_{\beta_i}(x) = \frac{b!}{(i-1)!(b-i)!}\left[F_\beta(x)\right]^{i-1}\left[1-F_\beta(x)\right]^{b-i} f_\beta(x), \text{ for } i \in \{1,2,\ldots,b\};$$
$$f_{\gamma_i}(x) = \frac{(N-b)!}{(i-1)!(N-b-i)!}\left[F_\gamma(x)\right]^{i-1}\left[1-F_\gamma(x)\right]^{N-b-i} f_\gamma(x), \text{ for } i \in \{1,2,\ldots,N-b\}. \tag{6.95}$$

Note that (6.90) and (6.91) reduce to (6.95) when all channel gains $|h_k|^2$ are equal.

Reliability Probability Functions

We require the CDFs and PDFs of α_{f_k}, a reliability value associated with an incorrect hard decision, and α_{g_k}, a reliability value associated with a correct hard decisions. At the receiver front end we have equalised symbols $r'_k = s_k + w'_k$, where s_k is a point from an M-ary PAM constellation with separation $2\sqrt{E_0}$ between points, and w'_k is a zero mean Gaussian random variable with variance denoted $\mathbb{E}\left[{w'_k}^2\right] = \sigma_k^2 = \frac{1}{|h_k|^2}\frac{N_0}{2}$. The reliability values α_k are defined in (6.76).

We first consider the case when the hard decision is known to be correct. We label the points in the M-ary PAM constellation as $s^{(0)}, s^{(1)}, \ldots, s^{(M)}$, as shown in Figure 6.1. The PDF $f_{\alpha_{g_k}}(x)$ is then the weighted sum of PDFs conditional on each $s^{(i)}$, for $i = 0, \ldots, M-1$, being transmitted. That is,

$$f_{\alpha_{g_k}}(x) = \sum_{i=0}^{M} \Pr\left(s^{(i)} \text{ sent}\right) f_{\alpha_{g_k}}\left(x \middle| s^{(i)} \text{ sent}\right) = \frac{1}{M}\sum_{i=0}^{M} f_{\alpha_{g_k}}\left(x \middle| s^{(i)} \text{ sent}\right) \tag{6.96}$$

assuming equiprobable transmission of constellation points. Then, substituting the expressions (E.4) and (E.10) from Appendix E, we may write the PDF of a reliability value α_{g_k},

for $\frac{E_0}{t_0\sigma_k^2} > 1$, as

$$f_{\alpha_{g_k}}\left(x, \frac{E_0}{t_0\sigma_k^2} > 1\right) = \begin{cases} \frac{M-2}{M}\frac{\operatorname{erf}\left(\sqrt{\frac{E_0}{2\sigma_k^2}\left[1-\frac{t_0\sigma_k^2}{E_0}\right]}\right)}{\operatorname{erf}\left(\sqrt{\frac{E_0}{2\sigma_k^2}}\right)} + \frac{2}{M}\frac{\operatorname{erfc}\left(\sqrt{\frac{E_0}{2\sigma_k^2}}\right)}{1+\operatorname{erf}\left(\sqrt{\frac{E_0}{2\sigma_k^2}}\right)} & \text{for } x = 0 \\ \frac{2t_0\sigma_k}{M\sqrt{E_0}\sqrt{2\pi}}\left[\frac{M-2}{\operatorname{erf}\left(\sqrt{\frac{E_0}{2\sigma_k^2}}\right)} + \frac{4}{1+\operatorname{erf}\left(\sqrt{\frac{E_0}{2\sigma_k^2}}\right)}\right]\exp\left(-\frac{E_0}{2\sigma_k^2}\left[1-\frac{t_0\sigma_k^2}{E_0}x\right]^2\right) & \text{for } 0 < x < 1 \\ \frac{4}{M}\cdot\frac{2\operatorname{erf}\left(\sqrt{\frac{E_0}{2\sigma_k^2}\left[1-\frac{t_0\sigma_k^2}{E_0}\right]}\right)}{1+\operatorname{erf}\left(\sqrt{\frac{E_0}{2\sigma_k^2}}\right)} & \text{for } x = 1. \end{cases} \tag{6.97}$$

In the case when $\frac{E_0}{t_0\sigma_k^2} \leq 1$, we may substitute (E.11) and (E.5) into (6.96) to write

$$f_{\alpha_{g_k}}\left(x, \frac{E_0}{t_0\sigma_k^2} \leq 1\right) = \begin{cases} \frac{2}{M}\frac{\operatorname{erfc}\left(\sqrt{\frac{E_0}{2\sigma_k^2}}\right)}{1+\operatorname{erf}\left(\sqrt{\frac{E_0}{2\sigma_k^2}}\right)} & \text{for } x = 0 \\ \frac{2t_0\sigma_k}{M\sqrt{E_0}\sqrt{2\pi}}\left[\frac{4}{1+\operatorname{erf}\left(\sqrt{\frac{E_0}{2\sigma_k^2}}\right)} + \frac{M-2}{\operatorname{erf}\left(\sqrt{\frac{E_0}{2\sigma_k^2}}\right)}\right]\exp\left(-\frac{E_0}{2\sigma_k^2}\left[1-\frac{t_0\sigma_k^2}{E_0}x\right]^2\right) & \text{for } 0 < x \leq \frac{E_0}{t_0\sigma_k^2}. \end{cases} \tag{6.98}$$

The CDF of α_{g_k} is obtained by integrating (6.97) and (6.98). First note that

$$\int_0^A \frac{2t_0\sigma_k}{\sqrt{E_0}\sqrt{2\pi}}\exp\left(-\frac{E_0}{2\sigma_k^2}\left[1-\frac{t_0\sigma_k^2}{E_0}x\right]^2\right)dx = \operatorname{erf}\left(\sqrt{\frac{E_0}{t_0\sigma_k^2}}\right) - \operatorname{erf}\left(\sqrt{\frac{E_0}{t_0\sigma_k^2}}\left[1-\frac{t_0\sigma_k^2}{E_0}A\right]\right). \tag{6.99}$$

We may then write the CDF for $\frac{E_0}{t_0\sigma_k^2} > 1$ as

$$F_{\alpha_{g_k}}\left(x|\frac{E_0}{t_0\sigma_k^2} > 1\right) =$$
$$\begin{cases} 0 & \text{for } x < 0 \\ 1 & \text{for } x \geq 1 \\ \frac{M-2}{M} \cdot \frac{\operatorname{erf}\left(\sqrt{\frac{E_0}{2\sigma_k^2}}\left[1-\frac{t_0\sigma_k^2}{E_0}\right]\right)}{\operatorname{erf}\left(\sqrt{\frac{E_0}{2\sigma_k^2}}\right)} + \frac{2}{M} \cdot \frac{\operatorname{erfc}\left(\sqrt{\frac{E_0}{2\sigma_k^2}}\right)}{1+\operatorname{erf}\left(\sqrt{\frac{E_0}{2\sigma_k^2}}\right)} & \text{for } x = 0 \\ 1 - \frac{M-2}{M} \cdot \frac{\operatorname{erf}\left(\sqrt{\frac{E_0}{2\sigma_k^2}}\left[1-\frac{t_0\sigma_k^2}{E_0}x\right]\right) - \operatorname{erf}\left(\sqrt{\frac{E_0}{2\sigma_k^2}}\left[1-\frac{t_0\sigma_k^2}{E_0}\right]\right)}{\operatorname{erf}\left(\sqrt{\frac{E_0}{2\sigma_k^2}}\right)} - \frac{2}{M} \cdot \frac{\operatorname{erf}\left(\sqrt{\frac{E_0}{2\sigma_k^2}}\left[1-\frac{t_0\sigma_k^2}{E_0}\right]\right)}{1+\operatorname{erf}\left(\sqrt{\frac{E_0}{2\sigma_k^2}}\right)} & \text{otherwise.} \end{cases} \tag{6.100}$$

Similarly, after integration of (6.98) we may write the CDF, for $\frac{E_0}{t_0\sigma_k^2} \leq 1$, as

$$\begin{aligned} & F_{\alpha_{g_k}}\left(x|\frac{E_0}{t_0\sigma_k^2} \leq 1\right) \\ &= \begin{cases} 0 & \text{for } x < 0 \\ \frac{2}{M} \cdot \frac{\operatorname{erfc}\left(\sqrt{\frac{E_0}{2\sigma_k^2}}\right)}{1+\operatorname{erf}\left(\sqrt{\frac{E_0}{2\sigma_k^2}}\right)} & \text{for } x = 0 \\ 1 - \frac{2}{M} \cdot \frac{\operatorname{erf}\left(\sqrt{\frac{E_0}{2\sigma_k^2}}\left[1-\frac{t_0\sigma_k^2}{E_0}x\right]\right)}{1+\operatorname{erf}\left(\sqrt{\frac{E_0}{2\sigma_k^2}}\right)} - \frac{M-2}{M} \cdot \frac{\operatorname{erf}\left(\sqrt{\frac{E_0}{2\sigma_k^2}}\left[1-\frac{t_0\sigma_k^2}{E_0}x\right]\right)}{\operatorname{erf}\left(\sqrt{\frac{E_0}{2\sigma_k^2}}\right)} & \text{for } 0 < x\frac{E_0}{t_0\sigma_k^2} \\ 1 & \text{for } x \geq \frac{E_0}{t_0\sigma_k^2}. \end{cases} \end{aligned} \tag{6.101}$$

We may similarly obtain the PDF of a reliability value α_{f_k} associated with an incorrect hard decision, by assuming that the transmitted point s_k was the second closest point $\hat{s}_k'$ to the

received point r_k. For the case when $\frac{E_0}{t_0\sigma_k^2} > 1$ we may use (E.16) to write

$$f_{\alpha_{f_k}}\left(x|I_k,\, \frac{E_0}{t_0\sigma_k^2} > 1\right) \approx f_{\alpha_{f_k}}\left(x|s_k = \hat{s}'_k,\, \frac{E_0}{t_0\sigma_k^2} > 1\right)$$
$$= \begin{cases} \frac{2t_0\sigma_k}{\sqrt{E_0}\sqrt{2\pi}} \frac{\exp\left(\frac{E_0}{2\sigma_k^2}\left[3-\frac{t_0\sigma_k^2}{E_0}x\right]^2\right) - \exp\left(\frac{E_0}{2\sigma_k^2}\left[1+\frac{t_0\sigma_k^2}{E_0}x\right]^2\right)}{\operatorname{erf}\left(3\sqrt{\frac{E_0}{2\sigma_k^2}}\right) - \operatorname{erf}\left(\sqrt{\frac{E_0}{2\sigma_k^2}}\right)} & \text{for } 0 \le x < 1 \\ \frac{\operatorname{erf}\left(\sqrt{\frac{E_0}{2\sigma_k^2}}\left[3-\frac{t_0\sigma_k^2}{E_0}\right]\right) - \operatorname{erf}\left(\sqrt{\frac{E_0}{2\sigma_k^2}}\left[1+\frac{t_0\sigma_k^2}{E_0}\right]\right)}{\operatorname{erf}\left(3\sqrt{\frac{E_0}{2\sigma_k^2}}\right) - \operatorname{erf}\left(\sqrt{\frac{E_0}{2\sigma_k^2}}\right)} & \text{for } x = 1 \\ 0 & \text{otherwise.} \end{cases} \tag{6.102}$$

Similarly, in the case when $\frac{E_0}{t_0\sigma_k^2} \le 1$ we may use (E.16) to write

$$\begin{aligned} & f_{\alpha_{f_k}}\left(x|I_k,\, \frac{E_0}{t_0\sigma_k^2} \le 1\right) \\ \approx\ & f_{\alpha_{f_k}}\left(x|s_k = \hat{s}'_k,\, \frac{E_0}{t_0\sigma_k^2} \le 1\right) \\ =\ & \begin{cases} \frac{2t_0\sigma_k}{\sqrt{E_0}\sqrt{2\pi}} \frac{\exp\left(-\frac{E_0}{2\sigma_k^2}\left[3-\frac{t_0\sigma_k^2}{E_0}x\right]^2\right) - \exp\left(-\frac{E_0}{2\sigma_k^2}\left[1+\frac{t_0\sigma_k^2}{E_0}x\right]^2\right)}{\operatorname{erf}\left(3\sqrt{\frac{E_0}{2\sigma_k^2}}\right) - \operatorname{erf}\left(\sqrt{\frac{E_0}{2\sigma_k^2}}\right)} & \text{for } 0 \le x \le \frac{E_0}{t_0\sigma_k^2} \\ 0 & \text{otherwise.} \end{cases} \end{aligned} \tag{6.103}$$

The CDF of α_{f_k} is obtained by integrating the above PDF expressions. Note that

$$\begin{aligned} \int_0^x \frac{2t_0\sigma_k}{\sqrt{E_0}\sqrt{2\pi}} \exp\left(-\frac{E_0}{2\sigma_k^2}\left[3-\frac{t_0\sigma_k^2}{E_0}y\right]^2\right) dy &= \operatorname{erf}\left(3\sqrt{\frac{E_0}{2\sigma_k^2}}\right) - \operatorname{erf}\left(\sqrt{\frac{E_0}{2\sigma_k^2}}\left[3-\frac{t_0\sigma_k^2}{E_0}x\right]\right) \\ \int_0^x \frac{2t_0\sigma_k}{\sqrt{E_0}\sqrt{2\pi}} \exp\left(-\frac{E_0}{2\sigma_k^2}\left[1+\frac{t_0\sigma_k^2}{E_0}y\right]^2\right) dy &= \operatorname{erf}\left(\sqrt{\frac{E_0}{2\sigma_k^2}}\left[1+\frac{t_0\sigma_k^2}{E_0}x\right]\right) - \operatorname{erf}\left(3\sqrt{\frac{E_0}{2\sigma_k^2}}\right). \end{aligned} \tag{6.104}$$

For $\frac{E_0}{t_0\sigma_k^2} > 1$ we may then integrate (6.102), and use (6.104) to write

$$\begin{aligned}
&F_{\alpha_{f_k}}\left(x|I_k, \frac{E_0}{t_0\sigma_k^2} > 1\right) \\
&\approx F_{\alpha_{f_k}}\left(x|s_k = \hat{s}'_k, \frac{E_0}{t_0\sigma_k^2} > 1\right) \\
&= \begin{cases} 0 & \text{for } x < 0 \\ \frac{1}{\mathrm{erf}\left(3\sqrt{\frac{E_0}{2\sigma_k^2}}\right) - \mathrm{erf}\left(\sqrt{\frac{E_0}{2\sigma_k^2}}\right)} \Bigg[\mathrm{erf}\left(\sqrt{\frac{E_0}{2\sigma_k^2}}\left[1 + \frac{t_0\sigma_k^2}{E_0}x\right]\right) & \\ \quad -\mathrm{erf}\left(\sqrt{\frac{E_0}{2\sigma_k^2}}\left[3 - \frac{t_0\sigma_k^2}{E_0}x\right]\right) + \mathrm{erf}\left(3\sqrt{\frac{E_0}{2\sigma_k^2}}\right) - \mathrm{erf}\left(\sqrt{\frac{E_0}{2\sigma_k^2}}\right)\Bigg] & \text{for } 0 \le x < 1 \\ 1 & \text{for } x \ge 1. \end{cases}
\end{aligned} \tag{6.105}$$

In the case when $\frac{E_0}{t_0\sigma_k^2} \le 1$ we integrate (6.103) to write

$$\begin{aligned}
&F_{\alpha_{f_k}}\left(x|I_k, \frac{E_0}{t_0\sigma_k^2} \le 1\right) \\
&\approx F_{\alpha_{f_k}}\left(x|s_k = \hat{s}'_k, \frac{E_0}{t_0\sigma_k^2} \le 1\right) \\
&= \begin{cases} 0 & \text{for } x < 0 \\ \frac{1}{\mathrm{erf}\left(3\sqrt{\frac{E_0}{2\sigma_k^2}}\right) - \mathrm{erf}\left(\sqrt{\frac{E_0}{2\sigma_k^2}}\right)} \Bigg[\mathrm{erf}\left(\sqrt{\frac{E_0}{2\sigma_k^2}}\left[1 + \frac{t_0\sigma_k^2}{E_0}x\right]\right) & \\ \quad -\mathrm{erf}\left(\sqrt{\frac{E_0}{2\sigma_k^2}}\left[3 - \frac{t_0\sigma_k^2}{E_0}x\right]\right) + \mathrm{erf}\left(3\sqrt{\frac{E_0}{2\sigma_k^2}}\right) - \mathrm{erf}\left(\sqrt{\frac{E_0}{2\sigma_k^2}}\right)\Bigg] & \text{for } 0 \le x < \frac{E_0}{t_0\sigma_k^2} \\ 1 & \text{for } x \ge \frac{E_0}{t_0\sigma_k^2}. \end{cases}
\end{aligned} \tag{6.106}$$

Although the above PDF and CDF expressions are verbose, they are readily calculable. We may substitute these expressions into (6.91) or (6.90) to obtain the PDF of the s^{th} largest value of α_{g_k} or α_{f_k}, as required for calculation of the probability of single stage GMD decoding error.

6.4.2 Simulations

We use the methods outlined in the previous sections to calculate analytical approximations to the probability of GMD decoding error rates with simulated error rates. We consider a 64 subcarrier OFDM system occupying 30MHz total bandwidth, with each subcarrier transmitting a 256-QAM constellation. Each OFDM Block is mapped from a point

in the 128 dimensional sphere packing P_{128}, described in Section 6.1. At the receiver we perform GMD decoding at each stage to obtain an estimate of the transmitted lattice point.

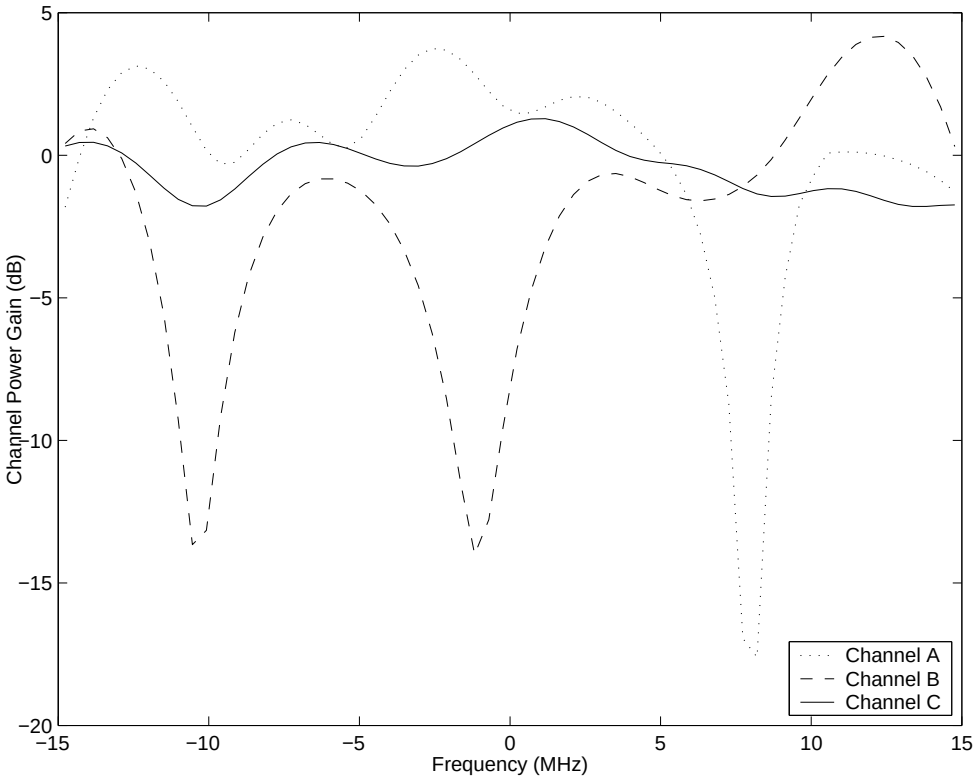

Figure 6.2 Channel Gains for Channels A, B and C

We consider the OFDM block error rate, equivalent to the lattice point error rate, for the AWGN channel and three randomly generated frequency selective channels. In all cases we assume perfect channel state information and synchronisation. The channel frequency responses are shown in Figure 6.2. Channels A and B are Rayleigh fading channels, with an exponential power delay profile and mean excess delay of 50ns. Channel C is a Rician channel with similar diffuse component statistics and a 10dB Rice factor.

The simulated error rates and the analytical upper bound approximation for the AWGN channel and channel A are shown in Figure 6.3. We also plot the block error rate for an uncoded 64 subcarrier OFDM system transmitting information bits at the same rate, with each subcarrier employing a 32-QAM cross constellation [110]. Similar results for channels B and C are displayed in Figure 6.4.

We also plot the performance of the same OFDM system encoded with the $(511, 313)$ BCH code [38], one of the most powerful known block codes of similar rate and length to our system. The decoding complexity for this code is equivalent to a single pass of the Berlekamp-

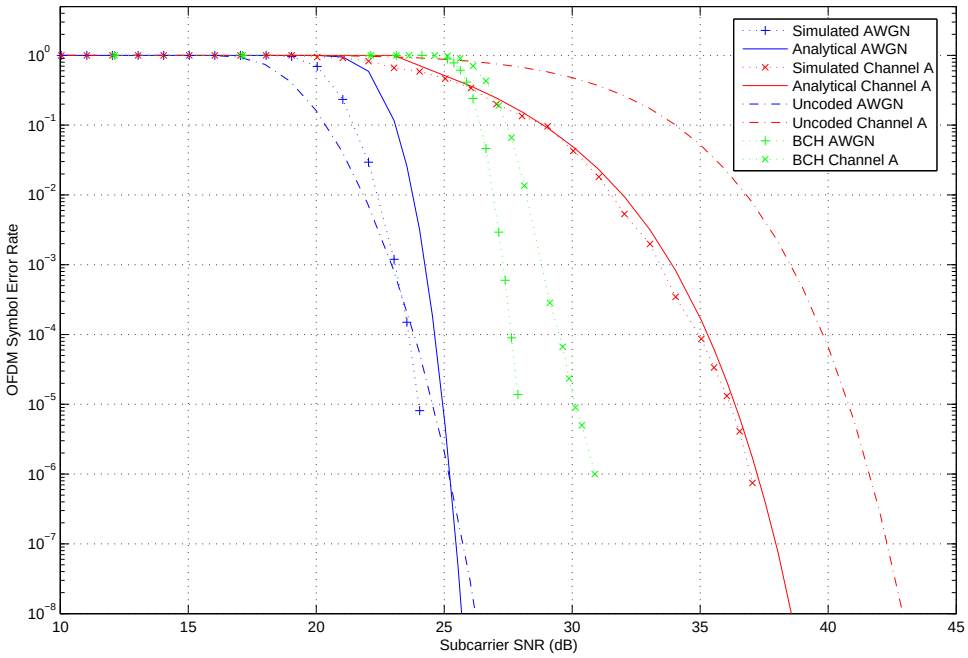

Figure 6.3 Analytical and simulated error rates for P_{128} encoded, GMD decoded, OFDM system transmitting over an AWGN channel and channel A

Massey algorithm [38]. Note that the P_{128} lattice encoded system exhibits superior performance over the AWGN channel, and channels B and C, at the cost of the complexity increase discussed in Section 6.3.3. However, performance of the P_{128} encoded system over channel A is poorer, due to the large fade in the channel response (Figure 6.2). The poorer performance of the P_{128} lattice on channel A is due to the poor lattice minimum product distance of P_{128}, despite its excellent minimum distance, as discussed in Section 6.2. The construction of lattices which provide far superior coding gains for channels with high frequency selectivity is beyond the scope of this thesis, however relevant results are found in [45] and [164].

We observe that the analysis provides good upper bounds, with accuracy within 1dB, 0.5dB, 2dB and 0.5dB, at an error rate of 10^{-5}, for the AWGN channel and channels A, B, and C, respectively. Note that we have used the derived analytical expressions to approximate upper bounds for very small error rates; error rates of 10^{-8} have been analytically calculated, although accurate simulation of the system at these error rates would require large computational expense.

The simulations and analysis both demonstrate the large coding gains provided by lattice encoding the OFDM symbol block for certain channels. For example, we estimate coding gain at an error rate of 10^{-6} to be approximately 1dB, 4.5dB, 1.2dB and 4dB for transmission

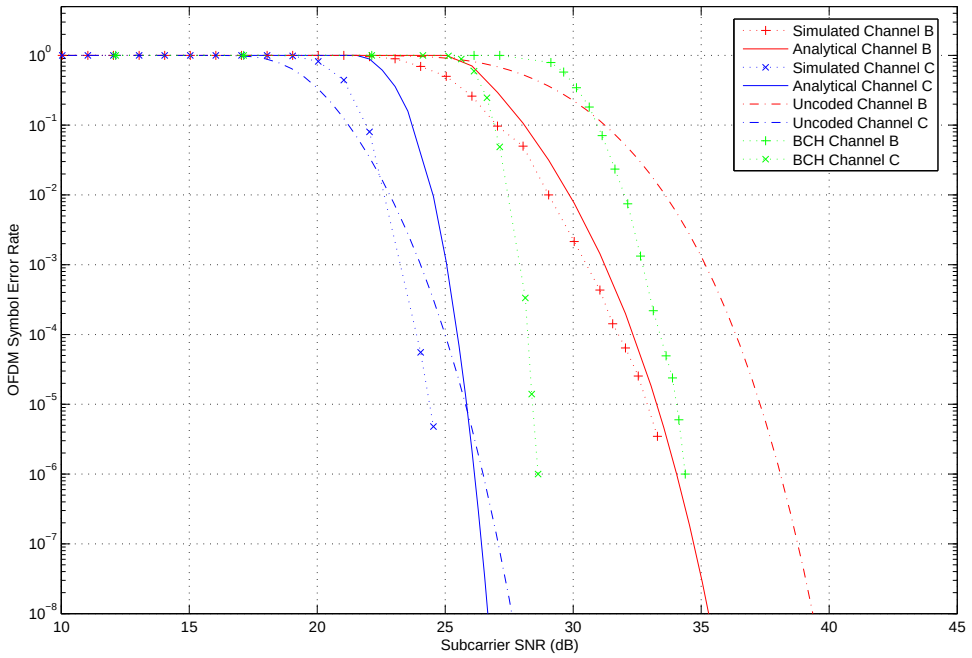

Figure 6.4 Analytical and simulated error rates for P_{128} encoded, GMD decoded OFDM system transmitting over channels B and C

over the AWGN channel, and channels A, B and C, respectively. Such large gains are due to the properties of the 128 dimensional sphere packing P_{128}. This comes at the cost of a decoding complexity of no more than $11,500$ real operations to decode each received lattice point, as compared to 512 operations for an uncoded system, as discussed in Section 6.3.3.

6.5 Summary

In this chapter we have proposed lattice encoding for wireless OFDM systems. Systems encoded with high dimensional lattices exhibit excellent coding gains, although maximum likelihood decoding is computationally infeasible. However, we have illustrated a practical decoding method for such systems, and outlined a method for analysis of its performance.

We have first considered encoding OFDM with lattices, and illustrated a simple mapping using the example of a Barnes-Wall lattice. The maximum likelihood decoding metric is derived, and shown to be the Euclidean distance from the equalised received point to the estimated point. We have then shown that the pairwise error probability of lattice encoded OFDM is proportional to the product distance of the underlying lattice, for systems operating over frequency selective channels. For a given lattice constellation and OFDM subchannel separation Δf, the pairwise error performance is dependent on the channel

rms excess delay τ_{rms}.

Maximum likelihood decoding of OFDM encoded with high dimensional lattices is not feasible due to the high computational expense. We have thus proposed generalised minimum distance (GMD) decoding as a low computational expense alternative. We have derived the optimal decoding metric for GMD lattice decoding, for OFDM systems operating over frequency selective channels. Then, using this metric we have derived probability functions for the reliability statistics and ordered reliability statistics. Using these probability functions we have been able to analytically approximate an upper bound on the error rate of GMD decoding high dimensional lattices.

Throughout this chapter we have illustrated the analysis with the example of a system encoded using the 128 dimensional Barnes-Wall lattice. We have demonstrated the large coding gains achievable using high dimensional lattices to encode OFDM systems, a consequence of the coding gains of the underlying lattices.

Chapter 7

Conclusions and Future Work

7.1 Conclusions

This thesis has undertaken analysis of the error performance of large wireless OFDM systems, that is, systems with a large number of subcarriers. We have firstly analysed the capacity and error rate performance of uncoded OFDM systems, and then proposed lattice coding as an error control method for large OFDM systems.

The capacity analysis of OFDM systems showed that, for large OFDM systems transmitting over frequency selective Rayleigh fading channels, the instantaneous capacity follows a fully describable Gaussian distribution. Furthermore, in the limit as the number of subcarriers, and system bandwidth, approaches infinity, we have shown that the capacity of such a large OFDM system approaches the capacity of a single carrier system occupying a flat fading channel with infinite bandwidth, or equivalently an infinite bandwidth, fading, frequency selective channel. We then analysed the error performance by first showing that the distribution of the number of symbol errors within an OFDM block is Poisson Binomial distributed, and may be approximated with the Poisson distribution. Furthermore, an upper bound on the approximation error was derived for Rayleigh fading channels. We then produced lower and upper bounds on the OFDM block error rate, for both Rician and Rayleigh fading channels. Calculation of the block error rate bounds necessitated derivation of simple expressions for the correlation between error rates on correlated narrowband Rayleigh or Rician fading channels. The uncoded OFDM analysis is applicable to a wide range of systems, since few restrictions are placed upon the system bandwidth, power or channel parameters. This analysis is useful in the design of error control methods for specific systems, since knowledge of the error performance of the system is critical for judicious choice of an error control coding scheme.

The second part of this thesis considered lattices for encoding large OFDM systems. This approach shows that very large coding gains may be achieved, since we exploited the high density of high dimensional lattices. We have shown a simple method for lattice encoding OFDM systems, and proved that the maximum likelihood decoding metric is the Euclidean distance. We then identified the optimal lattice property, for reduction of the pairwise error probability of lattice encoded OFDM transmitting over frequency selective channels, to be the product distance. However, we noted that maximum likelihood decoding of OFDM systems is computationally infeasible for the large constellations typically associated with high dimensional lattices. We thus proposed generalised minimum distance (GMD) decoding as a method for decoding such systems, and derived the optimal GMD decoding reliability metric for the frequency selective channel. A method for analysing the error performance of multistage GMD decoding of lattice encoded OFDM was then presented, requiring derivation of probability functions of reliability statistics and ordered reliability statistics. We illustrated our analysis with an example high data rate system, and showed that good error rate upper bounds are readily constructed. The simulated examples show that very high coding gains are available using high dimensional lattices.

7.2 Suggested Future Work

OFDM systems still command much research interest and, as processing power becomes less expensive, we can expect more complicated OFDM systems with greater expectations placed on these systems. The research presented in this thesis may be extended in many ways to cover further aspects of large OFDM systems. Some suggested topics for future research are listed below.

Although modern OFDM systems typically operate in slowly fading channels with reasonably good channel state information available, an obvious suggestion for future work is to remove the assumption of perfect channel state information. The capacity calculations of chapter four and error rate analysis of chapter five may be non-trivially extended to describe a receiver with imperfect subchannel gain estimates. We may similarly extend the analysis of chapter six to construct lattice coding systems more robust to imperfect subchannel gain estimates. However, the code error rate analysis may present an intractable problem, since such analysis is already difficult and requires some approximations.

We may similarly extend the analysis to OFDM systems with imperfect frequency and timing synchronisation. In this case subcarrier orthogonality is not preserved, and one would expect capacity to decrease and error rates to increase. However, analysis of these effects upon the capacity, distribution of the number of symbol errors, and block error rate has thus far proved difficult. Similarly, design of lattice codes to combat inter carrier interference could be undertaken.

Future work on high dimensional lattice codes could involve construction of lattices with high product distance. Although some of this is addressed by [164] and [45], the problem remains open, with the problem of constructing lattices with high product distance closely related to that of constructing high density lattices. This is in itself a vast research topic in mathematics, as documented by [7].

Note, from equation (6.46), that the union bound on the pairwise probability of lattice encoded OFDM error is derived as the lattice product distance divided by the determinant of the subchannel correlation matrix. From equation (6.48) note that this correlation matrix is Toeplitz. We require the determinant of this matrix, equal to the product of its eigenvalues. As such, we may be able to use the results presented in Gray's classic paper [179] on the limiting eigenvalues of Toeplitz matrices to draw conclusions on the limiting performance of lattice encoded OFDM operating over frequency selective channels, as the number of subcarrier approaches infinity. However, one would also require less available limiting results, or bounds, concerning the product distances of sphere packings as the dimension approaches infinity.

Although we have considered GMD decoding as a low complexity method for decoding high dimensional lattices, other soft decision decoding methods are applicable, including list based decoding [180]. Further work could consider the error performance of these alternative decoding methods for lattice encoded wireless OFDM.

Finally, it is possible that the error performance of multistage GMD decoding method may be improved by passing reliability information between the decoding stages. Such a method for improving multistage decoding is proposed in [181] and [182].

Appendix A

Pertinent Mathematical Expressions

This appendix lists mathematical expressions used throughout the thesis. Each expression may be found in [37] or [21]. The following notation is used: $\mathrm{J}_v(\cdot)$ is the v^{th} order Bessel function of the first kind, $\mathrm{I}_v(\cdot)$ is the v^{th} order modified Bessel function of the first kind, $\mathrm{Ei}(\cdot)$ is the exponential integral function, $\Gamma(\cdot)$ is the Gamma (factorial) function, $\Gamma(\cdot,\cdot)$ is the incomplete Gamma function, and $\mathrm{Q}(\cdot)$ is the Gaussian Q-function.

A.1 Alternative Integral Representations

$$\int_1^\infty \exp(-\mu x)\ln x = -\frac{1}{\mu}\mathrm{Ei}(-\mu), \text{ for } \mathrm{Re}[\mu] > 0 \tag{A.1}$$

$$\int_0^\infty \exp(-x^2)\left[\ln x\right]^2\, dx = \frac{\sqrt{\pi}}{8}\left[(\xi + 2\ln 2)^2 + \frac{\pi^2}{2}\right] \tag{A.2}$$

$$\int_0^\infty \exp(-\mu x)\left[\ln x\right]^2 = -\frac{1}{\mu}\left[\frac{\pi^2}{6} + (\xi + \ln\mu)^2\right], \text{ for } \mathrm{Re}[\mu] > 0 \tag{A.3}$$

$$\int x^n \exp(ax)dx = \exp(ax)\left(\frac{x^n}{a} + \sum_{k=1}^{n}(-1)^k\,\frac{n(n-1)\cdots(n-k+1)}{a^{k+1}}\,x^{n-k}\right) \tag{A.4}$$

$$\int_0^\infty \exp(-\alpha x)\mathrm{J}_0\left(\beta\sqrt{x}\right) = \frac{1}{\alpha}\exp\left(-\frac{\beta^2}{4\alpha}\right) \tag{A.5}$$

$$\int_0^\infty x^n \exp(-\mu x)dx = n!\mu^{-n-1} \text{ for } \mathrm{Re}[\mu] > 0 \tag{A.6}$$

$$\int_0^\infty \mathrm{erfc}\,(x) \exp\left(-\mu^2 x^2\right) dx = \frac{\arctan(\mu)}{\sqrt{\pi}\mu} \text{ for } \mathrm{Re}[\mu] > 0 \tag{A.7}$$

$$\int_u^\infty x^{v-1} \exp(-\mu x)dx = \mu^{-v}\Gamma(v, \mu u) \text{ for } \mathrm{Re}[\mu] > 0, u > 0. \tag{A.8}$$

A.2 The Error Function

$$\mathrm{erfc}(x) = 1 - \mathrm{erf}(x) = 2\mathrm{Q}(\sqrt{2}x) \triangleq \frac{2}{\sqrt{\pi}} \int_x^\infty \exp\left(-t^2\right)\, dt \tag{A.9}$$

$$\mathrm{erfc}(x) = \frac{2}{\pi} \int_0^{\frac{\pi}{2}} \exp\left(-\frac{x^2}{\sin^2\theta}\right)\, d\theta \tag{A.10}$$

A.3 Series Expansions

$$\mathrm{I_v}(x) = \left(\frac{x}{2}\right)^2 \sum_{k=0}^{\infty} \frac{\left(\frac{1}{4}x^2\right)^k}{k!\Gamma(v+k+1)}. \tag{A.11}$$

$$\mathrm{I}_0(x) = \left(\frac{x}{2}\right)^2 \sum_{k=0}^{\infty} \frac{\left(\frac{1}{4}x^2\right)^k}{(k!)^2}. \tag{A.12}$$

$$\mathrm{J_v}(x) = \left(\frac{x}{2}\right)^2 \sum_{k=0}^{\infty} \frac{\left(-\frac{1}{4}x^2\right)^k}{k!\Gamma(v+k+1)} \tag{A.13}$$

$$\mathrm{J}_0(x) = \left(\frac{x}{2}\right)^2 \sum_{k=0}^{\infty} \frac{\left(-\frac{1}{4}x^2\right)^k}{(k!)^2} \tag{A.14}$$

$$(a+x)^n = \sum_{k=0}^{n} \binom{n}{k} x^k a^{n-k}. \tag{A.15}$$

Appendix B

Ratio of Gaussian Random Variables

Consider two Gaussian random variables X and Y with means μ_X, μ_Y and variances σ_X^2, σ_Y^2, respectively. Furthermore let ρ be the coefficient of correlation between X and Y. We wish to find the distribution of the ratio $W = \frac{X}{Y}$. We show that $W' = \frac{a+U}{b+V}$, where U and V are standard Gaussian random variables and a and b are nonnegative constants, has the same distribution as $c + dW$, where c and d are constants.

Let $\tilde{X}$ and $\tilde{Y}$ be standard Gaussian random variables, with correlation coefficient ρ. We may write

$$\frac{X}{Y} = \frac{\mu_X + \sigma_X \tilde{X}}{\mu_Y + \sigma_Y \tilde{Y}} \tag{B.1}$$

and

$$\tilde{X} = \rho \tilde{Y} + \sqrt{1-\rho^2} Z \tag{B.2}$$

where Z is a standard Gaussian random variable, independent of both $\tilde{X}$ and $\tilde{Y}$. We can then write

$$\begin{aligned}
\frac{X}{Y} &= \frac{\mu_X + \sigma_X \rho \tilde{Y} + \sigma_X \sqrt{1-\rho^2} Z}{\mu_Y + \sigma_Y \tilde{Y}} \\
&= \frac{\sigma_X \rho}{\sigma_Y} + \frac{\mu_X - \sigma_X \sigma_Y^{-1} \rho \mu_Y + \sigma_X \sqrt{1-\rho^2} Z}{\mu_Y + \sigma_Y \tilde{Y}} \\
&= \frac{\sigma_X \rho}{\sigma_Y} + \frac{\sigma_X \sqrt{1-\rho^2}}{\sigma_Y} \times \frac{Z + \frac{1}{\sigma_X \sqrt{1-\rho^2}} \left[\mu_X - \sigma_X \sigma_Y^{-1} \rho \mu_Y\right]}{\tilde{Y} + \sigma_Y^{-1} \mu_Y} \\
&= c + d \frac{Z + a}{\tilde{Y} + b}
\end{aligned} \tag{B.3}$$

where

$$c = \frac{\rho\sigma_X}{\sigma_Y}, \qquad d = \frac{\sigma_X\sqrt{1-\rho^2}}{\sigma_Y}, \qquad a = \frac{\sigma_Y\mu_X - \rho\sigma_X\mu_Y}{\sigma_X\sigma_Y\sqrt{1-\rho^2}}, \qquad b = \frac{\mu_Y}{\sigma_Y}. \tag{B.4}$$

Thus, we may express the distribution of the ratio of correlated Gaussian random variables X and Y as the scaled and shifted ratio of the two independent standard Gaussian random variables Z and $\tilde{Y}$. From [183] the ratio W' of two shifted independent standard Gaussian random variables, has PDF

$$f_{W'}(t) = \frac{\exp\left(-\frac{a^2+b^2}{2}\right)}{\pi(1+t^1)}\left[1 + \frac{q}{\mathfrak{n}(q)}\int_0^q \mathfrak{n}(y)\,dy\right] \tag{B.5}$$

where $\mathfrak{n}(x)$ is the standard normal PDF and $q = \frac{b+at}{\sqrt{1+t^2}}$.

Appendix C

Inverse Correlation Matrix Determinant

We require the determinant of the matrix $\tilde{\mathbf{\Theta}}^{-1}$, defined as the $2|L| \times 2|L|$ matrix consisting of all $k, k+\frac{N}{2}$ rows and $k, k+\frac{N}{2}$ columns, such that $k \in L$, of $\left(\mathbf{\Theta}^{-1}_{\Psi\Psi\backslash\mathbf{S}_{(1)}} - \mathbf{\Theta}^{-1}_{\Psi\Psi\backslash\mathbf{S}_{(2)}}\right)$, where $L = \left\{k : S_{(1),k} \neq S_{(2),k},\, 1 \leq k \leq \frac{N}{2}\right\}$. Recall, from (6.27), that

$$\mathbf{\Theta}^{-1}_{\Psi\Psi\backslash\mathbf{S}_{(1)}} - \mathbf{\Theta}^{-1}_{\Psi\Psi\backslash\mathbf{S}_{(2)}} = \begin{bmatrix} \mathbf{0} & \frac{1}{N_0}\left(\mathbf{S}_{(1)} - \mathbf{S}_{(2)}\right) \\ -\frac{1}{N_0}\left(\mathbf{S}^{\dagger}_{(1)} - \mathbf{S}^{\dagger}_{(2)}\right) & \frac{1}{N_0}\left(\mathbf{S}^{\dagger}_{(1)}\mathbf{S}_{(1)} - \mathbf{S}^{\dagger}_{(2)}\mathbf{S}_{(2)}\right) \end{bmatrix}. \tag{C.1}$$

We may then write

$$\tilde{\mathbf{\Theta}}^{-1} = \begin{bmatrix} \mathbf{0} & \frac{1}{N_0}\left(\tilde{\mathbf{S}}_{(1)} - \tilde{\mathbf{S}}_{(2)}\right) \\ \frac{1}{N_0}\left(\tilde{\mathbf{S}}^{\dagger}_{(1)} - \tilde{\mathbf{S}}^{\dagger}_{(2)}\right) & \frac{1}{N_0}\left(\tilde{\mathbf{S}}^{\dagger}_{(1)}\tilde{\mathbf{S}}_{(1)} - \tilde{\mathbf{S}}^{\dagger}_{(2)}\tilde{\mathbf{S}}_{(2)}\right) \end{bmatrix} \tag{C.2}$$

where $\tilde{\mathbf{S}}_{(1)}$ and $\tilde{\mathbf{S}}_{(2)}$ are diagonal matrices, whose elements are the k^{th}, $k \in L$, elements of the diagonal matrices $\mathbf{S}_{(1)}$ and $\mathbf{S}_{(2)}$ respectively.

The determinant of $\tilde{\mathbf{\Theta}}^{-1}$ is then

$$\begin{aligned}
\det\left[\tilde{\mathbf{\Theta}}^{-1}\right] &= \det\left[\frac{1}{N_0}\left(\tilde{\mathbf{S}}_{(1)} - \tilde{\mathbf{S}}_{(2)}\right)\right]\det\left[-\frac{1}{N_0}\left(\tilde{\mathbf{S}}^{\dagger}_{(1)} - \tilde{\mathbf{S}}^{\dagger}_{(2)}\right)\right] \\
&= \frac{(-1)^{|L|}}{N_0^{2|L|}}\det\left[\tilde{\mathbf{S}}_{(1)} - \tilde{\mathbf{S}}_{(2)}\right]\det\left[\tilde{\mathbf{S}}^{\dagger}_{(1)} - \tilde{\mathbf{S}}^{\dagger}_{(2)}\right] \\
&= \frac{(-1)^{|L|}}{N_0^{2|L|}}\prod_{k=1}^{|L|}\left\{\tilde{S}_{(1),k} - \tilde{S}_{(2),k}\right\}\prod_{k=1}^{|L|}\left\{\tilde{S}^{\dagger}_{(1),k} - \tilde{S}^{\dagger}_{(2),k}\right\} \\
&= \frac{(-1)^{|L|}}{N_0^{2|L|}}\prod_{k\in L}\left|S_{(1),k} - S_{(2),k}\right|^2 .
\end{aligned} \tag{C.3}$$

Appendix D

GMD Reliability Probability Expressions

We presume reception of a point $r'_k = s_k + w'_k$ from an M-ary PAM constellation perturbed by additive white Gaussian noise w'_k with variance $\frac{N_0}{2|h_k|^2}$. We make a hard decision $\hat{s}_k$ as to the transmitted point, and denote the event that this hard decision is correct as G_k, and the event that it is incorrect as F_k. Given the log likelihood ratio $\mathcal{L}_k = \frac{\Pr(G_k, r_k)}{\Pr(F_k, r_k)}$, some relevant probability expressions are calculated.

We first calculate the probability of correct reception given that $\mathcal{L} \geq x$ for some $x > 0, x \in \mathbb{R}$. We recognise that the event of correct decision implies that the noise component magnitude $|w'_k| = |\hat{s}_k - r'_k|$, so that we may write

$$\begin{aligned} \Pr\left(G_k, \mathcal{L}_k \geq x\right) &= \Pr\left(G_k, \frac{4|h_k|^2 E_0}{N_0}\left[1 - \frac{|\hat{s}_k - r'_k|}{\sqrt{E_0}}\right] \geq x\right) \\ &= \Pr\left(|w'_k| \leq \frac{4|h_k|^2 E_0}{N_0}\sqrt{E_0} - \sqrt{E_0}x\right) \\ &= \operatorname{erf}\left(\sqrt{\frac{|h_k|^2 E_0}{N_0}}\left[\frac{4|h_k|^2 E_0}{N_0} - x\right]\right). \end{aligned} \tag{D.1}$$

Similarly, we may write

$$\begin{aligned}\Pr\left(G_k, 0 \leq \mathcal{L}_k \leq x\right) &= \Pr\left(G_k, 0 \leq \frac{4|h_k|^2 E_0}{N_0}\left[1 - \frac{|\hat{s}_k - r'_k|}{\sqrt{E_0}}\right] \leq x\right) \\ &= \Pr\left(\sqrt{E_0}\left[1 - \frac{N_0}{4|h_k|^2 E_0}x\right] \leq |w'_k| \leq \sqrt{E_0}\right) \\ &= \operatorname{erf}\left(\sqrt{\frac{|h_k|^2 E_0}{N_0}}\right) - \operatorname{erf}\left(\sqrt{\frac{|h_k|^2 E_0}{N_0}}\left[1 - \frac{N_0}{4|h_k|^2 E_0}x\right]\right).\end{aligned} \tag{D.2}$$

For the event F_k, we may approximate the required probabilities by assuming that the point $\hat{s}'_k$ is transmitted, the second closest point to r'_k, and point $\hat{s}_k$ is the hard decision. The noise component then satisfies $|w'_k| = 2\sqrt{E_0} - |\hat{s}_k - r'_k|$, and we may write

$$\begin{aligned}\Pr\left(F_k, \mathcal{L}_k \geq x\right) &= \Pr\left(F_k, \frac{4|h_k|^2 E_0}{N_0}\left[1 - \frac{|\hat{s}_k - r'_k|}{\sqrt{E_0}}\right] \geq x\right) \\ &\approx \Pr\left(F_k, \frac{4|h_k|^2 E_0}{N_0}\left[\frac{|w'_k|}{\sqrt{E_0}} - 1\right] \geq x\right) \\ &= \operatorname{erfc}\left(\sqrt{\frac{|h_k|^2 E_0}{N_0}}\left[\frac{N_0}{4|h_k|^2 E_0}x + 1\right]\right).\end{aligned} \tag{D.3}$$

Similarly, we may write

$$\begin{aligned}\Pr\left(F_k, 0 \leq \mathcal{L} \leq x\right) &= \Pr\left(F_k, 0 \leq \frac{4|h_k|^2 E_0}{N_0}\left[1 - \frac{|\hat{s}_k - r'_k|}{\sqrt{E_0}}\right] \leq x\right) \\ &\approx \Pr\left(0 \leq \frac{4|h_k|^2 E_0}{N_0}\left[\frac{|w'_k|}{\sqrt{E_0}} - 1\right] \leq x\right) \\ &= \operatorname{erfc}\left(\sqrt{\frac{|h_k|^2 E_0}{N_0}}\right) - \operatorname{erfc}\left(\sqrt{\frac{E_0}{N_0}}\left[1 + \frac{N_0}{4|h_k|^2 E_0}x\right]\right).\end{aligned} \tag{D.4}$$

We finally recognise that the log likelihood ratio is, by definition, nonnegative, so that

$$\Pr\left(G_k, \mathcal{L} < 0\right) = \Pr\left(F_k, \mathcal{L} < 0\right) = 0. \tag{D.5}$$

Appendix E

GMD Reliability PDFs

E.1 Correct Hard Decision Reliability

We presume the hard decision is correct, that is, the hard decision $\hat{s}_k$ is equal to the transmitted M-ary PAM point s_k. We denote this event as G_k. The points in the M-ary PAM constellation are labelled $s^{(0)}, s^{(1)}, \ldots, s^{(M)}$, as shown in Figure 6.1. From (6.76) we may write this reliability as

$$\alpha_k \triangleq \begin{cases} 0 & \text{for } |\hat{s}_k - r'_k| \geq \sqrt{E_0} \\ \frac{E_0}{t_0\sigma_k^2}\left(1 - \frac{|\hat{s}_k - r'_k|}{\sqrt{E_0}}\right) & \text{for } \sqrt{E_0}\left(1 - \frac{t_0\sigma_k^2}{E_0}\right) < |\hat{s}_k - r'_k| < \sqrt{E_0} \\ \frac{E_0}{t_0\sigma_k^2} & \text{for } |\hat{s}_k - r'_k| \leq \sqrt{E_0}\left(1 - \frac{t_0\sigma_k^2}{E_0}\right) \text{ and } \frac{E_0}{t_0\sigma_k^2} \leq 1 \\ 1 & \text{for } |\hat{s}_k - r'_k| \leq \sqrt{E_0}\left(1 - \frac{t_0\sigma_k^2}{E_0}\right) \text{ and } \frac{E_0}{t_0\sigma_k^2} > 1. \end{cases} \tag{E.1}$$

For transmission of $s^{(i)}$, with $i = 1, \ldots, M-2$, a correct hard decision is made if the noise element w'_k has magnitude $|w'_k| = |\hat{s}_k - r'_k| < \sqrt{E_0}$. That is, w'_k has the PDF of a two sided truncated Gaussian random variable, so that the magnitude $|\hat{s}_k - r'_k| = |w'_k|$ has PDF

$$f_{|\hat{s}_k - r'_k|}\left(x|\, G_k,\, s^{(i)} \text{ sent}\right) = \begin{cases} \frac{2}{\operatorname{erf}\left(\sqrt{\frac{E_0}{2\sigma^2}}\right)} \frac{1}{\sqrt{2\pi}\sigma} \exp\left(-\frac{x^2}{2\sigma^2}\right) & \text{for } 0 \leq x\sqrt{E_0} \\ 0 & \text{otherwise.} \end{cases} \tag{E.2}$$

We may then integrate this PDF to give the following probabilities

$$\begin{aligned}
\Pr\left(\left|\hat{s}_k - r'_k\right| > \sqrt{E_0}\right) &= 0 \\
\Pr\left(\left|\hat{s}_k - r'_k\right| \leq \left[1 - \frac{t_0\sigma_k^2}{E_0}\right]\sqrt{E_0}\right) &= \begin{cases} \dfrac{\operatorname{erf}\left(\sqrt{\frac{E_0}{2\sigma_k^2}}\left[1-\frac{t_0\sigma_k^2}{E_0}\right]\right)}{\operatorname{erf}\left(\sqrt{\frac{E_0}{2\sigma_k^2}}\right)} & \text{for } \frac{E_0}{t_0\sigma_k^2} > 1 \\ 0 & \text{for } \frac{E_0}{t_0\sigma_k^2} \leq 1 \end{cases} \\
\Pr\left(\left[1 - \frac{t_0\sigma_k^2}{E_0}\right]\sqrt{E_0} < \left|\hat{s}_k - r'_k\right| < \sqrt{E_0}\right) &= \begin{cases} 1 - \dfrac{\operatorname{erf}\left(\sqrt{\frac{E_0}{2\sigma_k^2}}\left[1-\frac{t_0\sigma_k^2}{E_0}\right]\right)}{\operatorname{erf}\left(\sqrt{\frac{E_0}{2\sigma_k^2}}\right)} & \text{for } \frac{E_0}{t_0\sigma_k^2} > 1 \\ 1 & \text{for } \frac{E_0}{t_0\sigma_k^2} \leq 1 \end{cases}.
\end{aligned} \tag{E.3}$$

Then, with the above probability expressions and the definition of α_k from (E.1), we use the transformation of random variables technique [184] to obtain the conditional PDFs that follow. Firstly, in the case when $\frac{E_0}{t_0\sigma_k^2} > 1$,

$$\begin{aligned}
&f_{\alpha_k}\left(x\middle|G_k,\, s_k = s^{(i)} :\, i \in \{1,\ldots,M-1\},\, \frac{E_0}{t_0\sigma_k^2} > 1\right) \\
&= \begin{cases} \dfrac{\operatorname{erf}\left(\sqrt{\frac{E_0}{2\sigma_k^2}}\left[1-\frac{t_0\sigma_k^2}{E_0}\right]\right)}{\operatorname{erf}\left(\sqrt{\frac{E_0}{2\sigma_k^2}}\right)} & \text{for } x = 1 \\ \dfrac{2}{\operatorname{erf}\left(\sqrt{\frac{E_0}{2\sigma_k^2}}\right)} \cdot \frac{t_0\sigma_k}{\sqrt{E_0}} \cdot \frac{1}{\sqrt{2\pi}} \exp\left(-\frac{E_0}{2\sigma_k^2}\left[1 - \frac{t_0\sigma_k^2}{E_0}x\right]^2\right) & \text{for } 0 < x \leq 1 \\ 0 & \text{otherwise;} \end{cases}
\end{aligned} \tag{E.4}$$

and in the case when $\frac{E_0}{t_0\sigma_k^2} \leq 1$ we may write

$$\begin{aligned}
&f_{\alpha_k}\left(x\middle|G_k,\, s_k = s^{(i)} :\, i \in \{1,\ldots,M-1\},\, \frac{E_0}{t_0\sigma_k^2} \leq 1\right) \\
&= \begin{cases} \dfrac{2}{\operatorname{erf}\left(\sqrt{\frac{E_0}{2\sigma_k^2}}\right)} \cdot \frac{t_0\sigma_k}{\sqrt{E_0}} \cdot \frac{1}{\sqrt{2\pi}} \exp\left(-\frac{E_0}{2\sigma_k^2}\left[1 - \frac{t_0\sigma_k^2}{E_0}x\right]^2\right) & \text{for } 0 \leq x \leq \frac{E_0}{t_0\sigma_k^2} \\ 0 & \text{otherwise.} \end{cases}
\end{aligned} \tag{E.5}$$

We next consider the case when a constellation end point is transmitted, $s_k = s^{(0)}$. Correct transmission then implies $w'_k < \sqrt{E_0}$, so that w'_k has the PDF of a one sided truncated

Gaussian random variable,

$$f_{w_k'}\left(x\middle|s_k=s^{(0)},\,G_k\right)=\begin{cases}\frac{2}{1+\mathrm{erf}\left(\sqrt{\frac{E_0}{2\sigma_k^2}}\right)}\cdot\frac{1}{\sqrt{2\pi\sigma_k^2}}\exp\left(-\frac{-x^2}{2\sigma_k^2}\right) & \text{for } x<\sqrt{E_0}\\ 0 & \text{otherwise.}\end{cases}\tag{E.6}$$

The magnitude $|\hat{s}_k - r_k'| = |w_k'|$ then has PDF

$$f_{|\hat{s}_k-r_k'|}\left(x\middle|s_k=s^{(0)},\,G_k\right)=\begin{cases}\frac{2}{1+\mathrm{erf}\left(\sqrt{\frac{E_0}{2\sigma_k^2}}\right)}\cdot\frac{1}{\sqrt{2\pi\sigma_k^2}}\exp\left(-\frac{-x^2}{2\sigma_k^2}\right) & \text{for } x>\sqrt{E_0}\\ \frac{4}{1+\mathrm{erf}\left(\sqrt{\frac{E_0}{2\sigma_k^2}}\right)}\cdot\frac{1}{\sqrt{2\pi\sigma_k^2}}\exp\left(-\frac{-x^2}{2\sigma_k^2}\right) & \text{for } 0\le x\le\sqrt{E_0}\\ 0 & \text{otherwise.}\end{cases}\tag{E.7}$$

We may then integrate this PDF to calculate the following probabilities

$$\begin{aligned}\Pr\left(\left|\hat{s}_k-r_k'\right|\ge\sqrt{E_0}\right)=&\frac{\mathrm{erfc}\left(\sqrt{\frac{E_0}{2\sigma_k^2}}\right)}{1+\mathrm{erf}\left(\sqrt{\frac{E_0}{2\sigma_k^2}}\right)}\\ \Pr\left(\left|\hat{s}_k-r_k'\right|\le\left[1-\frac{t_0\sigma_k^2}{E_0}\right]\sqrt{E_0}\right)=&\begin{cases}\frac{2\mathrm{erf}\left(\sqrt{\frac{E_0}{2\sigma_k^2}}\left[1-\frac{t_0\sigma_k^2}{E_0}\right]\right)}{1+\mathrm{erf}\left(\sqrt{\frac{E_0}{2\sigma_k^2}}\right)} & \text{for } \frac{E_0}{t_0\sigma_k^2}>1\\ 0 & \text{for } \frac{E_0}{t_0\sigma_k^2}\le 1\end{cases}\end{aligned}\tag{E.8}$$

and

$$\begin{aligned}&\Pr\left(\left[1-\frac{t_0\sigma_k^2}{E_0}\right]\sqrt{E_0}<\left|\hat{s}_k-r_k'\right|<\sqrt{E_0}\right)\\ &=\begin{cases}\frac{2\mathrm{erf}\left(\sqrt{\frac{E_0}{2\sigma_k^2}}\right)-2\mathrm{erf}\left(\sqrt{\frac{E_0}{2\sigma_k^2}}\left[1-\frac{t_0\sigma_k^2}{E_0}\right]\right)}{1+\mathrm{erf}\left(\sqrt{\frac{E_0}{2\sigma_k^2}}\right)} & \text{for } \frac{E_0}{t_0\sigma_k^2}>1\\ \frac{2\mathrm{erf}\left(\sqrt{\frac{E_0}{2\sigma_k^2}}\right)}{1+\mathrm{erf}\left(\sqrt{\frac{E_0}{2\sigma_k^2}}\right)} & \text{for } \frac{E_0}{t_0\sigma_k^2}\le 1.\end{cases}\end{aligned}\tag{E.9}$$

Then, with the above probability expressions and the definition of α_k from (E.1), we use the transformation of random variables technique [184] to write the following conditional

PDFs. Firstly, in the case when $\frac{E_0}{t_0\sigma_k^2} > 1$,

$$f_{\alpha_k}\left(x\middle|G_k,\, s_k = s^{(0)},\, \frac{E_0}{t_0\sigma_k^2} > 1\right)$$
$$= \begin{cases} \frac{\operatorname{erfc}\left(\sqrt{\frac{E_0}{2\sigma_k^2}}\right)}{1+\operatorname{erf}\left(\sqrt{\frac{E_0}{2\sigma_k^2}}\right)} & \text{for } x = 0 \\ \frac{4}{1+\operatorname{erf}\left(\sqrt{\frac{E_0}{2\sigma_k^2}}\right)} \frac{t_0\sigma_k}{\sqrt{E_0}\sqrt{2\pi}} \exp\left(-\frac{E_0}{2\sigma_k^2}\left[1-\frac{t_0\sigma_k^2}{E_0}x\right]^2\right) & \text{for } 0 < x < 1 \\ \frac{2\operatorname{erf}\left(\sqrt{\frac{E_0}{2\sigma_k^2}}\left[1-\frac{t_0\sigma_k^2}{E_0}\right]\right)}{1+\operatorname{erf}\left(\sqrt{\frac{E_0}{2\sigma_k^2}}\right)} & \text{for } x = 1 \\ 0 & \text{otherwise;} \end{cases} \tag{E.10}$$

and in the case when $\frac{E_0}{t_0\sigma_k^2} \leq 1$ we may write

$$f_{\alpha_k}\left(x\middle|G_k,\, s_k = s^{(0)},\, \frac{E_0}{t_0\sigma_k^2} \leq 1\right)$$
$$= \begin{cases} \frac{\operatorname{erfc}\left(\sqrt{\frac{E_0}{2\sigma_k^2}}\right)}{1+\operatorname{erf}\left(\sqrt{\frac{E_0}{2\sigma_k^2}}\right)} & \text{for } x = 0 \\ \frac{4}{1+\operatorname{erf}\left(\sqrt{\frac{E_0}{2\sigma_k^2}}\right)} \frac{t_0\sigma_k}{\sqrt{E_0}\sqrt{2\pi}} \exp\left(-\frac{E_0}{2\sigma_k^2}\left[1-\frac{t_0\sigma_k^2}{E_0}x\right]^2\right) & \text{for } 0 < x \leq \frac{E_0}{t_0\sigma_k^2} \\ 0 & \text{otherwise.} \end{cases} \tag{E.11}$$

It is readily shown that the reliability α_k, conditional on constellation point $s_k = s_{M-1}$ being transmitted and correctly received, follows the same distribution as in (E.10) and (E.11).

E.2 Incorrect Hard Decision Reliability

We now presume that some point s_k is transmitted, and the hard decision is incorrect. Thus, $\hat{s}_k \neq s_k$, an event denoted by F_k. The value α_k is again defined by (E.1). If the hard decision is incorrect, we may approximate the PDF of α_k by assuming that the actual transmitted point is the second closest point to the hard decision, so that $s_k = \hat{s}'_k$. Since $|\hat{s}_k - \hat{s}'_k| = 2\sqrt{E_0}$, we may then write

$$\left|\hat{s}_k - r'_k\right| = \left|2\sqrt{E_0} - |w'_k|\right| \tag{E.12}$$

where w'_k is the Gaussian distributed noise. Under the assumption that $s_k = \hat{s}'_k$, the noise has magnitude $\sqrt{E_0} < |w'_k| < 3\sqrt{E_0}$, with PDF

$$f_{|w'_k|}\left(x|s_k = \hat{s}'_k\right) = \begin{cases} \frac{2}{\operatorname{erf}\left(3\sqrt{\frac{E_0}{2\sigma_k^2}}\right) - \operatorname{erf}\left(\sqrt{\frac{E_0}{2\sigma_k^2}}\right)} \frac{1}{\sqrt{2\pi\sigma_k^2}} \exp\left(-\frac{x^2}{2\sigma_k^2}\right) & \text{for } \sqrt{E_0} < x < 3\sqrt{E_0} \\ 0 & \text{otherwise.} \end{cases} \tag{E.13}$$

We then write the PDF of $|\hat{s}_k - r'_k|$ as

$$f_{|\hat{s}_k - r'_k|}\left(x|s_k = \hat{s}'_k\right) = \begin{cases} \frac{2}{\operatorname{erf}\left(3\sqrt{\frac{E_0}{2\sigma_k^2}}\right) - \operatorname{erf}\left(\sqrt{\frac{E_0}{2\sigma_k^2}}\right)} \frac{1}{\sqrt{2\pi\sigma_k^2}} \left[\exp\left(-\frac{[2\sqrt{E_0}+x]^2}{2\sigma_k^2}\right) + \exp\left(-\frac{[2\sqrt{E_0}-x]^2}{2\sigma_k^2}\right)\right] & \text{for } 0 < x < \sqrt{E_0} \\ 0 & \text{otherwise.} \end{cases} \tag{E.14}$$

We may then integrate this PDF to obtain the following probability expressions

$$\begin{aligned} \Pr\left(\left|\hat{s}_k - r'_k\right| \leq \sqrt{E_0}\right) &= 0 \\ \Pr\left(\left|\hat{s}_k - r'_k\right| \geq \left[1 - \frac{t_0\sigma_k^2}{E_0}\right]\sqrt{E_0}\right) &= \begin{cases} \frac{\operatorname{erf}\left(\sqrt{\frac{E_0}{2\sigma_k^2}}\left[3 - \frac{t_0\sigma_k^2}{E_0}\right]\right) - \operatorname{erf}\left(\sqrt{\frac{E_0}{2\sigma_k^2}}\left[1 + \frac{t_0\sigma_k^2}{E_0}\right]\right)}{\operatorname{erf}\left(3\sqrt{\frac{E_0}{2\sigma_k^2}}\right) - \operatorname{erf}\left(\sqrt{\frac{E_0}{2\sigma_k^2}}\right)} & \text{for } \frac{E_0}{t_0\sigma_k^2} > 1 \\ 0 & \text{for } \frac{E_0}{t_0\sigma_k^2} \leq 1. \end{cases} \end{aligned} \tag{E.15}$$

Then, with the above probability expressions and the definition of α_k from (E.1), we use the transformation of random variables technique to write the following conditional PDFs. Firstly, in the case when $\frac{E_0}{t_0\sigma_k^2} > 1$,

$$\begin{aligned} & f_{\alpha_k}\left(x|s_k = \hat{s}'_k, \frac{E_0}{t_0\sigma_k^2} > 1\right) \\ &= \begin{cases} \frac{2t_0\sigma_k}{\sqrt{E_0}\sqrt{2\pi}} \frac{\exp\left(\frac{E_0}{2\sigma_k^2}\left[3 - \frac{t_0\sigma_k^2}{E_0}x\right]^2\right) - \exp\left(\frac{E_0}{2\sigma_k^2}\left[1 + \frac{t_0\sigma_k^2}{E_0}x\right]^2\right)}{\operatorname{erf}\left(3\sqrt{\frac{E_0}{2\sigma_k^2}}\right) - \operatorname{erf}\left(\sqrt{\frac{E_0}{2\sigma_k^2}}\right)} & \text{for } 0 \leq x < 1 \\ \frac{\operatorname{erf}\left(\sqrt{\frac{E_0}{2\sigma_k^2}}\left[3 - \frac{t_0\sigma_k^2}{E_0}\right]\right) - \operatorname{erf}\left(\sqrt{\frac{E_0}{2\sigma_k^2}}\left[1 + \frac{t_0\sigma_k^2}{E_0}\right]\right)}{\operatorname{erf}\left(3\sqrt{\frac{E_0}{2\sigma_k^2}}\right) - \operatorname{erf}\left(\sqrt{\frac{E_0}{2\sigma_k^2}}\right)} & \text{for } x = 1 \\ 0 & \text{otherwise.} \end{cases} \end{aligned} \tag{E.16}$$

In the case when $\frac{E_0}{t_0\sigma_k^2} \leq 1$ we may write

$$
\begin{aligned}
& f_{\alpha_k}\left(x|s_k = \hat{s}'_k,\ \frac{E_0}{t_0\sigma_k^2} \leq 1\right) \\
&= \begin{cases} \frac{2t_0\sigma_k}{\sqrt{E_0}\sqrt{2\pi}} \frac{\exp\left(\frac{E_0}{2\sigma_k^2}\left[3-\frac{t_0\sigma_k^2}{E_0}x\right]^2\right) - \exp\left(\frac{E_0}{2\sigma_k^2}\left[1+\frac{t_0\sigma_k^2}{E_0}x\right]^2\right)}{\operatorname{erf}\left(3\sqrt{\frac{E_0}{2\sigma_k^2}}\right) - \operatorname{erf}\left(\sqrt{\frac{E_0}{2\sigma_k^2}}\right)} & \text{for } 0 \leq x \leq \frac{E_0}{t_0\sigma_k^2} \\ 0 & \text{otherwise.} \end{cases}
\end{aligned}
\tag{E.17}
$$

References

[1] C. E. Shannon, "A mathematical theory of communication," *Bell Sys. Tech. J.*, vol. 27, pp. 379–423, 623–656, 1948.

[2] (2005) Statistics New Zealand. [Online]. Available: www.stats.govt.nz/quick-facts/comm-arts-science/telecommunications.htm

[3] S. Haykin and M. Moher, *Modern wireless communications*. Upper Saddle River, NJ: Pearson Prentice Hall, 2005.

[4] A. F. Molisch, Ed., *Wideband Wireless Digital Communications*. Upper Saddle River, NJ: Prentice-Hall, 2001.

[5] A. Calderbank, "The art of signaling: Fifty years of coding theory," *IEEE Trans. Inform. Theory*, vol. 44, no. 6, pp. 2561–2595, Oct. 1998.

[6] *Digital Video Broadcasting (DVB-T); Framing structure, channel coding, and modulation for digital terrestrial television*, ETSI Std. ETS 300 744, Dec. 2001.

[7] J. H. Conway and N. J. A. Sloane, *Sphere Packings, Lattices and Groups*. New York, NY: Springer - Verlag, 1999.

[8] S. Haykin, *Communications Systems*. New York, NY: John Wiley & Sons, 1994.

[9] J. G. Proakis, *Digital Communications*. New York, NY: McGraw-Hill, 1989.

[10] T. S. Rappaport, *Wireless Communications, Principles and Practice*. Upper Saddle River, NJ: Prentice Hall, 2002.

[11] W. C. Jakes, *Microwave Mobile Communications*. New York, NY: IEEE Press, 1994.

[12] P. A. Bello, "Characterization of randomly time-variant linear channels," *IEEE Trans. Commun.*, vol. 11, pp. 360–393, Dec. 1963.

[13] R. M. Gray, *Source Coding Theory*. New York, NY: Springer, 1989.

[14] R. Veldhuis and M. Breeuwer, *An Introduction to Source Coding*. Upper Saddle River, NJ: Prentice Hall, 1993.

[15] A. Monk and L. Milstein, "Open-loop power control error in a land mobile system," vol. 13, no. 2, pp. 205–212, Feb. 1995.

[16] A. Goldsmith, "Design and performance of high-speed communication systems over time-varying radio channels," Ph.D. dissertation, University of California, Berkeley, CA, 1994.

[17] K. Pahlavan and A. H. Levesque, *Wireless Information Networks*. New York, NY: John Wiley, 1995.

[18] A. Papoulis, *Probability, Random Variables, and Stochastic Processes*. New York, NY: McGraw-Hill, 1984.

[19] M. K. Simon, *Probability Distributions involving Gaussian random variables: a handbook for Engineers and scientists*. Boston, MA: Kluwer Academic Publishers, 2002.

[20] S. Rice, "Statistical properties of a sine wave plus random noise," *Bell Sys. Tech. J.*, vol. 24, pp. 109–157, 1948.

[21] I. S. Gradshteyn and I. M. Ryzhik, *Table of Integrals, Series, and Products*. New York, NY: Academic Press, 1965.

[22] S. Stein, "Fading channel issues in system engineering," *IEEE J. Select. Areas Commun.*, vol. 5, pp. 68–89, Feb. 1987.

[23] W. H. Tranter, K. S. Shanmugan, T. S. Rappaport, and K. L. Kosbar, *Principles of Communications Systems Simulation with Wireless Applications*. Upper Saddle River, NJ: Prentice-Hall, 2004.

[24] T. S. Rappaport, S. Y. Seidel, and R. Singh, "900-MHz multipath propagation measurements for U.S. digital cellular radiotelephone," *IEEE Trans. Veh. Technol.*, vol. 39, no. 2, pp. 132–139, May 1990.

[25] S. Y. Seidel and T. S. Rappaport, "Path loss and multipath delay statistics in four European cities for 900MHz cellular and microcellular communications," *IEEE Elec. Letters*, vol. 26, no. 20, pp. 1713–1715, Sept. 1990.

[26] S. Y. Seidel, T. S. Rappaport, S. Jain, M. L. Lord, and R. Singh, "Path loss, scattering, and multipath delay statistics in four European cities for digital cellular and microcellular radiotelephone," *IEEE Trans. Veh. Technol.*, vol. 40, no. 4, pp. 721–730, Nov. 1991.

[27] J. Parsons and J. Gardiner, *Mobile Communications Systems*. Glasgow, UK: Blackie, 1989.

[28] J. K. Cavers, *Mobile Channel Characteristics*. Boston, MA: Kluwer Academic, 2000.

[29] R. Clarke, "A statistical theory of mobile radio reception," *Bell Systems Tech. J.*, pp. 957–1000, July-August 1968.

[30] R. K. Mallik, "On multivariate Rayleigh and exponential distributions," *IEEE Trans. Inform. Theory*, vol. 49, no. 6, pp. 1499–1515, June 2003.

[31] H. Nakagami, *Statistical Methods and Radio Wave Propagation*. Oxford, England: Pergamon Press, 1960, pp. 3–36.

[32] W. Weibull, "A statistical function of wide distribution," *J. Appl. Mech.*, vol. 18, pp. 293–297, 1951.

[33] H. Hashemi, "The indoor radio propagation channel," *Proc. IEEE*, vol. 81, pp. 943–968, July 1993.

[34] A. J. Coulson, "Characterization of the mobile radio multipath channel," Ph.D. dissertation, University of Auckland, Auckland, New Zealand, 1998.

[35] M. C. Jeruchim, P. Balaban, and K. S. Shanmugan, *Simulation of Communication Systems*. New York, NY: Kluwer Academic, 2000.

[36] D. Verdin and T. Tozer, "Generating a fading process for the simulation of land-mobile radio communications," *IEEE Electronics Letters*, vol. 29, no. 5, pp. 490–492, Mar. 1993.

[37] M. Abramowitz and I. A. Stegun, Eds., *Handbook of Mathematical Functions*. New York, NY: Dover, 1965.

[38] S. B. Wicker, *Error Control Systems for Digital Communication and Storage*. Upper Saddle River, NJ: Prentice-Hall, 1995.

[39] S. Lin and D. J. Costello, *Error Control Coding*, 2nd ed. Upper Saddle River, NJ: Prentice-Hall, 2004.

[40] *Wireless LAN Medium Access Control (MAC) and Physical Layer (PHY) Specification*, IEEE Std. 802.11a, 1997.

[41] *Radio Broadcast Systems; Digital audio broadcasting (DAB) to mobile, portable, and fixed receivers*, ETSI Std. ETS 300 401, May 1997.

[42] R. de Buda, "Some optimal codes have structure," *IEEE J. Select. Areas Commun.*, vol. 7, no. 6, pp. 893–899, Aug. 1989.

[43] G. D. Forney, M. D. Trott, and S.-Y. Chung, "Sphere-bound-achieving coset codes and multilevel coset codes," *IEEE Trans. Inform. Theory*, vol. 46, no. 3, pp. 820–850, May 2000.

[44] R. Urbanke and B. Rimoldi, "Lattice codes can achieve capacity on the AWGN channel," *IEEE Trans. Inform. Theory*, vol. 44, no. 1, pp. 273–278, Jan. 1998.

[45] J. Boutros, E. Viterbo, C. Rastello, and J.-C. Belfiore, "Good lattice constellations for both Rayleigh fading and Gaussian channels," *IEEE Trans. Inform. Theory*, vol. 42, no. 2, pp. 502–518, Mar. 1996.

[46] W. K. Nicholson, *Introduction to Abstract Algebra*, 2nd ed. New York, NY: Wiley, 1999.

[47] E. Berlekamp, Ed., *Key Papers in the Development of Coding Theory*. New York, NY: IEEE Press, 1974.

[48] I. Reed and G. Solomon, "Polynomial codes over certain finite fields," *SIAM J. Appl. Math.*, vol. 8, pp. 300–304, 1960.

[49] R. Bose and D. Ray-Chaudhuri, "On a class of error correcting binary group codes," *Information and Control*, vol. 3, pp. 68–79, Mar. 1960.

[50] ——, "Further results on error correcting binary group codes," *Information and Control*, vol. 3, pp. 279–290, Sept. 1960.

[51] A. Hocquenghem, "Codes correcteurs d'erreurs," *Chiffres*, vol. 2, pp. 147–156, 1959.

[52] D. Muller, "Application of Boolean algebra to switching circuit design," *IEEE Trans. Computers*, vol. 3, pp. 6–12, Sept. 1954.

[53] I. Reed, "A class of multiple-error-correcting codes and a decoding scheme," *IEEE Trans. Inform. Theory*, vol. 4, pp. 38–49, Sept. 1954.

[54] E. Berlekamp, *Algebraic Coding Theory*. New York, NY: McGraw-Hill, 1968.

[55] J. Massey, "Shift register synthesis and BCH decoding," *IEEE Trans. Inform. Theory*, vol. IT-15, no. 1, pp. 122–127, Jan.

[56] G. D. Forney, "Generalized minimum distance decoding," *IEEE Trans. Inform. Theory*, vol. 12, pp. 125–131, 1966.

[57] G. D. Forney and A. Vardy, "Generalized minimum-distance decoding of Euclidean-space codes and lattices," *IEEE Trans. Inform. Theory*, vol. 42, no. 6, pp. 1992–2025, 1996.

[58] C. Schlegel, *Trellis Coding*. New York, NY: IEEE Press, 1997.

[59] C. Rogers, "A note on coverings," *Mathematika*, vol. 4, pp. 1–6, 1957.

[60] ——, *Packing and Covering*. Cambridge, UK: Cambridge Univ. Press, 1964.

[61] J. Leech, "Notes on sphere packings," *Can. J. Math.*, vol. 19, pp. 251–267, 1967.

[62] G. Kabatiansky and V. Levenshtein, "Bounds for packings on a sphere and in space," *Problems of Information Transmission (English trans.)*, vol. 14, no. 1, pp. 1–17, 1978.

[63] H. Minkowski, "Ausgewählte arbeiten zur zahlentheorie und zur geometrie [in German] (Selected papers on number theory and geometry)," 1989.

[64] C. F. Gauss, "Besprechung des Buchs von L.A.Seeber: Untersuchung über die Eigenschaften der positiven tern'"

[65] T. Gosset, "On the regular and semi-regular figures in space of n dimensions," *Messenger Math.*, vol. 29, pp. 43–48, 1900.

[66] H. Coexeter and J. Todd, "An extreme duodenary form," *Can. J. Math.*, pp. 384–392, 1953.

[67] H.-G. Quebbemann, "Lattices with theta functions for $g\sqrt{2}$ and linear codes," *J. Algebra*, vol. 105, pp. 443–450, 1987.

[68] E. Barnes and G. Wall, "Some extreme forms defined in terms of Abelian groups," *J. Austral. Math. Soc.*, vol. 1, pp. 47–63, 1959.

[69] G. Nebe, "Some cyclo-quaternionic lattices," *J. Algebra*, vol. 199, pp. 472–498, 1998.

[70] G. Ungerboek, "Channel coding with multileve/phase signals," *IEEE Trans. Inform. Theory*, vol. IT-28, pp. 55–67, 1982.

[71] G. D. Forney, "Coset codes - Part I: Introduction and geometrical classification," *IEEE Trans. Inform. Theory*, vol. 34, no. 5, pp. 1123–1151, 1988.

[72] ——, "Coset codes - Part II: Binary lattices and related codes," *IEEE Trans. Inform. Theory*, vol. 34, no. 5, pp. 1152–1187, 1988.

[73] G. D. Forney, R. G. Gallager, G. R. Lang, F. M. Longstaff, and S. U. Qureshi, "Efficient modulation for band-limited channels," *IEEE J. Select. Areas Commun.*, vol. SAC-2, no. 5, pp. 632–647, 1984.

[74] G. D. Forney and L.-F. Wei, "Multidimensional constellations - part I: Introduction, figures of merit, and generalized cross constellations," *IEEE J. Select. Areas Commun.*, vol. 7, no. 6, pp. 877–892, 1989.

[75] G. J. Pottie and D. P. Taylor, "Multilevel codes based on partitioning," *IEEE Trans. Inform. Theory*, vol. 35, no. 1, pp. 87–98, Jan. 1989.

[76] A. Calderbank, "Multilevel codes and multistage decoding," *IEEE Trans. Commun.*, vol. 37, no. 3, pp. 222–229, March 1989.

[77] U. Wachsmann, R. F. Fischer, and J. B. Huber, "Multilevel codes: Theoretical concepts and practical design rules," *IEEE Trans. Inform. Theory*, vol. 45, no. 5, pp. 1361–1391, July 1999.

[78] R. F. Fischer, J. B. Huber, and U. Wachsmann, "Multilevel coding: Aspects from information theory," in *Proc. Global Telcommunications Conference, 1996. GLOBECOM '96*, Nov. 1996, pp. 26–30.

[79] D. Agrawal and A. Vardy, "Generalized minimum distance decoding in Euclidean space: Performance analysis," *IEEE Trans. Inform. Theory*, vol. 46, no. 1, pp. 60–83, 2000.

[80] A. R. S. Bahai and B. R. Saltzberg, *Multi-Carrier Digital Communications*. New York, NY: Kluwer Academic, 1999.

[81] W. H. Press, *Numerical Recipes in C*, 2nd ed. Cambridge, NY: Cambridge University Press.

[82] R. Chang, "Synthesis of band-limited orthogonal signals for multichannel data transmission," *Bell Sys. Tech. J.*, vol. 45, Dec. 1966.

[83] B. Saltzberg, "Performance of an efficient parallel data transmission system," *IEEE Trans. Commun.*, vol. 15, pp. 805–811, Dec. 1967.

[84] S. B. Weinstein and P. M. Ebert, "Data transmission by frequency-division multiplexing using the discrete Fourier transform," *IEEE Trans. Commun.*, vol. com-19, no. 5, pp. 628–634, Oct. 1971.

[85] L. J. Cimini, Jr., "Analysis and simulation of a digital mobile channel using orthogonal frequency division multiplexing," *IEEE Trans. Commun.*, vol. com-33, no. 7, pp. 665–675, July 1985.

[86] *Network and Customer Installation Interfaces - Asymmetric Digital Subscriber Line (ADSL) Metallic Interface*, ANSI Std. ANSI TI.413-1998, 1998.

[87] *Broadband Radio Access Networks (BRAN); HIPERLAN Type 2; Physical (PHY) layer*, ETSI Std. TS 101 475, Dec. 2001.

[88] *Multi-band OFDM Physical Layer Proposal for IEEE 802.15 Task Group 3a*, IEEE Std. P802.15, November 2004.

[89] K. Zheng, L. Huang, W. Wang, and G. Yang, "TD-CDM-OFDM: Evolution of TD-SCDMA toward 4G," *IEEE Commun. Soc. Mag.*, pp. 45–52, Jan. 2005.

[90] B. Muquet, Z. Wang, G. B. Giannakis, M. de Courville, and P. Duhamel, "Cyclic prefixing or zero padding for wireless multicarrier transmissions?" *IEEE Trans. Commun.*, vol. 50, no. 12, pp. 2136–2148, Dec. 2002.

[91] P. Billingsley, *Convergence of Probability Measures*. New York, NY: John Wiley, 1968.

[92] Y. V. Prokhorov and V. Statulevičius, Eds., *Limit Theorems of Probability Theory*. Berlin, Germany: Springer-Verlag, 2000.

[93] P. Doukhan, G. Oppenheim, and M. S. Taqqu, Eds., *Theory and Applications of Long-Range Dependence*. Boston, MA: Birkhäuser, 2002.

[94] T. Keller and L. Hanzo, "Orthogonal frequency division multiplexing synchronization techniques for wireless local area networks," in *Proc. Personal Indoor and Mobile Radio Comm. (PIMRC) '96*, vol. 3, Taipei, Taiwan, Oct. 1996.

[95] L. Hazy and M. El-Tanany, "Synchronization of ofdm systems over frequency selective fading channels," in *Proc. Veh. Techol. Conf. (VTC) '97*, Phoenix, AZ, May 1997, pp. 2094–2098.

[96] T. Schmidl and D. Cox, "Robust frequency and timing synchronization for OFDM," *IEEE Trans. Commun.*, vol. 45, pp. 1613–1621, 1997.

[97] M. Speth, F. Classen, and H. Meyr, "Frame synchronization of OFDM systems in frequency selective fading channels," in *Proc. Veh. Techol. Conf. (VTC) '97*, Phoenix, AZ, June 1997, pp. 1807–1811.

[98] Z. Zhang and M. Zhao, "Joint frame synchronization and frequency offset estimation in OFDM system," in *Proc. Personal Indoor and Mobile Radio Comm. (PIMRC) 2003*, vol. 3, Sept. 2003, pp. 2249–2253.

[99] F. Classen and H. Meyr, "Frequency synchronization algorithms for OFDM systems suitable for communication over frequency-selective fading channels," in *Proc. Veh. Techol. Conf. (VTC) '94*, Stockholm, Sweden, June 1994, pp. 1655–1659.

[100] M. Russell and G. Stüber, "Interchannel interference analysis of OFDM in a mobile environment," in *Proc. Veh. Techol. Conf. (VTC) '95*, pp. 820–824.

[101] A. J. Coulson, "Maximum likelihood synchronization for OFDM using a pilot symbol: Algorithms," *IEEE J. Select. Areas Commun.*, vol. 19, no. 12, pp. 2486–2494, Dec. 2001.

[102] P. Moose, "A technique for orthogonal frequency division multiplexing frequency offset correction," *IEEE Trans. Commun.*, vol. 42, pp. 1590–1598, Oct. 1994.

[103] G. Armada and M. Calvo, "Phase noise and sub-carrier spacing effects on the performance of an OFDM communications system," vol. 2, no. 1, pp. 11–13, Jan. 1998.

[104] J. Armstrong, "Analysis of new and existing methods of reducing intercarrier interference due to carrier frequency offset in OFDM," *IEEE Trans. Commun.*, vol. 47, no. 3, pp. 365–369, Mar. 1999.

[105] P. Tourtier, R. Monnier, and P. Lopez, "Multicarrier modem for digital HDTV terrestrial broadcasting," *Signal Processing: Image Comm.*, vol. 5, no. 5/6, pp. 379–403, 1993.

[106] F. Daffara and O. Adami, "A new frequency detector for orthogonal multicarrier transmission techniques," in *Proc. IEEE Veh. Technol. Conf. '95*, vol. 2, Chicago, IL, 1995, pp. 804–809.

[107] M. Sandell, J. van de Beek, and P. Börjesson, "Timing and frequency synchronization in OFDM systems using the cyclic prefix," in *Proc. IEEE Intl. Symp. Synchronization*, 1995, pp. 16–19.

[108] J. van de Beek, M. Sandell, and P. Börjesson, "ML estimation of time and frequency offsets in OFDM systems," *IEEE Trans. Signal Processing*, vol. 45, no. 7, pp. 1800–1805, 1997.

[109] Y. Li, L. Cimini, and N. Sollenberger, "Robust channel esimtation for OFDM systems with rapid dispersive channels," *IEEE Trans. Commun.*, vol. 46, pp. 902–915, 1998.

[110] L. Hanzo, W. Webb, and T. Keller, *Single- and Multi-carrier Quadrature Amplitude Modulation*. New York, NY: John Wiley & Sons, 2000.

[111] V. Engels and H. Rohling, "Multilevel differential modulation techniques (64-DAPSK) for multicarrier transmission systems," *European Trans. Telecommunications*, vol. 6, no. 6, pp. 633–640, 1995.

[112] H. Ochiai and H. Imai, "On the distribution of the peak-to-average power ratio in OFDM signals," *IEEE Trans. Commun.*, vol. 49, no. 2, pp. 282–289, Feb. 2001.

[113] A. Jones and T. Wilkinson, "Combined coding for error control and increased robustness to system nonlinearities in OFDM," in *Proc. Veh. Techol. Conf. (VTC) '96*, Atlanta, GA, Apr. 1996, pp. 904–908.

[114] P. Fan and X.-G. Xia, "Block coded modulation for the reduction of the peak to average power ratio in OFDM systems," *IEEE Trans. Comsumer Electronics*, vol. 45, no. 4, pp. 1025–1029, Nov. 1999.

[115] H. Chen, H. Liang, and M.-C. Chiu, "Combined block coded modulation and peak-to-average power ratio reduction in OFDM systems," in *Proc. IEEE ISIT 2004*, Phoenix, AZ, June 2004, p. 424.

[116] H. Rohling and T. May, "OFDM systems with differential modulation schemes and turbo decoding techniques," in *Proc. 2000 Intl. Sem. on Broadband Comm.*, Zurich, Switzerland, Feb. 2000, pp. 251–255.

[117] X. Wang, T. Tjhung, and C. Ng, "Reduction of peak-to-average power ratio of OFDM system using acompanding technique," *IEEE. Trans. Broadcasting*, vol. 45, no. 3, pp. 303–307, Sept. 1999.

[118] X. Huang, J. Lu, J. Zheng, K. Letaief, and J. Gu, "Companding transform for reduction in peak-to-average power ratio of OFDM signals," *IEEE Trans. Wireless Comm.*, vol. 3, no. 6, pp. 2030–2039, Nov. 2004.

[119] A. J. Coulson, "Narrowband interference in pilot symbol assisted OFDM systems," *IEEE Trans. Wireless Commun.*, vol. 3, no. 6, pp. 2277–2287, Nov. 2004.

[120] C. Muschallik, "Influence of RF oscillators on an OFDM signal," *IEEE Trans. Consumer Electronics*, vol. 41, no. 3, pp. 592–603, 1995.

[121] G. Cuypers, K. Vanbleu, G. Ysebaert, and M. Moonen, "Egress reduction by intra-symbol windowing in DMT-based transmitters," in *IEEE Proc. Intl. Conf. Acoustics, Speech & Signal Processing '03*, vol. 4, 2003, pp. iv532–iv535.

[122] Y.-P. Lin, Y.-Y. Ban, C.-C. Su, and S.-M. Phong, "Windowed multicarrier systems with minimum spectral leakage," in *IEEE Proc. Intl. Conf. Acoustics, Speech & SIgnal Processing '04*, vol. 4, 2004, pp. iv749–iv752.

[123] M. Pauli and P. Kuchenbecker, "On the reduction of the out-of-band radiation of OFDM signals," in *Proc. IEEE Int'l. Conf. Comm. (ICC) '98*, vol. 3, Atlanta, GA, 1998, pp. 1304–1308.

[124] M. Engels, Ed., *Wireless OFDM systems : how to make them work?* Boston, MA: Kluwer Academic, 2002.

[125] S. Verdú, "Spectral efficiency of CDMA with random spreading," *IEEE Trans. Inform. Theory*, vol. 45, no. 2, pp. 622–640, Mar. 1999.

[126] ——, "On channel capacity per unit cost," *IEEE Trans. Inform. Theory*, vol. 36, no. 5, pp. 1019–1039, Sept. 1990.

[127] ——, "Spectral efficiency in the wideband regime," *IEEE Trans. Inform. Theory*, vol. 48, no. 6, pp. 1319–1343, June 2002.

[128] E. Biglieri, J. Proakis, and S. Shamai, "Fading channels: Information-theoretic and communications aspects," *IEEE Trans. Inform. Theory*, vol. 44, no. 6, pp. 2619–2690, Oct. 1998.

[129] N. A. Zervos and I. Kalet, "Optimized decision feedback equalization versus optimized orthogonal frequency division multiplexing for high-speed data transmission over the local cable network," in *Proc. IEEE Int'l. Comm. Conf.*, Boston, MA, June 1989, pp. 1080–1085.

[130] S. Verdú, "Recent results on the capacity of wideband channels in the low-power regime," *IEEE Wireless Commun. Mag.*, pp. 40–45, Aug. 2002.

[131] W. C. Lee, "Estimate of channel capacity in Rayleigh fading environment," *IEEE Trans. Veh. Technol.*, vol. 39, no. 3, pp. 187–189, Aug. 1990.

[132] M. S. Taqqu, "Weak convergence to fractional Brownian motion and to the Rosenblatt process," *Zeitschrift f. Wahrscheinlichkeitstheorie verw. Gebiete*, vol. 31, pp. 287–302, 1975.

[133] G. Szegö, *Orthogonal Polynomials*. New York, NY: American Mathematical Society, 1959.

[134] M. A. Arcones, "Limit theorems for nonlinear functionals of a stationary Gaussian sequence of vectors," *Ann. Prob.*, vol. 22, no. 4, pp. 2242–2274, 1994.

[135] M. V. S. de Naranjo, "A central limit theorem for non-linear functionals of stationary Gaussian vector processes," *Stat. Prob. Lett.*, vol. 22, pp. 223–230, 1995.

[136] J. E. Marsden and M. J. Hoffman, *Basic Complex Analysis*. New York, NY: W.H. Freeman and Company, 1987.

[137] J. M. Wozencraft and I. M. Jacobs, *Principles of Communication Engineering*. Prospect Heights, IL: Waveland Press, 1990.

[138] D. Agrawal, V. Tarokh, A. Naguib, and N. Seshadri, "Space-time coded OFDM for high data-rate wireless communication over wideband channels," in *Proc. Veh. Techol. Conf. (VTC) 1998*, vol. 3, Ottawa, Canada, May 1998, pp. 2232–2236.

[139] H. Yang, "A road to future broadband wireless access: MIMO-OFDM based air interface," *IEEE Commun. Soc. Mag.*, pp. 53–60, Jan. 2005.

[140] S. Ross, *A First Course in Probability*. New York, NY: MacMillan College, 1994.

[141] M. Zorzi and R. R. Rao, "Perspectives on the impact of error statistics on protocols for wireless networks," *IEEE Personal Communications*, vol. 6, no. 5, pp. 32–40, 1999.

[142] L. Kanal and A. Sastry, "Models for channels with memory and their applications to control," *Proc. IEEE*, vol. 66, pp. 724–744, July 1978.

[143] J. R. Yee and E. J. Weldon, "Evaluation of the performance of error-correcting codes on a Gilbert channel," *IEEE Trans. Commun.*, vol. 43, no. 8, pp. 2316–2323, Aug. 1995.

[144] J. Craig, "A new, simple and exact result for calculating the probability of error for two-dimensional signal constellations," in *Proc. IEEE MILCOM'91 Conf. Rec.*, Boston, 1991, pp. 25.5.1–25.5.5.

[145] M. K. Simon and M.-S. Alouini, *Digital Communication over Fading Channels*. New York, NY: John Wiley, 2000.

[146] M. K. Simon, "Comments on: `infinite-series representations associated with the bivariate Rician distribution and their applications'"

[147] K. Miller, R. Bernstein, and L.E.Blumenson, "Generalized Rayleigh processes," *Quarterly of Applied Mathematics*, vol. 16, no. 2, pp. 137–145, 1958.

[148] A. Clark, P. Smith, and D. Taylor, "Simple expressions for the correlation between fading channel error rates," in *Proc. IEEE Int. Symp. Info. Theory 2006*, Seattle, Wa., 2006.

[149] A. A. Saleh and R. A. Valenzuela, "A statistical model for indoor multipath propagation," *IEEE J. Select. Areas Commun.*, vol. SAC-5, no. 3, pp. 128–137, Feb. 1987.

[150] W. Feller, *An Introduction to Probability Theory and Its Applications, Vol. 1*, 2nd ed. New York, NY: John Wiley and Sons, 1957.

[151] A. Barbour and P. Hall, "On the rate of Poisson convergence," *Math. Proc. Camb. Phil. Soc.*, vol. 95, no. 3, pp. 473–480, 1984.

[152] I. Borisov and P. Ruzankin, "Poisson approximation for expectations of unbounded functions of independent random variables," *Ann. Prob.*, vol. 30, no. 4, pp. 1657–1680, 2002.

[153] K. Choi and A. Xia, "Approximating the number of successes in independent trials: Binomial versus Poisson," *Ann. Prob.*, vol. 12, no. 4, pp. 1139–1148, 2002.

[154] J. Hodges and L. Le Cam, "The Poisson approximation to the Poisson binomial distribution," vol. 31, no. 3, pp. 737–740, 1960.

[155] L. H. Chen, "On the convergence of Poisson binomial to Poisson distributions," *Ann. Prob.*, vol. 2, no. 1, pp. 178–180, 1974.

[156] J. K. Cavers and P. Ho, "Analysis of the error performance of trellis-coded modulations in Rayleigh-fading channels," *IEEE Trans. Commun.*, vol. 40, no. 1, pp. 74–83, Jan. 1992.

[157] R. van Nobelen and D. P. Taylor, "Analysis of the pairwise error probability of noninterleaved codes on the Rayleigh-fading channel," *IEEE Trans. Commun.*, vol. 44, no. 4, pp. 456–463, Apr. 1996.

[158] B. Noble and J. W. Daniel, *Applied Linear Algebra*. Upper Saddle River, NJ: Prentice-Hall, 1988.

[159] G. Turin, "The characteristic function of hermitian quadratic forms in complex normal variables," *Biometrika*, vol. 47, no. 1/2, pp. 199–201, June 1960.

[160] R. Berends, H. ter Morsche, J. van den Berg, and E. van de Vrie, *Fourier and Laplace Transforms*. Cambridge, UK: Cambridge University Press, 2003.

[161] W. R. LePage, *Complex Variables and the Laplace Transform for Engineers*. New York, NY: McGraw-Hill, 1961.

[162] E. Kreyszig, *Advanced Engineering Mathematics*, 8th ed. New York, NY: John Wiley & Sons, 1999.

[163] C. Chen and F. Qi, "The best bounds to $(2n)!/(2^{2n}(n!)^2)$," *Math. Gaz.*, vol. 88, no. 513, pp. 540–542, Nov. 2004.

[164] J. Boutros and E. Viterbo, "High diversity lattices for fading channels," in *Proc. 1995 IEEE Intl. Symp. Info. Theory (ISIT '95)*, Whistler, BC, Canada, 1995, p. 157.

[165] E. Bayer-Fluckiger, F. Oggier, and E. Viterbo, "New algebraic constructions of rotated $\mathbb{Z}^n$ lattice constellations for the Rayleigh fading channel," *IEEE Trans. Inform. Theory*, vol. 50, no. 4, pp. 702–714, Apr. 2004.

[166] P. Robertson, E. Villebrun, and P. Hoeher, "A comparison of optimal and sub-optimal MAP decoding algorithms operating in the log domain," in *Proc. IEEE Int'l Conf. Comm. (ICC) '95*, 1995, pp. 1009–1013.

[167] D. E. Knuth, *The Art of Computer Programming, vol. 3: Sorting and Searching*. Reading, MA: Addison-Wesley, 1973.

[168] K. Araki, M. Takada, and M. Morii, "The generalized syndrome polynomial and its application to the efficient decoding of reed-solomon codes based on the GMD criterion," in *Proc. IEEE Int. Symp. Info. Theory*, San Antonio, Tx., 1993, p. 34.

[169] U. Sorger, "Fast generalized-minimum-distance decoding," in *Proc. IEEE Int. Symp. Info. Theory*, San Antonio, Tx., 1993, p. 30.

[170] I. Dumer and R. Krichevskiy, "Soft-decision majority decoding of Reed-Muller codes," *IEEE Trans. Inform. Theory*, vol. 46, no. 1, pp. 258–264, Jan. 2000.

[171] S. Litsyn, "On decoding complexity of low-rate reed-muller codes (in Russian)," in *Proc. 9th All-Union Conf. Coding Theory and Info. Transmission*, Odessa, USSR, 1988, pp. 202–204.

[172] R. J. Vaughan and W. N. Venables, "Permanent expressions for order statistic densities," *J. Royal Stat. Soc., Ser. B*, vol. 34, no. 2, pp. 308–310, 1972.

[173] H. Minc, *Permanents*. Reading, MA: Addison-Wesley, 1978.

[174] P. Smith and B. Dawkins, "Estimating the permanent by importance sampling from a finite population," *J. Stat. Comput. Simul.*, vol. 70, pp. 197–214, 2001.

[175] M. Jerrum, A. Sinclair, and E. Vigoda, "A polynomial-time approximation algorithm for the permanent of a matrix with nonnegative entries," *J. Assoc. Computing Machinery*, vol. 51, no. 4, pp. 671–697, July 2004.

[176] M. Jerrum and A. Sinclair, "Approximating the permanent," *SIAM J. Computing*, vol. 8, no. 6, pp. 1149–1178, Dec. 1989.

[177] W. Jurkat and H. Ryser, "Matrix factorizations of determinants and permanents," *J. Algebra*, vol. 3, pp. 1–27, 1966.

[178] B. C. Arnold, N. Balakrishnan, and H. N. Nagaraja, *A First Course in Order Statistics*. New York, NY: John Wiley, 1992.

[179] R. M. Gray, "On the asymptotic eigenvalue distribution of Toeplitz matrices," *IEEE Trans. Inform. Theory*, vol. 18, no. 6, pp. 725–730, Nov. 1972.

[180] M. Fossorier and S. Lin, "Soft-decision decoding of linear block codes based on ordered statistics," *IEEE Trans. Inform. Theory*, vol. 41, pp. 1379–1396, Sept. 1995.

[181] P. A. Martin and D. P. Taylor, "On multilevel codes and iterative multistage decoding," *IEEE Trans. Commun.*, vol. 49, no. 11, pp. 1916–1925, Nov. 2001.

[182] P. A. Martin, "Adaptive iterative decoding : block turbo codes and multilevel codes," Ph.D. dissertation, University of Canterbury, Christchurch, New Zealand, 2001.

[183] G. Marsaglia, "Ratios of normal variables and ratios of sums of uniform variables," *J. Am. Stat. Assoc.*, vol. 60, no. 309, pp. 193–204, Mar. 1965.

[184] I. Miller and M. Miller, Eds., *John E. Freund's Mathematical Statistics*. Upper Saddle River, NJ: Prentice-Hall, 1999.